Adding new functions to insulin-like growth factor-I (IGF-I) via genetic codon expansion

Dissertation zur Erlangung des naturwissenschaftlichen Doktorgrades der

Julius-Maximilians-Universität Würzburg

vorgelegt von

Fang Wu

aus Loudi - China

Würzburg 2018

CC BY SA

Eingereicht bei der Fakultät für Chemie und Pharmazie am

Gutachter der schriftlichen Arbeit

1. Gutachter:

2. Gutachter:

Prüfer des öffentlichen Promotionskolloquiums

1. Prüfer:

2. Prüfer:

3. Prüfer:

Datum des öffentlichen Promotionskolloquiums

Doktorurkunde ausgehändigt am

Die vorliegende Arbeit wurde in der Zeit von November 2014 bis Oktober 2018 am Institut für Pharmazie und Lebensmittelchemie der Bayerischen Julius-Maximilians-Universität Würzburg unter der Anleitung von Herrn Prof. Dr. Dr. Lorenz Meinel angefertigt.

Table of Contents

Summary 1
Zusammenfassung 3
1. Introduction 7
1.1 IGF-I isoforms 7
1.1.1 IGF-I gene structure and alternative splicing 7
1.1.2 Processing of pre-pro-IGF-I peptides (signal peptide + IGF-I + E-peptide) 8
1.1.3 Potential functions of IGF-I splice variants 9
1.1.4 Potential actions of E-peptides (Ea, Eb & Ec) 11
1.1.5 Full-processed IGF-I 15
1.1.6 Naturally occurring analog of IGF-I: Des (1-3) IGF-I 15
1.1.7 Synthetic analog of IGF-I: long-R^3-IGF-I 16
1.2 IGF-I actions and signaling 16
1.3 IGF binding proteins 18
1.4 IGF-I decoration 22
1.5 Translation of bio-inspired systems into the pharmaceutical design scheme 26
1.6 Aim of the thesis 31
2. Materials & Methods 33
2.1 General materials 33
2.2 IGF-I variants preparation 41
2.2.1 Genetically engineered IGF-I variants containing N-terminally His_6-tagged thioredoxin and a thrombin cleavage site 41
2.3 Dual-functionalized IGF-I variants 52
2.3.1 Genetically engineered IGF-I Ea with two alkyne functionalities 52
2.3.2 Clickable plk-IGF-I Ea with TGase reactivity 54
2.3.3 Site-specific conjugation of plk-IGF-I Ea with azide-PCL-FGF2 56
3. Results 59
3.1 IGF-I variants preparation 59
3.1.1 Genetically engineered IGF-I variants containing N-terminally His_6-tagged thioredoxin and a thrombin cleavage site 59
3.2 Dual-functionalized IGF-I variants 72
3.2.1 Genetically engineered IGF-I Ea with two alkyne functionalities 72
3.2.2 Clickable plk-IGF-I Ea with TGase reactivity 76
3.2.3 Site-specific conjugation of plk-IGF-I Ea with azide-PCL-FGF2 79

4. Discussion 85
5. ACS Biomater. Sci. Eng. 2018 91
6. Conclusion & Outlook 113
References 119
Appendix 141
Abbreviations 145
Curriculum vitae 149
Acknowledgments 151
Documentation of authorship 153

Summary

Insulin-like growth factor-I (IGF-I) is a 70-amino acid polypeptide with a molecular weight of approximately 7.6 kDa acting as an anabolic effector. It is essential for tissue growth and remodeling. Clinically, it is used for the treatment of growth disorders and has been proposed for various other applications including musculoskeletal diseases. Unlike insulin, IGF-I is complexed to at least six high-affinity binding proteins (IGFBPs) exerting homeostatic effects by modulating IGF-I availability to its receptor (IGF-IR) on most cells in the body as well as changing the distribution of the growth factor within the organism.[1-3] Short half-lived IGF-I have been the driving forces for the design of localized IGF-I depot systems or protein modification with enhanced pharmacokinetic properties. In this thesis, we endeavor to present a versatile biologic into which galenical properties were engineered through chemical synthesis, e.g., by site-specific coupling of biomaterials or complex composites to IGF-I. For that, we redesigned the therapeutic via genetic codon expansion resulting in an alkyne introduced IGF-I, thereby becoming a substrate for biorthogonal click chemistries yielding a site-specific decoration.

In this approach, an orthogonal pyrrolysine tRNA synthetase (PylRS)/tRNAPyl CUA pair was employed to direct the co-translational incorporation of an unnatural amino acid—propargyl-L-lysine (plk)—bearing a clickable alkyne functional handle into IGF-I in response to the amber stop codon (UAG) introduced into the defined position in the gene of interest. We summarized the systematic optimization of upstream and downstream process alike with the ultimate goal to increase the yield of plk modified IGF-I therapeutic, from the construction of gene fusions resulting in (i) Trx-plk-IGF-I fusion variants, (ii) naturally occurring pro-IGF-I protein (IGF-I + Ea peptide) (plk-IGF-I Ea), over the subsequent bacterial cultivation and protein extraction to the final chromatographic purification. The opportunities and hurdles of all of the above strategies were discussed. Evidence was provided that the wild-type IGF-I yields were pure by exploiting the advantages of the pHisTrx expression vector system in concert with a thrombin enzyme with its highly specific proteolytic digestion site and multiple-chromatography steps. The alkyne functionality was successfully introduced into IGF-I by amber codon suppression. The proper folding of plk-IGF-I Ea was assessed by WST-1 proliferation assay and the detection of phosphorylated AKT in MG-63 cell lysate. The purity of plk-IGF-I Ea was monitored with RP-HPLC and SDS-PAGE analysis. This work also showed site-specific coupling an alkyne in plk-IGF-I Ea by copper (I)-catalyzed azide-alkyne cycloaddition (CuAAC) with potent activities *in vitro*. The site-specific immobilization of plk-IGF-I Ea to the model carrier (i.e., agarose beads) resulted in enhanced cell proliferation and adhesion surrounding the IGF-I-presenting particles. Cell proliferation and differentiation were enhanced in the accessibility of IGF-I decorated beads, reflecting the multivalence on cellular performance.

Next, we aimed at effectively showing the disease environment by co-delivery of fibroblast growth factor 2 (FGF2) and IGF-I, deploying localized matrix metalloproteinases (MMPs) upregulation as a surrogate marker driving the response of the drug delivery system. For this purpose, we genetically engineered FGF2 variant containing an (S)-2-amino-6-(((2-azidoethoxy)carbonyl)amino)hexanoic acid incorporated at its N-terminus, followed by an MMPs-cleavable linker (PCL) and FGF2 sequence, thereby allowing site-directed, specific decoration of the resultant azide-PCL-FGF2 with the previously mentioned plk-IGF-I Ea to generate defined protein-protein conjugates with a PCL in between. The click reaction between plk-IGF-I Ea and azide-PCL-FGF2 was systematically optimized to increase the yield of IGF-FGF conjugates, including reaction temperature, incubation duration, the addition of anionic detergent, and different ratios of the participating biopharmaceutics. The challenge here was that CuAAC reaction components or conditions might oxidize free cysteines of azide-PCL-FGF2 and future work needs to present the extent of activity retention after conjugation. Furthermore, our study provides potential options for dual-labeling of IGF-I either by the introduction of unnatural amino acids within two distinct positions of the protein of interest for parallel “double-click” labeling of the resultant plk-IGF-I Ea-plk or by using a combination of enzymatic-catalyzed and CuAAC bioorthogonal coupling strategies for sequentially dual-labeling of plk-IGF-I Ea.

In conclusion, genetic code expansion in combination with click-chemistry provides the fundament for novel IGF-I analogs allowing unprecedented site specificity for decoration. Considerable progress towards IGF-I based therapies with enhanced pharmacological properties was made by demonstrating the feasibility of the expression of plk incorporated IGF-I using *E. coli* and retained activity of unconjugated and conjugated IGF-I variant. Dual-labeling of IGF-I provides further insights into the functional requirements of IGF-I. Still, further investigation warrants to develop precise IGF-I therapy through unmatched temporal and spatial regulation of the pleiotropic IGF-I.

Zusammenfassung

Insulin-like growth factor-I (IGF-I) ist ein 70 Aminosäuren langes Polypeptid mit einem Molekuargewicht von 7,5 kDa, dass als anaboler Effektor wirkt und dadurch eine essentielle Rolle in Gewebewachstum und -umbau spielt. Klinisch wird IGF-I für die Behandlung von Wachstumsstörungen verwendet und ist für weitere Anwendungen wie muskuloskelettale Erkrankungen von Interesse. Im Gegensatz zu Insulin wird IGF-I von mindestens sechs hochaffinen Bindungsproteinen (IGFBPs) komplexiert, die homöostatisch regulierend wirken, indem sie die Verfügbarkeit von IGF-I zu seinem Rezeptor (IGF-IR) auf vielen Zellen modulieren und ebenso die Verteilung des Wachstumsfaktors im Körper steuern. Aufgrund der kurzen Halbwertszeit von IGF-I wurde die Entwicklung von lokalen IGF-I Depot-Systemen und von auf Proteinebene modifizierten IGF-I-Varianten mit verbesserten pharmakokinetischen Eigenschaften vorangetrieben. In der vorliegenden Arbeit sind wir bestrebt ein vielseitiges Biopharmazeutikum zu präsentieren, das hinsichtlich seiner galenischen Eigenschaften optimiert wurde, z. B. durch chemische Modifikation, wie ortsspezifische Kopplung von IGF-I an Biomaterialien oder komplexe Verbundstoffe. Für diesen Zweck wurde das Therapeutikum neu entworfen und über die Erweiterung des genetischen Codes eine Alkin-Funktionalität eingefügt. Durch dieses Alkin wird IGF-I zugänglich für die Modifizierung mit bio-orthogonaler, ortsspezifischer „Click-Chemie“.

In diesem Ansatz wird ein orthogonales Pyrrolysin tRNA-Synthase (PylRS)/tRNAPyl-CUA – Paar verwendet, um den co-translationalen Einbau einer unnatürlichen Aminosäure — Propargyl-L-lysine (Plk) —, die eine Alkin-Funktionalität für Click-Reaktionen enthält, an Stelle des Amber-Stop-Codons (UAG) im entsprechenden Gen, im IGF-I-Protein zu gewährleisten. Die systematische Optimierung von Up- und Downstream-Prozessen, mit dem Ziel die Ausbeute von Plk-modifiziertem IGF-I-Biopharmazeutikum zu erhöhen, wurden zusammengefasst: von der Konstruktion von Genfusionen, die in (i) einer Trx-plk-IGF-I Fusionsvariant und (ii) natürlich vorkommendem pro-IGF-I Protein (IGF-I + Ea peptide) (Plk-IGF-I Ea) resultierten, über die folgende Expression in Bakterien und Proteinextraktion, bis hin zur finalen chromatographischen Reinigung des Biopharmazeutikums. Die Möglichkeiten und Schwierigkeiten aller oben genannten Strategien wurden diskutiert. Es wurde gezeigt, dass die Wildtyp-IGF-I-Ausbeuten durch den Einsatz des vorteilhaften pHisTrx-Expressionsvektor-Systems zusammen mit dem Enzym Thrombin und seiner hochspezifischen proteolytischen Spaltstelle und mehrfacher chromatographischer Aufreinigung einen hohen Reinheitsgrad aufwiesen. Die Alkin-Funktionalität wurde erfolgreich durch Unterdrückung des Amber-Codons in IGF-I eingeführt. Die richtige Faltung von Plk-IGF-I Ea wurde durch den WST-1 Proliferationsassay und den Nachweis von phosphorylierten Akt in MG-63-Zelllysat nachgewiesen. Die Reinheit von Plk-IGF-I Ea wurde durch RP-HPLC- und SDS-PAGE-Analyse überwacht. In dieser Arbeit konnte auch gezeigt

werden, dass die ortspezifische Kopplung von Alkinen an Plk-IGF-I Ea durch Kupfer(I)-katalysierte Azid-Alkin Zykloaddition (CuAAC) in einem Produkt mit hoher *in vitro* Aktivität resultiert. Die ortspezifische Immobilisierung von Plk-IGF-I Ea an einem Modell-Trägersystem (hier: Agarosepartikel) führte zu einer verbesserten Zellproliferation und Zelladhäsion in der Umgebung der IGF-I-präsentierenden Partikel. Der vielfältige Einfluss von IGF-I auf Zellen wird durch die verbesserte Zellproliferation und -differenzierung durch die Verfügbarkeit von IGF-I präsentierenden Partikeln widergespiegelt.

Als Nächstes setzten wir uns zum Ziel den Krankheitseinfluss durch die gleichzeitige Anwendung von Fibroblast-Wachstumsfaktor 2 (FGF2) und IGF-I zu zeigen, indem wir uns der lokalen Hochregulierung von Matrixmetalloproteinasen (MMPS) als Surrogat-Krankheitsmarker bedienten, der die Antwort des Drug Delivery-Systems auslöst. Zu diesem Zweck wurde eine FGF2-Variante genetisch modifiziert, sodass sie am N-Terminus eine (S)-2-amino-6-(((2-azidoethoxy)carbonyl)amino)Hexansäure trägt - gefolgt von einen durch MMPs spaltbaren Verbindungsstück (PCL) und der FGF2 Sequenz - und dadurch die gezielte, spezifische Konjugation des resultierenden Azid-PCL-FGF2 mit dem vorher erwähnten Plk-IGF-I Ea ermöglicht, um definierte Protein-Protein-Konjugate, die mit einem PCL verbunden sind, zu erzeugen. Die Click-Reaktion zwischen Plk-IGF-I Ea und Azid-PCL-FGF2 wurde zur Erhöhung der IGF-FGF Ausbeute systematisch optimiert, indem die Parameter Temperatur, Inkubationsdauer, Zugabe von anionischem Tensid und verschiedene Eduktverhältnisse untersucht wurden. Es gilt zu bedenken, dass die in der CuAAC Reaktion eingesetzten Komponenten oder Reaktionsbedingungen freie Cysteinreste von Azid-PCL-FGF2 oxidieren können und es in Zukunft gilt, die verbleibende Aktivität nach Proteinkonjugation zu bestimmen. Des Weiteren zeigen unsere Untersuchungen potentielle Möglichkeiten für duale Konjugation von IGF-I entweder durch die Einführung einer unnatürlichen Aminosäure an zwei verschiedenen Positionen innerhalb des Proteins (Plk-IGF-I Ea-Plk) für parallele „Doppel-Click“-Konjugation oder durch die Kombination bioorthogonaler Kopplungsreaktionen - einer enzymkatalysierten Reaktion und CuAAC - für sequentielles duales Verknüpfen von Plk-IGF-I Ea.

Schlussendlich stellt die Erweiterung des genetischen Codes in Kombination mit Click-Chemie eine Grundlage für neue IGF-I-Analoga dar, die eine noch nie dagewesene Ortsspezifität für Konjugationen besitzen. Ein entscheidender Fortschritt hin zu IGF-I basierten Therapeutika mit verbesserten pharmakologischen Eigenschaften wurde durch die Expression, Reinigung und Konjugation von bioaktivem IGF-I mit Plk sowie konjugierten IGF-I Varianten erreicht. Duales Modifizieren von IGF-I erlaubt weitere Einblicke in die funktionalen Anforderungen an IGF-I. Dennoch sind weitere Untersuchungen nötig, um eine gezielte IGF-I Therapie trotz der unterschiedlichen zeitlichen und räumlichen Regulierung des pleiotropen IGF-I zu ermöglichen.

The data in the monograph (from **1.Introduction** to **4.Discussion section**) is unpublished.

1. Introduction

1.1 IGF-I isoforms

Insulin-like growth factor-I (IGF-I) is a potent survival factor that also stimulates axon growth in motoneurons, blocks atrophy in skeletal muscle fibers and maintains mass and regenerative capacity in senescent animals.[4-7] Given the prominent functions of IGF-I in normal tissue and cell homeostasis and tropism, numerous therapeutic applications have been envisaged and extensive trials with recombinant human IGF-I were performed, including treatment of growth disorders, insulin resistance and diabetes, musculoskeletal disorders, cardiovascular diseases, chronic liver disease, neurodegenerative diseases and aging.[8] Rescue effects with IGF-I have been observed in multiple models, such as improved muscle function, delayed disease progression, and extended survival.[9-15]

1.1.1 IGF-I gene structure and alternative splicing

The general consensus is that these biological functions are mediated by the mature IGF-I peptide, which is produced from *Igf1* gene. The *Igf1* gene contains 6 exons, which generates a heterogeneous pool of IGF-I transcripts by a combination of alternative transcription initiation sites located within the leader sequences (exon 1 and 2), alternative splicing at 5'- and/or 3'- end of the *Igf1* gene, and multiple polyadenylation sites usage within exon 6.[16, 17] More specifically, the different leader exons, which undergo differential splicing of exons 1 and 2 to the common exon 3, result in two IGF-I splice mRNA classes: class 1 mRNA variants have the leader sequences on exon 1, whereas class 2 transcripts use exon 2 as the leader exon (**Figure 1**). In particular, transcription initiation at promoter 1 are extensively expressed in various tissues, likely linked to the synthesis of paracrine IGF-I and may have an influence on interactions with IGF binding proteins (IGFBPs), or promote truncated IGF-I peptide formation.[18] While transcriptional start sites at promoter 2 are expressed predominantly in the liver (circulating IGF-I forms) and kidney[19] which are expected to be more GH-dependent[20-25] or comparably GH-responsive.[26, 27] However, both promoters are probably not mutually exclusive, and GH can also stimulate the tissue-specific (local form) transcripts expression, although the present evidence is still ambiguous.[28-33] Alternative splicing at 3'- end of the *Igf1* gene also results in distinct transcripts that contain exon 5, generally are designated as IGF-I Eb, or exon 6 termed as IGF-I Ea, or both exon 5 and 6 as the IGF-I Ec (corresponding to IGF-I Eb in rodents).[18, 34-36] Additionally, differential usage of polyadenylation sites further creates size heterogeneity of human IGF-I mRNAs, ranging from 1.1 to 7.6 kb in size.[37] Studies of transcript stability suggested the half-life of IGF-I mRNAs was inversely proportional to the length of their 3'-untranslated region (UTR) with the shortest transcript size having the greatest stability.[38]

Further regulations at a post-transcriptional level by methylation or microRNA (miRNA) repression are likely involved.[39] Examples of miRNA negatively associated with expression of IGF-I are found in cardiac and skeletal muscle under physiological and pathological conditions as miRNA-1[40] and in Alzheimer's disease (AD) as miRNA-98.[41]

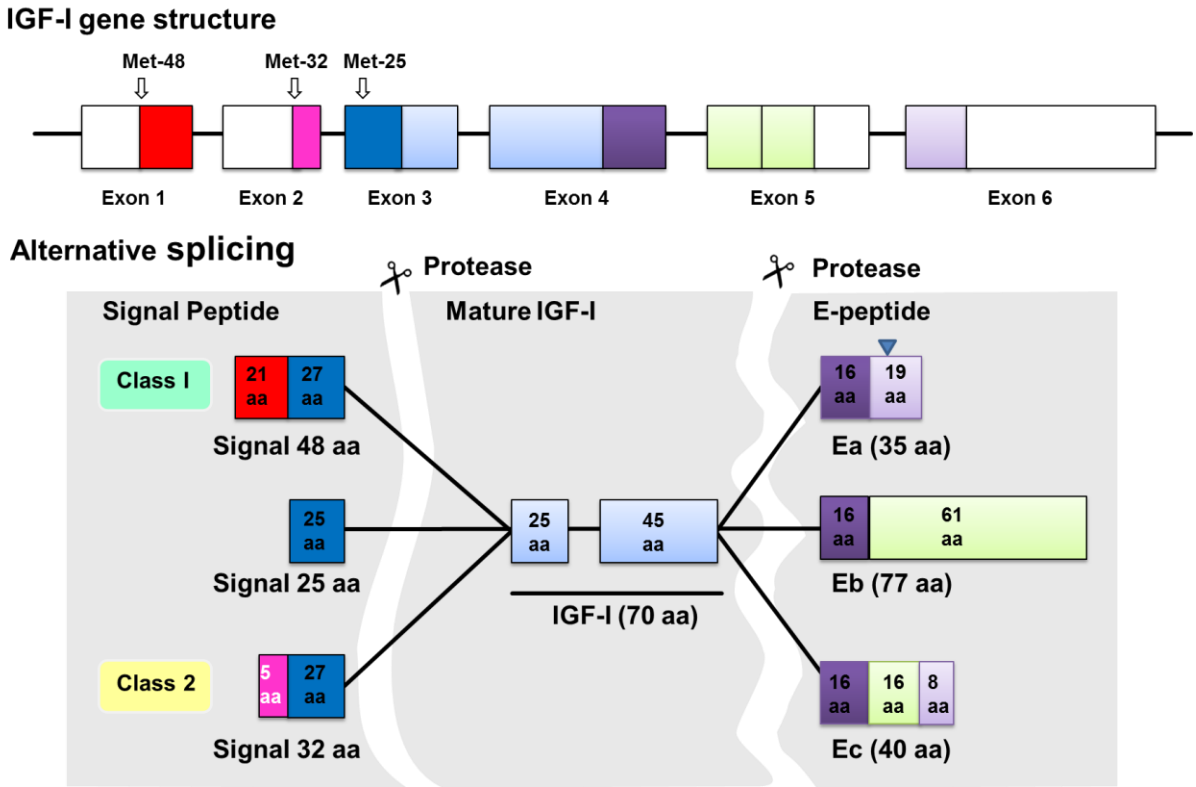

Figure 1. Schematic illustration of the human *Igf1* gene and alternative splicing. Multiple IGF-I mRNA variants can be generated using all possible combinations between leader sequence (encoding signal peptide) usage and terminal exon (5 or 6). The mature IGF-I peptide, coded by exon 3 and 4, is obtained from posttranslational processing of each of the various IGF-I precursor polypeptides by the removal of the signal and the E(a,b,c)-peptides (gaps mark the cleavage sites). Three different E-peptides are encoded by three mRNA variants resulted from alternative splicing at the 3′ end of the pro-IGF-I mRNA. The first 16 amino acids of the N-terminus E-peptides are coded by part of exon 4. Exons 5 and 6 encode distinct parts of the E-peptides with alternative C-terminal sequences by alternative splicing. An N-linked glycosylation site (N92) contained only in the Ea-peptide (▼).

1.1.2 Processing of pre-pro-IGF-I peptides (signal peptide + IGF-I + E-peptide)

These transcripts encode several different IGF-I precursor polypeptides,[34] which consist of a signal peptide directing excretion, the mature IGF-I, and a C-terminal extension called E-peptide.[42] Various isoforms are generated by alternative splicing, multiple promoter usage, and post-translational modification.[43, 44] However, they share the identical mature IGF-I peptide with B, C, A, and D domains.[1] Data from other model systems suggested that co- or post-translational

modification was of importance for protein stabilization, transmembrane transportation, and secretion.[45-47] In rodents, pro-IGF-I precursor polypeptides generated from classes 1 and 2 transcripts can have 48, 32 and 22 amino acids long signal peptides, which can further undergo post-translational processing.[17] Evidence of *in vitro* glycosylation showed that glycosylation process did not occur in the pro-IGF-I precursor with the 48-residue signal peptide, and a precursor with the 32 amino acids long signal sequence was glycosylated to the lesser extent than 22-residue pre-peptide.[48] Again, alternative splicing and alternate promoter usage at the 5'-end of IGF-I mRNAs resulting in different signal peptides could influence the precise N-terminal cleavage site of the signal sequence,[49] suggesting that alternate signal peptides could trigger cleavage at a position three amino acids downstream of the routine cleavage site to generate an N-terminal truncated IGF-I or pro-IGF-I (mature IGF-I plus an E-peptide).[50, 51] After the cleavage of the signal peptide, additional processing for the pro-IGF-I can be performed prior to secretion. This includes proteolytic removal of the E-peptides to release mature IGF-I for secretion,[52] maintenance of the intact pro-IGF-I to be secreted,[53-55] or N-glycosylation in the predominant IGF-I isoform (IGF-I Ea) prior to secretion[56] (reviewed in [57]). Thus, three forms of IGF-I protein could exist in the extracellular situation: mature IGF-I, non-glycosylated pro-IGF-I (three isoforms in human, IGF-I Ea, IGF-I Eb, IGF-I Ec), and glycosylated pro-IGF-I. Further, removal of the entire E-peptide could be achieved probably by furin protease or by pro-protein convertase subtilisin/kexin type 6 (e.g., PACE4) and subsequently mature IGF-I is released for receptor binding when needed.[57, 58] The differential expression of the IGF-I isoforms was observed in various conditions or pathologies in humans, such as exercise-induced skeletal muscle damage,[59, 60] endometriosis[61] or prostate,[62] cervical[63] and colorectal cancer,[64] implying an underlying complexity of IGF-I actions.[65, 66]

1.1.3 Potential functions of IGF-I splice variants

Class 2 IGF-I Ea transcript represents the main (endocrine) pro-IGF-I mRNA produced in liver[67] and is similar to the predominant class 1 IGF-I Ea isoform locally expressed in other tissues[68] which may be linked to the autocrine/paracrine form of IGF-I.[67] Of the three human IGF-I isoforms, IGF-I Ea is the only isoform which contains an N-linked glycosylation at Asn92 (marked in red, **Table 1**) based on the consensus sequence Asn–Xaa–Ser/Thr, where Xaa present any amino acid except proline.[69, 70] In murine skeletal muscle, glycosylated pro-IGF-I and non-glycosylated pro-IGF-I are predominant IGF-I forms and overexpressed in the media from IGF-I Ea-transfected cells, suggesting a biological purpose for (non- or) glycosylated Ea.[71] Non-glycosylated pro-IGF-I possessed equivalent activity as mature IGF-I, whereas glycosylated form significantly reduced IGF-I receptor (IGF-IR) activation in IGF-IR activation assays.[71] Although an N-glycosylation process has been reported to be a critical step in producing a fully functional protein (e.g., insulin receptor)[72] and regulate the circulatory half-life of other peptide hormones (e.g., growth hormone),[73, 74] its significance to IGF-I function has yet to be identified. In muscle, pro-IGF-I could

be directly bound (possibly not through IGFBP stabilization) to the extracellular matrix (ECM) for subsequent activity by cleavage,[75] while glycosylation status of pro-IGF-I impaired this association. This observation may explain the significance of preserved E-peptide extension as it increases local IGF-I bioavailability through enhanced ECM retention and prevents their release into circulation. Provided as a muscle-specific transgene, IGF-I Ea induced muscle hypertrophy and regeneration post injury,[7, 76, 77] modulated inflammation response and reduced fibrosis.[78] In the hindlimb muscle reload model, disuse atrophy was reverted by both mature IGF-I and IGF-I Ea, while mature IGF-I did more rapidly for promoting skeletal muscle recovery.[79]

Protective mechanisms of cardiac muscle from oxidative stress by constitutively overexpressed IGF-I Ea form in the heart, was achieved via Sirtuin 1 (SirT1)/c-Jun N-terminal kinase 1 (JNK1) activity, whereas circulating IGF-I did not influence SirT1 activity.[80, 81] Interestingly, overexpressed IGF-I Ea triggered the phosphorylation of IGF-IR but with the activation of novel signaling intermediates 3-phosphoinositide-dependent protein kinase-1 (PDK1) and serum/glucocorticoid regulated kinase 1 (SGK1), as well as SirT1 in transgenic mice, likely accounting for its unique effects (e.g. delayed cell proliferative response) on the heart.[82, 83] Also, supplemental expression of local-specific IGF-I Ea transgene, in heart[84] and skin,[85] facilitated tissue protection and repair without the increase of serum IGF-I levels, supporting the previous hypothesis that E-peptides may play a role in local IGF-I action and retention of IGF-I in the tissue of synthesis. In contrast, transgenic overexpressed IGF-I (without E-peptide) showed increased circulating IGF-I levels,[86, 87] whereas raised serum IGF-I is positively associated with cancer.[88] Structurally, the E-peptide extension at C-terminus of IGF-I faces away from the ligand binding site on IGF-IR, and may not interfere with mature IGF-I/IGF-IR association,[89] resembling the PEGylated IGF-I.[90] These observations may offer an appealing pharmaceutical design choice in reducing pharmaceuticals diffusion and preventing systemic circulation, implying the impact of naturally occurring pro-IGF-I on local treatment efficiency.[75]

Human IGF-I Eb was initially identified in the liver,[42] may be GH responsive and represent an endocrine role of IGF-I, but it was also found in skeletal muscle.[30] The E domain of human IGF-I Eb seems unique given the fact that it is less conserved among primate species beyond apes in comparison with those of IGF-I Ea and IGF-I Ec. Moreover, the unique splicing pattern of human IGF-I Eb is nonexistent in rodents. Human IGF-I Ec, corresponding to IGF-I Eb in rodent, was also firstly detected in human liver.[36] The term is also coined as mechano growth factor (MGF) due to its remarkable upregulation by muscle stretch or damage, indicating that MGF probably induces the regeneration of senescent skeletal muscle as a separate growth factor.[91] Its expression also has been found in various tissues and cells such as endometrium,[61] prostate,[62] as well as in osteoblast-like osteosarcoma cells.[92] MGF was reported to activate satellite cells in muscle leading to hypertrophy or regeneration,[93] and to display its neuroprotective ability in brain ischemia.[94, 95]

In skeletal muscle, IGF-I Ea and MGF are predominant isoforms. Although robust elevated MGF was observed after high resistance training in young men with no significant increase in IGF-I Ea mRNA levels,[96] the transcripts levels of class 1 IGF-I Ea were always much higher than those of MGF in resting muscles of rats and humans.[96, 97] In C2C12 myogenic cell lines, both isoforms (IGF-I Ea and MGF) increase myoblast proliferation, IGF-I Ea promoted the fusion whereas MGF further prolongs proliferation and seemed to inhibit myoblast differentiation.[98] Further, selectively blocking IGF-IR provided evidence that MGF E domain-mediated its mitogenic activity via a different signaling pathway.[98] Moreover, after viral-mediated delivery of murine IGF-I isoforms (IGF-I Ea & IGF-I Eb) into skeletal muscle, both isoforms caused increased phosphorylation of the IGF-IR, increased expression of murine IGF-I Eb (MGF) drove both PI3K/AKT pathway and the MAPK pathway downstream of IGF-IR, whereas murine IGF-I Ea overexpression caused increased AKT phosphorylation only.[99] These studies suggest that IGF-I effects are isoform-specific irrespective of any potential receptor(s) activation (vide infra).

1.1.4 Potential actions of E-peptides (Ea, Eb & Ec)

Synthetic E-peptide analogs, derived from unique regions of the E domains, were shown to possess mitogenic,[61, 62, 92, 100-102] angiogenic[103] and migratory activity,[102, 104, 105] and regulate cell differentiation[101, 104] in various human cells or cell lines, suggesting the E-peptides of human pro-IGF-I may act as independent growth factors. Human Eb-peptide also reported its antitumor effect in some cancer cells.[106] Especially, rodent Ea derived peptides have recently been reported bioactive.[107] Besides, murine Ea- and Eb-peptides were shown to increase cell entry of IGF-I from the media, giving proof of possible modulated properties for IGF-I, beyond their independent activity.[108] Differential roles of the synthetic Ec-peptide and mature IGF-I in cell proliferation and differentiation in the presence of IGF-IR neutralizing antibodies, suggest that the Ec-peptide acts via a different receptor.[98, 104, 109] However, concerns about the effectiveness of a monoclonal antibody antagonist to the IGF-IR have been raised, as they may induce receptor internalization activating the downstream signaling unintentionally, or change IGF-IR conformation to facilitate an E-peptide action.[107] Nevertheless, the bioactivity of fully-processed IGF-I seemed to be inhibited in those cells with IGF-IR neutralizing antibodies. Interestingly, a synthetic analog of the Eb peptide (residues 103–124 amino acid, **Table 1**) with C-terminal amidation has been reported IGF-IR-independent bioactivity, including binding specifically to surface molecules of human bronchial epithelial cells, and initiating mitogenic activity. Furthermore, neither ligand binding was inhibited by IGF-I or insulin competition, nor did IGF-IR neutralizing antibodies inhibit the proliferation induced by the synthetic Eb, suggesting that Eb may mediate its effect through a specific high-affinity receptor.[100] Latter data in human neuroblastoma cells model indicated that the initial step of E-peptide action was mediated through the interaction with conserved and specific putative membrane receptors on a cell surface.[101, 110]

Table 1. The protein sequence, expression and biological roles of 3 different human IGF-I isoforms (i.e., IGF-I Ea, IGF-I Eb, IGF-I Ec) and of mature peptide, E-peptides (i.e., Ea, Eb, Ec) as well as IGF-I analogs. The intact IGF-I sequence is marked in blue, N-glycosylation site in IGF-I Ea is highlighted in red. The common 16 amino acid of N-terminal E-peptide is marked in purple.

Isoforms	Protein sequence	Expression	Functions	Mode of function	Signaling
IGF-I Ea	GPETLCGAELVDALQFVCGDRGFYFNKPTGYGSSSRRAPQTGIVDECCFRSCDLRRLEMYCAPLKPAKSARSVRAQRHTDMPKTQKEVHLKNASRGSAGNKNYRM	Produced in liver[67] as well as in other tissues[68]	Induce muscle hypertrophy and enhance regeneration after injury when provided as a muscle-specific transgene,[76, 77, 111] modulate inflammation response and reduce fibrosis,[78] facilitate tissue protection and repair	Endocrine, autocrine /paracrine action[67]	Act through IGF-I receptor and also trigger alternate signaling intermediates (e.g., PDK1 and SGK1, SirT1) by the phosphorylation of IGF-IR[82, 83]
IGF-I Eb	GPETLCGAELVDALQFVCGDRGFYFNKPTGYGSSSRRAPQTGIVDECCFRSCDLRRLEMYCAPLKPAKSARSVRAQRHTDMPKTQKYQPPSTNKNTKSQRRKGWPKTHPGGEQKEGTEASLQIRGKKKEQRREIGSRNAECRGKKGK	Initially identified in the liver,[42] but it was also found in skeletal muscle[30]	Little information about much-less conserved human IGF-I Eb, more attention was paid to Eb activity	Likely act in both endocrine[42] and autocrine /paracrine fashions[112]	Act through IGF-I receptor
IGF-I Ec (MGF)	GPETLCGAELVDALQFVCGDRGFYFNKPTGYGSSSRRAPQTGIVDECCFRSCDLRRLEMYCAPLKPAKSARSVRAQRHTDMPKTQK**YQPPSTNKNTKSQRRKGSTFEERK**	Markedly increased in exercised and damaged muscle[59, 113]	Serve as a local tissue repair factor in acute injury models of muscle,[93] cardiac muscle[114] and neurons,[94, 115] increase myoblast proliferation and inhibit terminal differentiation,[98] neuroprotective[116-118]	Autocrine /paracrine fashion[113]	Act both through a yet common IGF receptor and through yet unknown specific receptor recognizing a unique MGF E-domain[98]

Ea peptide	RSVRAQRHTDMPKTQKEVHLKNASRGSAGNKNYRM	Only been detected *in vivo* as part of pro-IGF-I[53]	Enhance cell proliferation and migration,[107] induce morphological differentiation and inhibit the anchorage-independent cell growth in human neuroblastoma cells[101]	__	Dependent on IGF-I receptor, affect growth via modulating IGF-I signaling[107]
Eb peptide	RSVRAQRHTDMPKTQKYQPPSTNKNTKSQRRKGWPKTHPGGEQKEGTEASLQIRGKKKEQRREIGSRNAECRGKKGK	Unknown, partly due to the lack of an appropriate and specific antibody, and it is localized to nuclei of transfected cells[119]	Promote cell proliferation and induce morphological differentiation,[100, 101] suppress cancer cell growth and cancer-induced angiogenesis,[106] induce cell attachment and lamellipodia outspread via clathrin-mediated endocytosis[120]	Unknown	Act through novel binding candidates that were not IGF-IR or insulin receptor to conduct biological functions[100, 110]
Ec peptide	RSVRAQRHTDMPKTQK**YQPPSTNKNTKSQRRKGSTFEERK**	Ec peptide and a stable 24-amino-acid MGF (bold marked in the left panel) derived from *Igf1* gene in biological systems were not detected[121]	Promote cell proliferation and migration, act as a local tissue repair factor in acute injury models of muscle,[109] cardiac muscle[114] and neurons[94, 115]	__	Act through yet unknown specific receptor recognizing a unique MGF E-domain[98]
Human IGF-I	GPETLCGAELVDALQFVCGDRGFYFNKPTGYGSSSRRAPQTGIVDECCFRSCDLRRLEMYCAPLKPAKSA	Mainly produced by the liver, also expressed in many other tissues. (Detailed	Important in normal body growth and development,[122] promote cell proliferation,	Endocrine, autocrine /paracrine functions	Act through binding to type I IGF-I receptor (IGF-IR), insulin receptor

		in **Appendix A**)	differentiation, anti-apoptosis, and survival[3, 123-130]		(IR), cation-independent mannose-6-phosphate receptor, IR/IGF-IR hybrid[131-133]
Des(1-3)IGF-I	~~GPE~~TLCGAELVDALQFVCGDRGFYFNKPTGYGSSSRRAPQTGIVDECCFRSCDLRRLEMYCAPLKPAKSA	Found in brain[53, 54]	Stimulate protein accumulation in cultured myoblasts,[134, 135] support differentiated neuronal growth more effectively than native IGF-I[136]	Probably autocrine /paracrine fashion[137]	Act through IGF receptor
Long-R^3-IGF-I	MFPAMPLSSLFVNGP**R**TLCGAELVDALQFVCGDRGFYFNKPTGYGSSSRRAPQTGIVDECCFRSCDLRRLEMYCAPLKPAKSA	__	More potent than IGF-I in stimulating protein and DNA synthesis in the myoblasts,[138] prolonged hypoglycemic action than IGF-I in pigs and marmoset monkeys,[139] more potent growth and survival factor than either insulin or IGF-I in embryonic kidney cells during serum free cultures[140]	__	Act through IGF receptor[138, 139]

Furthermore, a 24-residues Ec-peptide (highlighted in bold, **Table 1**) corresponding to the unique portion beyond that common 16 residues sequence (marked in purple, **Table 1**), possessed bioactivity in some human cells, possibly mediated via an IGF-IR- and IR-independent mechanism.[61, 62, 92] In particular, through exogenous administration of synthetic Ec to these cell lines, peptide bioactivity was not suppressed by either IGF-IR neutralizing antibody or the siRNA knock-out of IGF-IR or IR. This unique Ec peptide activated only ERK1/2 and not AKT,[33, 59, 62, 141] indicating distinct signaling as compared with mature IGF-I. Recently, it has been proposed that E-peptides may affect IGF-I receptor internalization and localization.[107, 108] Also, synthetic peptides

for rodent Ea and Eb domain sequences did not directly induce phosphorylation of IGF-IR in mouse fibroblasts (P6 cells) in a kinase receptor activation assay.[107] Intriguingly, the activation of IGF-IR by IGF-I was enhanced in the presence of either E-peptide in the murine C2C12 cell line, further implying that E-peptides may modulate IGF-I activity.[107] A further conclusion was drawn from the findings of that platform as to that E-peptides signaling as well as mitogenic and motogenic were IGF-IR dependent and plausibly reflected pro-IGF-I actions,[107] indicating that IGF-I splice variants may perform their actions through only mature IGF-I,[142] or by supporting the biological activity of pro-IGF-I forms.[71] Furthermore, the role of murine pro-IGF-I forms[75, 142, 143] or E-peptides[107] is controversial, especially in cell differentiation (see review in [58]).

1.1.5 Full-processed IGF-I

The mature IGF-I is derived from each of the pro-IGF-I isoforms after the removal of the E-peptides. Of the well-characterized growth factors, IGF-I is unique in that it has been reported to promote both cellular proliferation and differentiation[124, 144] depending on the time course and intracellular conditions in the stage of post injury.[145, 146] FDA-approved Mecasermin (an analog of human IGF-I) is for long-term treatment of growth failure with therapeutic value in other aspects such as atrophic musculoskeletal, neurodegenerative disorders and myocardial infarction.[65, 147, 148] However, adverse effects such as hypoglycemia,[149] diabetic retinopathy[150] and neoplastic cell growth,[151, 152] after systemic administration of short-lived IGF-I lead to the development of locally implanted IGF-I depot systems, enabling sustained IGF-I release for bone regeneration after implantation,[153-156] or localized administration,[157, 158] or systemically application of PEGylated version of IGF-I.[90, 159-161]

1.1.6 Naturally occurring analog of IGF-I: Des (1-3) IGF-I

In addition to the full-length IGF-I, two other protein forms are believed to be produced by post-translational processing of pro-IGF-I precursor protein[162] (vide supra) and have been identified in the brain.[50] A truncated analog of human IGF-I (Des(1-3)IGF-I), lacking the first three amino acids of the B domain of mature peptide, exhibits enhanced biological effects (neurotrophic) that is modulated by the IGF-I receptor.[137, 163] The other product is the tripeptide Gly–Pro–Glu, which corresponds to amino-terminal tripeptide of IGF-I.[50] In the central nervous system, the tripeptide may regulate the release of neurotransmitter through binding to the N-methyl-D-aspartate (NMDA) receptor.[50, 163] The removal of N-terminal tripeptide Gly–Pro–Glu may be exploited for enhancing the potency of IGF-I, due to its reduced IGFBPs binding compared to the unprocessed protein.[1, 136, 139]

1.1.7 Synthetic analog of IGF-I: long-R^3-IGF-I

Long-R^3-IGF-I is a synthetic analog of IGF-I comprising the intact IGF-I with an arginine substitution for glutamic acid at position 3, and an additional 13 amino acids peptide at its N-terminus (**Table 1**). It was specifically engineered for enhancing cell performance. These modifications dramatically reduced its affinity for IGFBPs, suggesting the shorter half-life for long-R^3-IGF-I *in vivo* than native IGF-I. Work from Robertson et al.[164] and Bastian et al.[165] supported the above hypothesis that exogenous long-R^3-IGF-I were cleared more rapidly than regular IGF-I from wound fluid, plasma. Plasma IGF-I was predominantly associated with IGFBPs, while the majority of long-R^3-IGF-I was detected as free peptide.[165] The maximal activation ability of the IGF-IR generated by 0.1 μg/mL long-R^3-IGF was similar to that induced by 0.5 μg/mL recombinant human IGF-I. However, the stimulatory ability decreased at a higher concentration (0.5 μg/mL), suggesting that a dose-response curve of long-R^3 IGF-I may be bell-shaped.[140] Despite the shorter half-life, long-R^3-IGF-I showed prolonged hypoglycemic action than native IGF-I in pigs and marmoset monkeys,[139] due to its dramatically reduced affinities for the IGFBPs in plasma.[139, 165] Long-R^3-IGF-I may be a more potent growth and survival factor *in vivo*, resembling other analogs such as Des(1-3)IGF-I, R^3-IGF-I, long-IGF-I with deletions, substitutions, or insertion at the N-terminal end[136, 138, 139, 162, 166] exhibiting superior potent but decreased IGFBPs affinity.

Taken together, the complexity generated by the *Igf1* gene splicing, posttranscriptional regulation, and posttranslational modification, leading to multiple IGF-I isoforms, probably indicate the distinguishing roles and bioactivity of the various IGF-I isoforms in the aspects of physiological conditions and disease.

1.2 IGF-I actions and signaling

IGFs exerts the biological actions through binding to their receptors including the type I (IGF-IR) and type II (IGF-IIR) IGF receptor, the insulin receptor (IR), and some atypical receptors such as the hybrid IGF-IR/IR.[131-133] Nevertheless, the cellular responses to IGFs are predominantly mediated by the tyrosine kinase activity[3, 167] of IGF-IR which binds with higher affinity to IGF-I than IGF-II, insulin. IGF-I has been indicated to stimulate myoblast proliferation through mitogen-activated protein (MAP) kinase signaling and, subsequently, to promote myogenic differentiation via phosphatidylinositol 3 kinase (PI3K) activation.[168-170] The PI3K signaling is also involved in the regulation of protein turnover, alteration in intracellular calcium as well as in the cell survival process (**Figure 2**). Later evidence implied calcineurin and the calcium-calmodulin-dependent protein kinase (CamK) in skeletal muscle cell differentiation.[168]

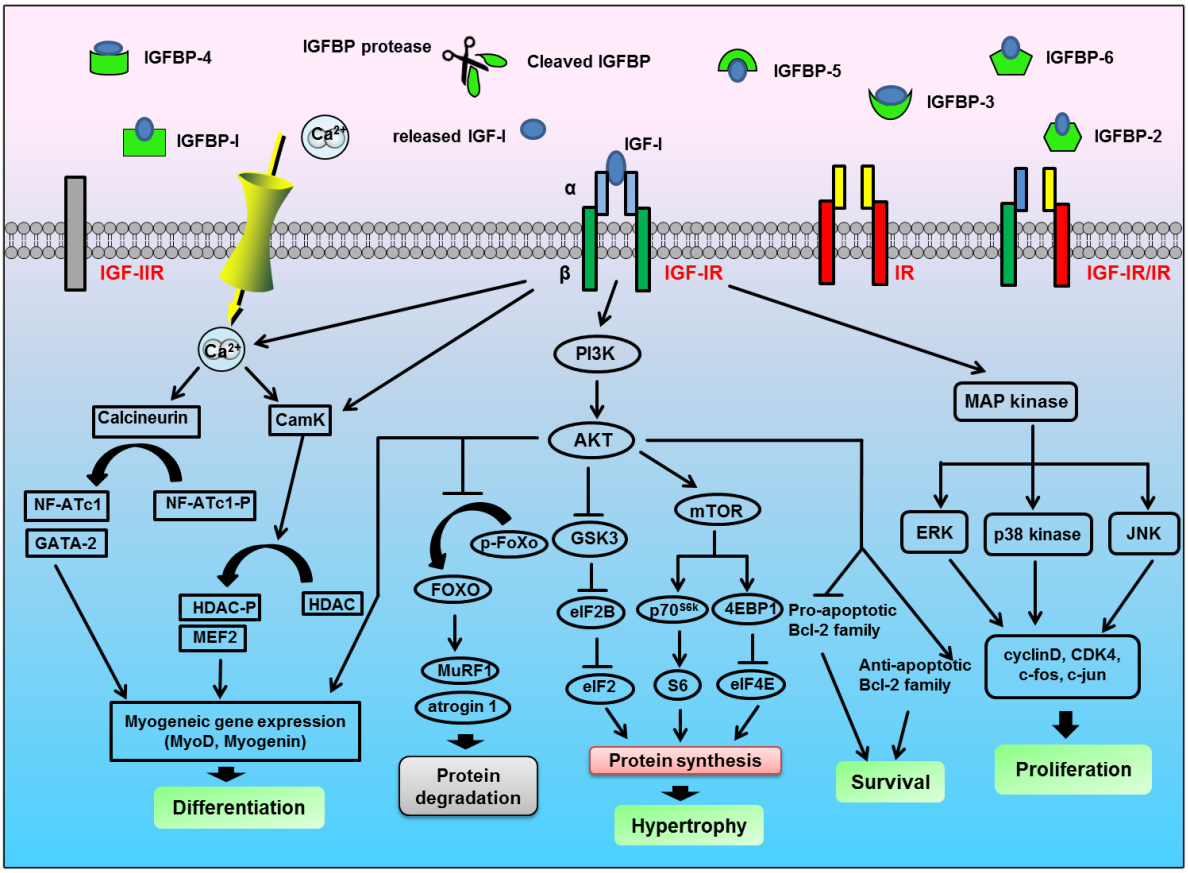

Figure 2. Signal transduction pathways activated by IGF-I, triggering diverse cellular responses including cell proliferation, differentiation, protein synthesis as well as survival.

The binding of mature IGF-I to IGF-IR triggers receptor phosphorylation, which in turn recruits members of insulin receptor substrate (IRS) family (IRS 1–4) to directly to their PTB and SH2 domains, and indirectly to the growth receptor binding protein -2 (Grb2) and the p85 subunit of PI3K through specific motifs in the IRSs.[171-173] IRS-1 acts as a mediator and docking protein for some downstream signaling molecular including PI3K. PI3K activation results in the generation of inositol triphosphate and subsequent activation of AKT kinase. AKT can mediate cell differentiation by positively regulating the expression of terminal muscle differentiation markers, such as p21, MyoD, myocyte enhancer factor 2 (MEF2) and myogenin.[168] Direct and indirect targets downstream of AKT including mammalian target of Rapamycin (mTOR) and glycogen synthase kinase 3 (GSK3) cascade involved in translation and protein synthesis[174-176] as well as skeletal muscle hypertrophy.[169, 170] In addition to the classical PI3K/AKT kinase cascade, the CamK pathway has been shown to induce myogenesis via association of MEF2 myogenic transcriptional factor with histone deacetylases (HDACs).[177, 178] Cam-dependent phosphatase, calcineurin, plays a role in early skeletal muscle cell differentiation by regulating the expression of transcription factors MEF2, MyoD, and myogenin.[179] L6MLC/IGF-I hypertrophic myocytes dephosphorylated NFATc1 and induced expression of GATA-2 transcription factor, a marker of skeletal muscle

hypertrophy.[180] It is a matter of debate whether calcineurin also involved promoting skeletal muscle hypertrophy.

Some findings showed that overexpressed activated calcineurin was sufficient to induce the slow fiber gene regulatory program[181, 182] and cyclosporine A (a calcineurin inhibitor) can block hypertrophy of cultured skeletal myocytes.[180] However, transgenic mice constitutive expression of calcineurin in skeletal muscle did not result in hypertrophy,[182, 183] consistent with the absence of calcineurin up-regulation in hypertrophying muscle.[169] Also, both global- and muscle-specific calcineurin deficient mice showed no defects in muscle growth in response to IGF-I stimulation or mechanical overload, but this study suggested roles of calcineurin in myogenesis and fiber-type switching.[184]

The PI3K-AKT pathway also involves in cell survival by the inhibition of pro-apoptotic Bcl-2 family (Bax, Bad) and Caspase 9, and the activation of the anti-apoptotic Bcl-2 family (Bcl-2, Bcl-X) (**Figure 2**). AKT can regulate phosphorylation of FOXO protein, a subgroup of the transcription factor forkhead box. Activation of AKT also represses FOXO and downregulates expression of the E3 ubiquitin ligases Muscle Atrophy F-box (MAFbx), Muscle Ring Finger1 (MuRF1) and atrogin-1, which are responsible for muscle degradation.[6, 185] Another important IGF-I – activated signaling pathway is linked to the proliferative response by the stimulation of a family of MAP kinase cascade, besides ERK 1/2, including Jun kinase (JNK)-1 and -2 and p38 MAP kinase.

1.3 IGF binding proteins

Upon synthesis by various cell types and release into the interstitial fluid, IGF-I circulates in the blood at relatively high concentrations (150–400 ng/mL).[186] Most of IGF-I in blood and tissues is bound to six high-affinity IGF binding proteins[3] (IGFBPs, IGFBP-1 to -6) (**Figure 2**) with nanomolar affinities.[187-190] In human circulation, IGFBP-3 is the most abundant IGFBPs and has the highest affinity for IGF-I, accounting for 75–80% of the total carrying capacity. The IGF-I–IGFBP-3 binary complex can bind to a third protein – acid-labile subunit (ALS).[191, 192] IGFBP-5 could also form the ternary complex with IGF-I and ALS but in considerably less abundant proportion.[193, 194] The remaining bound IGF-I is believed to carried in binary complexed (without ALS) with each of the six IGFBPs. These complexes greatly extended the half-life of free IGF-I from several min to 20–30 min for the binary complex, even to 16–24 h for the ternary complexes (**Figure 3**).[21, 176, 179]

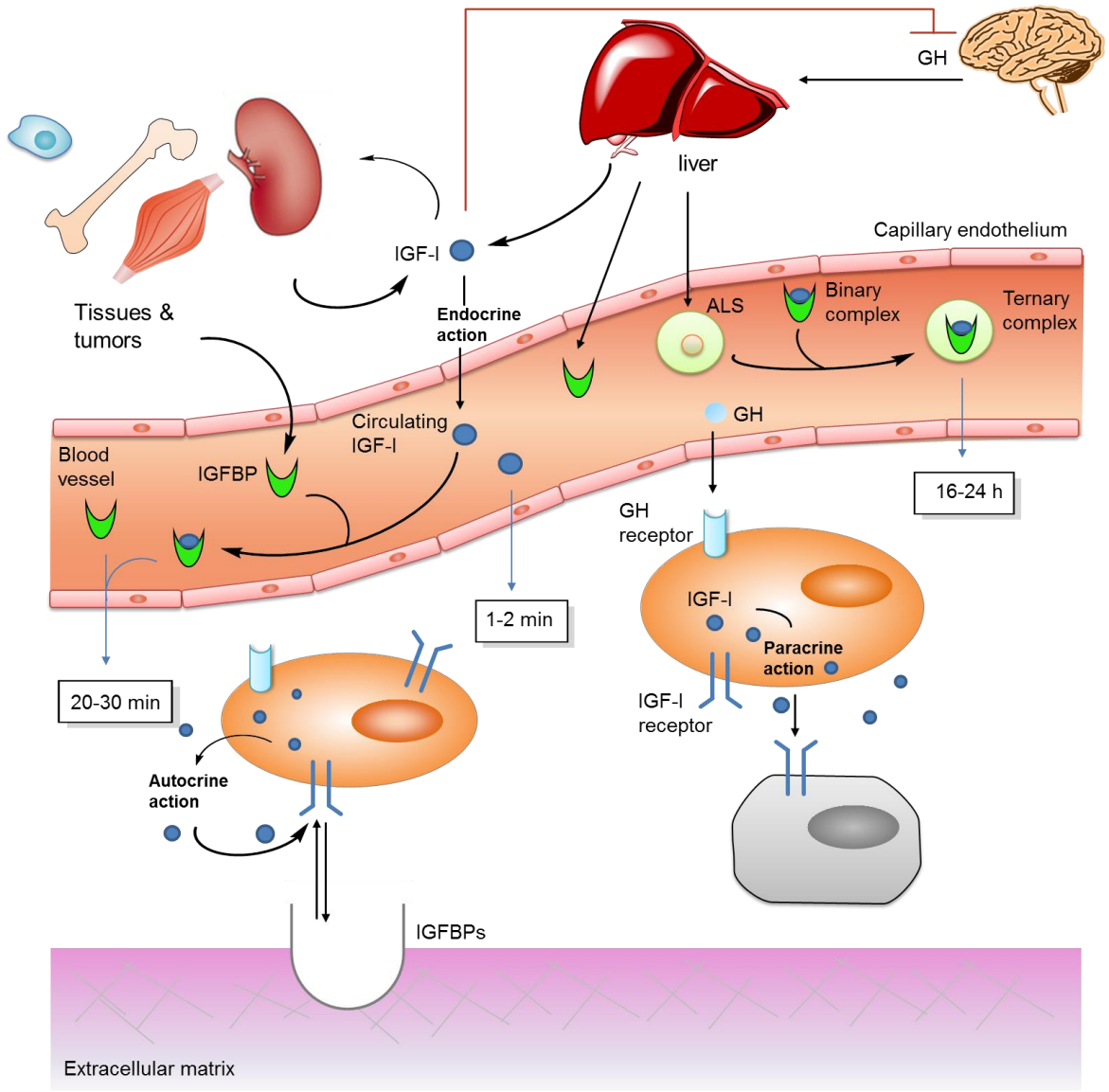

Figure 3. IGF-I can act both systemically as a hormone and locally in the autocrine/paracrine fashion.[201, 206-212] Although liver-derived IGF-I contributes to the main circulating source of IGF-I, many tissues, including the brain, muscle, and bone, produce IGF-I for the autocrine/paracrine mode of action.[17-19, 174-178] IGF-I can enter the bloodstream, forming binary complexes with each of the six high-affinity binding proteins (IGFBPs). A binary complex containing IGFBP-3 or IGFBP-5 can associate with ALS to obtain ternary complexes. The circulating half-lives of free IGF-I, binary complex, as well as IGFBPs and ternary complexes, are marked. Further, locally produced IGF-I can bind to IGFBPs (e.g., IGFBP-5) localized in the extracellular matrix as a reservoir of IGF-I.

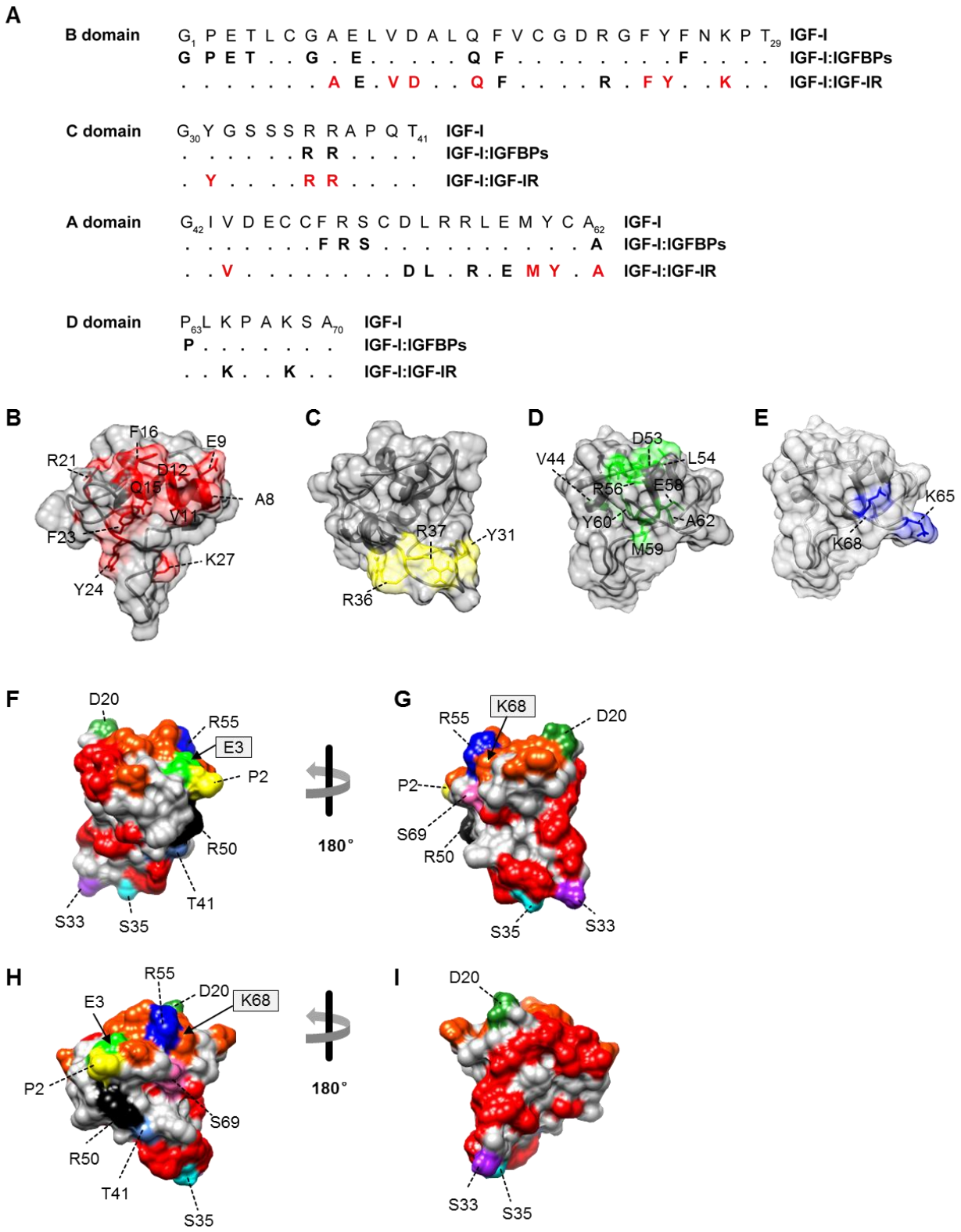

Figure 4. (A) Summary of essential amino acid residues of IGF-I for IGFBPs and receptor interaction.[1, 213, 214] The site 1 (primary ligand-receptor binding site)-engaging residues of IGF-I are highlighted in red, site 2 (secondary ligand-receptor binding site)-engaging residues of IGF-I are marked in black. The surface representations (B–E) of IGF-I are shown in four orientations. The essential amino acid residues of IGF-I for receptor association are highlighted for the (B) B domain (red), (C) C domain (yellow), (D) A domain

(green), and (E) D domain (blue). (F–I) from different orientations showed the site 1-engaging residues (red), site 2-engaging residues of IGF-I (orange-red), and potential alternative sites for modification. E3 was selected as a replacement site for uAA in this thesis, and modification site K68 was often reported in the literature.[90, 159, 160, 215-217] Potential alternative sites (P2, D20, S33, S35, T41, R50, R55, and S69) for E3 were annotated. The IGF-I structure (PDB ID: 2GF1) was used to build this diagram by UCSF Chimera (version 1.13.1rc).

IGF-I bind to IGFBPs with ~ 10-fold stronger affinity than its binding to the IGF receptor,[195] therefore regulating the local availability of IGF-I.[1, 2] The active release of IGF-I in response to the enzymatic degradation of IGFBPs through specific proteases expressed by host cells entails that IGFBPs govern the availability of the growth factor in response to cellular signals.[186] Some IGFBPs (IGFBP-2, -3, and -5), containing the von Willebrand factor, can bind to ECM components (e.g., collagen I, fibronectin, or heparin sulfate),[196] for example, IGFBP-3 is expressed in articular cartilage in which it can specifically bind to fibronectin.[197] Evidence also showed that IGF-I could interact with IGFBP-3/fibronectin complex in the circulation,[198] suggesting the possible role of IGFBP-3/fibronectin in the sequestration of IGF-I in the interstitial ECM. The enhancing effects of IGFBP-5 were shown to involve association of IGFBP-5 to ECM molecules, which lowers its affinity for IGF-I about 8-fold, allowing IGF-I to better equilibrate with its receptors.[199] No apparent change in IGFBP-2 affinity for IGF with matrix association was observed.[200] The described natural concept shed light on potential roles of the location of IGFBPs in the ECM in the control of local IGF-I bioavailability and activity.[186]

In summary, IGFBPs can both inhibit IGF-induced functions by binding to IGFs and preventing the binding of IGFs to its receptors and stimulate the effects of IGF-I (see review in [201]) by maintaining a “reservoir” of biologically “inactive” IGF-I and enhancing delivery of IGF-I to its receptor on the cell surface.[1-3] Alternatively, IGF-I, six soluble IGFBPs, and IGF receptors act together to fine control a variety of important biological outcomes including cell proliferation, differentiation, anti-apoptosis, and survival (**Figure 2**).[3, 123-130] These cellular activities are linked with a role in tissue formation and remodeling, musculoskeletal growth, brain development and energy metabolism, which all ultimately have an influence on body size and longevity. Dysregulation of the IGF system involves several pathophysiology processes including cancers.[88, 202, 203] To manipulate the IGF system for the treatment of certain disorders, it is of particular interest to understand the complex molecular interactions of IGF-I and its binding proteins as well as its receptors.

The three-dimensional structure of IGF-I is well defined, but not for IGFBPs. IGFBP-1 to -6 are approximately 30 kDa proteins that share a common domain organization consisting of cysteine-rich N- and C-terminal domains that are connected by a cysteine-poor flexible linker segment. IGF-binding sites are located on both N- and C-terminal fragments of IGFBPs, which are mostly conserved. Further, IGFBP-6 C-terminal fragments perturb a large number of residues on the IGF-

II surface and may interfere with IGF binding to the IGF-IR, providing a structural basis for the inhibitory potency of intact IGFBPs on IGF actions.[204] IGF-I residues involved in binding IGFBPs, as well as receptors, have been identified using a range of approaches, including amino acid mutations, deletions, and residue or domain swapping with insulin (see review in[1, 205]).

Replacing the IGF-I B domain for the respective insulin B domain endowed IGFBP binding ability on insulin,[218] and exchange of B domain of IGF-I with insulin B domain reduced serum IGFBP binding.[219] Grafting the IGF-I C domain into the insulin molecule increases the affinity of insulin for IGF-IR to 19–28% of that of IGF-I.[220] By site-directed mutagenesis and deletion analyses, Glu3 of IGF-I was shown to involve in the IGFBP interaction[221] but not crucial for IGF-IR binding (**Figure 4**). Gln15 and Phe16 residues in IGF-I B domain are also crucial for peptide association with binding proteins, together with Glu3 and Thr4 to the corresponding insulin residues, leading to dramatically lower binding to serum IGFBP by up to 600 fold.[219] Residues Ala8, Val11, Phe23 and Tyr24 of the IGF-I B domain have been shown to be essential for IGF-IR binding(**Figure 4**).[1] Alanine-scanning mutagenesis of the entire IGF-I molecule determined B domain residues Gly7, Leu10 and Phe25 association with IGFBP-1 interaction.[188] Further, mutation of Glu3 and Phe49 to Ala reduced binding to IGFBP-1 by 34- and 100-fold, but had a negligible effect on IGFBP-3 binding. Alanine substitution of Arg21 caused a 3-fold decrease in IGF-IR binding. This residue locates on the opposite side of the IGF-IR binding surface comprising residues Ala8, Val11, Phe23 and Tyr24, may be part of a second binding surface. Sequential deletions of the N-terminus of IGF-I revealed that removal of residues up to Thr4 increased potency, which was not attenuated by the reduced affinity to binding proteins.[221] Literature-derived data[1, 213, 214] regarding the effect of mutations on IGF-I binding to IGF-IR or IGFBPs are summarized in **Figure 4.**

1.4 IGF-I decoration

As mentioned above, the half-life and tissue distribution of potent IGF-I is strictly controlled by a suite of six IGFBPs in Nature. However, the translation of IGF-I into clinical applications is limited due to its short biological half-life, instability in the circulation, and several systemic side effects (vide supra). Sophisticated biomimetic strategies emerged with the ultimate aim of maximizing pharmaceutical performances of this protein *in vivo* and controlling pharmacokinetics (see review in [222]). Protein immobilization techniques, including physical adsorption, affinity interaction, encapsulation/immobilization as well as covalent immobilization of growth factors, combined with biomaterial matrix mimic the natural healing cascade during tissue regeneration by sustained localized growth factor delivery and effectivity (see review in [223]). Taking inspiration from the natural interactions between ECM and heparin-binding growth factors, bioengineers have decorated IGF-I with a heparin-binding motif (HB–IGF-I) to sequester its binding affinity to endogenous heparin sulfate and glycosaminoglycan in cartilage explants. Local delivery of HB–

IGF-I variant has shown selective retention in proteoglycan-rich environments without compromise of bioactivity.[224] Further, covalent immobilization of growth factors addresses many of the challenges associated with delivering freely-diffusible growth factors and shows a promise in achieving sustained localized growth factor presentation (reviewed in [225]). In addition, the IGF-I decoration generate effective systemic administration targeting, expanding the choice for optimized deployment of growth factor therapy, including PEGylated IGF-I (IGF-I attached to PEG),[90, 159-161, 215, 226] and fusion proteins such as Fc fusion proteins,[227, 228] fusion to human serum albumin (HSA),[229] naturally occurring pro-IGF-I protein (IGF-I plus E-peptides),[230] and other polypeptide fusion approaches[148, 231] (e.g. IGF-I–hGH[228]).

Traditional amine-targeting strategies, including *N*-hydroxysuccinimide (NHS)-chemistry, rely upon the accessibility of the 4 amino groups presented in the IGF-I, ending up with random heterogeneous pharmaceutical products (reviewed in [232], **Figure 5A**). This may impact its activity and increase the immunological risks. Site-specific PEGylation of IGF-I (PEG–IGF- I)[90, 226] was generated by the mutation of Lys27 and Lys65 to Arg and adding $PEG_{40\ kDa}$ to Lys68. Arg substitution of Lys65 or Lys68 inhibited MCF-7 breast cancer cells migration, and this modification dramatically reduced IGF-IR phosphorylation (**Figure 4E**) and AKT activation[233]. Analogously, PEG–IGF-I showed a decreased affinity for IGF-IR and IGFBPs binding but maintaining sustained anabolic activity *in vitro*. Desirable effects of PEG–IGF-I form *in vivo* included extended half-life, decreased renal clearance and providing sustained levels of IGF-I to the periphery and brain.[90, 160, 215] Besides NHS-PEGylation, transglutaminase-catalyzed crosslinking proofed instrumental for site-specifically PEGylated IGF-I due to its high selectivity and mild reaction conditions.[217] Transglutaminases (TGases) induce the formation of a ε-(γ-glutamyl) -lysine isopeptide bond by catalyzing an acyl-transfer reaction.[234] Excitingly, Lys68 of IGF-I is the very substrate for FXIIIa transglutaminase.[233] IGF-I was enzymatically conjugated with PEG_{30kDa} and had protease-sensitive peptide linker (PSL) insert to enable inflammation-mediated IGF-I release. Consistent with the previous observations,[161, 233] PEGylation impaired the biological activity and endocytosis of IGF-I, while the potency was later rescued by the bioresponsive release of IGF-I from PEG molecular trigged by the upregulation of proteases.[217]

Although PEG has been FDA-approved as generally recognized as safe (GRAS) molecule, some reports linked PEGs to vacuolization of renal cortical tubular epithelium cells[235] and immunological risks,[236-238] steering the need for alternative compound[239] (ideally nature-derived materials). IGF-I was covalently immobilized to fibrin matrices during normal thrombin/factor XIIIa-mediated polymerization via an incorporated α_2-plasmin inhibitor-derived peptide sequence ($\alpha_2PI_{1–8}$). The variant, α_2PI_{1-8}–IGF-I, was created by the recombinant fusion of 8-residue sequence (NQEQVSPL) at N-terminus of IGF-I and showed equivalent bioactivity compared to wild-type IGF-I. Incorporation of $\alpha_2PI_{1–8}$–IGF-I within 3D fibrin matrices demonstrated more robust proliferative

response in smooth muscle cells compared to wild-type IGF-I. Sustained local IGF-I availability at bladder lesion sites *in vivo* enhanced smooth muscle regeneration.[148] Bioinspired from the endogenous release profiles of growth factors triggered by local enzymatic activity during ECM degradation, this group developed multi-layered sandwich scaffold comprising of a bioactive fibrin layer laminated decorated with an engineered IGF-I variant between two collagen sheets. The cell-mediated IGF-I release was achieved by integration of a matrix metalloproteinases-cleavage linker between α_2PI_{1-8} and IGF-I. In a rat bladder model, the IGF-I loaded bioactive collagen-fibrin hybrid scaffolds resulted in host smooth muscle cell invasion in a dose-dependent fashion and smooth muscle bundle formation with re-urothelialization 28 days after surgery.[231] Apart from fibrin, other ECM proteins including fibronectin and collagen II, are natural transglutaminase substrates, allowing site-directed coupling of modified biologics by enzymatic introduction accordingly bypass the biomaterial modification.[240] In the examples of fibrin-bound therapeutic proteins, biologics are released dependent on the matrix degradation rate by the action of cell-associated proteases (e.g., matrix metalloproteinases, plasmin).

Peptide-Fc fusion proteins have been developed for improving the pharmacokinetics of peptides, as chimeric proteins generated by genetically linking an active peptide with the Fc-domain of immunoglobulin G (IgG). The plasma half-life of the peptide is dramatically extended, as Fc portion binds the neonatal Fc receptor (FcRn) in the endosome in a pH-dependent manner, allowing FcRn-bound proteins to be targeted back to the cell surface for recycling back into the circulation resulting in delayed lysosomal degradation,[214, 223] while non-FcRn-bound proteins are degraded by lysosome. Engineered IGF-I–Fc chimera (Fc fragments was endowed at C-terminus of IGF-I) dramatically prolonged the plasma half-life of IGF-I and was cleaved at Lys65 or Lys68 in serum after three days. With mutations of Lys65 and Lys68 to alanine or glycine, such variant showed greater stability and half-life than corresponding constructs with the lysine at position 65 or 68 of the IGF-I fusion polypeptide. IGF-I–Fc or IGF-I–hGH (with hGH as the fusion partner) was active, whereas Fc-tag or hGH protein fused at the N-terminus of IGF-I was found little or no activity in the aspects of IGF-IR phosphorylation and AKT activation or Stat5 phosphorylation. IGF-I–Fc protein showed improved ability to increase muscle mass in SCID mice suffering from muscle atrophy caused by an atrophy-causing agent and was also effective in decreasing blood glucose.[228] At present, there are eleven FDA-approved Fc-fusion proteins. Moreover, many novel Fc-fusion proteins are at different stages of pre-clinical and clinical development. Aside from Fc fragments, IGF-I was fused to long-circulating serum protein HSA and showed high-yield expression (100 mg/L) in CHO cells. The fusion protein demonstrated its ability on NIH3T3 cells proliferation, IGF-IR binding and activation *in vitro*.[229] Apart from acting as a fusion partner, albumin has been extensively used as an excipient to stabilize pharmaceutical proteins.[196]

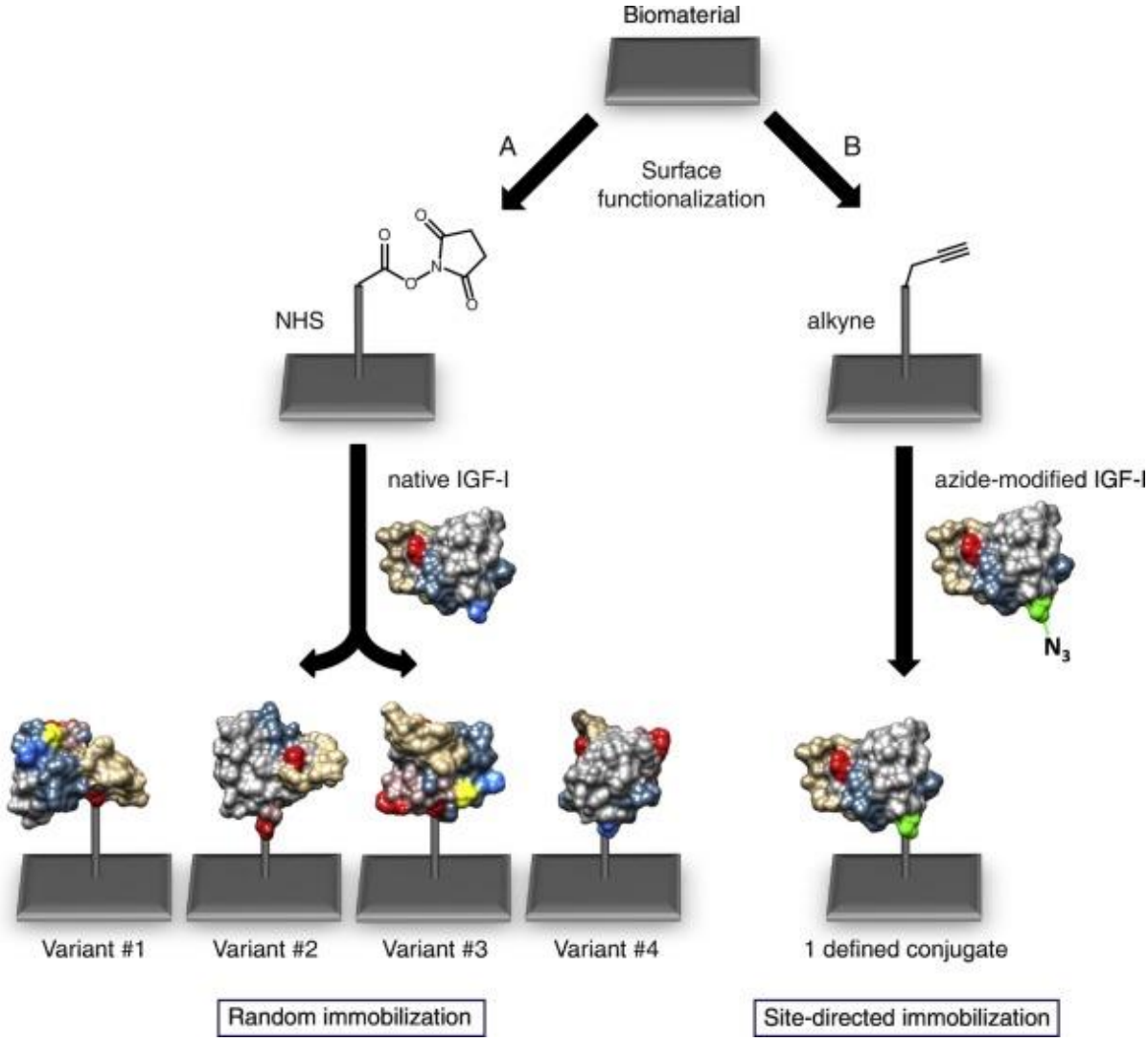

Figure 5. Schematic illustration of random immobilization (A) and site-directed immobilization (B) of IGF-I onto a biomaterial. Reprinted from Ref.[232]. Copyright (2018), with permission from Elsevier.

Naturally occurring E-peptides (Ea, Eb & Ec) with modulated properties for IGF-I *in vivo* (vide supra) provides insights into the translation of advanced IGF-I variants for therapeutic application. IGF-I Ea, IGF-I Eb, and IGF-I Ec demonstrated their ability on cell proliferation, migration and differentiation (**Table 1**). E-peptide prolonged IGF-I variants increased the size of IGF-I and were shown to stabilize IGF-I in serum especially with deletion of the dibasic protease cleavage site at position 71 and 72 (Arg–Ser),[230] suggesting its potential applications for systemic administration. IGF-I was successfully engineered with an Ea-peptide extension in *Escherichia coli* (*E. coli*).[222] The introduction of functionalized unnatural amino acids (uAAs) such as pyrrolysine (Pyl) derived analogs at a predefined site within the protein backbone, via orthogonal translation based on a pyrrolysine tRNA synthetase (PylRS)/tRNAPyl CUA pair from arche bacteria (e.g., *Methanosarcina barkeri*[241-245]), offers an elegant approach for site-specific decoration (**Figure 5B**, see below for further information).[239, 241]

1.5 Translation of bio-inspired systems into the pharmaceutical design scheme

Functional immobilization strategy

As highlighted above, growth factors like the IGF-I signal protein are essential in regulating processes involved in cell proliferation, differentiation, and tissue regeneration, and are therefore considered as significant building blocks in many tissue engineering strategies. Clinical use of growth factors is complicated by problems of delivery, retention, orientation, or desorption rate.[246] One way of addressing these challenges is by covalent immobilization of growth factors to biomaterial matrices to improve the stability and persistence of therapeutics delivered into cells or tissues.[225] Immobilization strategies may provide extended localized activity through spatial control and reduced protein quantities required for paracrine action. Also, the presentation of growth factors in an immobilized form is also found in the physiological environment, as exemplified by the growth factor storage in the ECM, such as affinity binding of FGFs to sulfated glycosaminoglycans, and binding of IGF-I to the ECM protein through IGFBPs.[196]

Conventional chemical decoration approaches to modify therapeutic proteins are limited to the *N*-terminal amino group, the *C*-terminal carboxylic acid, the ε-amino group of lysine or thiol-groups like cysteine. However, multiple accessible lysine and cysteine within a protein challenge selective modification and frequently lead to heterogeneous pharmaceutical products. Additionally, the lack of selectivity modification can impair the biological activity of proteins and possibly increase the immunogenicity.[247] In contrast, deploying an expanded genetic code allows the site-specific introduction of uAAs (particularly interesting in clickable uAAs) into proteins in live biological systems, thereby enabling novel functionalities selectively incorporated into the interest of proteins for engineering novel biological properties (as illustrated in **Figure 5B**). One major advantage of such labeling is site-specific decoration with single residue precision at any position in a protein. An orthogonal aminoacyl tRNA synthetase (RS) /tRNA pair is employed to decode a unique codon (e.g., amber stop codon UAG (often), ochre stop codon UAA, opal stop codon UGA, quadruplet codon) as the desired unnatural amino acid. One or more UAG codons can be introduced in the coding gene of a target protein and a UAA or UGA codon is adopted as a “real” stop codon. Meanwhile, the anticodon of an orthogonal tRNA is mutated to CUA to recognize the in-frame UAG codon. In principle, the UAG codon should not be decoded by any cellular components in the absence of a charged amber suppressor tRNA, and with the formation of truncated proteins instead. The full-length protein can only be expressed by reading-through amber codon as a sense codon in the presence of an aminoacylated suppressor tRNA. Further, multiple tRNA/RS pairs target existing distinct nonsense codons that allow for the incorporation of distinct uAAs for the subsequent coupling reactions.

Examples for bioorthogonal click chemistry are engaged in reactive side chain of uAAs, like aliphatic alkynes reacting with azides via classic copper (I)-catalyzed azide-alkyne cycloaddition (CuAAC), ketone with hydroxylamine via oxime ligation reactions, strained alkynes with azides via cooper-free strain-promoted azide-alkyne cycloaddition (SPAAC) and strained alkynes or alkenes with tetrazines via inverse-electron-demand Diels–Alder cycloaddition.[248, 249] The reaction of an alkyne with azide-containing probes through CuAAC reaction has been widely used for the *in vitro* labeling of biomolecules. Propargyl-L-lysine (Plk) has been genetically incorporated into proteins in *E. coli* using an orthogonal PylRS/tRNAPyl CUA pair, and proteins were modified selectively with azide-containing probes by CuAAC chemistry.[239, 250-253] Furthermore, the promiscuity of PylRS/tRNAPyl CUA pair allows to incorporate (S)-2-amino-6-(((2-azidoethoxy)carbonyl)amino)hexanoic acid into proteins in *E. coli*.[254] Purified azide-modified proteins can be labeled *in vitro* with fluorescent dye or polymer in SPAAC or CuAAC reaction. Together, cellular incorporation of uAAs enables site-specific single- or dual- even multiple-labeling of recombinant proteins with other molecular, such as small entities, proteins,[251] polymer, surface,[250, 251, 253] to improve pharmacokinetic properties and protein stabilities, and to visualize in living biological systems as well as to generate homogeneous therapeutic conjugates.

Besides chemical conjugation strategies, TGase-mediated acyl transfer reaction provides an advantageous option of covalent polymer attachment for proteins due to its high selectivity and mild reaction conditions. It is particularly attractive for proteins without multiple TGase-reactive glutamines or lysines,[255-258] as shown here for IGF-I. As highlighted in **section 1.4 IGF-I decoration**, the TGase-catalyzed reaction between specific glutamine in the PEG_{30kDa}–PSL molecule and lysine residue within the IGF-I substrate leads to a homogeneous outcome.[217] Factor XIIIa (FXIII)—a plasma transglutaminase—is responsible for cross-linking fibrin monomers and plays a crucial role in the stabilization and fibrinolysis of the provisional ECM during wound healing.[234, 259] Applications of conjugation by FXIIIa were presented in the incorporation of exogenous peptides into fibrin gels,[260] the controllable cross-linking in biological or synthetic hydrogels, surface functionalization[261, 262] and site-specific protein PEGylation.[217]

Sites for modification

Tremendous efforts of related work were based on commercially available mature IGF-I which may limit the decoration strategy to its unique proteinogenic amino acid (e.g., NHS-chemistry on the lysine, **Figure 5A**). In this thesis, we focused on the expansion of decoration strategies of potent IGF-I through the genetic incorporation of novel functionalities to enable flexible chemo- and site-selective protein modification. The first step was to identify IGF-I positions that serve as appropriate anchor sites and fulfill the following criteria: (i) replacement by the uAA does not affect protein folding and stability; (ii) the mutation does not influence protein function (or protein-

receptor association); (iii) the insertion site presenting the uAA is sterically favored for chemical immobilization (e.g., surface-exposed residues).

As elaborated in **section 1.16 & section 1.3**, the N-terminal residues (Gly1, Pro2, and Glu3) of the B domain in the IGF-I molecule are suitable sites for modification, as exemplified by the retained potency of a naturally truncated variant Des(1-3)IGF-I[1, 269] and unaltered IGF-IR binding affinity of such IGF-I variants with deletion or mutations.[230] C domain of IGF-I (residues 30–41, **Figure 4C**) was found to be essential for its function.[263, 264] Double mutation of Arg36–Arg37 into Ala36–Ala37 severely reduced binding of this mutant to IGF-IR[265] and IGFBP-1.[189] The existence of overlapping binding surfaces explains the competition between IGF-IR and IGFBPs binding to IGF-I. Further, a double replacement of Arg36–Arg37 to Glu36–Glu37 suggested a partial antagonism of IGF-IR, i.e., the analog demonstrated an impaired intracellular signaling[266] and suppressed tumorigenesis[267] albeit still bound to IGF-IR. Mutation of Val44 of B domain of IGF-I to Met causes dwarfism,[268] and mutation to Leu at the homologous Val of A3 position in insulin Wakayama causes diabetes,[269] with reduced affinity of both mutants for their cognate receptor to less than 1%.

In comparison with insulin's structure, the superfluous D domain and non-homologous C domain in IGF-I have been reported to participate in determining binding specificity for the IGF-I receptor. In particular, positively charged side chains in C and D domains of IGF-I contribute to the binding preference of the IGF-IR towards IGF-I,[265] with a 10-fold decrease in IGF-IR affinity for Lys65Ala/Lys68Ala variant. A contrasting finding showed that deletion of the D domain had a negligible effect.[263] NMR spectroscopy studies showed most residues in the D domain (Pro63, Lys65, Pro66, & Lys68–Ala70) to participate in IGFBP-1 binding,[189] which contributes to mediate IGF-I bioavailability. Contacts between IGF-I and the primary ligand-binding site (site 1) elements on the L1-CR-L2 domains of the IGF-IR was computability docked,[214, 270] with site 1 engaging residues of IGF-I are localized on the B, C and A domains of IGF-I (e.g., Phe23, Tyr24, Tyr31, Arg36, Arg37, Val44, Tyr60, and Ala62),[270] and do not include Lys68 (**Figure 4**). PEGylation at this site is likely to sterically hinder both receptor interaction and closing of the receptor dimer through the secondary binding site (site 2). Both of these effects most likely explain why PEGylated IGF-I had reduced *in vitro* affinity for IGF-I & insulin.[90] Recent molecular dynamic studies of an atomic structural model for complexes of IGF-I: IGF-IR ectodomain further support the engagement of Lys68 in site 2 receptor binding, suggesting partial contacts for Lys68 (IGF-I) with Lys306 in site 2 of the IGF-IR.[213]

Some site 2 substitutions in the case of insulin binding to IR can reduce the association rate of ^{125}I-labeled insulin up to 20-fold and slow down the dissociation rate, in which the prototype is hagfish insulin (a natural insulin variant).[271] Also, the slow on-rate association impact fast response of such

insulin analogues thereby leading to a low metabolic potency, while the increased residence time on the receptor enhances growth-promoting signaling, together contributing to improved mitogenic and metabolic potency ratio of hagfish insulin (3.8) [271] that is consistent with that of other insulins modified in the site 2.[272, 273] Given the fact that IGF-I bound to IGF-IR in a fashion effectively identical to that seen in IR binding mechanism,[270, 274] it is reasonable to extrapolate the consequences of impaired site 2 interaction to PEG–IGF-I. Indeed, PEGylated IGF-I (at site Lys68) demonstrated lower potency than wild-type IGF-I driven by rapid receptor binding, while longer incubation decreased their differences.[90] The other design takes advantage of the impaired receptor affinity of PEGylated IGF-I (at site Lys68), e.g., the placement of PCL between the IGF-I and PEG molecule, IGF-I activity was recovered after the cleavage of PCL as triggered by the upregulation of matrix metalloproteinases.[217]

Like the above-mentioned large PEG molecule (at site Lys68 of IGF-I), C-terminal E-peptide extension faces away from the site 1 binding area, suggesting the retained E-peptide in IGF-I might have no significant effect on IGF-IR binding. Indeed, naturally occurring pro-IGF-I (IGF-I+E-peptide) does not seem to impede receptor phosphorylation, and shows equivalent IGF-IR phosphorylation than mature IGF-I.[275] Little is known about the structures of pro-IGF-I and its interaction with receptors. Intriguingly, E-peptides are thought to enhance IGF-I storage by the interaction with the ECM components, to modulate IGF-I action by increasing the cell entry of IGF-I from media, and to act independently (see **section 1.1**). Also, recombinantly expressed E-peptide prolonged IGF-I variants (devoid of the dibasic protease cleavage site Arg71–Ser72) were shown to stabilize IGF-I in serum due to improved IGFBPs interaction with unaltered therapeutic activity.[230] In this respect, we engineered a novel IGF-I therapeutic with a 33-residue Ea peptide prolongation at its C-terminus (IGF-I Ea) for the incorporation of uAA. The improper folding of IGF-I or IGF-I Ea in *E. coli* causes protein aggregation, thus uAA incorporated or wild-type IGF-I (without Ea extension) was also expressed in forms of N-terminally fused to thioredoxin to improve the expression and solubility of IGF-I protein in *E. coli*[288, 319, 320] (as elaborated in **Results, Discussion section**).

Based on literature-derived data and modeled molecular structure of IGF-I, a hydrophilic (and surface-exposed) Glu at position 3 at the N-terminus, which did not engage the IGF-IR association and was ease of genetic manipulation & downstream purification, formed an attractive replacement site for uAA.

Beyond Glu3 of IGF-I, other residues fulfilling the required specifications can be used as alternative sites. An alternative site at N-terminus is surface-exposed hydrophobic Pro2 (**Figure 4F, G, and H,** highlighted in yellow). The comparison of IGF-I within various species will provide us information not only on the evolution of the molecule but also on the relationship between IGF-I

structure and activity. Some amino acids were highly conserved during evolution led to the suggestion that this cluster of residues located on the surface of the molecule was involved in receptor binding and biological activity.[276] Amino acid sequence comparison of human and animal IGF-I is presented in **Appendix B**. Based on this information, several less-conservation of hydrophilic residues (Asp20, Asn26, Ser33, Ser34, Ser35, Gln40, Thr41, Arg50, Asp53, Ser69) were rationally selected and further scanned through 3D model of IGF-I, with surface-exposed amino acids (Asp20, Ser33, Ser35, Thr41, Arg50, Ser69) selected as potential alternative sites (**Figure 4F, G, H, I**). Interestingly, none of them are included in the known ligand: IGF-IR binding sites. Asp20 (highlighted in forest green) and Arg50 (marked in black) might be alternative sites for modification. Intriguingly, residue Ser33 is localized closely to IGF-IR-engaging (site-1-engaging) residues of IGF-I. "On-demand activation" of IGF-I can be designed by steric blocking this site with a large molecule to impair its intracellular signaling ("inactivated" state) and by the removal of this molecule to recover IGF-I functions only when needed ("activated" state). Such a profile is also available for other residues (Ser35, Thr41, and Ser69). Cautions should be taken when the mutation site is near the C-terminus (Ser69), as an immediate conundrum is that purification of full-length uAA incorporated protein from the truncated form. Efforts to solve the "truncation problem" have focused upon nontrivial manipulations of the *E. coli* translation system, including genetic deletion of release factor 1 or reassignment of all of the UAG stop codons in the bacterium,[277] which may lead to comprised cell health and lower levels of protein production[278] (as elaborated in **Discussion section**). Intriguingly, surface-exposed conservative residue Arg55 (located on the helix) is not directly involved in stabilizing its cognate receptor binding, albeit spatially closed to Arg56 and Arg21 (which are involved in site 2 engagement). Also, arginine to alanine substituted IGF-I variant at position 55 showed a slower IGFBP-1 association.[189] The conservation of this residue may suggest that it is important for other functions. Arg55–Arg56 was reported to be responsive (in part) for the lower affinity of IGF-I for the type 2 IGF receptor/cation-independent mannose-6-phosphate receptor,[219] a clearance receptor (in the case of IGF-II),[279] suggesting its role in IGF receptor specificity. This insight may make Arg55 an interesting site for modification.

Upon selection of the insertion site (Glu3), we introduced the uAA with clickable functionality (plk) into IGF-I backbone during protein synthesis in *E. coli*. Optimization of uAA incorporation using amber codon suppression includes (i) variation of IGF-I genetic sequence and bacterial strains, (ii) variation of culture parameters (uAA concentration, culture time, IPTG concentration), (iii) downstream purification of the desired product. In combination with CuAAC, plk incorporated IGF-I could be site-specifically coupled to other molecules, including polymer, model carrier, and growth factor. In particular, an attempt has been made to investigate the dual-labeling of IGF-I

either by the introduction of uAA within two distinct positions of the protein of interest or by exploitation of clickable plk-IGF-I Ea with a unique proteinogenic TGase-reactive lysine.

1.6 Aim of the thesis

Overall Aim

To expand the decoration strategies of potent IGF-I through the genetic incorporation of novel functionalities to enable flexible chemo- and site-selective protein modification

Specific Aims

1. Engineered plk-modified IGF-I analog via genetic codon expansion and presented a defined strategy to bio-orthogonally immobilize IGF-I variant to azide presenting agarose particles for spatial controlled cell proliferation. Two strategies were deployed to increase the yield of plk-modified IGF-I analog, including (i) genetically engineered IGF-I variants (Trx-plk-IGF-I) containing an N-terminal His_6[280]-tagged thioredoxin[281] – thrombin cleavage site and a non-natural amino acid, propargyl-protected lysine derivative (plk) incorporated at Glu-3 of IGF-I; (ii) engineered indigenous IGF-I Ea therapeutic (plk-IGF-I Ea) with the exchange of Glu-3 against plk.

2. Dual-functionalized IGF-I variant either by engineered IGF-I Ea variant with two alkyne functionalities or by exploitation of “clickable” plk-IGF-I Ea with TGase-reactivity lysine

3. Bio-responsive co-delivery of FGF2 and IGF-I based on genetic incorporation of clickable unnatural amino acids

2. Materials & Methods

2.1 General materials

DNA manipulation. Standard molecular biology techniques were used throughout.[282] Site-directed mutagenesis and insertion of genes were carried out by polymerase chain reaction (PCR).

Enzyme	Application
EcoRI-HF® (NEB)	G⇓AATT C C TTAA⇑G
BamHI-HF® (NEB)	G⇓GATC C C CTAG⇑G
NdeI (NEB)	CA⇓TA TG GT AT⇑AC
SapI (NEB)	GCTCTTC$(N)_1$⇓ CGAGAAG$(N)_4$⇑
BglII (NEB)	A⇓GATC T T CTAG⇑A
Pfu DNA Polymerase (kindly provided by Dr. Joachim Nickel, Würzburg, Germany)	High fidelity PCR
T4 DNA ligase (NEB)	Joining double-stranded DNA molecules with cohesive or blunt ends
Antarctic phosphatase (NEB)	Preventing re-ligation of linearized DNA vectors by removing phosphate groups from both 5’ termini
GeneRuler 1 Kb plus DNA ladder (Thermo Fisher Scientific)	75–20000 bp reference
dNTPs mix (Thermo Fisher Scientific)	PCR

Bacterial strains.

***Escherichia coli* (*E. coli*) strain**	**Application**	**Description**
DH5α (NEB)	Plasmid amplification	Blue/white color screening with *lac*ZΔM15; high insert stability due to *rec*A1 mutation; high yield and quality of DNA due to *end*A mutation.
BL21 (DE3) (NEB)	Protein expression	Chemically competent *E. coli* cells suitable for transformation and protein expression; T7 Expression Strain; deficient in proteases Lon and OmpT that degrade abnormal and outer membrane proteins, respectively.
SHuffle T7 (NEB)	Protein expression	Chemically competent *E. coli* B cells engineered to form proteins containing disulfide bonds in the cytoplasm; suitable for T7 promoter driven protein expression; enhanced BL21 derivative.
Rosetta 2 (Novagen)	Protein expression	BL21 derivatives designed to enhance the expression of eukaryotic proteins that contribute tRNAs for 7 codons (AUA, AGG, AGA, CGG, CUA, CCC, and GGA) rarely used in *E. col*; bear a chloramphenicol-resistant plasmid pRARE.
Rosetta (DE3) (Novagen)	Protein expression	BL21 derivatives designed to enhance the expression of eukaryotic proteins that contribute tRNAs for 6 codons (AGG, AGA, AUA, CUA, CCC, GGA) rarely used in *E. coli*; bear a chloramphenicol-resistant plasmid pRARE; the host is a lysogen of λDE3, and carries a chromosomal copy of the T7 RNA polymerase gene under control of the *lacUV5* promote; suitable for production of protein from target genes cloned in pET vectors by induction with IPTG.
C321.ΔA. exp (Addgene)	Protein expression	Recoded *E. coli* with all UAG codons and release factor 1 (RF1) removed (UAG termination abolished); decreased mutation rate; 37 °C growth tolerated; contain a zeocin resistance cassette.

Protein expression vectors.

Vector type	Antibiotic Resistance	Promoter	Inductor	Notes
pHisTrx	ampicillin	T7	IPTG	The gene encoding N-terminal His_6-tagged Trx and a thrombin cleavage site[283]
pET-11a	ampicillin	T7	IPTG	lacI gene and the tRNAPyl gene
pRSFDuet-1vector	kanamycine	T7	IPTG	lacI gene and PylRS gene

Culture media & antibiotics. All solutions were prepared in Milli-Q water. Lysogeny broth (LB) medium was used for the growth of DH5α, BL21 (DE3), SHuffle T7, Rosetta 2, Rosetta (DE3), and C321.ΔA.exp strains. Terrific broth (TB) medium was used for recombinant protein expression. SOC Medium was used for DH5α, BL21 (DE3), SHuffle T7, Rosetta 2, Rosetta (DE3), and C321.ΔA.exp strains growth during transformation protocol. All purchased chemicals were used without further purification.

LB broth media (1 L)	10 g Tryptone; 5 g Yeast extract; 5 g NaCl; 5 g $MgSO_4 \cdot 7H_2O$; 1 g Glucose; Add H_2O to 1 L; Sterilize by autoclaving
LB agar media (200 mL)	2 g Tryptone;1 g Yeast extract; 2 g NaCl; 1 g Glucose; 3 g Agar; Adjust the pH to 7.5; Add H_2O to 200 mL
SOC media (1 L)	20 g Tryptone; 5 g Yeast extract; 0.58g NaCl; 0.19g KCl; 0.92g MgCl2; 1.21g MgSO4; 3.6 g glucose; Add H_2O to 1 L
TB broth media (900 mL)	12 g Tryptone; 24 g Yeast extract; 4 mL Glycerine; Add H_2O to 900 mL
LB glycerol media (100 mL)	20 mL Glycerin; 80 mL LB medium; Sterilize by autoclaving
Antibiotics (Working concentration)	❖ 100 µg/mL carbenicillin ❖ 34 µg/mL kanamycin ❖ 34 µg/mL chloramphenicol

Agarose gel electrophoresis buffers.

50x TAE buffer (250 mL)	60.5 g Tris base; 14.3 mL Glacial acetic acid; 7.3 g EDTA; Adjust the pH to 8.5; Add H_2O to 250 mL

1% Agarose/Midori Green/1x TAE gel (70 mL)	0.7 g Tris base; 70 mL of 1x TAE; Heat until the solution is clear; Add 3.5 µL Midori Green after cooling

General buffers.

10x PBS (1 L)	80 g NaCl; 2 g KCl; 6.1 g Na_2HPO_4; 2 g KH_2PO_4; Add H_2O to 1 L
10x TBS (1 L)	18.6 g Tris base; 80 g NaCl; Adjust the pH to 7.6; Add H_2O to 1 L
1x TBST (1 L)	100 mL 10xTBS; 1 mL Tween 20; Add H_2O to 1 L
10x Thrombin cleavage buffer (1 L)	24 g Tris base; 87.7 g NaCl; Add H_2O to 800 mL; Adjust the pH to 8.4; Add H_2O to 1 L

SDS-PAGE gel electrophoresis buffers.

SDS electrophoresis buffer (5x)	15.1 g Tris base; 72 g Glycine; 5g SDS; Add H_2O to 1 L
Reducing SDS sample buffer (6x)	1g SDS; 7 mL 4xTris· Cl/SDS (pH 6.8); 3 mL glycerol; 0.93 g 1,4-Dithiothreitol (DTT); 1.2 mg Bromophenol blue; Add H_2O to 10 mL
Non-reducing SDS sample buffer (6x)	1g SDS; 7 mL 4xTris·Cl/SDS (pH 6.8); 3 mL glycerol; 1.2 mg Bromophenol blue; Add H_2O to 10 mL
Coomassie blue staining (1 L)	1 g Coomassie Brilliant Blue; 500 mL Methanol; 100 mL Glacial acetic acid; Add H_2O to 1 L
Destaining solution (1 L)	200 mL Methanol; 100 mL Glacial acetic acid; Add H_2O to 1 L
4xTris·Cl/SDS (pH 6.8)	6.05 g Tris base; 40 mL H_2O; Adjust to pH 6.8 with HCl; Add H_2O to 100 mL total volume; Filter solution through a 0.45 µm filter; 0.4 g SDS;
4xTris·Cl/SDS (pH 8.8)	91 g Tris base; 300 mL H_2O; Adjust to pH 8.8 with HCl; Add H_2O to 500 mL total volume; Filter solution through a 0.45 µm filter; 2 g SDS

Transfer and blotting buffers for Western Blot.

10x Western Blot buffer (1 L)	30.3 g Tris base; 144 g Glycine; Add H_2O to 1 L
1x Western Blot buffer (1 L)	100 mL of 10x WB buffer; 200 mL Methanol; Add H_2O to 1 L
Blocking solution (100 mL)	10 mL of 10x Roti®-Block; 90 mL 1x TBS

Antibody wash buffer (1 L)	1 L of 1x TBST; 2 mL Tween 20
Ponceau S solution (200 mL)	10 mL Glacial acetic acid; 0.2 g Ponceau S; Add H_2O to 200 mL
Stripping buffer (100 mL)	780 µL β-mercaptoethanol; 6.25 mL of 1M Tris-HCl (pH 6.8); 2 g SDS; Add H_2O to 100 mL

Protein purification buffers.

Histidine tagged recombinant protein purification.

Sonication buffer (100 mL)	100 mL His_6-tag binding buffer (pH 7.5); 1 mL PMSF
His_6-tag binding buffer (1 L)	2.4 g Na_2HPO_4; 0.36 g NaH_2PO_4; 29 g NaCl; 1.4 g Imidazole; Add H_2O to 1 L; pH 7.5; Filter solution through a 0.45 µm filter
His_6-tag elution buffer (1 L)	2.4 g Na_2HPO_4; 0.36 g NaH_2PO_4; 29 g NaCl; 34 g Imidazole; Add H_2O to 1 L; pH 7.5; Filter solution through a 0.45 µm filter

Azide-PCL-FGF2/IGF-FGF protein purification.

Sonication buffer (100 mL)	100 mL Heparin binding buffer (pH 7.4); 200 µL of 0.5 M EDTA; 15.4 mg DTT; 1 mL PMSF
Heparin binding buffer (1 L,)	1.37 g Na_2HPO_4; 0.27 g NaH_2PO_4; 17.53 g NaCl; Add H_2O to 1 L; pH 7.4; Filter solution through a 0.45 µm filter
Heparin elution buffer (1 L)	1.37 g Na_2HPO_4; 0.27 g NaH_2PO_4; 87.81 g NaCl; Add H_2O to 1 L; pH 7.4; Filter solution through a 0.45 µm filter

IGF-I variant purification (Reverse-phase HPLC, RP-HPLC).

Eluent solution A (1 L)	1 L H_2O; 1 mL TFA; Degas by sonication before use
Eluent solution B (1 L)	1 L Acetonitrile; 1 mL TFA; Degas by sonication before use

IGF-I variant purification (cation-exchange chromatography).

Binding buffer (1 L)	6.8 g Acetate sodium trihydrate; 800 mL H_2O; Adjust the pH to 4.5 with acetic acid; add H_2O to 1 L; Filter solution through a 0.45 µm filter
Elution buffer (1 L)	6.8 g Acetate sodium trihydrate; 58.4 g NaCl; 800 mL H_2O; Adjust the pH to 4.5 with acetic acid; Add H_2O to 1 L; Filter solution through a 0.45 µm filter

Recombinant protein purification from inclusion bodies.

Sonication buffer (100 mL)	0.607 g Tris base, 0.29 g NaCl, 0.029 g EDTA; 100 µL PMSF; 80 mL H_2O; Adjust the pH to 8.0; Add H_2O to 100 mL
Unfolding buffer (100 mL)	0.607 g Tris base, 0.29 g NaCl, 0.029 g EDTA; 100 µL PMSF; 57.32 g Guanidine HCl; 61.4 mg reduced glutathione; 12.2 mg oxidized glutathione; 80 mL H_2O; Adjust the pH to 8.0; Add H_2O to 100 mL

Unnatural amino acid (uAA). Propargyl-chloroformate was purchased from Sigma-Aldrich. Boc-protected L-lysine was obtained from Chem-Impex Int'l Inc. Propargyl-L-lysine (Plk) as HCl-salt was synthesized in-house as described by Milles et al.[284] and Li et al.[285] The product was confirmed by a Bruker Advance 400 MHz NMR spectrometer as reported elsewhere.[250] (S)-2-Amino-6-(((2-azidoethoxy)carbonyl)amino)hexanoic acid (azido-L-lysine) was kindly provided by Martina Raschig.

Resins/devices for protein purification.

Resins/devices for protein purification	Type	Application
P-aminobenzamidine agarose (Sigma-Aldrich)	Affinity chromatography resin	Removal/purification of serine proteases (e.g., thrombin) after the cleavage of the fusion protein
HisPur Ni-NTA resin (Thermo Fisher Scientific)	Affinity chromatography resin (Nickel-NTA resin)	Affinity purification of His-tagged fusion proteins; Pulling down polyhistidine protein
1-mL HisTrap FF crude column (GE Healthcare)	Affinity chromatography column	Histidine-tagged protein purification
1-mL HiTrap SP HP (GE Healthcare)	cation-exchange resin	Protein purification
Jupiter C18 300A column (Phenomenex Inc., Torrance, CA)	Reversed-phase HPLC column	Protein, peptide purification
SOURCE™ 15RPC ST 4.6/100 column (GE Healthcare)	Reversed phase chromatography column	Protein purification

Zip Tip pipette tips (Millipore)	C18 resin	Fast and efficient capture, concentration, desalting and elution of peptides for MALDI mass spectrometry and other methods.
HiTrap Desalting 5-mL column (GE Healthcare)	Desalting column	Scale-up protein desalting
HiTrapTM Heparin HP 1 ml (GE Healthcare)	Affinity chromatography column	Protein purification
FPLC AKTApurifier system™ (GE Healtcare)	_____	Protein purification
Vivaspin 2, Vivaspin 6 & Vivaspin 500 (Sartorius)	Disposable ultrafiltration devices	Protein concentration and buffer exchange
Zorbax 300SB-CN column (Agilent)	Reversed-phase chromatography column	Protein/peptide analysis
Dialysis Membrane (Spectrum Laboratories)	Dialysis	Buffer exchange
Slide-A-Lyzer MINI dialysis devices (Thermo Fisher Scientific)	Dialysis	Buffer exchange

Antibodies.

Primary antibody	**Description**	**Company**
Insulin-like growth factor-I antibody	Goat polyclonal	Sigma-Aldrich #I8773
Insulin-like growth factor-I antibody	Mouse monoclonal	Sigma-Aldrich #I9909
Anti-FGF2 antibody	Mouse monoclonal	Merck #05-118
Anti-phospho-AKT (Ser473)	Rabbit polyclonal	Cell Signaling #9271

AKT Antibody	Rabbit polyclonal	Cell Signaling #9272
α-tubulin antibody	rabbit monoclonal	Cell Signaling #2125S
Myosin heavy chain (MyHC) antibody	Mouse monoclonal	R&D Systems #MAB4470
Second antibody	**Description**	**Company**
Anti-mouse IgG-HRP conjugate	Goat polyclonal	Sigma-Aldrich #A4416
Anti-rabbit IgG-HRP conjugate	Goat	Cell signaling #7074S
Anti-goat IgG-HRP conjugate	Mouse polyclonal	Sigma-Aldrich #AP186P
Anti-Mouse IgG secondary antibody	Goat, Alexa Fluor 488 labeled	Invitrogen #A11001

Molecular biological commercial kits.

E.Z.N.A.R Gel extraction kit	Omega bio-tek, #D2500-1
E.Z.N.A.R plasmid mini Kit	Omega bio-tek, #D6942-02
NucleoBond® Xtra Maxi kits	Macherey-Nagel, #740414.50
Bradford Protein Assay Kit	Pierce, #23200
Pierce BCA Protein Assay Kit	Thermo Fisher Scientific, #23225
Thrombin kits	Novagen, #69671-3
SuperSignal® West Pico Chemiluminescent Substrate	Thermo Fisher Scientific, #34078
M-PER mammalian protein extraction reagent	Thermo Fisher Scientific, #78501

2.2 IGF-I variants preparation

2.2.1 Genetically engineered IGF-I variants containing N-terminally His_6-tagged thioredoxin and a thrombin cleavage site

2.2.1.1 DNA sequence of the IGF-I fusion protein (Trx-IGF-I)

```
                 His6-tag          Trx →
  1  ATG GGT CAT CAC CAT CAC CAT CAC GGT TCT GGT ATG AGC GAT AAA ATT ATT
  1   M   G   H   H   H   H   H   H   G   S   G   M   S   D   K   I   I

 52  CAC CTG ACT GAC GAC AGT TTT GAC ACG GAT GTA CTC AAA GCG GAC GGG
 18   H   L   T   D   D   S   F   D   T   D   V   L   K   A   D   G

100  GCG ATC CTC GTC GAT TTC TGG GCA GAG TGG TGC GGT CCG TGC AAA ATG
 34   A   I   L   V   D   F   W   A   E   W   C   G   P   C   K   M

148  ATC GCC CCG ATT CTG GAT GAA ATC GCT GAC GAA TAT CAG GGC AAA CTG
 50   I   A   P   I   L   D   E   I   A   D   E   Y   Q   G   K   L

196  ACC GTT GCA AAA CTG AAC ATC GAT CAA AAC CCT GGC ACT GCG CCG AAA
 66   T   V   A   K   L   N   I   D   Q   N   P   G   T   A   P   K

244  TAT GGC ATC CGT GGT ATC CCG ACT CTG CTG CTG TTC AAA AAC GGT GAA
 82   Y   G   I   R   G   I   P   T   L   L   L   F   K   N   G   E

292  GTG GCG GCA ACC AAA GTG GGT GCA CTG TCT AAA GGT CAG TTG AAA GAG
 98   V   A   A   T   K   V   G   A   L   S   K   G   Q   L   K   E
                                                   ← Trx   Thrombin site
340  TTC CTC GAC GCT AAC CTG GCC GGT TCT GGT TCT GGC CTG GTT CCG CGT
114   F   L   D   A   N   L   A   G   S   G   S   G   L   V   P   R
                 IGF-I
388  GGA TCC GGA CCG GAG ACG CTC TGC GGG GCT GAG CTG GTG GAT GCT
130   G   S   G   P   E   T   L   C   G   A   E   L   V   D   A

433  CTT CAG TTC GTG TGT GGA GAC AGG GGC TTT TAT TTC AAC AAG CCC
145   L   Q   F   V   C   G   D   R   G   F   Y   F   N   K   P

478  ACA GGG TAT GGC TCC AGC AGT CGG AGG GCG CCT CAG ACA GGC ATC
160   T   G   Y   G   S   S   S   R   R   A   P   Q   T   G   I

523  GTG GAT GAG TGC TGC TTC CGG AGC TGT GAT CTA AGG AGG CTG GAG
175   V   D   E   C   C   F   R   S   C   D   L   R   R   L   E
                                     IGF-I
568  ATG TAT TGC GCA CCC CTC AAG CCT GCC AAG TCA GCT
190   M   Y   C   A   P   L   K   P   A   K   S   A
```

Figure 6. Nucleotide and deduced amino acid sequences of Trx-IGF-I. The hexahistidine tag was overlined, the thrombin cleavage site was distinguished in the square, and the mature IGF-I was in black boldfaced letters.

The DNA sequence of the IGF-I fusion protein referred to as Trx-IGF-I cDNA (**Figure 6**), encodes for *E. coli* thioredoxin (Trx) with an N-terminal His_6 tag and a thrombin cleavage site,[283] followed by (human) IGF-I wild-type protein.

2.2.1.1.1 Subcloning

Primer design. The followed primers were designed to introduce a BamHI site (5'- GGATCC - 3') at the 5' end, and two TAA stop codons (marked in italics) followed by an EcoRI site (5'- GAATTC - 3') at the 3' end of human IGF-I cDNA.

Forward primer (FP_B/IGF): 5'- CCC GGATCC GGA CCG GAG ACG CTC TGC - 3'
Reverse primer (RP_IGF/E): 5'- CCC GAATTC *TTA TTA* AGC TGA CTT GGC AGG CTT GA - 3'

PCR amplification. IGF-I cDNA was PCR-amplified from the pCMV6-XL4 vector (Origene, Herford, Germany) using high fidelity *Pfu* DNA Polymerase. The components and final concentrations for a typical 50 µL reaction (**Table 2**) were as follows.

Table 2. PCR reaction

Component	50 µL reaction	Final Concentration
10x *Pfu* Buffer (Promega)	5 µL	1x
10 mM dNTPs	1 µL	200 µM
5 µM Forward Primer	2.5 µL	0.25 µM (0.05–1 µM)
5 µM Reverse Primer	2.5 µL	0.25 µM (0.05–1 µM)
Template DNA	variable	~ 200 ng
Pfu DNA Polymerase	0.4 µL	1 unit/50 µL PCR
Nuclease-free water	to 50 µL	

The routine PCR was carried out by thermal cycler under the following conditions: 95 °C for 5 min, 35 cycles of 95 °C for 30 s, 65 °C for 30 s, and 68 °C for 1 min, and a final extension at 68 °C for 5 min.

Agarose gel electrophoresis. DNA fragments were mixed with 6x DNA Gel Loading Buffer (Thermo Fisher Scientific) and run on 1% agarose/Midori Green/1x TAE gel. 5 µL GeneRuler 1 Kb plus DNA ladder (Thermo Fisher Scientific) was used as a standard. The obtained fragments were recovered using an E.Z.N.A Gel Extraction Kit according to the manufacturer's instruction.

Restriction digestion & ligation. Both, amplified PCR product and recipient vector (pHisTrx), were digested by a High-Fidelity version of BamHI and EcoRI at 37 °C for 4 h (**Table 3**).

Table 3. 50 µL of the digestion system

8 µL	200 µg/mL pHisTrx vector	8 µL	150 µg/mL PCR product
1 µL	BamHI-HF®	1 µL	BamHI-HF®
1 µL	EcoRI-HF®	1 µL	EcoRI-HF®
5 µL	10x CutSmart buffer	5 µL	10x CutSmart buffer
35 µL	H_2O	35 µL	H_2O

To prevent self-ligation, the digested plasmid was treated with Antarctic phosphatase to remove the 5'- phosphate groups according to the following steps: 50 µL pHisTrx mixture + 5.66 µL 10x Antarctic phosphatase buffer + 1 µL Antarctic phosphatase were mixed and incubated for 30 min at 37 °C. Gel extraction was applied to purify the digested PCR product. Required insert and vector volumes for ligation at molar ratio insert/vector 3:1 was calculated (https://nebiocalculator.neb.com/#!/ligation). The two fragments (**Table 4**) were then ligated at 16 °C overnight to construct the expression vector pHisTrx/ Trx-IGF-I.

Table 4. Ligation (molar ratio insert: vector =3:1)

Volume (µL)	Component
2.5	pHisTrx vector (50 ng)
1.2	insert DNA (6 ng)
1	10x T4 DNA ligase buffer
0.5	T4 DNA ligase
4.8	H_2O

Transformation. The transformation was performed using the standard protocol as follows; 4 µL of above ligation mixture was added to 50 µL of thawed competent *E. coli* DH5α cells and mixed gently. The suspensions were kept on ice for 20 min, followed a heat shock at 42 °C for 45 s, and immediately placed on ice bath for another 5 min. Then 500 µL of SOC media was added, and the cells were allowed to recover at 37 °C for 1 h. In the end, 100 µL of recovered cells were spread onto agar plates containing 100 µg/mL carbenicillin and incubated overnight at 37 °C. Several colonies were randomly picked and each inoculated into a 5-mL culture of LB medium

supplemented with 100 µg/mL carbenicillin. The cultures were grown overnight at 37 °C, following plasmid DNA extraction using E.Z.N.A.R plasmid mini Kit according to the manufacture instruction. Double-enzyme (SapI & NdeI) digestion of the purified plasmid DNA (with and without an insert) followed by agarose gel electrophoresis, was used to check if the vector contained the expected size insert. PCR amplification of the plasmid using insert-specific primers: forward primer (FP_B/IGF) and reverse primer (RP_IGF/E), followed by electrophoresis can also determine if the construct contained the DNA fragment of interest. Positive results were further confirmed by DNA sequencing using T7 primers (Eurofins Genomics, Ebersberg, Germany).

2.2.1.1.2 Protein expression

The verified vector pHisTrx/ Trx-IGF-I was finally transformed into *E. coli* BL21 (DE3), *E. coli* SHuffle T7 and *E. coli* Rosetta 2, respectively. A fresh clone of *E. coli* harboring the expression vector was inoculated in 5 mL LB medium supplemented with 100 µg/mL carbenicillin for BL21 (DE3), 100 µg/mL carbenicillin for SHuffle T7, 100 µg/mL carbenicillin and 34 µg/mL chloramphenicol for Rosetta 2, respectively. 1 mL of the resulted seed culture was then transferred into 100 mL TB medium in 500 mL flask. The protein expression was induced using 0.2 mM of isopropyl-β-D-thiogalactopyranoside (IPTG) at OD_{600} = 0.6 ~ 0.8 at certain conditions according to optimization purpose. Cells were harvested by centrifugation at 5000 g for 30 min, and stored at -80 °C until further usage.

2.2.1.1.3 Protein extraction

The cell pellet was resuspended in His_6-tag binding buffer (**section 2.1**) supplemented with 1 mM phenylmethylsulfonylfluoride (PMSF). The suspended cells were disrupted by sonication (5 cycles for 1 min: 1 s pulse, 0.8 s pause, 70% amplification with 2 min pause between cycles). Subsequently, the cell lysate was clarified by centrifugation at 5000 g for 30 min, then at 10,000 g for 60 min at 4 °C to separate from insoluble sediment. Small amounts of soluble and insoluble fractions were then prepared in 1x reducing SDS-loading buffer, heated at 95 °C for 5 min, and analyzed by sodium dodecyl sulfate-polyacrylamide gel electrophoresis (SDS-PAGE).

The Trx-IGF-I fusion protein was purified from the supernatant of cell lysate by immobilized metal affinity chromatography (IMAC). All steps were performed on an FPLC system (GE Healthcare Äkta Purifier, Life sciences, Freiburg, Germany) setup with 1 mL HisTrap FF column for affinity chromatography. The column was equilibrated with His_6-tag binding buffer (**section 2.1**). After the soluble sample was loaded onto the column, the bound recombinant fusion protein was eluted by His_6-tag elution buffer at the flow rate of 1 mL/min. The gradient was set up as follows: a linear gradient of 0 to 50% elution buffer for 25 column volumes (CV), a step gradient of 50% elution buffer for 15 CV, a linear gradient of 50% to 100% elution buffer for 1 CV, flushing at 100%

elution buffer and re-equilibrate to 100% binding buffer. Eluted fusion proteins were analyzed by SDS-PAGE and assayed by Bradford method[286] with bovine serum albumin (BSA) as a standard. Briefly, 5 µL of protein sample was mixed with 195 µL of Bradford Reagent (Sigma) and the absorbance measured at 595 nm. The protein concentration was determined by comparison with a standard curve, prepared with BSA samples of known concentration ranging from 0.1 to 1 mg/mL. The target proteins were pooled together and then buffer-exchanged into 1x thrombin digestion buffer (20 mM Tris, 150 mM NaCl, pH=8.4) by dialysis or gel filtration chromatography by using the HiTrap Desalting column (Sephadex G-25 resin, GE Healthcare).

Small-scale parallel digestion of fusion protein by thrombin from two different manufacturers (GE Healthcare vs. Novagen) was conducted to optimize the cleavage efficiency. The digestion was optimized by varying the thrombin concentration (1, 5, and 10 U "GE Healthcare" thrombin/mg fusion protein; 1, 2, and 5 U "Novagen" thrombin/mg fusion protein), the duration of the reaction, and the addition of additives ($CaCl_2$, urea). The corresponding aliquots were collected and analyzed by SDS-PAGE, and in some cases followed by Western Blot with antibody to IGF-I. The cleavage reaction was stopped with 1 mM PMSF. The above mixture was then incubated with p-aminobenzamidine agarose to trap the thrombin protease at room temperature for 1 h. Removal of the His_6-tag from Trx-IGF-I fusion was achieved by the second round of affinity chromatography. Tag-free IGF-I was then obtained in the flow-through fraction after passing through a HisTrap FF column. The samples were adjusted to 0.1% trifluoroacetic acid (TFA) and loaded on a Jupiter C18 reverse-phase high-performance liquid chromatography column (Phenomenex Inc., Torrance, CA) as a final purification step. A linear gradient, from 0% to 60% acetonitrile in 0.1% TFA was run. The peak fractions were collected and analyzed by SDS-PAGE. After identification of IGF-I protein, the pooled fractions were lyophilized.

2.2.1.1.4 SDS-PAGE

Expressed proteins and cleavage reaction were analyzed by standard Tris-glycine SDS-PAGE. The SDS-PAGE gel was prepared according to the following recipe (**Table 5**). (Note: Perform a 5% separating gel for SDS-denatured proteins of 60 to 200 kDa and a 15% gel for 10 to 50 kDa; 15 % SDS-PAGE gel was used throughout this thesis unless specifically noted)

The samples were mixed with 6x reducing SDS sample buffer prior to heating at 95 °C for 5 min. The denatured proteins and a prestained protein ladder (Thermo Fisher Scientific) were loaded into the gel (Bio-Rad Laboratories GmbH, München, Germany) and electrophoresis was run at 80 V for 15 min, then at 120 V until the tracking dye reached the bottom of the gel. Gels were stained with 0.1% Coomassie Brilliant Blue G250 solution for 2 h at room temperature and destained with 20% methanol, 10% glacial acetic acid in H_2O. Microwave heating was also used to decrease the time required for staining and destaining of SDS-PAGE gels.

Table 5. Recipes for Laemmli resolving gel.

Stock solution	Separation gel		Stacking gel
	5%	15%	3.9%
30%Acrylamide/0.8% bisacrylamide (Bio-Rad)	2.5 mL	7.5 mL	0.65 mL
4x Tris-HCl/SDS, pH 6.8	___	___	1.25 mL
4x Tris-HCl/SDS, pH 8.8	3.75 mL	3.75 mL	___
H_2O	8.75 mL	3.75 mL	3.05 mL
10% (w/v) ammonium persulfate	50 µL	50 µL	25 µL
TEMED	10 µL	10 µL	5 µL
Total volume	15 mL	15 mL	5 mL

2.2.1.1.5 Western Blot analysis

The proteins were separated by SDS-PAGE gel electrophoresis and electrotransferred to nitrocellulose membranes (BioTrace®NT, PN 66485, Pall Life Sciences, Ann Arbor, MI, USA) with 1× Western Blot buffer containing 20% ethanol (**section 2.1**). Membranes were blocked with 1x Roti®-Block (Carl Roth GmbH, Karlsruhe, Germany) for 1 h at room temperature before addition of goat anti-human IGF-I antibodies (1:1000 dilution) in Tris-buffered saline (TBS) solution containing 0.1 % (v/v) Tween 20 (TBST) at 4 °C for overnight. After washing three times with TBST for 10 min, membranes were incubated with a peroxidase-conjugated rabbit anti-goat IgG at a dilution of 1:2000 in TBST solution for 1 h at room temperature. Detection was performed with a chemiluminescent substrate kit (SuperSignal® West Pico Chemiluminescent Substrate, Thermo Fisher Scientific, Lausanne, CH) and photographed using a FluorChem FC2 imaging system.

2.2.1.1.6 MALDI analysis

Matrix-assisted laser desorption/ionization time-of-flight mass spectrometry (MALDI-TOF-MS) was used to identify the molecular mass of proteins. MALDI mass spectrum of protein was recorded by using sinapinic acid as matrix and acquired in the positive linear mode by using an Autoflex II LRF instrument from Bruker Daltonics Inc. (Bremen, Germany) equipped with a nitrogen laser operating at 337 nm. Mass calibration was externally accomplished by using a mixture of calibrates containing insulin, ubiquitin, myoglobin and cytochrome C (Bruker Daltonics

Inc., Bremen, Germany). Theoretical masses of wild-type proteins were predicted with PeptideMass (http://web.expasy.org/peptide_mass).

2.2.1.1.7 HPLC analysis

Protein purity was evaluated by reversed-phase HPLC using a VWR Hitachi LaChromUltra HPLC system. Briefly, samples were injected to a Zorbax 300SB-CN reversed-phase chromatography column (4.6 mm x 150 mm, 5 µm, Agilent) at 40 °C with detection at 214 nm, equilibrated by water containing 0.1 % TFA. Mobile phase A was 0.1% TFA in water, while mobile phase B was 0.1% TFA in acetonitrile. Commercial IGF-I (cIGF-I, reference, Genentech) and purified IGF-I from Trx-IGF-I fusion protein (own) were separated at a flow rate of 0.8 mL/min with a gradient program that allowed for 5 min at 100% A followed by a linear gradient to 100% mobile phase B in 30 min. Afterward, washing at 100% B and equilibration at 100% A were performed in a total analysis time of 45 min.

2.2.1.2 DNA sequence of the IGF-I mutant fusion protein (Trx-plk-IGF-I)

The DNA sequence of the IGF-I mutant fusion protein, referred to as Trx-plk-IGF-I cDNA, is almost the same sequence as that of wild-type IGF-I fusion protein, except the mutation of Glu-3 of IGF-I into an amber codon (TAG) for the incorporation of the uAA.

2.2.1.2.1 Subcloning

The plasmid pCMV6-XL4/IGF-I was used as a template for the amplification of mutant E3(TAG)-IGF-I genes by using the followed primers.

Forward primer (FP_B/IGF mut): 5′ - CCC <u>GGATCC</u> GGA CCG **TAG** ACG CTC TGC - 3′
Reverse primer (RP_IGF/E): 5′ - CCC <u>GAATTC</u> *TTA TTA* AGC TGA CTT GGC AGG CTT GA - 3′

The forward primer contained a BamHI site (5'- GGATCC - 3') and an amber codon (**TAG**), whereas the reverse primer comprised an EcoRI site (5'- GAATTC - 3') and two TAA stop codons (marked in italics). PCR thermocycling conditions were as follows: 95 °C for 5 min, 35 cycles of 95 °C for 30 s, 65 °C for 30 s, and 68 °C for 1 min, and final heating at 68 °C for 5 min. Amplified E3(TAG)-IGF-I cDNA was cloned with the restriction endonucleases BamHI and EcoRI into the backbone of a pHisTrx vector (**Figure 7**). DH5α competent cells were subsequently transformed with the mutated plasmid (pHisTrx/Trx-plk-IGF-I) using the heat shock method as described previously (**section 2.2.1.1.1**). The DNA sequence of Trx-plk-IGF-I gene was confirmed by T7-promotor DNA sequencing. For the expression of Trx-plk-IGF-I in *E. coli*, the plasmid pET-11a/ Trx-plk-IGF-I was constructed. Primers (FP_N/Trx-plk-IGF-I & RP_Trx-plk-IGF-I/BglII) were

used to amplify Trx-plk-IGF-I from recombinant pHisTrx/Trx-plk-IGF-I, resulting in a product with NdeI (5'- CATATG - 3') and BglII (5'- AGATCT - 3') at the 5′ and 3'-ends, respectively.

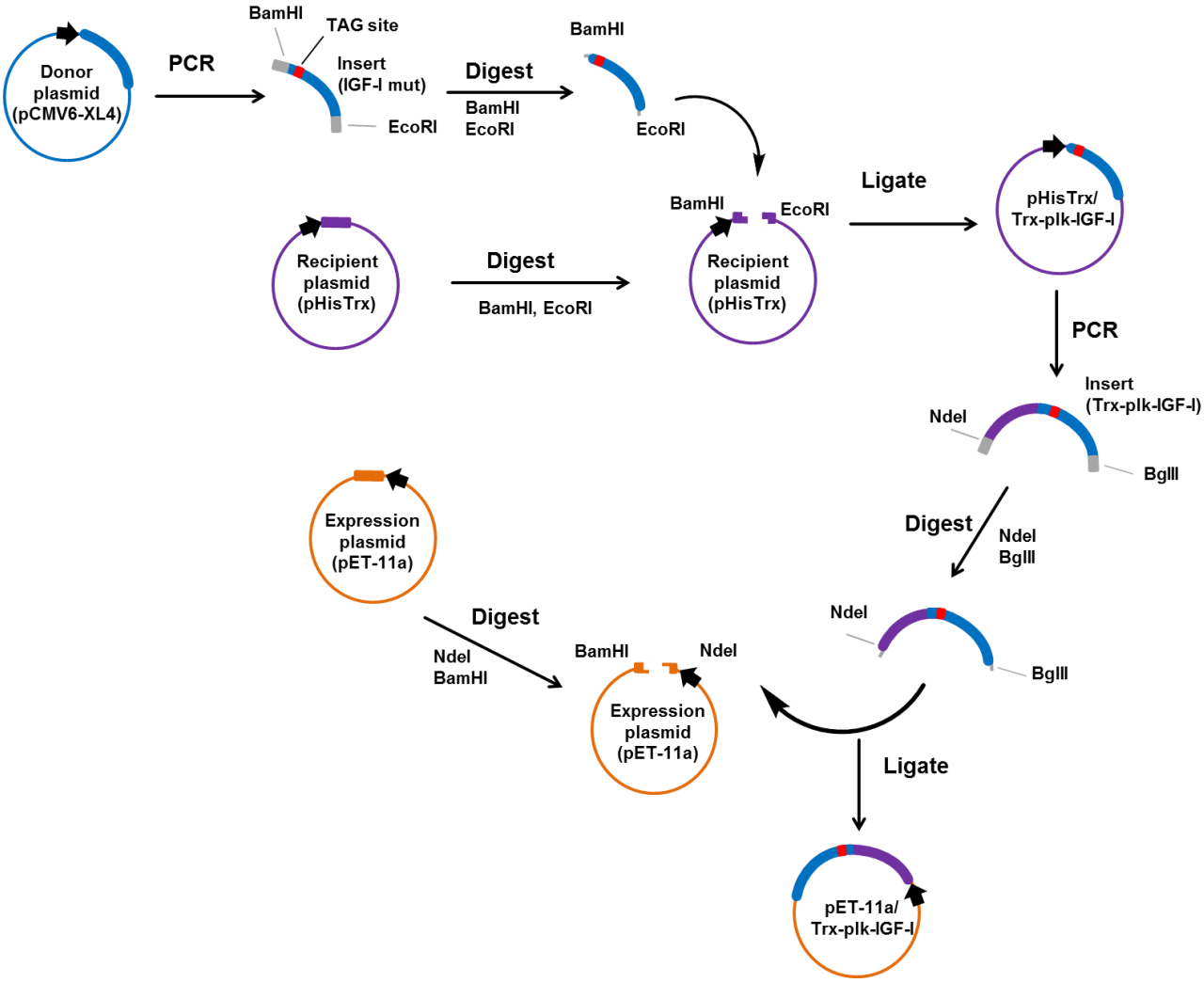

Figure 7. A cartoon image about the overview of the cloning process.

Forward primer (FP_N/Trx-plk-IGF-I): 5′ - CAAGAA <u>CATATG</u> ATG GGT CAT CAC CAT CAC CAT - 3′

Reverse primer (RP_Trx-plk-IGF-I/BglII): 5′ - CAAGAA <u>AGATCT</u> *TTA TTA* AGC TGA CTT GGC AGG CTT GA - 3′

The PCR product of Trx-plk-IGF-I gene was digested with NdeI and BglII, followed by heat inactivation of the enzymes. The insert was then ligated into pET-11a vector that had been previously digested with BamHI & NdeI and phosphatase treated, to give rise to pET-11a/Trx-plk-IGF-I (**based on the compatible cohesive ends produced by BglII to those of BamHI**). Correct insert sequences of all constructs were confirmed by DNA sequencing.

2.2.1.2.2 Protein expression

Cotransformation. The plk incorporation was accomplished in different *E. coli* cells (BL21 (DE3), SHuffle T7, Rosetta (DE3) and C321.ΔA.exp) by cotransformation of two plasmids, pET-11a/Trx-plk-IGF-I containing an amber mutation and the pRSFDuet-1 construct encoding for PylRS gene. Briefly, 50 µL of each strain (BL21 (DE3), SHuffle T7, Rosetta (DE3) and C321.ΔA.exp competent cells) were thawed on ice for 10 min before the addition of 250 ng of each plasmid (pET-11a/Trx-plk-IGF-I, pRSFDuet-1). The vials were mixed thoroughly and kept on ice for 20 min. The cells were heat shocked at 42 °C for 45 s and immediately returned to an ice bath for another 5 min. 250 µL of SOC medium was then added to bacteria and incubated for 60 min at 37 °C with vigorously shaking. Subsequently, 100 µL of the cells were spread onto a selection agar plated with 100 µg/mL carbenicillin and 34 µg/mL kanamycin for BL21 (DE3), 100 µg/mL carbenicillin and 34 µg/mL kanamycin for SHuffle T7, 100 µg/mL carbenicillin, and 34 µg/mL kanamycin and 25 µg/mL chloramphenicol for Rosetta (DE3), 100 µg/mL carbenicillin and 34 µg/mL kanamycin for C321.ΔA.exp, respectively. The plates were incubated at 37 °C overnight. A fresh colony of each strain was inoculated into 100 mL LB medium supplemented with corresponding selection antibiotic and cultured at 37 °C overnight. The cells were harvested by centrifugation at 4 °C with 4000 g for 10 min. Glycerol stocks of *E. coli* (BL21 (DE3), SHuffle T7, Rosetta (DE3) and C321.ΔA.exp) harboring the expression vectors were prepared by resuspending each yielded pellet in their corresponding 5 mL LB-glycerol medium (**section 2.1**) and frozen in a cryotube at -80 °C.

General IPTG-induction protein expression. General IPTG-induction protein expression was performed to optimize conditions for Trx-plk-IGF-I production.[250, 252, 287] Briefly, the saturated culture of *E. coli* was inoculated into fresh TB medium containing 100 µg/mL carbenicillin and 34 µg/mL kanamycin for BL21 (DE3), 100 µg/mL carbenicillin and 34 µg/mL kanamycin for SHuffle T7, 100 µg/mL carbenicillin, and 34 µg/mL kanamycin and 25 µg/mL chloramphenicol for Rosetta (DE3), 100 µg/mL carbenicillin, 34 µg/mL kanamycin and 25 µg/mL zeocin for C321.ΔA.exp (with all 321 UAG codons changed to UAA and RF1 knock-out),[288] respectively. Plk was added at OD_{600} = 0.3 ~ 0.4. Protein expression was induced using 1 mM IPTG at OD_{600} =0.6 ~ 0.8. After incubation at 37 °C for 6–8 h, bacteria were harvested by centrifugation at 5000 g for 30 min at 4 °C and stored at -80 °C. SDS-PAGE and Western Blot were performed to compare the protein expression in four different *E. coli* hosts.

2.2.1.2.3 Protein extraction

Protein detection using polyhistidine protein pull-down assay. To determine if most of the target protein expressed in soluble form or as inclusion body, polyhistidine protein from the soluble part and insoluble sediment of small-scale bacterial culture (**Figure 8**) were pulled down and analyzed by SDS-PAGE and Western Blot.

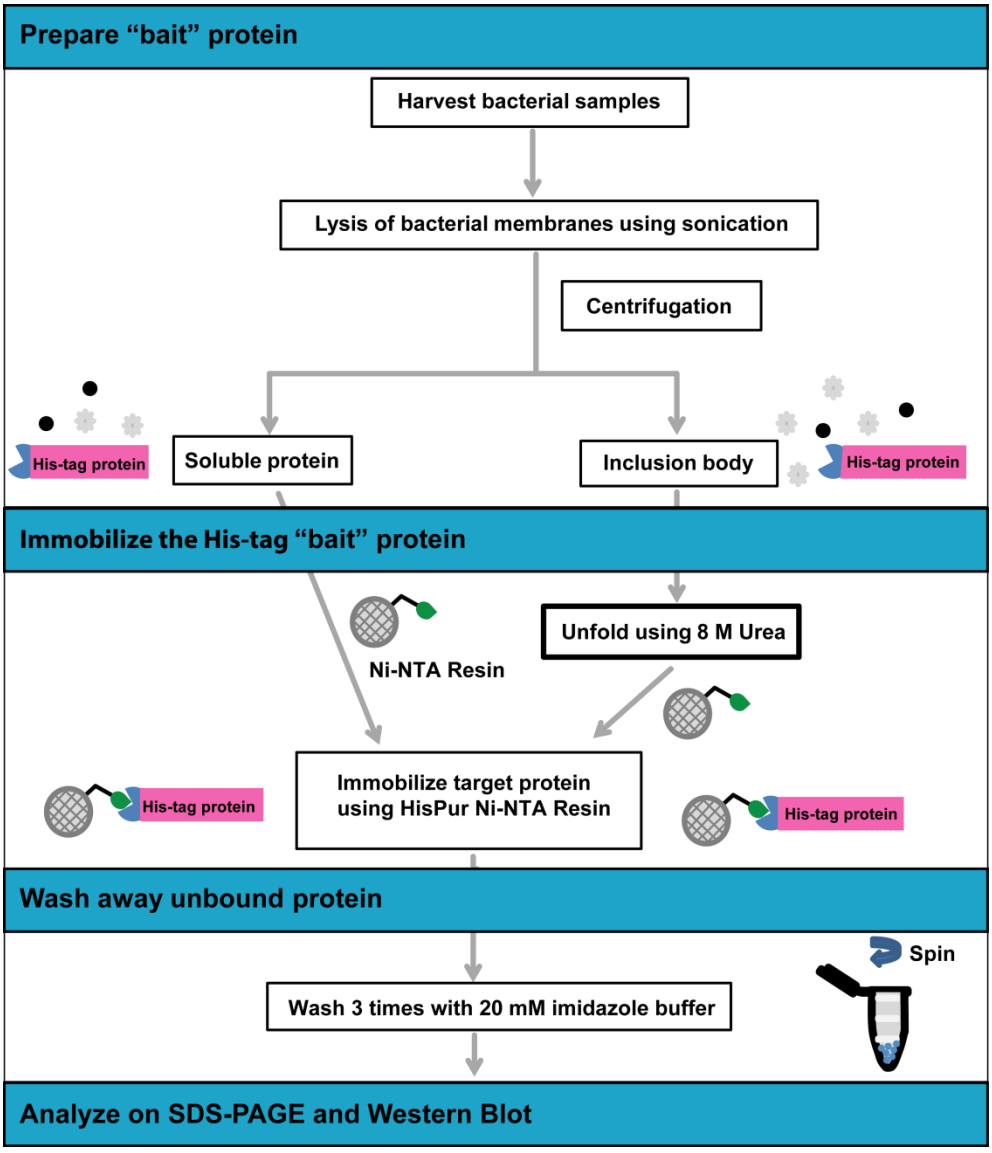

Figure 8. Procedure summary for histidine-tag pull-down assay.

The expression system of BL21 (DE3) harboring pET-11a/Trx-plk-IGF-I and pRSFDuet-1 was used for polyhistidine-tagged bait protein (Trx-plk-IGF-I) preparation. Protein expression with different plk amounts (2 mM vs. 10 mM) was performed according to the previous procedures (**section 2.2.1.2.2**). After expression, cells were resuspended in 1 mL of sonication buffer (50 mM Tris-HCl with 1 mM PMSF, pH 7.4) per 5 mL of original culture volume and lysed by sonication. Following clarification of the lysate by centrifugation at 5000 g for 30 min, the supernatant was incubated with 100 µL Ni-NTA agarose beads (HisPur Ni-NTA resin, Thermo Fisher Scientific) for 1 h at 4 °C (**Figure 8**). Trx-plk-IGF-I bound beads were washed 3 times with 20 mM imidazole buffer to remove unbound protein. After wash, Trx-plk-IGF-I protein-bound beads were transferred into a 1.5 mL Eppendorf tube. After adding 30 µL of 1x SDS-loading buffer to the beads, the mixture was cooked at 95 °C for 5 min and analyzed by SDS-PAGE and Western Blot. Analogously, the immobilization of Trx-plk-IGF-I from inclusion body was achieved by unfolding

in the dissolution buffer (50 mM Tris-HCl, 8M Urea, 1 mM DTT and 1 mM PMSF, pH 7.4) for 1 h at room temperature, clarifying by centrifugation followed by incubation with 100 µL Ni-NTA agarose beads for 1 h at 4 °C. After wash, 30 µL of 1x SDS-loading buffer were added into denatured Trx-plk-IGF-I protein coated beads before analysis by SDS-PAGE and Western Blot.

General protein extraction. After expression, cell pellets were resuspended in the His_6-tag binding buffer (17 mM Na_2HPO_4, 3 mM NaH_2PO_4, 500 mM NaCl, 20 mM imidazole, pH=7.5) with 1 mM PMSF and lysed via sonication (70% amplitude, 6 times) on ice. After clarification by centrifugation, the supernatant, containing soluble Trx-plk-IGF-I was directly purified by nickel affinity chromatography using an FPLC system (GE Healthcare, Äkta Purifier), whereas the pellet was prepared for unfolding and refolding experiment according to previously published protocols[289] with the following modifications. The resulting pellet containing the insoluble Trx-plk-IGF-I was washed with inclusion body washing buffer (50 mM Tris-HCl, 50 mM NaCl, 1 mM EDTA, 3 M urea, 0.1 mM PMSF, pH=8.0) for twice. The washed pellet was resuspended in unfolding buffer (**section 2.1**) supplemented with 0.1 mM PMSF (1 g crude cell pellet: 9 mL unfolding buffer) and incubated at room temperature for 1 h with gentle mixing. The solution was clarified by centrifugation at 5000 g for 30 min to remove any insoluble materials. The cleared solution was added into a five-volume refolding buffer (50 mM Tris-HCl, pH 8.0, 2 mM reduced glutathione, 0.2 mM oxidized glutathione and 50 mM NaCl), dropwise at ~1 drop per 1–2 s while stirring at room temperature. The diluted denatured protein was refolded through dialysis against the same refolding buffer at room temperature for 4 h. Precipitates were removed by centrifugation at 4000 g for 15 min at 4 °C. The supernatant was subsequently dialyzed against His_6-tag binding buffer overnight at 4 °C, filtered through 0.22 µm cellulose acetate membrane and then loaded onto a 1 mL HisTrap FF crude column (GE Healthcare) pre-equilibrated with binding buffer.

After washing with the same buffer, the linear gradient program immediately started from 100% His_6-tag binding buffer to 50% His_6-tag elution buffer (**section 2.1**) for 25 CV, a step gradient of 50% elution buffer for 15 CV, to 100% elution buffer for 1 CV at 1 mL/min. Trx-plk-IGF-I was eluted at ~50% elution buffer. Afterward the purified fusion protein was buffer-exchanged into 1x thrombin digestion buffer (pH=8.4) or phosphate-buffered saline (pH=7.2) and digested with restriction grade thrombin (Novagen) at room temperature. The optimization of cleavage efficiency was achieved by the variation of thrombin concentration (1, 2, and 5 U/mg fusion protein), incubation time (6, 12, and 24 h) and reaction pH levels (pH=8.4, 7.2 and 6). The corresponding aliquots were collected and analyzed by Western Blot. After cleavage, plk-IGF-I was obtained by using p-aminobenzamidine-agarose beads to remove thrombin protease and using reverse-phase HPLC as the final purification step. The purified plk-IGF-I was analyzed by SDS-PAGE followed by Western Blot.

2.3 Dual-functionalized IGF-I variants

2.3.1 Genetically engineered IGF-I Ea with two alkyne functionalities

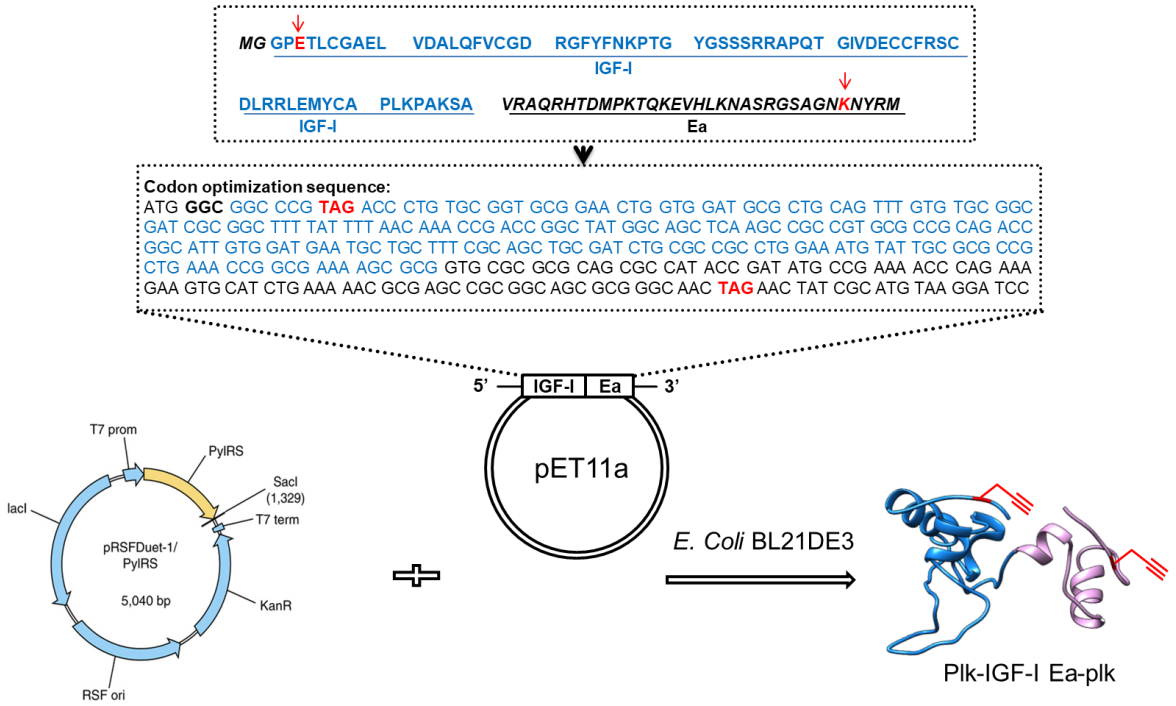

Figure 9. Schematic representation of the construction of plk-IGF-I Ea-plk. Vector pRSFDuet-1/PylRS was reprinted by permission from Macmillan Publishers Ltd.: Nature Protocols (Ref.[290]), copyright (2015). Glu-3 and Lys-99 of IGF-I Ea were replaced by plk (highlighted in red). Ribbon structure of IGF-I Ea (UCSF Chimera) was based on the IGF-I structure (indicated in blue) (PDB ID: 2GF1) and an *in silico* peptide structure Pep-fold[291, 292] prediction of Ea peptide (marked in purple).

The DNA sequence of the IGF-I Ea variant, referred to as plk-IGF-I Ea-plk, is almost the same as that of plk-IGF-I Ea,[293] except the substitution of Lys-99 of IGF-I Ea into an amber codon (TAG) (two TAG codons highlighted in red, **Figure 9**).

2.3.1.1 Plk-IGF-I Ea-plk expression

BL21 (DE3) glycerol stocks harboring plasmids pET-11a/plk-IGF-I Ea-plk and pRSFDuet-1/PylRS were kindly provided by Dr. Schultz. Protein expression was performed as previously described (**section 2.2.1.2.2**) with the following modification. An overnight culture of BL21 (DE3) cells in 100 mL of LB medium containing 100 µg/mL carbenicillin and 34 µg/mL kanamycin were harvested by centrifugation. The pellet was then resuspended in 1 L TB medium supplemented with 100 µg/mL carbenicillin and 34 µg/mL kanamycin, and grown at 37 °C. 10 mM of plk were added at OD_{600} = 0.3 ~ 0.4. 1 mM of IPTG was added at OD_{600} =0.6 ~ 0.8 to induce the production of plk-IGF-I Ea-plk. 1 mL of bacterial suspension of each expression was collected at a given time

point and pelleted by centrifugation. The obtained pellets were mixed with 1x SDS-reduced loading buffer, cooked at 95 °C for 5 min and followed by centrifugation. The lysate supernatants were then analyzed by SDS-PAGE followed by Western Blot. The protein expression method was also performed at 27 °C induced by different IPTG concentrations (0.1 mM, 0.5 mM, & 1 mM). Cells were harvested by centrifugation at 5000 g for 30 min at 4 °C, and stored at -80 °C until required.

2.3.1.2 Solubilization of inclusion bodies

Plk-IGF-I Ea-plk extraction was performed as previously described (**section 2.2.1.2.3**), with the following modifications. For washing of inclusion bodies, the pellets were suspended in the same washing buffer and incubated for 10 min on ice, and then centrifuged at 10,000 g for 30 min at 4 °C. This wash step was repeated twice.

2.3.1.3 Refolding and purification of refolded Plk-IGF-I Ea-plk

To optimize the refolding process, refolding buffer with various additives was screened based on the turbidity of solutions at 320 nm, in which condition giving lower turbidity demonstrated less protein aggregation.[294] The detailed procedure was as follows:

1. Prepare washed inclusion bodies solubilized in the above-solubilized buffer (3–5 mg/mL) and centrifuged to remove any insoluble material.
2. Prepare a set of test solutions (**Table 6**) based on the variables and additives that may be used to facilitate protein refolding (**Appendix C**)
3. Pipette 10 μL of solubilized protein into each well of a 96-well plate.
4. Perform 20-fold rapid dilution by quickly adding 190 μL of the test refolding solution and mixing the solution thoroughly.
5. Place them at room temperature or 4 °C for 60 min, and then read the absorbance of the plate at 320 nm using a Spectramax 250 microplate reader (Molecular Devices, Sunnyvale, USA).
6. Graph the absorbance readings with the plate absorbance subtracted.
7. Choose the best conditions which show the lowest turbidity for the scale-up refolding process.

Subsequently, the best condition giving low turbidity was chosen for the further optimization. The denatured protein was diluted with 9 times volume of refolding buffer (50 mM Tris-HCl, 50 mM NaCl, 1 mM EDTA, 0.4 M L-arginine, 2 mM reduced and 0.2 mM oxidized glutathione, pH 8.0) and stirred either (Method I) at 4 °C for 36 h, or (Method II) at room temperature for 1 h. Precipitates were removed by centrifugation at 2500 g for 15 min at 4 °C. The supernatant fraction was collected, dialyzed against PBS (pH 7.4) at 4 °C, and then concentrated either by lyophilization or PES ultrafiltration membrane (molecular weight cutoff, 3K; Vivaspin 6, Sartorius) to a 14-fold increase of the concentration of protein samples. Except for the concentrated supernatant by a Vivaspin-6 3K filter and reconstructed freeze-dried samples, the deposition of small amounts of

aggregated proteins on PES membrane was also collected for SDS-PAGE and Western Blot analysis.

Table 6. Test solutions used in this study, consisting of Tris buffer (50 mM Tris, 50 mM NaCl, 1 mM EDTA, 2 mM reduced glutathione, 0.2 mM oxidized glutathione) and supplement reagent.

No.	Supplement reagent			
	L-Arginine	PEG 3000	Ethanol	pH
A1	0.4 M	-----	-----	8.0
A2	0.4 M	-----	-----	8.5
A3	0.4 M	-----	-----	9.0
A4	0.4 M	0.5%	-----	8.0
A5	0.4 M	0.5%	-----	8.5
A6	0.4 M	0.5%	-----	9.0
A7	0.4 M	-----	20%	8.0
A8	0.4 M	-----	20%	8.5
A9	0.4 M	-----	20%	9.0

2.3.1.4 In-gel tryptic digestion and mass spectrometry

SDS-PAGE followed by Coomassie Blue staining was utilized to visualize protein samples.[295] The appropriate band was excised, and in-gel reduction with DTT and alkylation with iodoacetamide (IAM) were performed as previously described.[296, 297] The presence of plk-IGF-I Ea-plk was confirmed by in-gel tryptic digestion and ESI-MS analysis. This procedure was performed by Dr. Werner Schmitz at the Department of Biochemistry and Molecular Biology (University of Wuerzburg, Germany).

2.3.2 Clickable plk-IGF-I Ea with TGase reactivity

2.3.2.1 Cross-linking of plk-IGF-I Ea to Q-peptide by TGase-catalyzed reaction

2.3.2.1.1 Synthesis and purification of the Q-peptide

Q-peptide (NQEQVSPLA(N_3)G), derived from the TGase substrate sequence of α-2 plasmin inhibitor (α_2PI_{1-8}), was synthesized manually by Fmoc solid phase peptide synthesis as described.[298] In brief, 2-chlorotrityl chloride resin (2-CTC, 170 mg, 0.2 mmol) as solid support was

loaded into a plastic syringe fitted with a polyethylene frit (MultiSynTech GmbH, Witten, Germany). The first Fmoc-Gly-OH amino acid (1 equiv.) was esterified to the resin in the presence of N,N-Diisopropylethylamine (DIPEA) (6.5 equiv.) in dichloromethane (DCM) for 2 h at room temperature. The remaining active site of the resin was capped by adding 1.5 mL methanol into the mixture and stirred for 15 min at room temperature. The resin was washed with DCM (3 times × 2 mL), N,N-Dimethylformamide (DMF) (3 times × 2 mL), DCM (3 times × 2 mL) and methanol (3 times × 2 mL) and dried overnight. After the esterification of Fmoc-Gly-OH on 2-CTC resin, Fmoc-deprotection was performed using 40% (V/V) piperidine in DMF for 3 min followed by 20% (V/V) piperidine in DMF for 10 min. Following each deprotection or coupling step, the resin was washed with DMF (6 times × 4 mL). The Fmoc-amino acids (5 equiv.) dissolved in 0.5 M 1-hydroxybenzotriazole hydrate (HOBT) in DMF with 160 µL N, N′-Diisopropylcarbodiimide (DIC) and 176 µL DIPEA was added into the resin and allowed to couple for at least 3 h. Fmoc-deprotection and coupling steps were iteratively repeated until the desired peptide chain was obtained.

After cleavage from resin with the splitting solution TFA/H_2O (95:5), the peptide was loaded into a Jupiter 15u C18 300A column (21.2 mm× 250 mm, Phenomenex Inc., Torrance, CA) pre-equilibrated with 5% (V/V) acetonitrile /H_2O containing 0.1% TFA. Elution was performed at 1 mL/min using an acetonitrile/water gradient in 0.1% TFA (from 3% to 20% over 5 CV, from 20% to 45% over 20 CV, and from 45% to 70% over 8 CV). The Q-peptide eluted as a broad peak at ~30% acetonitrile was confirmed by LC-MS analysis and recovered as a pure peptide after lyophilization.

2.3.2.1.2 Cross-linking of plk-IGF-I Ea to Q-peptide in the presence of Factor XIIIa (FXIIIa)

The expressed plk-IGF-I Ea (as previously described in [293]) and IGF-I wild-type (Genentech) incubated with a 5-fold molar excess of Q-peptide in the presence of 11 µL of 10 U/mL FXIIIa. These reactions were incubated at 37 °C for 30 min in 100 µL reaction volumes with slight agitation in the presence of 2.5 mM $CaCl_2$ and 20 mM Tris-HCl (pH adjusted to 7.6 at room temperature). These reaction products were subjected to Vivaspin 6 ultrafiltration spin columns (3000 MWCO PES membranes, Sartorius, Gottingen, Germany) to remove the excess Q peptide. After that, copper-free strain-promoted alkyne-azide cycloaddition (SPAAC) reaction was performed to label the azide group of the Q-peptide and the coupling product with a fluorescent dye (DBCO-5,6-carboxyrhodamine 110) in 20 mM Tris buffer (20 mM Tris-HCl, 150 mM NaCl, pH 7.6) for 1 h at room temperature in the dark. After coupling, the reaction mixture was directly transferred to a 15% SDS-PAGE gel and visualized on a Gene flash Doku system (Syngene, Cambridge, UK) for fluorescence detection of the protein-dye conjugate followed by Coomassie brilliant blue staining.

The plk-IGF-I Ea presenting agarose beads (prepared as described in [293]) were coupled with Q-peptide by TGase-catalyzed reaction as described above. After the reaction, beads were briefly spun down and washed several times with 20 mM Tris buffer (20 mM Tris-HCl, 150 mM NaCl, pH 7.6). 100 µL of 1.25 µg/mL DBCO-Cy5 dyes in 20 mM Tris buffer was added to the beads and incubated for 1 h at room temperature in the dark. The resulted products were subsequently imaged using a Zeiss Observer Z1 epifluorescence microscope at 10-fold magnification.

2.3.3 Site-specific conjugation of plk-IGF-I Ea with azide-PCL-FGF2

2.3.3.1 Expression and purification of azide-PCL-FGF2

The expression system BL21 (DE3), cotransformed with pET-11a/8(TAG)-PCL-FGF2 and pRSFDuet-1 vector were inoculated directly from glycerol stock (kindly provided by Marcus Gutmann) in LB media containing 100 µg/mL carbenicillin and 40 µg/mL kanamycin for 16 h at 33 °C with shaking. 100 mL of the saturated seed culture was then transferred into 2 L fresh TB medium supplemented with 2 mM $MgSO_4$, 100 µg/mL carbenicillin and 40 µg/mL kanamycin in 4× 2 L baffled flasks. Cells were incubated at 37 °C and 3 mM azido-L-lysine was added at an OD600 of 0.3, and protein expression was induced at an OD600 of 0.7 with 1 mM IPTG. Cells were harvested after 6 h and spun at 4500 g for 20 min at 4 °C.

The cell pellet was resuspended in heparin binding buffer (12 mM sodium phosphate, 300 mM NaCl, pH 7.4, supplemented with 1 mM PMSF) and ultrasonicated at 4 °C. The cell lysate was centrifuged at 4500 g for 30 min at 4°C, again at 10,000 g for 60 min at 4°C and filtered with a 0.22 µm syringe filter. The filtered supernatant containing azide-PCL-FGF2 was applied to a 1-mL heparin-sepharose high-performance resin column (GE Healthcare, HiTrap Heparin HP affinity column) previously equilibrated in heparin binding buffer using an FPLC system (GE Healthcare, Äkta purifier). The column was washed with 15 CV of binding buffer, and bound protein was eluted with a linear gradient of NaCl in 12 mM phosphate buffer (pH 7.4) (0.3–1.5 M over 45 CV at 1 mL/min). 5-mL fractions were collected, and the fraction containing azide-PCL-FGF were dialyzed against PBS containing 1 mM DTT at 4°C and stored in PBS containing 3 mM DTT at -80 °C. Concentration was determined using the Bradford assay with BSA as a standard. Purified azide-PCL-FGF2 was analyzed by SDS-PAGE.

2.3.3.2 Click reaction between plk-IGF-I Ea and azide-PCL-FGF2

IGF-FGF conjugate was synthesized performing CuAAC of plk-IGF-I Ea with engineered azide-PCL-FGF2 as reported previously.[293] In brief, plk-IGF-I Ea solution and azide-PCL-FGF2 were mixed in various molar ratios (1:1, 1:3) with 250 µM THPTA, 2.5 mM sodium ascorbate and 50 µM $CuSO_4$. The mixture was incubated with gentle agitation.

The coupling efficiency was optimized by varying the temperature (room temperature, 4 °C, 37 °C) and incubation time (overnight, 0.5 h, 1 h, 2 h). At last, the reaction was stopped by addition of 5 mM EDTA, before analysis by SDS-PAGE.

2.3.3.3 Purification of tandem IGF-FGF conjugate

The purification of the resulted product was performed using different methods.

(i: Heparin affinity chromatography) After the click reaction, the resulted mixture was loaded on a HiTrap Heparin HP column (GE Healthcare, Freiburg, Germany) pre-equilibrated with 12 mM phosphate buffer containing 300 mM NaCl (pH 7.4). After washing with the same buffer, IGF-FGF was eluted with a NaCl gradient in 12 mM phosphate buffer (pH 7.4): 0.3–1.5 M. After purification, peak fractions were dialyzed against PBS and analyzed by Western Blot with antibody to FGF2 (produced in mouse, Merck).

(ii: Ultrafiltration purification) After CuAAC reaction, the reaction mixture was subjected into Vivaspin 2 ultrafiltration spin column (20,000 MWCO, CTA membranes, Sartorius Stedium, Goettingen, Germany) followed by centrifugation at 4000 g for 30 min at 4 °C. A small aliquot of the concentrated sample was analyzed by SDS-PAGE, and the rest was stored at -20 °C until further usage.

3. Results

3.1 IGF-I variants preparation

3.1.1 Genetically engineered IGF-I variants containing N-terminally His_6-tagged thioredoxin and a thrombin cleavage site

3.1.1.1 Cloning of IGF-I into the pHisTrx vector

After amplification of the IGF-I gene by PCR, the target DNA fragments (234 bp, indicated by an arrow) were detected on the agarose gel (**Figure 10A**). IGF-I insert (234 bp) were subsequently double digested with high fidelity version of BamHI and EcoRI, followed by extraction from 1% agarose gel, and then cloned into the pHisTrx backbone to generate pHisTrx/Trx-IGF-I. Restriction digestion of pHisTrx/Trx-IGF-I with SapI and NdeI followed by 1% agarose gel electrophoresis was utilized to screen recombinant clones (**Figure 10B**).

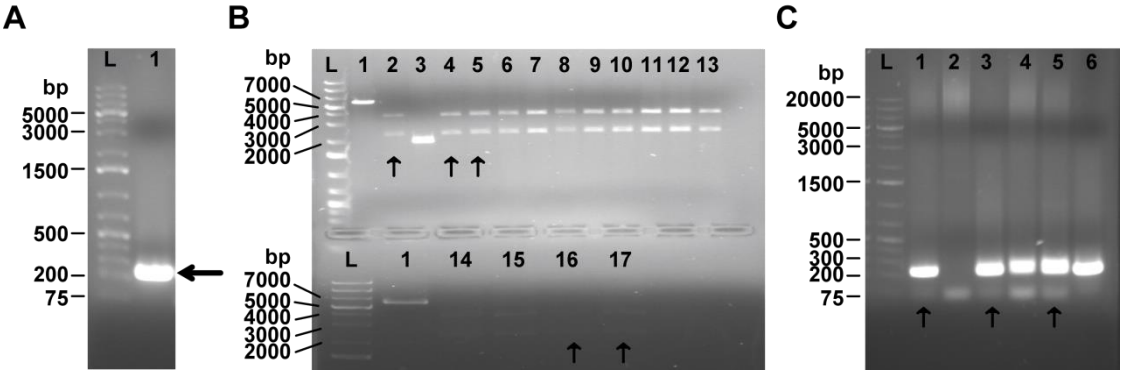

Figure 10. Agarose gel electrophoresis. DNA ladder (lane #L) in the range from 75–20000 bp. (A) PCR amplified product of IGF-I gene (lane #1) was fractionated on 1% agarose gel electrophoresis. (B) Double digested recombinant pHisTrx/Trx-IGF-I by SapI and NdeI was applied. Lane #1, digested pHisTrx as a control, suggesting poor digestion by SapI and NdeI. Lane #2 – #17, referred to as recombinant clones 1–16, respectively. Lane #2, #4 – #17 demonstrated the similar cleavage pattern, and thus five of them was randomly selected (indicated with up arrow symbols) to be further screened and using recombinant clone 2 (lane #3) as a control. (C) Agarose gel electrophoresis of PCR assays for the identification of the recombinant clone 1 (lane #1), clone 2 (lane #2), clone 3 (lane #3), clone 4 (lane #4), clone 15 (lane #5) and clone 16 (lane #6). Recombinant clone 1 (lane #1), clone 3 (lane #3), and clone 15 (lane #5) were sent for DNA sequencing (indicated with up arrow symbols).

DNA fragments of different sizes were observed on the agarose gel, and the majority of selected recombinant vectors showed the similar cleavage pattern except for recombinant clone 2 (**Figure 10B**, lane #3). Note that the control vector pHisTrx (without insert) failed to be cleaved into two fragments, making the diagnostic restriction digestion assay a less precise strategy to determine the

correct insert. Therefore, several recombinant plasmids with the similar cleavage pattern were randomly selected (indicated by the up-arrow symbols), with recombinant clone 2 (**Figure 10B**, lane #3) as a negative control, to be further screened by PCR amplification using primer pair FP_B/IGF & RP_IGF/E (**Figure 10C**). The amplified fragments (**Figure 10C**, lane #1, #3, #4, #5 and #6) were detected between 200 and 300 bp which was in line with the size of the IGF-I gene, and recombinant clones 1 (**Figure 10C**, lane #1), 3 (**Figure 10C**, lane #3) and 15 (**Figure 10C**, lane #5) were subsequently sequenced. DNA sequences and deduced amino acids of Trx-IGF-I gene (recombinant clones 3 and 15) were aligned with the known amino acid sequences of IGF-I. Thus either clone can be used for the following experiments.

3.1.1.2 Expression of the IGF-I fusion protein (Trx-IGF-I) in different *E. coli* strains

The expression of recombinant Trx-IGF-I was compared in three different *E. coli* hosts including BL21 (DE3), Rosetta 2 and SHuffle T7, respectively. When the culture was propagated (37 °C, 140 rpm) to at OD_{600} = 0.7, the expression was induced by 0.2 mM IPTG, and then followed by 6 h-cultivation at 37 °C. As shown in **Figure 11A, B and C**, the target protein (Trx-IGF-I), which is about 21.6 kDa, was effectively expressed in all these three strains. SHuffle T7 was more efficient for the expression of Trx-IGF-I and thus was further employed for the optimization of expression conditions. Increasing the induction time from 0–6 h increased Trx-IGF-I expression (**Figure 11A, B, and C**). Bacteria cultivation at reduced temperatures has been used favorably to improve the recombinant protein solubility.[299-301] The *E. coli* SHuffle T7/pHisTrx/Trx-IGF-I expression system was induced for 6 h at 33 °C, or overnight at 25 °C, respectively. The expression levels were analyzed by SDS-PAGE to determine the preferable expression temperature. The results in **Figure 11D** revealed that the productivity of fusion protein at 37 °C and 33 °C was similar (**Figure 11C, D**) and the highest production of target fusion protein was achieved at 25 °C. Thus, the preferable induction temperature was set up at 25 °C. The proportion of soluble and insoluble Trx-IGF-I was roughly determined by analyzing crude cell lysate, clarified cytosolic extract and pellet taken from sonicated BL21 (DE3) and SHuffle T7 cells. The results were shown in **Figure 11E**. The greater proportion of soluble fusion proteins produced relative to the amounts of insoluble counterparts was observed, especially in SHuffle T7 expression system.

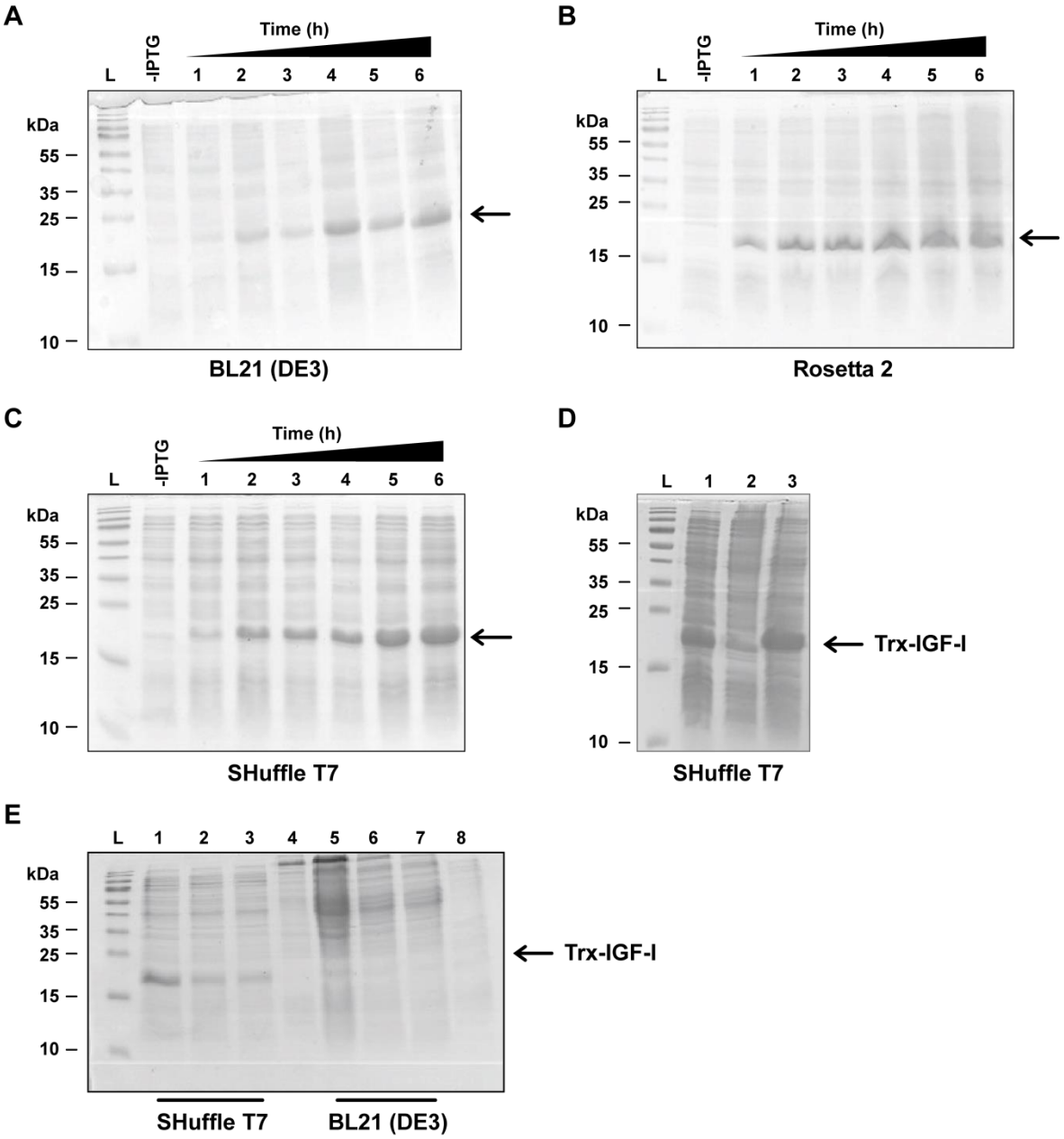

Figure 11. SDS-PAGE analyses of Trx-IGF-I expression in different strains, including BL21 (DE3) (A), Rosetta 2 (B), and SHuffle T7 (C & D). (A-C) target protein (MW=21.6 kDa) were induced by 0.2 mM IPTG for 1–6 h at 37 °C, respectively; (D) Lane #L, protein ladder; Lane #1, target protein (MW=21.6 kDa) induced by 0.2 mM IPTG for 6 h at 33 °C; Lane #2, target protein without IPTG induction as control; Lane #3, target protein induced by 0.2 mM IPTG overnight at 25 °C. (E) SDS-PAGE analysis after BL21 (DE3) & SHuffle T7 cell lysis. Trx-IGF-I with the size of 21.6 kDa was observed (indicated with a black arrow). Lane #L, protein ladder; Lane #1 and #5, crude cell lysate; Lane #2 and #6, supernatant after the first centrifugation at 5000 g for 30 min; Lane #3 and #7, supernatant after the second centrifugation at 10,000 g for 60 min; Lane #4, pellet of BL21 (DE3) after the first centrifugation; Lane #8, pellet of SHuffle T7 after the first centrifugation.

3.1.1.3 Purification of Trx-IGF-I protein

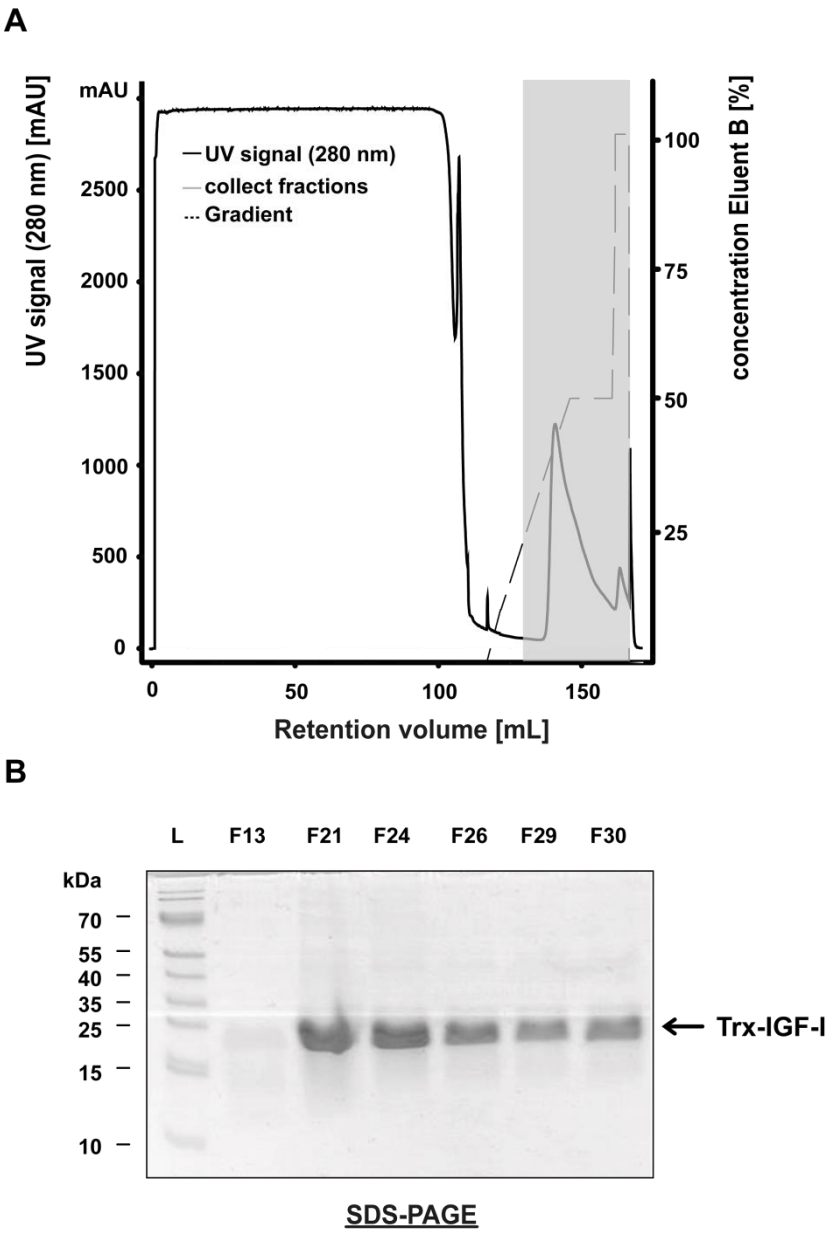

Figure 12. (A) The curve of affinity chromatographic purification of Trx-IGF-I, showing a small peak at the beginning of elution step (Fraction F13) followed a major peak at the retention volume of ~ 150 mL (fractions F21 to F30, marked in grey), all peak fractions were then collected for further analysis. (B) SDS-PAGE analysis of collected eluate samples of affinity chromatography. All the fractions showed the target fusion protein (MW=21.6 kDa) with high purity, were then pooled for the further experiments.

The cultivation was subsequently scaled up to 1 L to obtain sufficient raw material to start the purification process. The target fusion protein having N-terminal His-tag was purified from soluble fraction through routine nickel affinity chromatography, and the affinity chromatography curve of UV280 nm was shown in **Figure 12A**. After the resin binding step, 500 mM imidazole elution buffer was used to elute the target fusion protein and the eluate was analyzed by 15% SDS-PAGE

for the collection of refined IGF-I fusion protein, which exhibited a single band between 15 to 25 kDa corresponding to the molecular weight of Trx-IGF-I (21.6 kDa) protein (**Figure 12B**), suggesting that the fusion proteins were purified to apparent homogeneity by one-step purification. Approximately 21 mg of the purified soluble IGF-I fusion protein was obtained from 1 L of *E. coli* SHuffle T7 culture.

3.1.1.4 Cleavage of Trx-IGF-I protein by thrombin

Even though the Trx sequence could facilitate protein folding and disulfide bond formation,[281, 302-305] its relatively larger size (than IGF-I) may interfere with IGF-I functions to some extent. Therefore, thrombin was employed to remove the fusion partner from IGF-I in the sense that it can specifically cleave target proteins containing the recognition sequence (LVPR ↓GS).

To optimize specificity and efficiency of cleavage, three different ratios of thrombin (GE, Freiburg, Germany) to fusion protein (1 U/mg, 5 U/mg and 10 U/mg) and incubation time (6 h, 12 h, and 24 h) were chosen for small-scale cleavage reactions testing. The reaction was allowed to proceed in the cleavage buffer at room temperature with or without the addition of 1 M urea. The corresponding aliquots were collected and analyzed at different time points. SDS-PAGE and Western Blot were used to analyze the cleavage efficiency of the fusion protein by thrombin. The results demonstrated that the cleavage efficiency was concentration-dependent as well as time-dependent. However, the addition of urea showed negative effect on the cleavage efficiency (**Figure 13A, B**). No clear changes were observed by the effect of $CaCl_2$ concentrations on cleavage of recombinant Trx-IGF-I under the tested conditions. The best cleavage condition found was 10 units for 1 mg fusion protein at room temperature for 24 h. Note that the low yielded IGF-I was almost undetectable in the Coomassie-stained gel (**Figure 13A**).

The small-scale cleavage reaction was also repeated by restriction grade thrombin (Novagen). The cleavage efficiency was optimized by the variation of thrombin concentration (1, 2, 5 U thrombin/mg fusion protein) and reaction time (16, 24 h). A truncated analog of the Trx-IGF-I fusion protein (Trx-IGF-I variant), lacking the last carboxyl-terminal 6-amino acid D region of IGF-I, was used against restriction grade thrombin to evaluate the cleavage efficiency and samples were analyzed by SDS-PAGE (15% gel) followed by staining with Coomassie blue. The production of IGF-I was not enhanced with further increases in the incubation time (24 h) and thrombin concentration (2 U/mg, 5 U/mg) (**Figure 13C**). This result suggested a plateau tendency of cleavage under all treatments. Therefore, 1 U/mg was employed for further optimization.

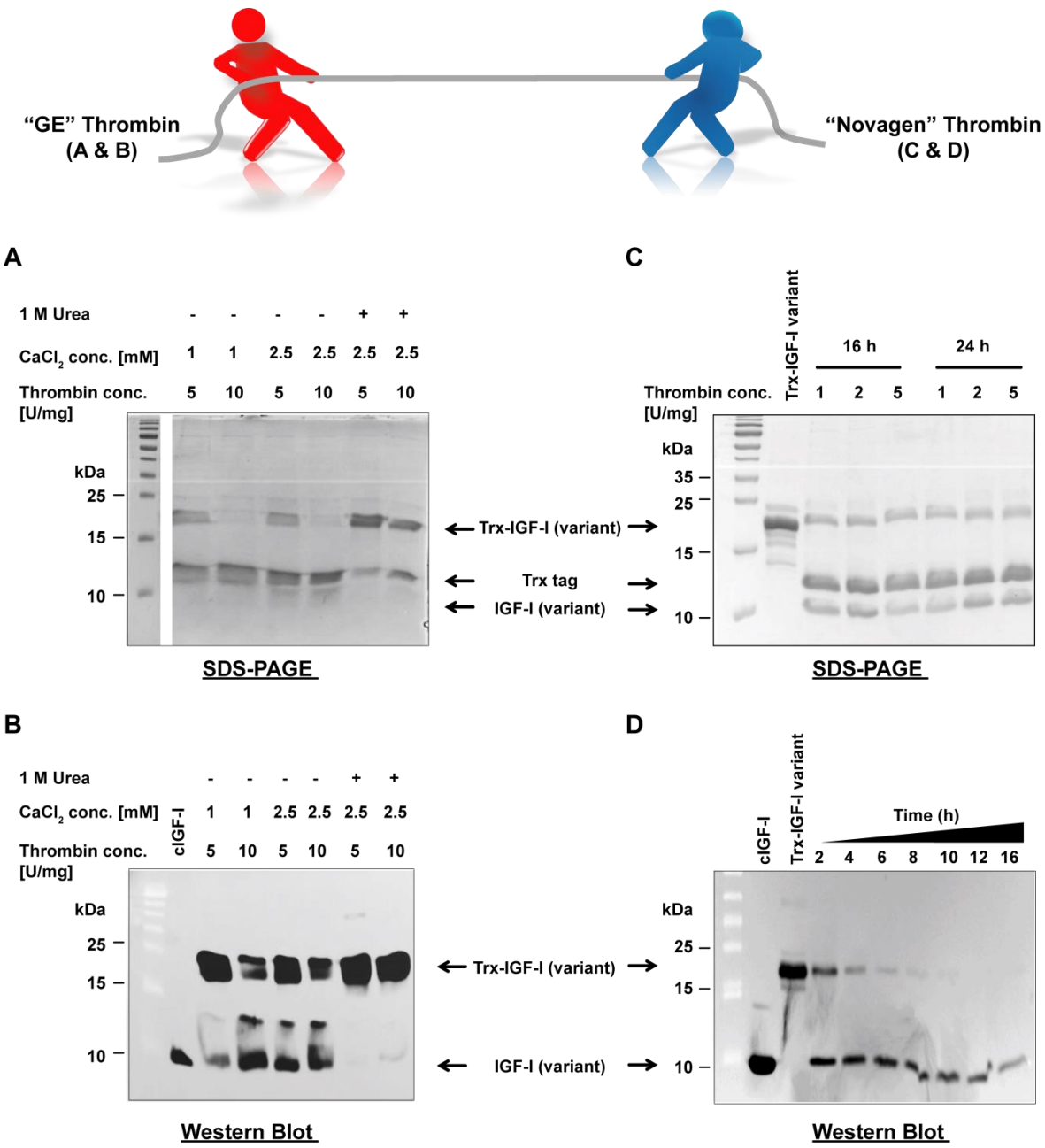

Figure 13. Cleavage efficiency of fusion protein with different amounts of thrombin (GE, Freiburg, Germany) as followed by (A) SDS-PAGE (15%) and (B) Western Blot using an anti-IGF-I antibody. Note: 5 U, 10 U of thrombin was added to 1 mg of fusion protein in 1x thrombin cleavage buffer (pH 8.4) for 24 h, respectively. Samples treated with 1 U/mg of thrombin for 6 h, 12 h, 24 h and by 5 U/mg, 10 U/mg of thrombin for 6 h, 12 h were not shown here. (C-D) Cleavage efficiency of Trx-IGF-I variant (which lacks the last carboxyl-terminal 6-amino acid D region of IGF-I) with restriction grade thrombin (Novagen). (C) SDS-PAGE analysis of the cleavage pattern of the fusion protein with different thrombin amounts. Samples were cleaved at room temperature in 1x thrombin cleavage buffer (pH 8.4) with 1, 2, and 5 U/mg of thrombin and collected at 16 h and 24 h of incubation for SDS-PAGE analysis. (D) Time course of thrombin cleavage of Trx-IGF-I variant protein. One unit of thrombin was added to 1 mg of the fusion protein in 1x thrombin cleavage buffer

(pH 8.4). The reaction was incubated at room temperature, and aliquotes were taken at various time points and analyzed by Western Blot using an anti-IGF-I antibody.

The time-course study of Trx-IGF-I variant cleavage by restriction grade thrombin was performed to optimize the digest conditions. Samples were taken from the digest mixture at various time points (2, 4, 6, 8, 10, 12, and 16 h) and analyzed by Western Blot to estimate the preferable incubation time. **Figure 13D** demonstrated the time-dependent progression of the thrombin digest, with nearly complete processing of the fusion protein in 6 h and thus was used in the scale-up cleavage study.

3.1.1.5 Purification of wild-type IGF-I

After stopping the cleavage reaction with 1 mM PMSF, IGF-I was purified through p-aminobenzamidine resin to trap the thrombin protease and subsequently by nickel affinity chromatography to bind the histidine-tagged Trx sequence. Then, the flow-through containing IGF-I without His-tag sequence was collected and loaded onto a C18 column for further purification. The RP-HPLC fraction eluting at the retention volume of ~ 450 mL contained the protein of interest (**Figure 14**).

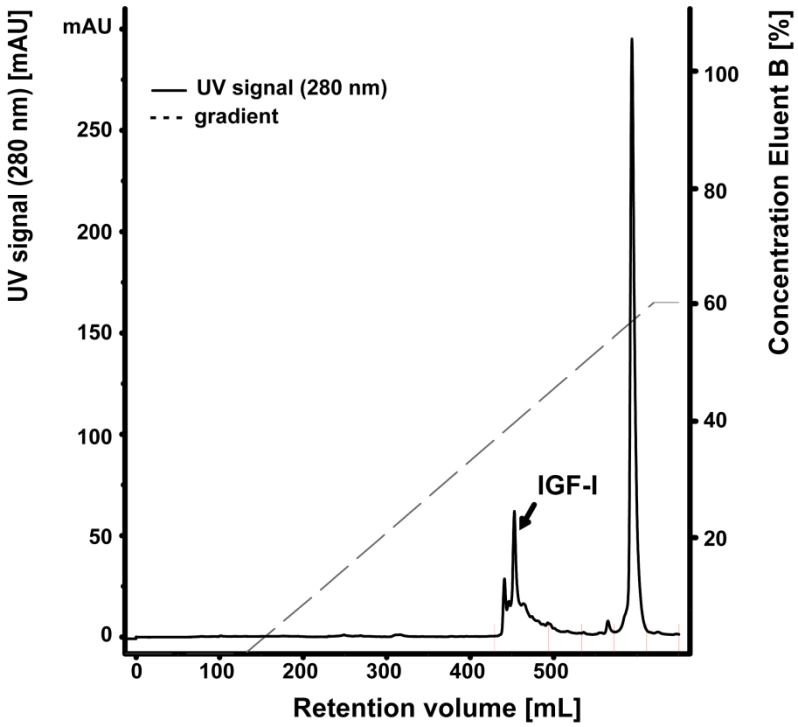

Figure 14. Representative reverse phase HPLC elution profile with single peaks containing IGF-I. The target protein was indicted by a black arrow. Elution was by acetonitrile gradient.

3.1.1.6 Characterization analysis of wild-type IGF-I

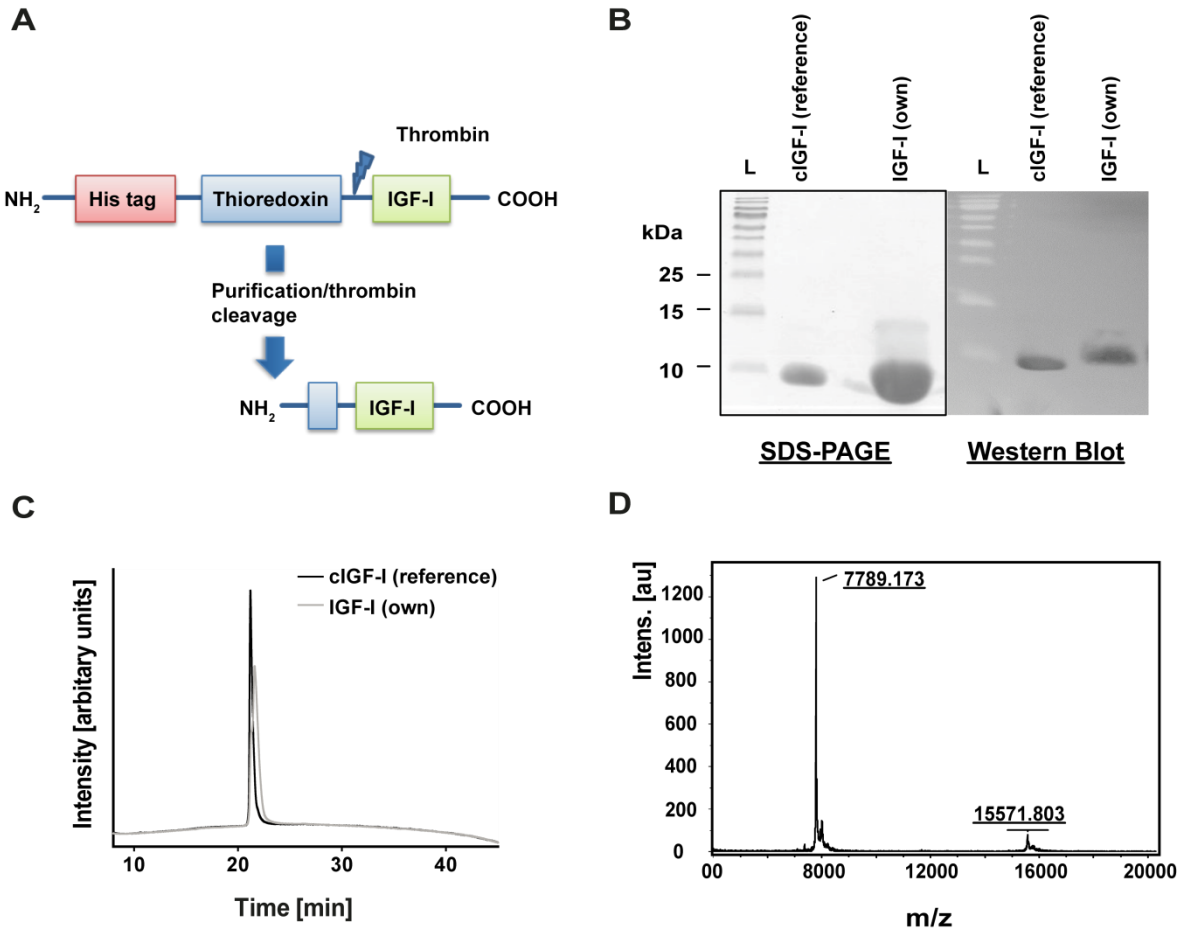

Figure 15. (A) Scheme of IGF-I as Trx fusion protein; the final purification step by thrombin cleavage yielded IGF-I with two additional amino acids (GS) at its N-terminus. (B) Coomassie blue staining (left panel) and Western Blot (right panel) analysis of purified IGF-I after reverse phase HPLC. The right panel showed that the Western Blot analysis of IGF-I using an anti-IGF-I antibody. cIGF-I: commercial IGF-I (Genentech). (C) HPLC graph of purified IGF-I (own, light gray) and commercial IGF-I (cIGF-I, dark gray). (D) MALDI MS spectra of purified IGF-I (Obs. average mass = 7789.173 Da, calc. oxidized average mass = 7792.867 Da)

Figure 15B displayed SDS-PAGE and Western Blot analysis of the purified IGF-I from Trx-IGF-I fusion protein after thrombin cleavage (**Figure 15A**). Multiple-step purification of IGF-I resulted in a single band with high purity as determined by SDS-PAGE. Moreover, the identity of purified IGF-I was shown by Western Blot analysis using an anti-IGF-I antibody and reverse phase HPLC profile in comparison to commercial IGF-I (**Figures 15B & C**). MALDI/TOF MS analysis of the purified protein suggested that the Gly–Ser dipeptide remained to the IGF-I sequence after successful cleavage with thrombin (Obs. average mass = 7789.173 Da, calc. oxidized average mass = 7792.867 Da). MS data (**Figure 15D**) showed a major peak having an average intensity of

7789.173 Da corresponding to the monomeric state of the protein, whereas a weak peak having an average intensity of 15571.803 Da corresponding to the dimer state of the protein of interest.

3.1.1.7 Construction of the expression vector pET-11a/Trx-plk-IGF-I

Once the fusion strategy for wild-type IGF-I production had been established, mutant IGF-I was assessed. Gene-specific primers were designed to incorporate TAG codon into IGF-I cDNA sequence, and the fragment was amplified from pCMV6-XL4/IGF-I by PCR. The amplicon was then cloned into the vector pHisTrx to generate Trx-plk-IGF-I fragment, followed by subcloning into pET-11a vector to generate pET-11a/ Trx-plk-IGF-I for IGF-I mutant protein expression.

```
Synthesized IGF-I mut   1    ATGGGTCATCACCATCACCATCACGGTTCTGGTATGAGCGATAAAATTATTCACCTGACT
                             ||||||||||||||||||||||||||||||||||||||||||||||||||||||||||||
   Theoretic IGF-I mut  1    ATGGGTCATCACCATCACCATCACGGTTCTGGTATGAGCGATAAAATTATTCACCTGACT

Synthesized IGF-I mut   61   GACGACAGTTTTGACACGGATGTACTCAAAGCGGACGGGGCGATCCTCGTCGATTTCTGG
                             ||||||||||||||||||||||||||||||||||||||||||||||||||||||||||||
   Theoretic IGF-I mut  61   GACGACAGTTTTGACACGGATGTACTCAAAGCGGACGGGGCGATCCTCGTCGATTTCTGG

Synthesized IGF-I mut   121  GCAGAGTGGTGCGGTCCGTGCAAAATGATCGCCCCGATTCTGGATGAAATCGCTGACGAA
                             ||||||||||||||||||||||||||||||||||||||||||||||||||||||||||||
   Theoretic IGF-I mut  121  GCAGAGTGGTGCGGTCCGTGCAAAATGATCGCCCCGATTCTGGATGAAATCGCTGACGAA

Synthesized IGF-I mut   181  TATCAGGGCAAACTGACCGTTGCAAAACTGAACATCGATCAAAACCCTGGCACTGCGCCG
                             ||||||||||||||||||||||||||||||||||||||||||||||||||||||||||||
   Theoretic IGF-I mut  181  TATCAGGGCAAACTGACCGTTGCAAAACTGAACATCGATCAAAACCCTGGCACTGCGCCG

Synthesized IGF-I mut   241  AAATATGGCATCCGTGGTATCCCGACTCTGCTGCTGTTCAAAAACGGTGAAGTGGCGGCA
                             ||||||||||||||||||||||||||||||||||||||||||||||||||||||||||||
   Theoretic IGF-I mut  241  AAATATGGCATCCGTGGTATCCCGACTCTGCTGCTGTTCAAAAACGGTGAAGTGGCGGCA

Synthesized IGF-I mut   301  ACCAAAGTGGGTGCACTGTCTAAAGGTCAGTTGAAAGAGTTCCTCGACGCTAACCTGGCC
                             ||||||||||||||||||||||||||||||||||||||||||||||||||||||||||||
   Theoretic IGF-I mut  301  ACCAAAGTGGGTGCACTGTCTAAAGGTCAGTTGAAAGAGTTCCTCGACGCTAACCTGGCC

Synthesized IGF-I mut   361  GGTTCTGGTTCTGGCCTGGTTCCGCGTGGATCCGGACCGTAGACGCTCTGCGGGGCTGAG
                             ||||||||||||||||||||||||||||||||||||||||||||||||||||||||||||
   Theoretic IGF-I mut  361  GGTTCTGGTTCTGGCCTGGTTCCGCGTGGATCCGGACCGTAGACGCTCTGCGGGGCTGAG

Synthesized IGF-I mut   421  CTGGTGGATGCTCTTCAGTTCGTGTGTGGAGACAGGGGCTTTTATTTCAACAAGCCCACA
                             ||||||||||||||||||||||||||||||||||||||||||||||||||||||||||||
   Theoretic IGF-I mut  421  CTGGTGGATGCTCTTCAGTTCGTGTGTGGAGACAGGGGCTTTTATTTCAACAAGCCCACA

Synthesized IGF-I mut   481  GGGTATGGCTCCAGCAGTCGGAGGGCGCCTCAGACAGGCATCGTGGATGAGTGCTGCTTC
                             ||||||||||||||||||||||||||||||||||||||||||||||||||||||||||||
   Theoretic IGF-I mut  481  GGGTATGGCTCCAGCAGTCGGAGGGCGCCTCAGACAGGCATCGTGGATGAGTGCTGCTTC

Synthesized IGF-I mut   541  CGGAGCTGTGATCTAAGGAGGCTGGAGATGTATTGCGCACCCCTCAAGCCTGCCAAGTCA
                             ||||||||||||||||||||||||||||||||||||||||||||||||||||||||||||
   Theoretic IGF-I mut  541  CGGAGCTGTGATCTAAGGAGGCTGGAGATGTATTGCGCACCCCTCAAGCCTGCCAAGTCA

Synthesized IGF-I mut   601  GCTTAATAA  609
                             |||||||||
   Theoretic IGF-I mut  601  GCTTAATAA  609
```

Figure 16. DNA sequence alignment of synthesized and theoretic Trx-plk-IGF-I mutant using the NCBI's database and BLAST program, showing 100% sequence identity. The mutation site was highlighted in red.

The confirmation of recombinant clones was carried out by a combination of diagnostic restriction digestion (by SapI and NdeI) and PCR assay using primer pair FP_N/Trx-plk-IGF-I and RP_IGF/E, as well as DNA sequencing. Synthesized Trx-plk-IGF-I gene shared 100% sequence identity with

the theoretic Trx-plk-IGF-I fragment (**Figure 16**). The IGF-I mutant contained the amber stop codon TAG coding for the unnatural amino acid, propargyl-L-lysine (plk), at Glu-3 (marked in red) of IGF-I [GAG (E) → TAG (Plk)].

3.1.1.8 Effects of strains on Trx-plk-IGF-I expression

Genetic code expansion was utilized to site-specifically incorporate plk into Trx-IGF-I. More specifically, expression of Trx-plk-IGF-I mutant with an amber codon (TAG) introduced in Glu-3 of IGF-I (**Figure 16**) required co-expression of an orthogonal amber suppressor PylRS/ tRNAPyl CUA pair from *Methanosarcina barkeri*.[242-245] This PylRS/ tRNAPyl CUA pair was encoded by two plasmids, pET-11a/Trx-plk-IGF-I, and the pRSFDuet-1 construct, inducible with IPTG. Limitations for the codon expansion strategy are its low suppression yields and truncated protein formation, which is possibly caused by the competition between endogenous RF1 and orthogonal $tRNA_{CUA}$ for recognizing the UAG stop codon (**Figure 17A)**.[277, 306] To optimize the yield of full-length Trx-plk-IGF-I, we qualitatively screened several culture parameters including the concentration of plk added to the medium, bacterial strains and the expression time by SDS-PAGE and (in certain cases) Western Blot. Western Blot image (**Figure 17B)** demonstrated the target Trx-plk-IGF-I with a molecular weight of 21.6 kDa expressed in all *E. coli* strains [BL21 (DE3), SHuffle T7 and Rosetta (DE3)]. Furthermore, not only full-length Trx-plk-IGF-I but also a shorter form (truncated protein, MW=14.1 kDa) (**Figure 17C)**, most probably corresponding to premature translation termination caused by the amber codon, were observed in the bacterial lysates. Recoded *E. coli* (C321.ΔA.exp) with UAG termination abolished[307, 308] decreased the truncated protein expression over conventional strains in the SDS-PAGE analysis (**Figure 17C)**. Despite this modification, the expression of full-length soluble protein did not increase in the recorded C321.ΔA.exp (**Figure 17C**). Increasing plk concentration (10 mM) facilitated the production of Trx-plk-IGF-I (**Figure 17B, C &D)**, and thus was applied for the further study. Trx-plk-IGF-I was expressed from 2 h post induction. However, the decreased signal was observed at certain time points dependent on the stain used. Due to co-express the bulk of endogenous host proteins and low specificity of Coomassie gel staining, endogenous bacterial contaminants with the similar electrophoretic mobility as the target protein could not be ruled out. Thus polyhistidine pull-down assay followed by SDS-PAGE analysis was used to identify the protein of interest more accurately. After 8 h-induction, *E. coli* BL21 (DE3) was harvested for the pull-down assay. In accord with our previous results, increased plk amount enhanced the formation of Trx-plk-IGF-I. In the presence of strong denaturing agents such as 8 M urea, Trx-plk-IGF-I in the pellet was soluble, and then detected by SDS-PAGE followed by Coomassie blue staining (**Figure 17D**, upper panel), and further confirmed by Western Blot using IGF-I antibody (**Figure 17D**, bottom panel).

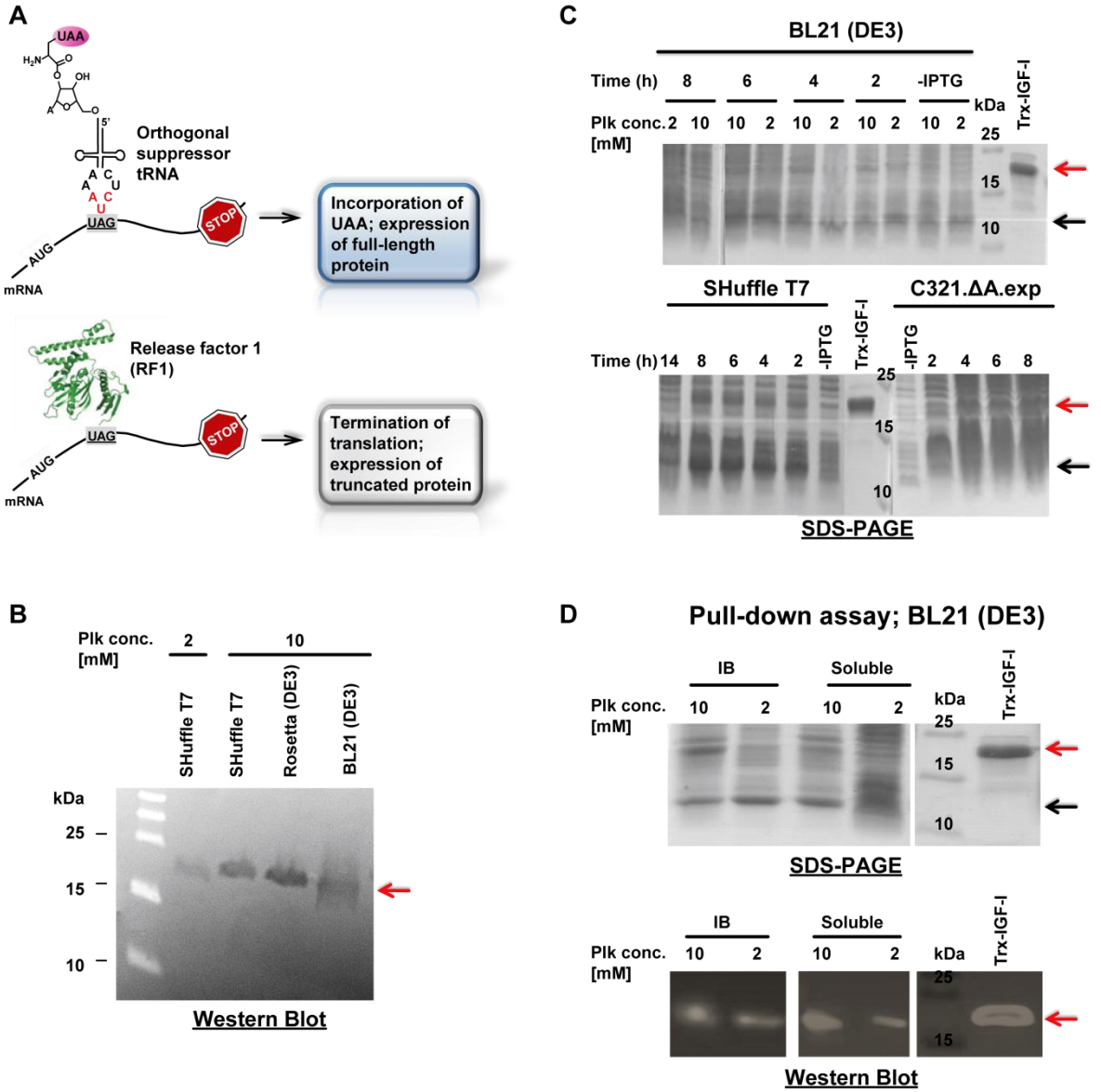

Figure 17. (A) RF1 mediated termination competes with the incorporation of uAA in response to the UAG stop codon. Adapted from Ref.[309] with permission from The Royal Society of Chemistry. (B) Western Blot analysis of the expression level of Trx-plk-IGF-I in various *E. coli* expression strains [BL21 (DE3), SHuffle T7 and Rosetta (DE3)] with the addition of different plk amounts (2 mM vs. 10 mM). The primary antibody used was an anti-IGF-I antibody (Goat). (C) SDS-PAGE analyses of Trx-plk-IGF-I expression in BL21 (DE3), SHuffle T7, and C321.ΔA.exp under different induction time. (D) Pull-down assay with Trx-plk-IGF-I. SDS-PAGE (upper panel) and Western Blot (bottom panel) analysis of soluble and insoluble fractions (inclusion body, IB) of BL21 (DE3) cultures expressing Trx-plk-IGF-I recovered from the pull-down fraction. Full-length Trx-plk-IGF-I (MW=21.6 kDa) was indicated by a red arrow, while the truncated protein (MW=14.1 kDa) was indicated by a black arrow.

Expression of the soluble recombinant was also confirmed by Western Blot (**Figure 17D**, bottom panel), showing signal to a similar extent in comparison with that of pellet fraction, and thus both cytosolic fraction and pellet were collected for the following Trx-plk-IGF-I extraction.

3.1.1.9 Purification & cleavage of Trx-plk-IGF-I

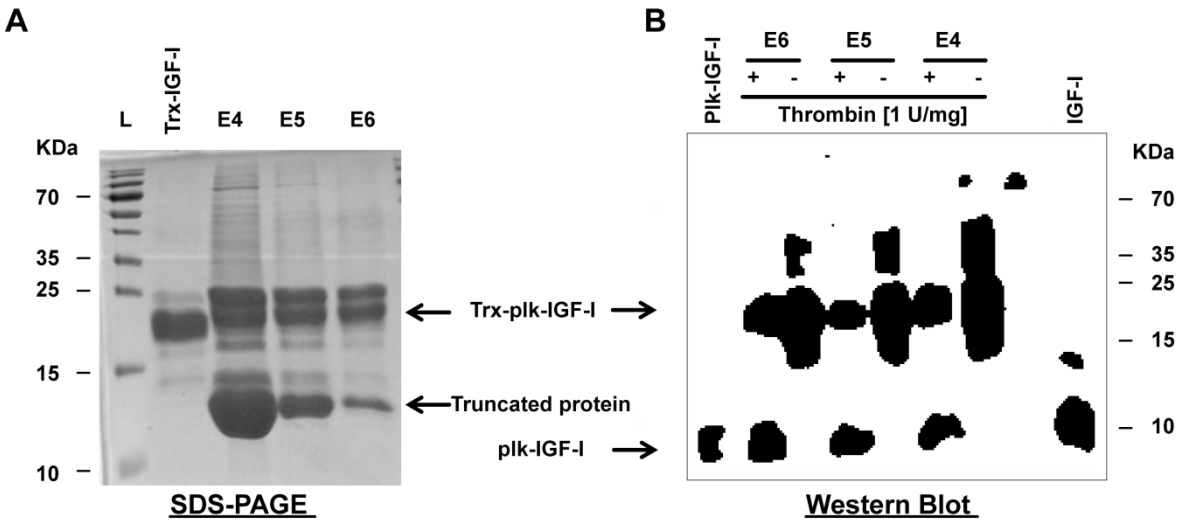

Figure 18. (A) SDS-PAGE analysis of collected eluate samples (E4, E5 & E6) of affinity chromatography. All the fractions showed the full-length target protein (MW=21.6 kDa) and truncated protein (MW=14.1 kDa). (B) Western Blot analysis of thrombin digestion. 1 U of thrombin was subjected into 1 mg fusion protein in 1x thrombin cleavage buffer (pH=8.4). After incubation for 6 h at room temperature, thrombin-treated samples and samples without thrombin treatment were detected on Western Blot probed with the anti-IGF-I antibody. After cleavage, plk-IGF-I was purified through the p-aminobenzamidine resin and reverse phase HPLC and was then identified by Western Blot. Note that protein precipitated in 1x thrombin cleavage buffer (pH=8.4), and decreasing pH level was thus employed in the following optimization study.

Besides the full-length Trx-plk-IGF-I, the truncated product was also riched by nickel affinity chromatography (**Figure 18A**). Purified Trx-plk-IGF-I was digested using restriction grade thrombin (Novagen) to yield plk-IGF-I. To optimize the cleavage efficiency, we screened several reaction parameters including thrombin concentrations (1, 2, and 5 U thrombin/mg fusion protein), incubation time (6, 12, and 24 h) and reaction pH levels (pH=8.4, 7.2 and 6) (**Figure 18B**, **Table 7**). Thrombin-treated reaction was allowed to proceed at room temperature. The corresponding aliquots were collected and analyzed by Western Blot. Although elevated pH levels (pH=8.4) demonstrated positive effects on the cleavage of Trx-plk-IGF-I by thrombin, precipitation was observed under this condition (data not shown). The pH of the cleavage buffer was changed by dialysis against 1x PBS (pH=7.2 or 6) to decrease the precipitation of protein during the cleavage process. No clear differences were observed on the yield of plk-IGF-I between reaction pH=7.2 and pH=6 used. The results suggested time-dependent, as well as concentration-dependent cleavage efficiency, the general overview of the presence of plk-IGF-I signal in Western Blot, was shown in **Table 7**.

Table 7. Effect of pH, thrombin concentration, incubation time on cleavage efficiency. The presence of plk-IGF-I was detected by Western Blot with anti-IGF-I.

Processed parameters			**Western Blot results**
pH	$C_{thrombin}$ [U/mg]	$T_{incubation}$ (h)	Plk-IGF-I signal
6	1	6	✕
6	1	12	✕
6	1	24	✓
6	2	6	✕
6	2	12	✓
6	2	24	✓
6	5	6	✓
6	5	12	✓
6	5	24	✓
7.2	1	6	✕
7.2	1	12	✓
7.2	1	24	✓
7.2	2	6	✓
7.2	2	12	✓
7.2	2	24	✓
7.2	5	6	✓
7.2	5	12	✓
7.2	5	24	✓

The optimized cleavage condition found was 2 units of thrombin for 1 mg fusion protein at pH=6 for 12 h and thus were employed in the scale-up cleavage study. Purified plk-IGF-I (lane #plkIGF-I) was successfully demonstrated by Western Blot (**Figure 18B**). Although many efforts have been made, including the optimization of the bacterial culture parameters and downstream protein purification process, initial attempts to produce plk-IGF-I using thioredoxin fusion strategy failed, due to a particularly low yielding cleavage reaction and poor stability of plk-IGF-I in the cleavage

buffer. Similarly, the use of E-peptide prolonged IGF-I will prevent the small protein from degradation in *E. coli* and managed to bypass a majority of problems associated with *in vitro* cleavage reactions; the results were published in ACS Biomaterials Science & Engineering.

3.2 Dual-functionalized IGF-I variants

3.2.1 Genetically engineered IGF-I Ea with two alkyne functionalities

3.2.1.1 Optimization of Plk-IGF-I Ea-plk expression

In order to monitor plk-IGF-I Ea-plk (MW=11.8 kDa) expression in *E. coli* BL21 (DE3), cells were grown and then induced with 0.1 mM, 0.5 mM or 1.0 mM of IPTG at 27 ºC or 37 ºC, whereupon the induced proteins were detected by Western Blot analysis with an anti-IGF-I antibody (**Figure 19**, **Table 8**).

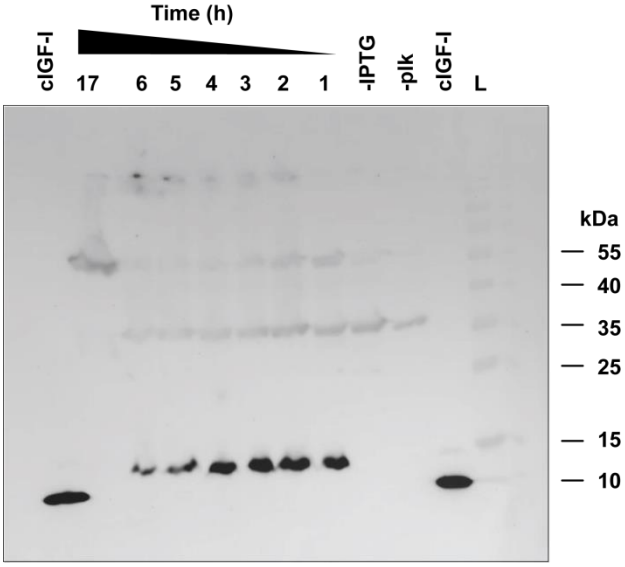

Figure 19. Western Blot analysis of the expression level of plk-IGF-I Ea-plk in *E. coli* BL21 (DE3) with different incubation time at 37 °C by 1 mM IPTG. The primary antibody used was an anti-IGF-I antibody (Goat). Lane #L, protein ladder; commercial IGF-I (cIGF-I) as the control.

Table 8. Effect of cultivation temperature, IPTG concentration, incubation time on plk-IGF-I Ea-plk expression. The presence of plk-IGF-I Ea-plk was detected by Western Blot with anti-IGF-I.

Process parameters			**Western Blot results**
Temp. (°C)	C_{IPTG} [mM]	$T_{incubation}$ (h)	Plk-IGF-I Ea-plk signal
37	1	1–6	✓
37	1	17	✕
27	1	1–6	✓
27	1	18	✕
27	0.5	1-6	✓
27	0.1	1–2	✕
27	0.1	3	✓
27	0.1	4	✕
27	0.1	5	✓
27	0.1	6	✕

The expression in TB medium at 37 ºC with 10 mM plk resulted in a strong band between 10 and 15 kDa after 1 h (**Figure 19**), and the signals increased by increasing the induction time until 4 h followed by a decreased signal over time, and no plk-IGF-I Ea-plk signal was observed at 17 h, suggesting proteolytic degradation. Also, several faint impurity bands were observed between 35 and 55 kDa for all plotted cell lysate samples. A similar trend was also found in the samples cultured at 27 ºC with 1 mM or 0.5 mM IPTG (general overview was shown in **Table 8**). No clear differences in the protein expression at 27 ºC were observed between 0.5 mM IPTG and 1 mM IPTG induction. The lower IPTG concentration (0.1 mM) negatively influenced the expression of plk-IGF-I Ea-plk. Although the expression of plk-IGF-I Ea-plk was detected successfully on Western Blot, it was unrecognizable by Coomassie blue staining irrespective of the optimization condition used (data not shown here).

3.2.1.2 Optimization of the refolding process

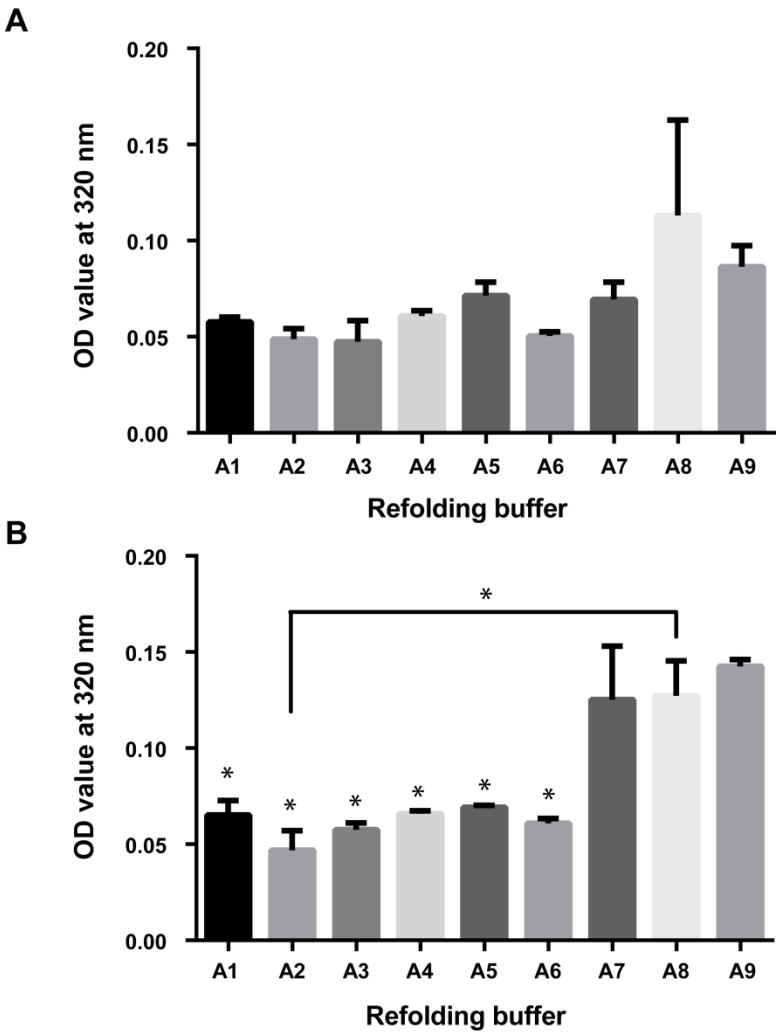

Figure 20. Nine refolding conditions were tested at (A) room temperature and at (B) 4 °C. A refolding condition giving low turbidity showed low protein aggregation. An asterisk ($p < 0.05$) located above the turbidity columns indicated significance between the other refolding buffer and A9 condition. An asterisk ($p < 0.05$) located above the black line indicated significance between the A2 condition and A8 condition. The statistical analysis used was the one-way ANOVA test. Bars on graph indicated standard deviation (n=3).

As collected from published literature, most of IGF-I proteins expressed in *E. coli* were insoluble as inclusion bodies due to its ineffective and inefficient refolding process in bacterial cells.[310] After scale-up to 1 L cultivation at 37 °C, recombinant plk-IGF-I Ea-plk in the pellet was unfolded with 6 M guanidine HCl and refolding buffer were screened as described in **section 2.3.1.3**. No significant differences in aggregates formation were observed among the nine refolding buffers used at room temperature (**Figure 20A**), whereas the addition of ethanol resulted in high turbidity levels (more aggregates formation) during the refolded process at 4 °C (**Figure 20B**). No significant differences in the turbidity levels among A1, A2, A3, A4, A5, A6 buffers were found

during the refolded process at 4 °C, thus either one of the above six buffers could be used for the further optimization of the refolding experiment.

Unfolded proteins were refolded in A1 buffer either at 4 °C for 36 h (Method I) or at room temperature for 1 h (Method II). The refolded plk-IGF-I Ea-plk was dialyzed against PBS and concentrated through PES ultrafiltration membrane or lyophilization. The precipitation of protein samples was observed during concentration in a spin device (Vivaspin 6). The concentrated supernatant, aggregation via Vivaspin 6 and reconstructed freeze-dried samples were loaded into SDS-PAGE followed by Western Blot analysis. The presence of plk-IGF-I Ea-plk in the inclusion body was confirmed by Western Blot (**Figure 21A**). Additionally, the refolding temperature influenced the outcome, with the absence of plk-IGF-I Ea-plk signal in concentrated supernatant via Vivaspin 6 (data not shown), and the presence of a weak plk-IGF-I Ea-plk signal (MW= 11.8kDa) (**Figure 21A**, lane #2) detected in the precipitation sample after concentrating using Vivaspin 6 by Method I. Refolding through Method II, no plk-IGF-I Ea-plk signal was found in aggregates after concentrating using Vivaspin 6 (data not shown), whereas concentrated supernatant via Vivaspin 6 showed a strong plk-IGF-I Ea-plk signal (**Figure 21A**). No plk-IGF-I Ea-plk signal was detected in reconstructed freeze-dried samples by either Method (data not shown). Thus, the concentrated supernatant (Method II) was subjected to SDS-PAGE followed by Coomassie blue staining (**Figure 21B**) for the further analysis.

3.2.1.3 In-gel tryptic digestion and mass analysis

Many impurities were found on SDS-PAGE (**Figure 21B,** lane #2), the area with expected size (11.8 kDa, indicated by a square) was further excised and subjected to trypsin digestion followed by ESI/MS analysis. The spectrum of plk-IGF-I Ea-plk showed 4 peptide fragments [amino acid 38 to 50: m/z = 1438.646; amino acid 22 to 36 (carbamidomethylation (CAM) modified): m/z = 1724.843; amino acid 37 to 55 (CAM modified): m/z = 2340.170; amino acid 38 to 68 (CAM modified): m/z = 3570.772 Da] (**Figure 21C**), implying that plk-IGF-I Ea-plk was expressed successfully. However, we are not aware if plk-IGF-I Ea-plk expressed as a full-length protein or the truncated form (stopped at the second mutation site) as the low protein amount was not sufficient to detect the residual fragments. The low expression yield hindered us from further chromatographic purification, and another strategy was needed for the development of dual functionalized biologics with modification at two distinct positions.

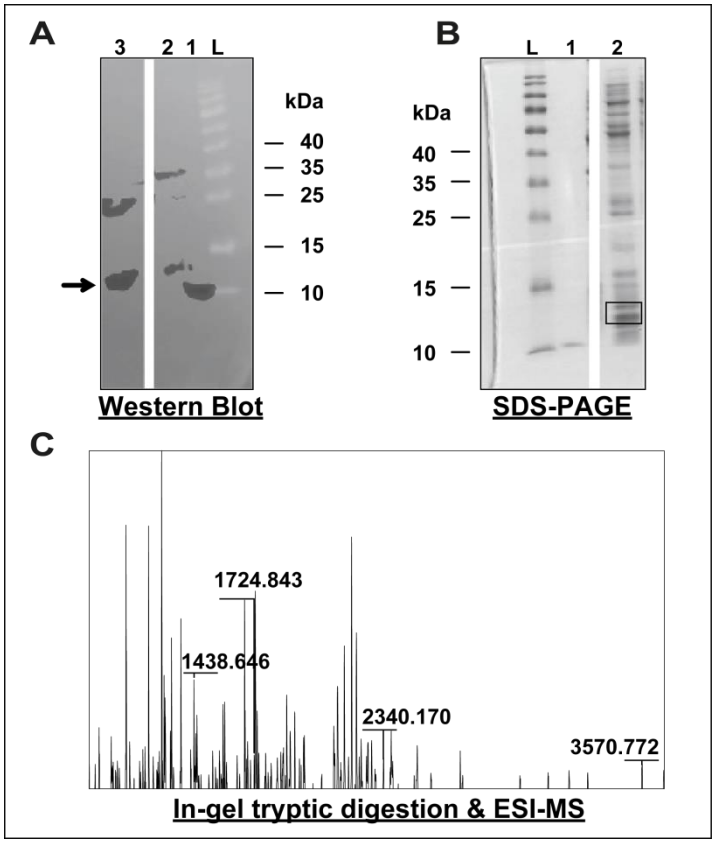

Figure 21. (A) Western Blot analysis of refolded plk-IGF-I Ea-plk. Lane #L, protein ladder; Lane #1, commercial IGF-I as control; Lane #2, precipitation of protein (Method I) after concentrating via Vivaspin; Lane #3, concentrated supernatant (Method II) via Vivaspin. The protein of interest, plk-IGF-I Ea-plk (MW=11.8 kDa), was indicated by a black arrow. (B) SDS-PAGE analysis of the concentrated supernatant sample via a spin device. Lane #L, protein ladder; Lane #1, commercial IGF-I as control; Lane #2, concentrated supernatant (Method II) via Vivaspin 6. (C) Mass chromatogram of plk-IGF-I Ea-plk after in-gel tryptic digestion and ESI-MS.

3.2.2 Clickable plk-IGF-I Ea with TGase reactivity

3.2.2.1 Characterization of Q-peptide

The mass of synthetic Q-peptide was verified using LC-MS (Obs. mass: 1097 Da, Calc. mass: 1097.096 Da) (**Figure 22**).

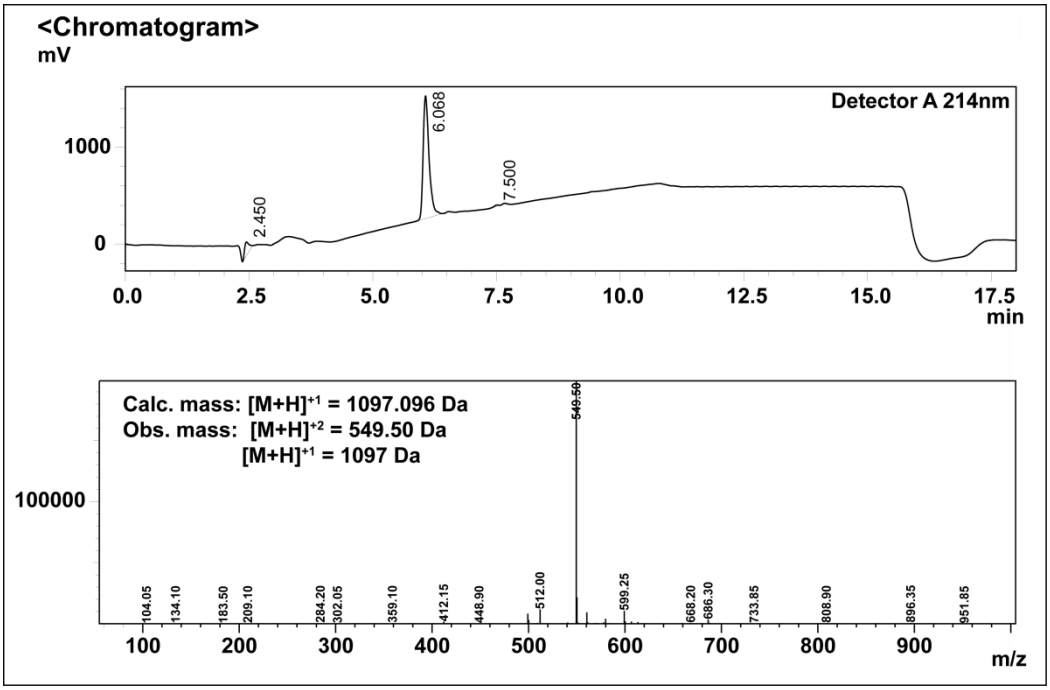

Figure 22. LC-MS analysis of the Q-peptide for evaluation of peptide purity.

3.2.2.2 Tag plk-IGF-I Ea with Q-peptide by TGase-catalyzed reaction

To identify whether plk-IGF-I Ea is a lysine substrate to TGases, plk-IGF-I Ea was incubated with a glutamine substrate modeled from the N-terminus of alpha-2 plasmin inhibitor (Q peptide) in the presence and absence of FXIIIa enzyme, with wild-type IGF-I as a positive control.[217, 233] FXIIIa mediated acyl transfer reaction was followed by SPAAC reaction with DBCO-5,6-carbozyrhodamine as detective conjugation partners (**Figure 23A**). As a positive control in case of the enzymatic transamidation reaction, wild-type IGF-I was crosslinked to glutamine substrate in the presence of FXIIIa before ultrafiltration to remove the unreacted Q-peptide, followed by labeling the azide functionality of the IGF-I: Q-peptide conjugate with DBCO-dye.

A fluorescent band of the IGF-I conjugate with the expected electrophoretic mobility was visualized by SDS-PAGE and fluorescence imaging (**Figure 23B**), whereas negative controls (in the absence of FXIIIa in the first coupling step) exclusively displayed an excess of unconjugated fluorescent dye in the gel. Analogously, cross-linking of recombinant engineered plk-IGF-I Ea to Q-peptide in the presence of FXIIIa was visible as a fluorescent band of ~ 13 kDa molecular weight. This demonstrated for the first time that Ea-extended IGF-I was a lysine donor substrate to TGases.

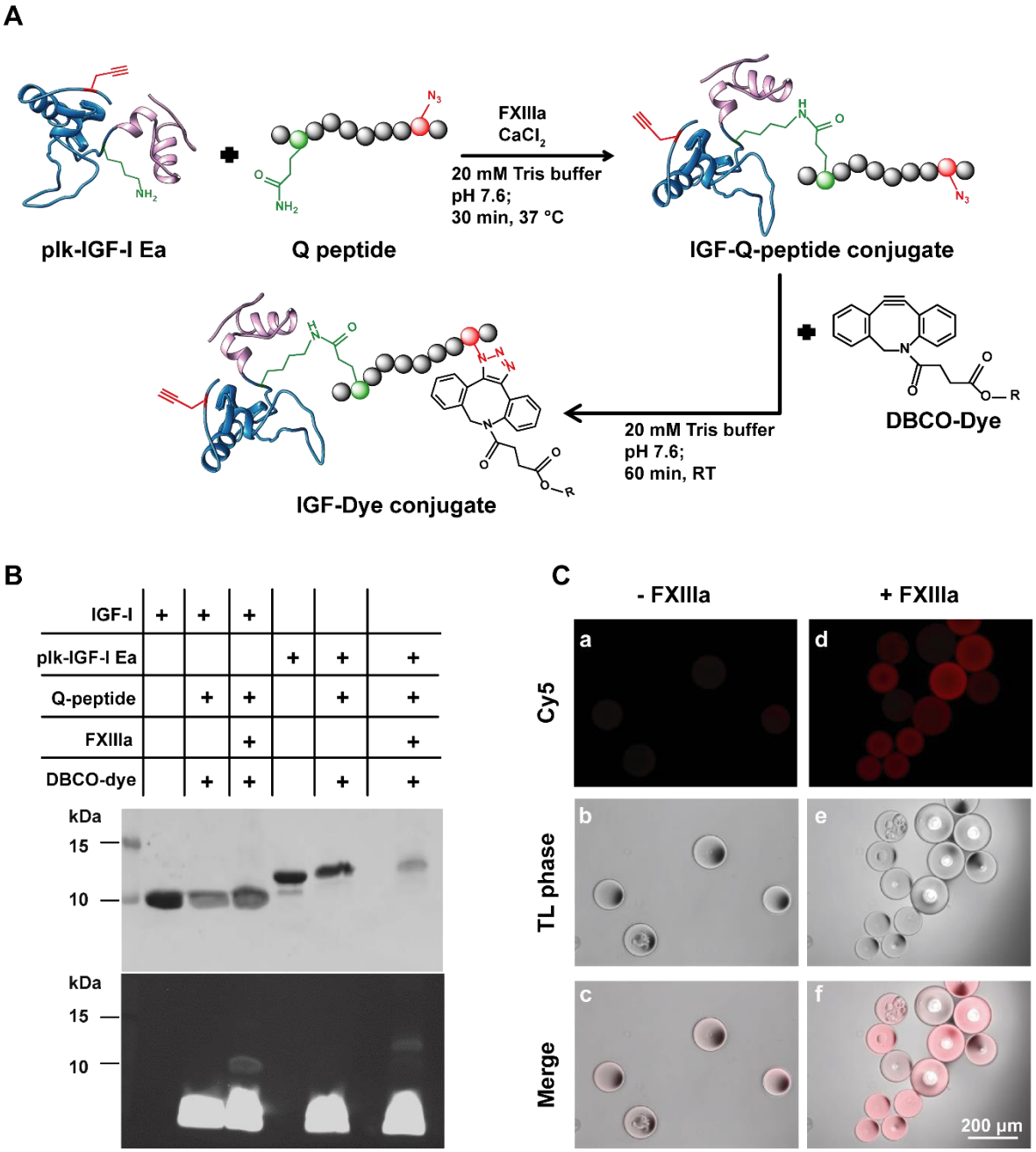

Figure 23. (A) Reaction scheme detailing the synthesis of IGF-I Ea-Dye conjugate via TGase-catalyzed reaction and SPAAC coupling. (B) Conjugation reactions assessed by SDS-PAGE, followed by fluorescence detection of dye-protein conjugates (bottom panel) and Coomassie brilliant blue staining (upper panel). (C) Plk-IGF-I Ea presenting beads were prepared as described in[293] followed by coupling with Q-peptide in the presence (d, e, f) and absence (a, b, c) of FXIIIa, respectively. The conjugates were visualized by fluorescent microscopy via labeling the azide group of the conjugate with DBCO-Cy5.

Moreover, TG reactivity of plk-IGF-I Ea was further verified by fluorescence microscopy image of Q-peptide and plk-IGF-I Ea presenting beads labeled with DBCO-Cy5 dye (**Figure 23C**). Q-peptide was coupled to plk-IGF-I Ea presenting beads in the presence and absence of FXIIIa with the approach described herein. After coupling, the beads were washed intensively to remove FXIIIa

and Q-peptide that was only physically adsorbed to the polymer surface. The enzymatic transamidation was then confirmed by labeling the azide group of the conjugate with DBCO-Cy5, allowing their visualization by fluorescent microscopy. In the absence of FXIIIa, the coupling of Q-peptide to plk-IGF-I Ea-coated agarose beads resulted in a weak fluorescence signal, possibly due to the nonspecific and noncovalent adsorption of Q-peptide to the beads surface (**Figure 23C**, a, c). Strong fluorescence signals were observed when plk-IGF-I Ea-coated beads incubated with Q-peptide in the presence of FXIIIa (**Figure 23C**, d, f).

3.2.3 Site-specific conjugation of plk-IGF-I Ea with azide-PCL-FGF2

3.2.3.1 Optimization of reaction efficiency

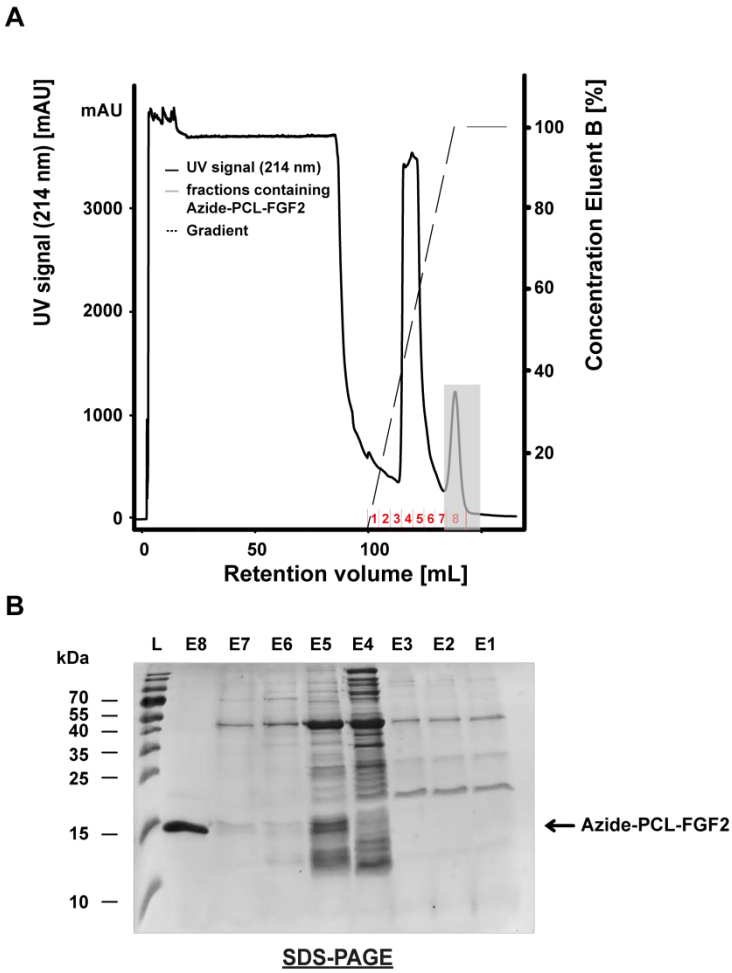

Figure 24. (A) The curve of affinity chromatographic purification of azide-PCL-FGF2. All peak fractions (E1, E2, E3, E4, E5, E6, E7, and E8) were then collected for further analysis. (B) SDS-PAGE analysis of collected eluate samples of affinity chromatography. E8 fraction showed the target protein (MW=17 kDa) with high purity, were then chosen for the further experiments.

To obtain IGF-FGF conjugate, we used an FGF2 variant (azide-PCL-FGF2, MW=17 kDa) containing an azide partner ("clickability"), a matrix metalloproteinase (MMP) – sensitive linker

(GPQGIAGQ) and FGF2 sequence[250] that enabled site-specific conjugation with plk-IGF-I Ea via CuAAC reaction (**Figure 25A**). The recombinant FGF2 variant was expressed in *E. coli* and purified on a heparin affinity column, showing a high purity as judged by SDS-PAGE (**Figure 24**).

To increase the efficiency of plk-IGF-I Ea conjugation with azide-PCL-FGF2, we first decided to use different ratios of the participating therapeutics and lower the reaction temperature to prevent FGF2 aggregation (**Figure 25B**). Caution was also taken by flushing the catalytic Cu (I) mixture with nitrogen for 10 min. The precise labeling was tested at 3:1, and 1:1 azide-PCL-FGF2: plk-IGF-I Ea molar ratios, with their corresponding mixture without copper as a negative control. When subjected the same total amount of proteins for click reaction, no clear differences on the yield of IGF-FGF conjugates (~28 kDa) were observed between the two molar ratios used (**Figure 25B**), while the molar ratios varied ending up with different amounts of unreacted plk-IGF-I Ea (MW=11.6 kDa). Owing to limited source availability, difficulty in isolation, and demand for large amounts of plk-IGF-I Ea, precise labeling with 3:1 azide-PCL-FGF2: plk-IGF-I Ea molar ratio was performed in the following optimization.

Next, a series of experiments were performed by varying the reaction duration and temperature (room temperature and 37 °C). The maximal conjugation with azide-PCL-FGF2 was observed after the reaction at 37 °C for 30 min (**Figure 25C, marked in the red cycle**). Upon SDS-PAGE of the reaction mixture, the bands of conjugates became faint as the increase of incubation time regardless of the incubation temperature (room temperature, 37 °C). Protein precipitation was observed after 1 h incubation, and the best condition (37 °C, 30 min) for labeling was repeated 3 times (**Figure 25D**). Low concentrations of SDS (0.001%, 0.002%) under the best condition did not affect the reaction yield or caused protein precipitation[311] (**Figure 25D**).

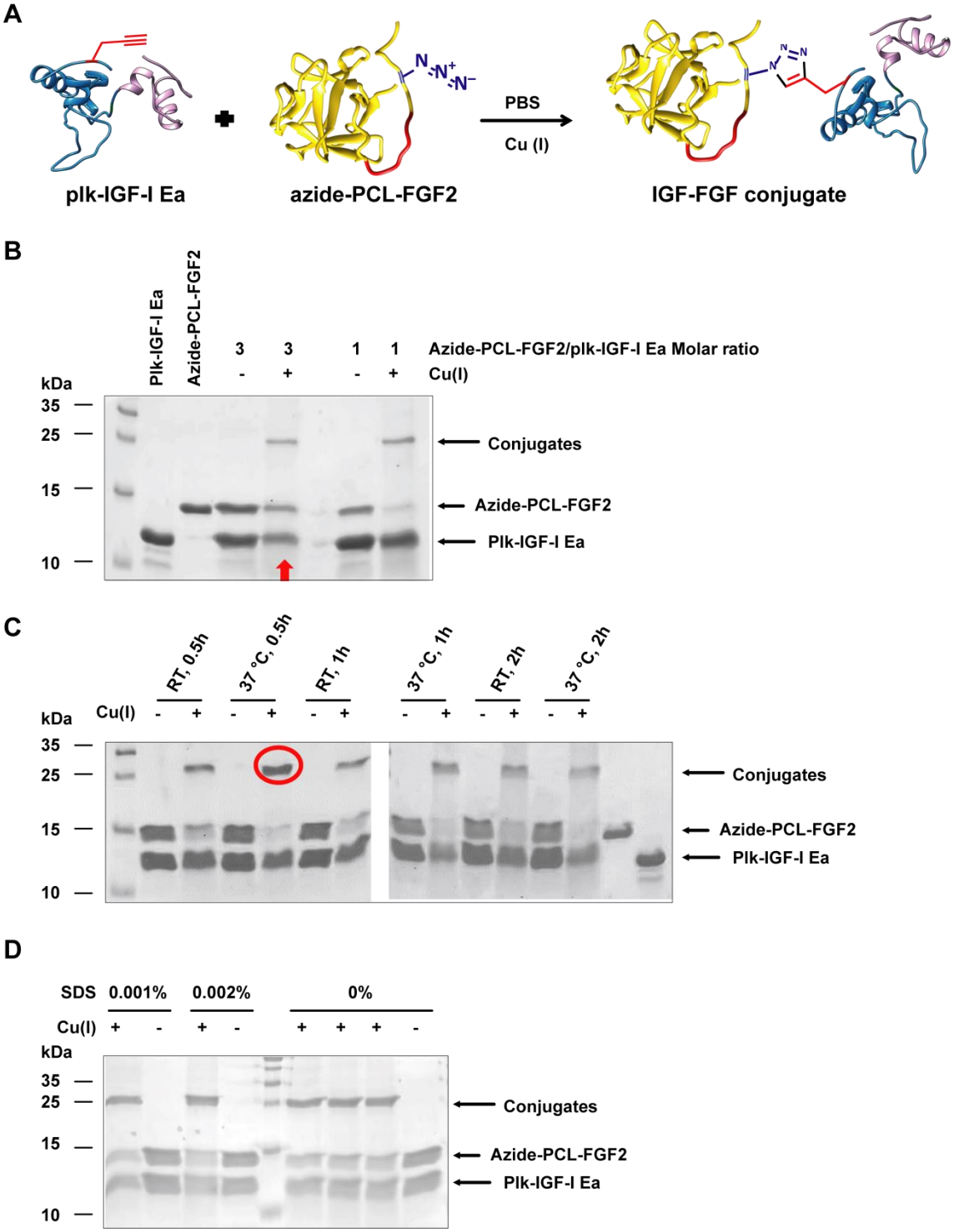

Figure 25. Labeling of plk-IGF-I Ea with azide-PCL-FGF2 (FGF2 PDB ID: 1BLD). (A) Scheme of reaction schemes detailing the synthesis IGF-FGF conjugate via CuAAC reaction. PCL: protease cleavable linker. (B) The CuAAC reaction was performed at 4 °C overnight with 3:1, and 1:1 azide-PCL-FGF2: plk-IGF-I Ea molar ratios, with their corresponding mixture without copper as a negative control. The 3:1 molar ratio of azide-PCL-FGF2: plk-IGF-I Ea was employed in the following study (indicated with a red arrow). (C) CuAAC reaction yield depended on the reaction time (0.5, 1 and 2 h) and temperature (room temperature and 37 °C). The condition giving maximal reaction efficiency (indicted with a red cycle) was referred to as the

best condition. (D) Influence of anionic detergent (SDS) on CuAAC reaction efficiency. The best condition was repeated for 3 times (n=3), and after the addition of SDS, the reaction mixture was incubated for 30 min at 37 °C.

3.2.3.2 Optimization of purification methods

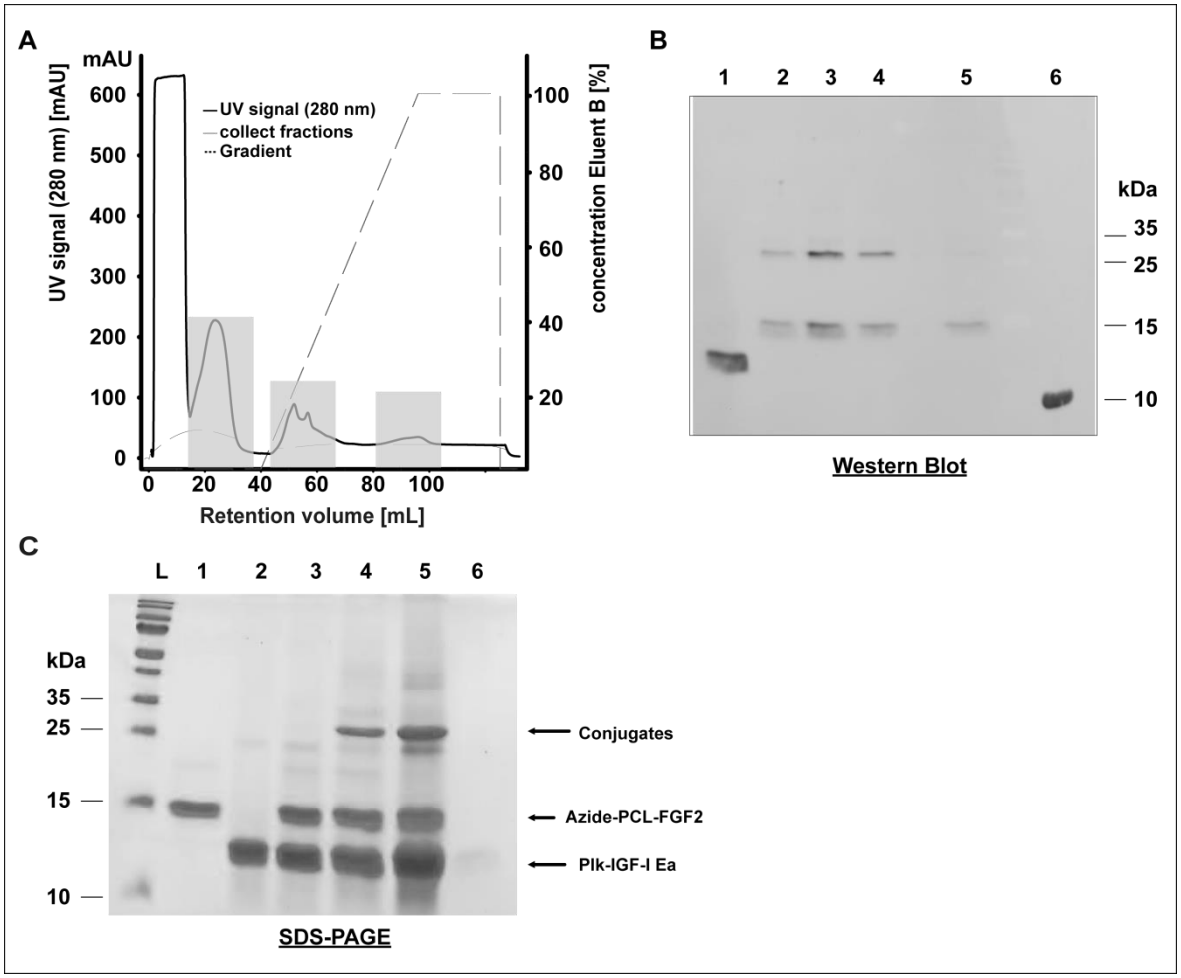

Figure 26. Purification of IGF-FGF conjugates. (A) The reaction mixture was applied to a Heparin Sepharose column. Free azide-PCL-FGF2 was washed out by 1.5 M NaCl, and IGF-FGF conjugate was eluted by ~ 450 mM NaCl. Peak fractions (indicated by grey squares), including flow-through fraction eluted at the retention volume of ~ 20 mL, were analyzed by Western Blot (B) using anti-FGF2 antibody. Lane #1: the flow-through sample; Lane #2 – 4: eluate fractions at the retention volume of ~ 50 mL; Lane #5: eluate fraction at the retention volume of ~ 90 mL; Lane #6: commercial IGF-I. (C) SDS-PAGE analysis of IGF-FGF conjugates purification via an ultrafiltration device. Lane #L: protein ladder; Lane #1: azide-PCL-FGF2; Lane #2: plk-IGF-I Ea; Lane #3: reaction mixture without the catalytic copper as a negative control; Lane #4: reaction mixture; Lane #5: protein samples after concentrating the reaction mixture via a spin device (20,000 MWCO, CTA membrane); Lane #6: filtrate after concentrating the reaction mixture via a spin device (20,000 MWCO, CTA membrane). Note: A larger-scale click reaction (2 mL) decreases the yield of the conjugate (Lane #4).

Several methods, including heparin affinity chromatography, ultrafiltration, have been applied to explore the purification of IGF-FGF conjugate. Since FGF2 (or azide-PCL-FGF2) exhibits high affinity for heparin only when it is natively folded, in general, the unconjugated FGF2 (or azide-PCL-FGF2) is eluted at 1.5 M NaCl (100% elution buffer) (**Figure 24A**). In our case, the conjugated azide-PCL-FGF2 was eluted at ~ 450 mM NaCl (**Figure 26A**). The purified conjugate was undetectable in SDS-PAGE and was visualized by Western Blot using anti-FGF2 antibody (mouse) (**Figure 26B**). In parenthesis non-specific interactions between the antibodies and IGF-I (or plk-IGF-I Ea) was observed. Partial of unconjugated azide-PCL-FGF2 was co-eluted with the expected conjugate. A separation and enrichment strategy based on centrifugal ultrafiltration was employed in this case to reduce the loss of protein samples during purification. Sartorius Vivaspin tangential membrane (20,000 MWCO, CTA membrane) was effective in the recovery and enrichment, but not in the separation of all the proteins used (**Figure 26C**, lane #5).

4. Discussion

Numerous research and efforts have been devoted to assessing the enormous variety of effects of commercially available mature IGF-I on different cells types and tissues during pre- and postnatal development stages. However, as noted in the **Introduction section**, its short biological half-life and several systemic side effects limit the translation of IGF-I into clinical applications. Therefore, the need for enhanced pharmacological properties of IGF-I has become a crucial prerequisite for novel IGF-I based therapies. The site-specific incorporation of uAA with unique chemistries into proteins biosynthetically is a valuable methodology for better therapeutic value. Such reactive handles are of particular importance for the bio-orthogonal modification to label biomolecules with small entities, to generate homogenous polymer-protein and protein-protein conjugates,[287] and for defined surface decoration.[250, 253, 287]

My research is focused on the production of recombinant human IGF-I in *E. coli*. In particular, the project concerns uAA modification of IGF-I with maximal pharmaceutical control over the modification site. The work presented here documents two strategies adopted to obtain uAA incorporated IGF-I, including (i) genetically engineered IGF-I fusion variants (Trx-plk-IGF-I); (ii) engineered indigenous IGF-I Ea therapeutic (plk-IGF-I Ea). This study also provides a possibility for further investigations into the dual functionality of IGF-I to modify the biologic at both positions. Also, preliminary studies about co-delivery of growth factors are performed by the conjugation of plk-IGF-I Ea and FGF2 with a protease cleavable linker in between, reflecting major implications on therapy-oriented research.

Genetically engineered IGF-I fusion variants

Owing to the ineffective and inefficient refolding process, major recombinant (human) IGF-I proteins were found in insoluble fraction of *E. coli*, which completely lost its bioactivity.[312] In comparison to *Bacillus subtillis* and yeast expression systems, *E. coli* expression system is the first choice host for recombinant proteins production due to its cost-effectiveness, the ease of genetic manipulation, rapid growth rate, and the capability for continuous fermentation.[313, 314] Around 30% of the approved recombinant proteins are currently being produced in *E. coli*.[315] The strategy of fusing the therapeutics (such as EGF, FGF2, IGF-I, etc.) with the Trx proved to be very efficient to achieve high-level soluble expression in *E. coli*.[281, 316, 317]

As described in **section 2.2.1.1**, we genetically engineered IGF-I fusion protein (Trx-IGF-I), containing mature human IGF-I, fused to N-terminal His_6-tagged Trx to (i) enhance the solubility and facilitate disulfide bond formation of target protein,[281, 302-305] (ii) allow a high level of protein purification through nickel affinity chromatography by 6x His tag.[318-322] Our results showed that the fusion of Trx could facilitate the soluble IGF-I fusion protein expression, but this efficiency was

significantly varied in different host cells (**Figure 11**). The results had revealed that the productivity of Trx-IGF-I protein was increased dramatically when *E. coli* SHuffle T7 was applied as the host. Besides the elimination of glutathione reductase (gor) and thioredoxin reductase (trxB) gene product, this strain has engineered to overexpress DsbC, which acts as a disulfide bond isomerase and "shuffle" mis-oxidized cysteine pairs, thus allows the recombinant target protein to achieve its properly folded confirmation in the cytoplasm.[323] After systematic optimization of the expression conditions, the expression level of Trx-IGF-I protein was greatly improved when the culture was effectively induced at OD600=0.7 with 0.2 mM IPTG for overnight at 25 °C (**Figure 11D**). The soluble fusion IGF-I protein was purified efficiently by nickel affinity chromatography (**Figure 12**). The overall productivity of soluble Trx-IGF-I (21 mg/L) was achieved. The thrombin cleavage site (LVPR↓GS), which segregates the Trx and the IGF-I protein, permitted the recovery of the IGF-I protein from the fusion protein through thrombin digestion. The SDS-PAGE analysis and Western Blot showed a major band corresponding to IGF-I, with a molecular weight of 7.8 kDa (**Figure 15**). The preparations are homogeneous as determined by HPLC and SDS-PAGE analysis (**Figure 15**). The identity of Gly–Ser–IGF-I (i.e., an additional Gly–Ser dipeptide at the N-terminus) after thrombin cleavage was confirmed by MALDI-MS (**Figure 15D**).

Our developed strategy to produce wild-type IGF-I was then extrapolated to the production of mutant IGF-I. In this variant, the Glu-3 of mature IGF-I is exchanged into an amber stop codon for the incorporation of plk, as this site is not crucial for receptor binding (**Figure 4**). The protein expression at 37 °C for 6–8 h resulted in a signal between 15 and 25 kDa, implying the formation of Trx-plk-IGF-I (**Figure 17**). Competition with RF1 is a limiting factor that depresses the yield of uAA-containing protein[324] (**Figure 17A**). Engineered RF1-deficient *E. coli* strains have been proved its ability to enhance UAG translation efficiency,[278, 288, 325-327] especially for multiple uAAs incorporation[328] (see below for further information). In agreement with recently published data,[325, 327] we found that recorded *E.coli* strain C321.ΔA.exp (i.e., UAG termination abolished) was more efficient at eliminating the truncated proteins. Despite the competition between plk insertion and RF1 in BL21 (DE3) or SHuffle T7, the fraction of Trx-plk-IGF-I produced was higher partly due to higher cell density compared to C321.ΔA.exp.[325] Sufficient amounts of the full-length fusion protein (~ 2 mg/L) were promoted by optimizing induction time, plk amounts and varying the strain. The recovery of plk-IGF-I was obtained by the addition of thrombin (**Figure 18B**). The cleavage efficiency varied depending on the substrates[329] and buffer used with the target protein and other variables (e.g., urea) (**Figure 13A & B**). Although its preferential recognition of the –L–V–P–R–G–S– sequence and cleavage at the R–G bond, thrombin was reported to cleave at secondary sites non-specifically.[329-331] This may partly account for undetectable IGF-I signals in the SDS-PAGE after "GE" thrombin cleavage (**Figure 13B**). This was improved by shorter duration exposure to lower concentrations of restriction grade "Novagen" thrombin (**Figure 13C**). However,

the production of plk-IGF-I was too low arguably as the mutant protein got precipitated during the cleavage study (pH 8.4). Buffer components and pH levels can influence the stability of IGF-I.[157] Adjusting the pH levels of the fusion protein away from the pI of IGF-I (8.3)[332] but still located in the optimum pH range (6–8) of thrombin cleavage activity[333] is rational to increase the yield of the target protein. PBS was reported to be an alternative cleavage buffer for thrombin.[317] After buffer exchanged to PBS (7.2 or 6), protein aggregation was greatly reduced, however, compromised cleavage efficiency of thrombin was observed during the tested pH conditions. One possibility to overcome this issue is replacing the thrombin cleavage site by enterokinase recognized sequence (Asp–Asp–Asp–Asp–Lys-↓-X) with broader reaction scope (temperature range: 4–45 °C; pH range: 4.5–9.5).[334-336] The other possible reason for the presence of precipitation and low cleavage efficiency may be the use of the solubility-enhancing tag, which still maintains their fusion protein (non-native or aggregates conformation) in a soluble state in *E. coli* and may not be readily accessible to an endoprotease[337] (as elaborated further in **Conclusion & Outlook section**).

Naturally occurring IGF-I Ea therapeutic

An alternative strategy is fusing IGF-I with E-peptides (Ea, Eb, Ec) to bypass the obstacles during *in vitro* cleavage process (e.g., low cleavage efficiency, nonspecific cleavage at variant sites). Indigenous pro-IGF-I (IGF-I + E-peptides) demonstrated maintained bioactivity (vide supra), and the deletion of the first dipeptide (Arg–Ser) of Ea-peptide showed increased stability in the presence of serum.[230] Accordingly, we engineered a bioactive and serum stabilized IGF-I Ea with the mutation of Glu-3 into plk, allowing the site-specific conjugation of IGF-I Ea to a fluorophore and carrier particles by CuAAC. Cell proliferation and differentiation were enhanced in close proximity to IGF-I-decorated carrier particles, implying the effect of designed multi-valence on decorated materials.[293]

The dual functionality of IGF-I Ea

Furthermore, we have site-specifically incorporated two uAAs simultaneously into IGF-I Ea therapeutics expressed in *E. coli*, the mutation of Glu-3 of IGF-I and additionally the Lys-29 of the Ea-peptide. Western Blot analysis after the expression at 37 °C showed the signal of plk-IGF-I Ea-plk within 6 h (**Figure 19**). Bacteria cultivation at reduced temperatures has been used favorably to enhance the yield of soluble protein.[299-301] Hence, we expanded the experiments and performed protein expression at 27 °C with various IPTG concentrations. Likewise, the protein expression induced by either 0.5 mM or 1 mM IPTG at 27 °C over 6 h resulted in a signal between 10 and 15 kDa, implying the formation of plk-IGF-I Ea-plk. Despite systematic optimization of the expression conditions, including the use of baffled flasks to increase the gas exchange, the supplement of magnesium sulfate[338] and antifoam agent (poly(propylene glycol)),[339-341] no clear increase in the production of the recombinant protein was observed.

Low protein yields can be attributed to the low efficiency of translation stop codon suppression in producing proteins containing multiple uAAs.[277, 306, 328] Less than 1% efficiency was obtained when it came to incorporating uAA into two sites.[342] Evolved ribosomes, Ribo-X developed by J. Chin and coworkers,[342] increased its efficiency for amber codon suppression (~20% for 2 amber codon sites). The Ribo-X discriminates the orthogonal mRNA by a designed sequence that allows only the synthesis of uAA encoded proteins. They speculated that Ribo-X has a decreased functional interaction with RF1, allowing the suppressor tRNACAU to more effectively compete for A-site binding in the presence of a UAG amber codon on the mRNA.[343] Again, the competition of amber suppressor tRNA with endogenous RF1 is responsible for low uAA incorporation in response to the UAG codon (vide supra). This has been successfully addressed with RF1 targeting strategy, including the use of RF1 knockout strain[278] (vide supra) and CRISPRi-mediated RF1 repression.[277] In comparison with Ribo-X, an RF1 knockout in the JX33 strain showed higher uAA incorporation of a reporter protein with multiple amber codon sites.[328] As amber codon suppression takes advantage of the host cell's translational machinery, proper interactions between the aminoacyl-tRNA synthetase(s) (aaRS) /tRNA pair and cellular components are highly appreciated. Previous work highlighted the potential of improving uAA incorporation efficiency through the optimization of the interaction between suppressor tRNA charged with uAA and elongation factor Tu (EF-Tu).[344, 345] Also, the use of an orthogonal translation system (e.g., Ribo-Q[346] and Ribo-X[342]) which is only responsible for the suppression of nonsense codon provides beneficial options for efficient uAA incorporation (reviewed extensively in [347]). Adjusting other experimental details, such as evolved sequence contexts flanking nonsense codons,[348] the development of expression vectors (e.g., pEVOL vector[349] and pUltra plasmid[350]), and the virus-based gene delivery system,[351] may also help to improve the uAA incorporation system.

For further analysis, priority was given to the refolding of plk-IGF-I Ea-plk from inclusion bodies. An ideal approach for all the refolding screens is to provide a readout that indicates which condition works best, such as bioactivity assay,[289] fluorescence testing for GFP,[352] enzymatic activity assay.[353] However, IGF-I is either not enzymes or has a long journey towards biological assay. A general and practical, rational procedure is applied based on the turbidity of solutions where protein aggregation has occurred.[294, 354, 355] Kinetic competition (as follows) between aggregation and other processes, including folding, exists in most instances of aggregation.

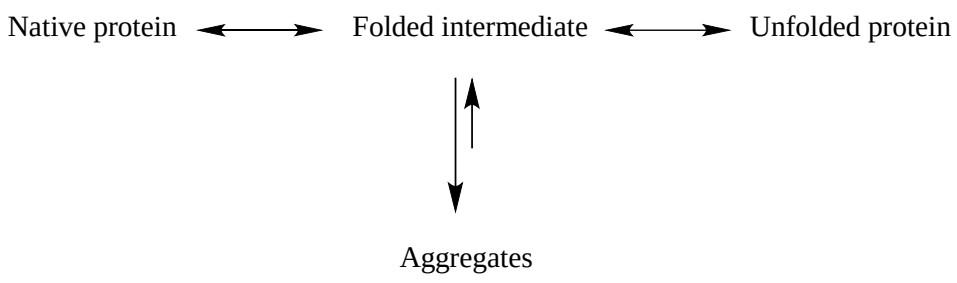

As discussed in the "**Genetically engineered IGF-I fusion variants" section**, recombinantly expressed insoluble protein (as inclusion bodies) can be addressed by decreasing culture temperatures, screening of different bacterial strains, fusion protein constructs (e.g., maltose binding protein, Trx). Protein aggregation during lyophilization greatly depends on the water content of the system.[356-361] Sporadically, dehydration of proteins by lyophilization results in denaturation,[362, 363] probably due to aggregation formation from partially folded intermediates during the ensuing rehydration. Free Cys residues in proteins (either the native or non-native conformations) can be oxidized easily to form disulfide bond linkages or initiate thio-disulfide exchanges[364, 365] or disulfide exchanges via β-elimination (in the disulfide-bonded conformations of protein),[366, 367] leading to protein aggregation. Also, a range in the denaturant solubility of insoluble proteins was described from relatively resistant to solubilization to much more readily dissolved in denaturant.[368] Taken together, these may be the reason for the undetectable plk-IGF-I Ea-plk signal in Western Blot after freeze-dried treatment. Exceeding the solubility limit of a partially folded intermediate, and the presence of intramolecular misfolding due to the nature of the expressed protein (e.g., multiple domains) are probably two common reasons for the formation of aggregates during renaturation.[368] To minimize aggregation, low protein concentrations were utilized by flash dilution of the solubilized protein in refolded buffer. Next, we carried out a preliminary refolding screening (**Figure 20**) focusing on several critical parameters, including temperature, pH levels and additives (see **Appendix C**).[369] The study gives an overall picture, but more in-depth research (bioactivity assay) is urgently needed to find out the optimized condition for a maximum yield of correctly oxidized protein. Refolding inclusion bodies to active IGF-I protein represents a huge challenge, as oxidative refolding of IGF-I *in vitro* yields two disulfide isomers of similar thermodynamic stability: (i) native IGF-I (Cys 6 – Cys 48; Cys 18 – Cys 61; Cys 47 – Cys 52, 60% yield); (ii) scrambled IGF-I (Cys 6 – Cys 47; Cys 18 – Cys 61; Cys 48 – Cys 52, 40% yield).[370] Although the supplement of ethanol increased protein aggregation (**Figure 20B**), it was reported that methanol or ethanol could facilitate the production of the correctly folded IGF-I.[369] The other strategy is to modify the IGF-I sequence, such as the additional positive charge on the Met-end of IGF-I.[371]

Myriad technological hurdles related to plk-IGF-I Ea-plk project lead us to conceive a different strategy to develop dual functionalities of IGF-I variant. As Lys-68 of wild-type, IGF-I was shown to be the sole substrate for FXIIIa[233]; we hypothesized that engineered "clickable" plk-IGF-I Ea[293] was also a substrate for FXIIIa. Next, TGase reactivity of E-peptide extended IGF-I was explored by fluorescent labeled plk-IGF-I Ea through a Q-peptide linker. Very preliminary results obtained by SDS-PAGE and fluorescence microscope, plk-IGF-I Ea cross-linked to glutamine substrate in the presence of FXIIIa. As this did not yet confirm the precise cross-linking site and number of available functional groups, further investigation of these findings with more quantitative and

molecular evidence will be necessary to examine the precise cross-linking site(s) within plk-IGF-I Ea.

Conjugation of IGF-I Ea with FGF2

As we were interested in the synergistic effects of IGF-I, we provided plk-IGF-I Ea in conjunction with a second therapeutic FGF2 via click chemistry, that was thought to be different from the physical combination of FGF2 with IGF-I.[372-374] Engineered azide-PCL-FGF2 contains an azide partner ("clickability"), followed by matrix metalloproteinase (MMP)—sensitive linker (GPQGIAGQ) and FGF2 sequence.[250] MMPs are upregulated in some compromised tissues, including inflamed tendons or tendinitis.[375] The MMP-responsive IGF-FGF conjugates use the protease as a proxy for sensing the disease state of the tendinitis liberating IGF-I and FGF2 only at times of flare.

The presence of copper during the CuAAC reaction leads to concerns relating to traces toxicity in the final product or protein precipitation.[376] The formation of reactive oxygen species (ROS) by the interaction between copper ions and reducing agent (sodium ascorbate) may result in oxidation processes of certain amino acids (e.g., lysine, arginine, cysteine),[377, 378] the cleavage[379] and cross-linking of proteins.[380] The optimal-performing click reaction condition (50 µM $CuSO_4$, 250 µM THPTA, and 2.5 mM sodium L-ascorbate) was also shown to be compatible with NIH 3T3 fibroblasts and HEK 293-F cells.[376] Thus, we carried out the following click reaction at 50 µM copper to minimize these above effects. The conjugation was further optimized by the variation of temperature (4°C, 37 °C, room temperature), reaction time (0.5 h, 1 h, 2 h, overnight) and the addition of anionic detergent SDS (0.001%, 0.002%)[311] (**Figure 25**). Moderate yield for conjugation with azide-PCL-FGF2 was achieved after 30 min at 37 °C. Future work needs to present mass analysis results to confirm the identity of the conjugates. A common procedure to purify FGF2 is heparin affinity chromatography.[250, 311, 317] We achieved small signals in the chromatogram after heparin affinity chromatography and an insufficient separation and yield of the conjugates. Ineffective separation was observed when CTA ultrafiltration membrane (20,000 MWCO) was applied (**Figure 26C**). A well-established strategy to purify protein is size exclusion chromatography[281, 381, 382] and could also afford an opportunity for IGF-FGF conjugates. There are still many possibilities for the improvement in all steps of the process, from the reaction efficiency to the change of purification method. The other option to reduce the copper-induced toxicity is to adopt copper-free click chemistry, for which strained alkyne functional group is genetically incorporated into the protein of interest (IGF-I Ea).[383, 384]

5. *ACS Biomater. Sci. Eng.* 2018

Site specifically conjugated Insulin-like growth factor-I (IGF-I) for anabolic therapy

*Fang Wu[1], Alexandra Braun[1], Tessa Lühmann[1], Lorenz Meinel[1]**

[1]Institute of Pharmacy and Food Chemistry, University of Würzburg, Am Hubland, 97074, Würzburg, Germany

This chapter was originally published in ACS Biomaterials Science & Engineering.

Reprinted with permission from Wu, F., Braun, A., Lühmann, T., Meinel, L. (2018). Site-Specific Conjugated Insulin-like Growth Factor-I for Anabolic Therapy. ACS Biomaterials Science & Engineering 2018 Feb 12, DOI: 10.1021/acsbiomaterials.7b01016. Copyright 2018 American Chemical Society.

ACS Biomaterials SCIENCE & ENGINEERING Letter
Cite This: ACS Biomater. Sci. Eng. 2018, 4, 819−825

Site-Specific Conjugated Insulin-like Growth Factor-I for Anabolic Therapy

Fang Wu,[†] Alexandra Braun,[†] Tessa Lühmann,[†] and Lorenz Meinel*,[†]

[†]Institute of Pharmacy and Food Chemistry, University of Würzburg, Am Hubland, 97074 Würzburg, Germany

Supporting Information

ABSTRACT: Insulin-like growth factor-I (IGF-I) is an inducer of skeletal muscle hypertrophy and blocks skeletal muscle atrophy, rendering it a good therapeutic option for the treatment of severe burn injury for which localized treatment options are particularly interesting. For that, the therapeutic was redesigned via amber codon expression, leading to a propargyl-L-lysine (plk) modified IGF-I (plk-IGF-I Ea) with Ea peptide prolongation at the C-terminus, thereby becoming a substrate for copper(I)-catalyzed azide alkyne cycloaddition (CuAAC) and other bio-orthogonal click chemistries. The plk-IGF-I Ea was site-specifically immobilized to agarose particles, resulting in homogeneous product outcome with retained potency while providing the necessary tools to maximize local and minimize systemic exposure. IGF-I decorated particles outperformed soluble IGF-I in C2C12 induced myotube formation, reflecting the impact of controlled multivalence on decorated materials.

KEYWORDS: *insulin-like growth factor I, IGF-I, bio-orthogonal immobilization, genetic codon expansion, CuAAC, proliferation, myotube formation*

Human insulin-like growth factor-I (IGF-I) is a small, single-chain polypeptide (M_w = 7649 g/mol) stimulating skeletal-muscle cell proliferation and differentiation in culture,[3−7] promoting the synthesis of proteins and nucleic acids,[8] and inducing skeletal muscle hypertrophy and blocking skeletal muscle atrophy.[9−11] The IGF-I gene is alternatively spliced, resulting in IGF-I precursor peptides with extensions of 35−77 amino acids at its C-terminus, referred to as Ea-, Eb- or Ec-peptides.[12] The mature IGF-I peptide consists of 70 amino acids and is posttranslationally processed by the proteolytic removal of their E-peptides. Recombinant human IGF-I (Mecasermin) is approved for treatment of growth failure and shows promising potential in other indications such as atrophic musculoskeletal and neurodegenerative diseases and myocardial infarction.[13−15] However, systemic administration of IGF-I shows adverse effects reflecting its pleiotropic functions,[16] including hypoglycemia,[17] diabetic retinopathy,[18] and neoplastic cell growth.[19,20] These limitations sparked interest in the development of parental IGF-I depot systems, enabling controlled IGF-I release from poly(D,L-lactide-*co*-glycolide) acid (PLGA) and silk fibroin derived materials to warrant maximal efficacy and safety while minimizing systemic exposure.[21−24]

Site-specific decoration strategies allow for homogeneous coupling of proteins to interfaces with precise spatial control, avoiding random immobilization through heterogeneous modification of, for example, endogenous thiol, amine, or carboxyl-groups.[25] Among them, amber codon suppression has evolved as an elegant approach to introduce functionalized unnatural amino acids (uAA) at a predefined site within the protein backbone during protein translation by deploying a pyrrolysine tRNA synthetase (PylRS)/tRNAPyl CUA pair from archaebacteria, including *Methanosarcina barkeri*.[26−29] The incorporation of pyrrolysine (Pyl) derived analogues into recombinantly expressed proteins in *Escherichia coli* was previously shown to allow for bio-orthogonal modification to tag biomolecules with small entities to generate polymer−protein and protein−protein conjugates[30] and for defined surface decoration.[30−32]

Here, we focused on the design, recombinant expression, and site-specific modification of a Ea-peptide prolonged IGF-I therapeutic (IGF-I Ea) by introducing the uAA propargyl-protected lysine (plk) into the biologic's backbone at a predefined site through amber codon suppression[26−32] with the design criteria to retain potency as compared to the unmodified IGF-I with maximal pharmaceutical control over the modification site. The IGF-Ea transcript represents the main pro-IGF-I mRNA in liver[33] and was therefore chosen for site-specific modification. Recombinantly expressed E-peptide prolonged IGF-I variants with deletion of the dibasic protease cleavage site at position 71 and 72 (Arg-Ser) were shown to stabilize IGF-I in serum due to improved IGFBP (IGF-I binding protein) interaction with unaltered therapeutic activity.[34] It is for the retained bioactivity why *N*-terminal amino acids Gly-1, Pro-2, and Glu-3 in the IGF-I molecule display suitable sites for modification.[34] Moreover, a naturally

Received: December 22, 2017
Accepted: February 12, 2018
Published: February 12, 2018

 © 2018 American Chemical Society
DOI: 10.1021/acsbiomaterials.7b01016
ACS Biomater. Sci. Eng. 2018, 4, 819−825

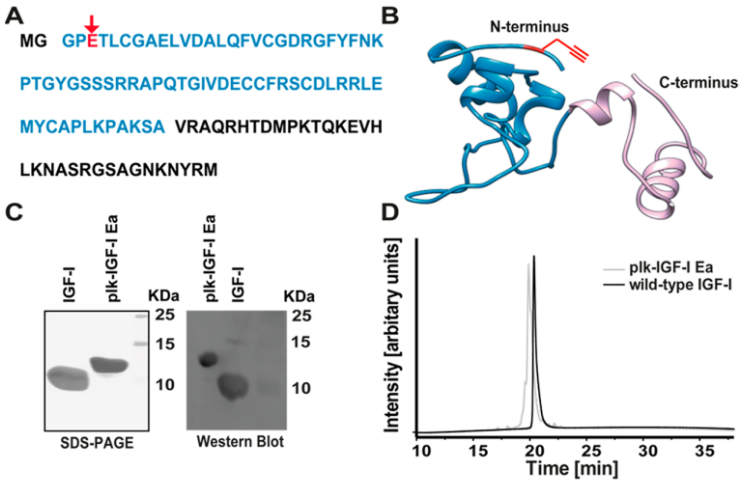

Figure 1. (A) The amino acid sequence of IGF-I Ea was extended with one Gly after initial Met and the unnatural amino acid were incorporated at the position of the amber stop codon TAG, which was introduced at position 3 of wild-type IGF-I (IGF-I sequence marked in blue) using Plk. The depicted Ea peptide lacks the amino acids 71 and 72. (B) Ribbon computer graphics representation of the model of the IGF-I Ea structure (UCSF Chimera). The structure of IGF-I (indicated in blue) is based on IGF-I (PDB ID: 2GF1) solution nuclear magnetic resonance spectroscopy with Glu 3 highlighted in red, and the structure of the Ea peptide (marked in purple) was predicted according to Pep-fold 3.0.[1,2] (C) SDS-PAGE and Western blot of purified plk-IGF-I Ea in comparison to wild-type IGF-I. (D) RP-HPLC analysis of wild-type IGF-I (black) and plk-IGF-I Ea (gray).

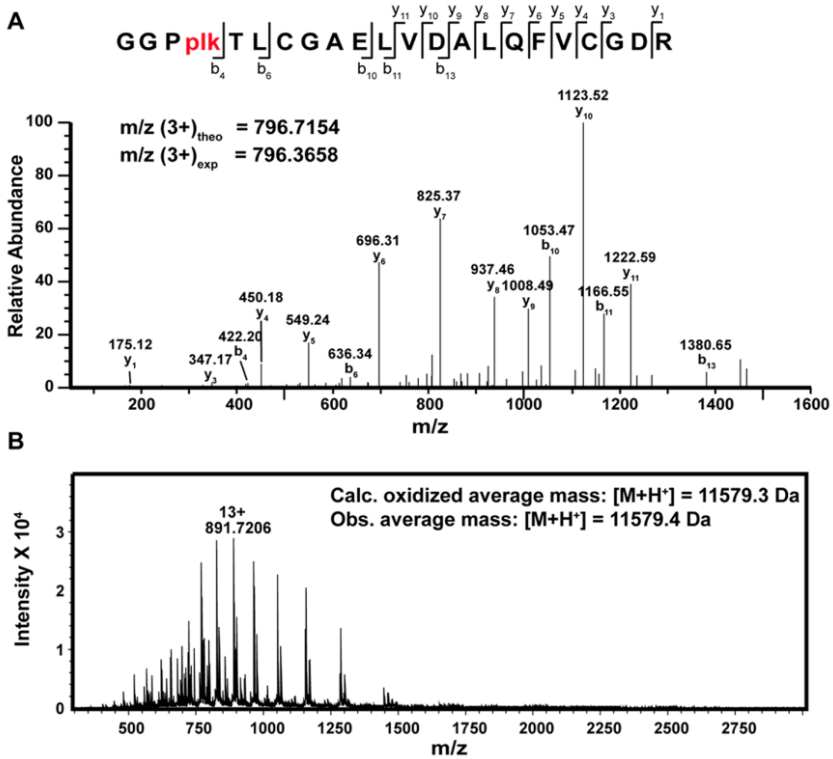

Figure 2. (A) Peptide fragments of trypsinized plk-IGF-I Ea as analyzed by LC-MS/MS. All b and y ions marked in the peptide sequence were found. (B) ESI-MS mass analysis of plk-IGF-I Ea. Obs average mass = 11579.4 Da; calcd oxidized average mass = 11579.3 Da.

truncated variant of human IGF-I (Des(1−3)IGF-I) with the tripeptide Gly-Pro-Glu absent from the *N*-terminus naturally exists,[35] demonstrating unaltered IGF-1R binding affinity and reduced IGF binding protein binding compared to those of the unprocessed protein.[36,37]

To this end, a novel IGF-I therapeutic was engineered with a 33 amino acid Ea peptide extension, lacking the amino acids 71 and 72 (Arg, Ser) and with the incorporation of the uAA plk at the *N*-terminus (Figures 1A and B), rendering this serum stabilized IGF-I variant available for bio-orthogonal click

DOI: 10.1021/acsbiomaterials.7b01016
ACS Biomater. Sci. Eng. 2018, 4, 819−825

chemistries such as copper catalyzed alkyne−azide cycloaddition (CuAAC).[38] Figure 1B depicts the crystal structure of IGF-I Ea, in which the location with plk-exchange (Glu-3-plk) and deletion of amino acids 71 and 72 is highlighted. Accordingly, we introduced an unnatural plk residue into IGF-I through amber codon (UAG) suppression using a pyrrolysyl-tRNA synthethase/$tRNA^{Pyl}_{CUA}$ pair originated from *M. barkeri*.[39,40]

One of the major limitations of the codon expansion strategy is the competition of $tRNA_{CUA}$ with release factor 1 (RF1) at the UAG stop codon, leading to low efficiency of UAA incorporation and inevitable even dominant truncated protein forms.[41,42] Therefore, we qualitatively screened several culture parameters by end point Western blot detection, including bacterial strains, IPTG induction time, plk concentration, and culture media with respect to their potential to promote plk-IGF-I Ea product formation (Figure S1). Expression in the bacterial strain *E. coli* BL21 (DE3) in the presence of 6 mM plk by following a modified Studier autoinduction strategy resulted in a maximal detection of plk-IGF-I Ea (Figures S1B and C). Plk-IGF-I Ea was expressed in inclusion bodies, refolded, and purified by ion-exchange chromatography, followed by reversed-phase high-performance liquid chromatography (RP-HPLC) with an overall yield of 0.4 mg/L. Figure 1C displays SDS-PAGE and Western blot analysis of the purified plk-IGF-I-Ea variant. Purification of plk-IGF-I-Ea resulted in a single band with high purity as determined by SDS-PAGE. Moreover, identity of plk-IGF-I Ea was shown by Western blot analysis and RP-HPLC in comparison to wild-type IGF-I (Figures 1C and D). The introduction of plk at position 3 of IGF-I-Ea peptide was confirmed after trypsin digest and liquid chromatography-tandem mass spectrometry (LC-MS/MS) analysis (Figure 2A). Electrospray ionization mass spectrometry (ESI-MS) analysis of the purified plk-IGF-I Ea protein suggested that the initial Met was removed upon translation by *E. coli* derived methionine amino peptidase (obs average mass = 11579.4 Da; calcd oxidized average mass = 11579.3 Da) (Figure 2B).

The alkyne functionality of plk-IGF-I Ea was further studied for chemical decoration by covalently anchoring a small azide fluorophore to the molecule by CuAAC using copper(II) sulfate as catalyst along with sodium L-ascorbate as mild reductant and the water-soluble base tris(3-hydroxypropyltriazolylmethyl) amine (THPTA) as previously described.[43] After click reaction, a fluorescent band of the plk-IGF-I Ea conjugate with the expected electrophoretic mobility was visualized by SDS-PAGE and fluorescence imaging (lane 7), whereas controls (wild-type IGF-I or coupling plk-IGF-I Ea in absence of copper(II) sulfate) displayed exclusively an excess of unconjugated fluorescent dye in the gel (lanes 5, 6, and 8) (Figure 3). Moreover, functionalization of plk-IGF-I Ea with the azide Fluor 488 fluorophore was detailed by ESI-MS mass analysis and revealed an equimolar decoration of plk-IGF-I Ea with the fluorescent dye after CuAAC (obs average mass = 12153.7 Da; calcd average mass = 12153.9 Da) (Figure S2).

To investigate the interference with IGF-I bioactivity resulting from an exchange of Glu-3 against plk, proliferation of the human osteosarcoma MG-63 cells was assessed by a WST-1 colorimetric read-out, as previously reported.[36] Stimulation of MG-63 cells with plk-IGF-I Ea resulted into a similar mitogenic activity as wild-type IGF-I (Figure 4A). We also analyzed downstream signaling of the plk-IGF-I Ea variant after short time exposure (30 min) by phosphorylation of AKT

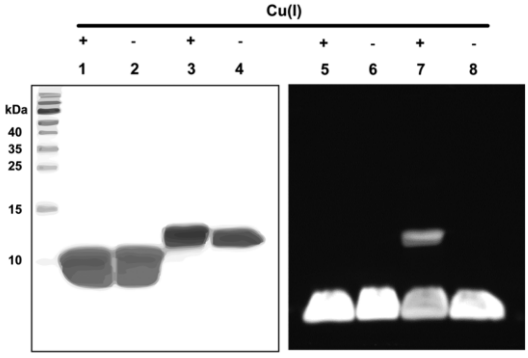

Figure 3. Click reactions between plk-IGF-I Ea, wild-type IGF-I, and the fluorophores Azide Fluor 488 as analyzed by SDS-PAGE. Protein staining by Coomassie brilliant blue is on the left; fluorescence of the gel for the detection of plk-IGF-I Ea -dye conjugate is on the right. Click reactions between plk-IGF-I Ea and dye Azide Fluor 488 in the presence (lanes 3 and 7) or absence (lanes 4 and 8) of copper(I). Reactions between wild-type IGF-I and dye Azide Fluor 488 in the presence (lanes 1 and 5) or absence (lanes 2 and 6) of copper(I).

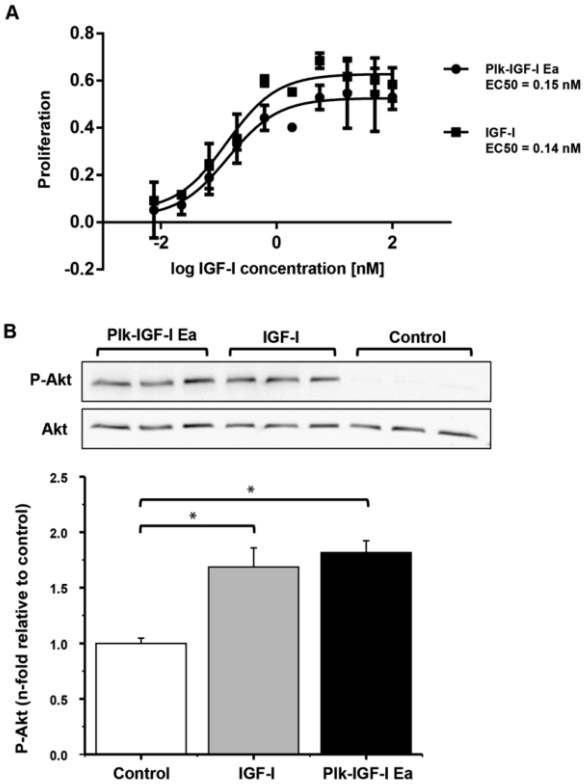

Figure 4. Biological activity of IGF-I. (A) MG-63 cell proliferation assay for plk-IGF-I Ea and wild-type IGF-I as positive control (mean ± SD, $n = 3$, blank $n = 12$). Results normalized to cells untreated with IGF-I that correspond to 0. 95% confidence intervals for EC-50 values are 0.065−0.0325 nM for Plk-IGF-Ea and 0.078−0.245 nM for IGF-I. (B) Top: Representative Western blot analysis of Akt activation by plk-IGF-I Ea and wild-type IGF-I at 100 nM. Bottom: Quantitated pAkt values were related to total Akt values with the control (no IGF-I, medium control) set to 1. Bars represent mean values ± SD of three experiments, and asterisks indicating statistical significant differences (ANOVA followed by Tukey post hoc test; $p \leq 0.05$).

DOI: 10.1021/acsbiomaterials.7b01016
ACS Biomater. Sci. Eng. 2018, 4, 819−825

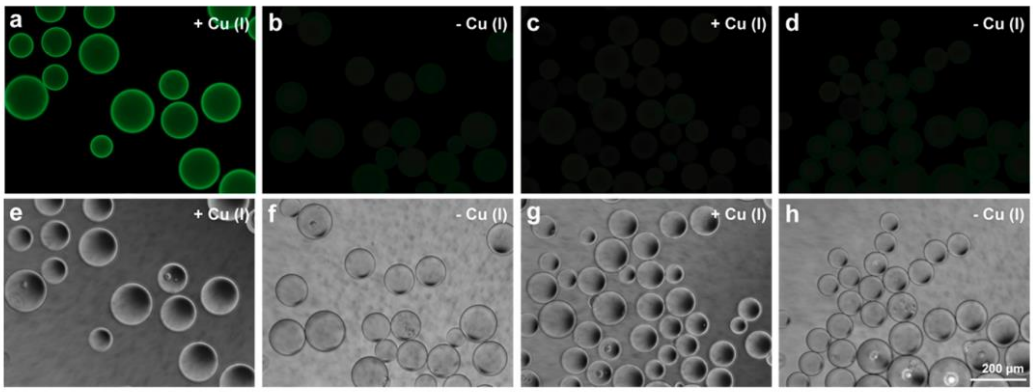

Figure 5. Site-specific immobilization of plk-IGF-I Ea onto azide and hydroxyl groups presenting agarose beads. Decoration of agarose particles with aminoundecanazide and ethanolamine. From top to bottom, fluorescence images and corresponding phase contrast images of plk-IGF-I Ea after CuAAC on aminoundecanazide (a and e) and ethanolamine (c and g) in the presence of copper(II) sulfate or absence of copper(II) sulfate (b, f, d, and h), labeled with anti-IGF-I antibody and Alexa Fluor 488 (green) secondary antibody conjugate.

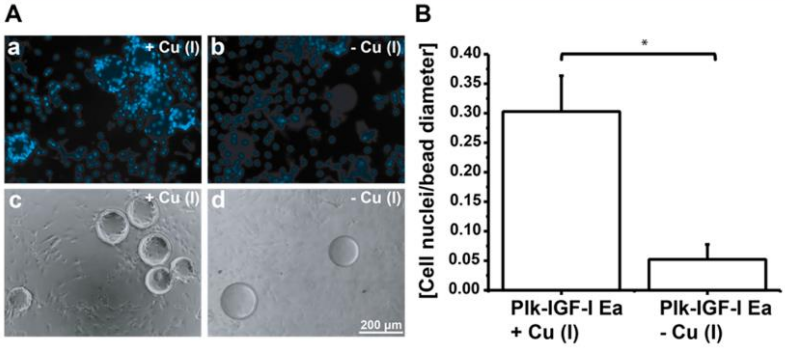

Figure 6. MG-63 cell proliferation on plk-IGF-I Ea presenting agarose beads in serum depleted medium. (A) Cell nuclei (DAPI) staining of MG-63 cells cultured on plk-IGF-I Ea immobilized to aminoundecan-azide decorated agarose beads by CuAAC (a and c) and in the absence of Cu(I) (b and d). Fluorescence images: a and b; corresponding phase contrast images: c and d. (B) Proliferation of MG-63 cells as determined by DAPI positive cells per bead diameter. At least 14 beads were analyzed per condition. The asterisk highlights significant differences ($*p \leq 0.05$). DAPI is blue.

in MG-63 cells in comparison to wild-type IGF-I and nonstimulated controls (Figure 4B). The plk-IGF-I Ea variant induced AKT phosphorylation normalized to total AKT expression as strong as the wild-type protein and significantly stronger than unstimulated controls. Together, both results indicate that the exchange of Glu3 against Plk did not affect bioactivity as determined by long-term exposure and receptor signaling (short-term exposure) and as analyzed by AKT phosphorylation.

Due to their biocompatibility and versatility in surface functionalization, agarose particles were selected as model carrier for site-directed immobilization of plk-IGF-I Ea via CuAAC as previously described.[30−32] To this end, we used amino-undecan-azide and ethanolamine to introduce azide and hydroxyl functional groups onto the agarose beads by amine coupling deploying NHS (*N*-hydroxysuccinimide) chemistry. Plk-IGF-I Ea was covalently immobilized by CuAAC to azide or hydroxyl groups presenting surfaces of agarose beads in the presence or absence of copper(II) sulfate, and plk-IGF-I Ea immobilization was determined by immunofluorescence thereafter (Figure 5). Specific and strong fluorescent signals of plk-IGF-I Ea on azide-functionalized agarose beads were observed in the presence of copper(II) sulfate (Figure 5a). In contrast, controls (CuAAC on hydroxyl-functionalized agarose beads (Figure 5b) or in absence of copper(II) sulfate on azide-functionalized agarose beads (Figure 5c)) showed only weak fluorescence signals on the bead surface after intensive washing, indicating the highly specific covalent coupling of plk-IGF-I Ea on azide-activated agarose beads in the presence of the copper catalyst.

Loading of plk-IGF-I Ea onto azide particles was determined by BCA assay[32] and revealed an average concentration of 28 μg plk-IGF-I Ea/mg particles after CuAAC, whereas control beads (prepared in absence of copper(II) sulfate during the reaction) displayed an average concentration of 8 μg surface adsorbed plk-IGF-I Ea/mg particles, respectively (Figure S3).

We then assessed the mitogenic effects of surface immobilized plk-IGF-I Ea on agarose carriers. To this end, MG-63 cells were incubated in serum-free medium in the presence of plk-IGF-I Ea decorated agarose beads (azide presenting groups and after CuAAC) and in the presence of control agarose beads (azide presenting groups and in absence of copper(II) sulfate during CuAAC with plk-IGF-I Ea) for 48 h. Cell proliferation around the agarose carriers was monitored by DAPI staining for visualization and quantification of cell nuclei (Figure 6), which were confined to cells in close proximity to plk-IGF-I Ea decorated agarose beads in comparison to controls (prepared in absence of copper(II)

DOI: 10.1021/acsbiomaterials.7b01016
ACS Biomater. Sci. Eng. 2018, 4, 819−825

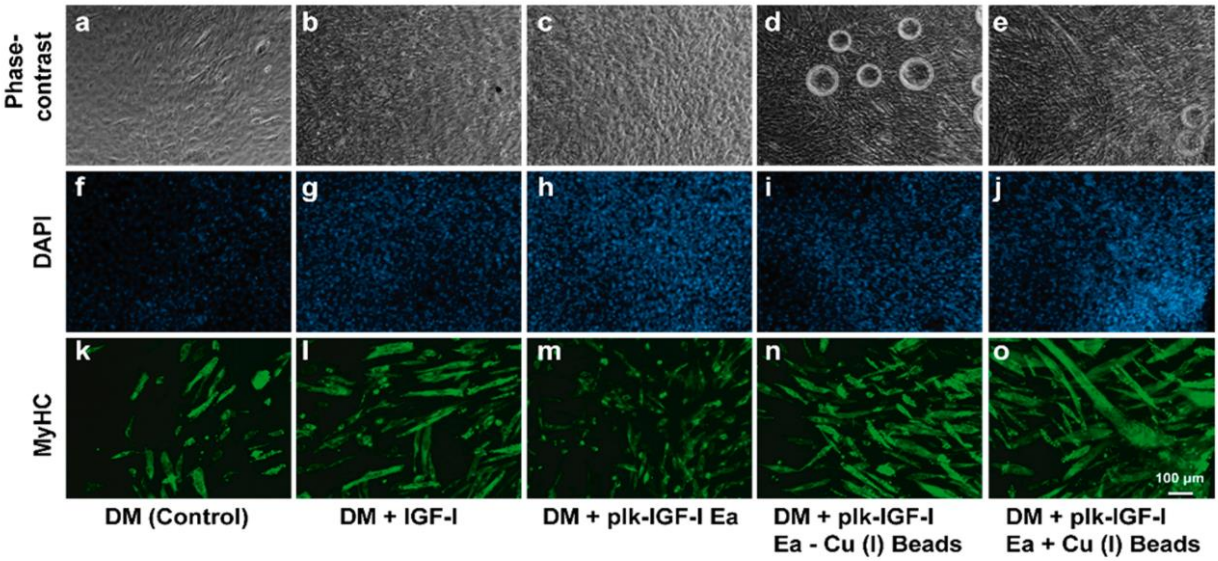

Figure 7. C2C12 cells differentiation after treatment with 1 nM IGF-I or 1 nM plk-IGF-I Ea or plk-IGF-I Ea + Cu (I) agarose beads or plk-IGF-I Ea − Cu (I) beads in differentiation medium. Representative immunostaining of myosin heavy chain (MyHC, green, k−o) or DAPI (blue, f−j) performed in C2C12 myotubes. Corresponding phase contrast images (a−e) are shown in upper panel.

sulfate during reaction; Figure 6A). Mitogenic activity of CuAAC treated agarose particles was significantly and 6-fold increased as determined by cell nuclei per bead (0.30 ± 0.06) compared to agarose particles incubated with plk-IGF-I Ea incubated agarose beads in the absence of copper(II) sulfate (control; 0.05 ± 0.02) (Figure 6B).

To assess the performances of the IGF-I and its clickable plk-IGF-I Ea variant on C2C12 cell differentiation, we performed immunofluorescence staining (Figure 7) and Western blot (Figure 8) analyses of myosin heavy chain (MyHC), a marker of terminal muscle differentiation. Cells were exposed to differentiation medium alone (DM, negative control) or 1 nM IGF-I supplemented DM or 1 nM plk-IGF-I Ea supplemented DM or plk-IGF-I Ea − Cu (I) beads supplemented DM or plk-IGF-I Ea + Cu (I) agarose beads supplemented DM for eight days followed by immunohistochemical visualization of the cell nuclei (DAPI) and differentiated myotubes (MyHC), respectively. In the negative control (Figure 7k), C2C12 cells were qualitatively observed to be fused to myotubes to a lower extent compared to C2C12 cells incubated with 1 nM IGF-I (Figure 7l) or plk-IGF-I Ea (Figure 7m), respectively. Plk-IGF-I Ea − Cu (I) beads (Figure 7n) formed myotubes to a similar extent as untreated C2C12 cells in DM (Figure 7k). Incubation with Plk-IGF-I Ea + Cu (I) beads resulted in an increased size and number of myotubes as qualitatively observed (Figure 7o).

These immunohistochemical outcomes (Figure 7) were confirmed at protein levels, which were quantified by Western blot followed by standard immunoblotting with a MyHC antibody using α-tubulin as internal control (Figure 8). Expression levels of MyHC relative to tubulin were indistinguishable in C2C12 cell lysates treated with IGF-I, IGF-Ea, or differentiation medium (negative control) (Figure 8). In contrast, Plk-IGF-I Ea presentation on beads significantly increased MyHC expression levels compared to negative controls, which lacked the copper catalyst and IGF-I or plk-IGF-I Ea, respectively (Figure 8).

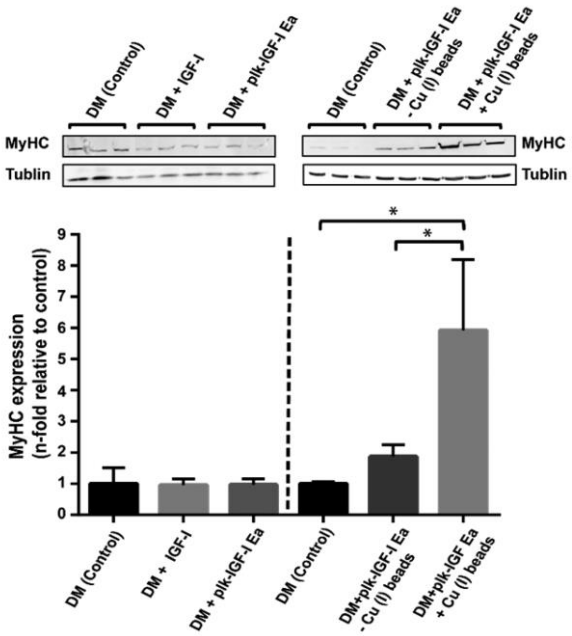

Figure 8. Immunoblotting of C2C12 cell lysates after eight days differentiation in the presence of 1 nM IGF-I or 1 nM plk-IGF-I Ea or plk-IGF-I Ea-free beads or plk-IGF-I Ea-presenting beads, respectively. The cell lysates were immunoblotted with anti-MyHC antibody, and equal loading was monitored with anti-α-tublin antibody. The data were shown as mean values ± SD (n = 3, $^*p \leq 0.05$).

In this work, we aimed at expanding the decoration strategies of IGF-I to enable site-specific modification with unprecedented spatial control over the modification site. For that, we engineered a bioactive and serum stabilized IGF-I Ea therapeutic with an unnatural amino acid bearing an alkyne function via amber codon suppression at the N-terminal site.

DOI: 10.1021/acsbiomaterials.7b01016
ACS Biomater. Sci. Eng. 2018, 4, 819−825

Plk-IGF-I Ea was immobilized by covalent CuAAC reaction to spatially direct its mitogenic effects to the surrounding of a model carrier, providing proliferative signals in a paracrine manner. We observed that cell proliferation and differentiation was significantly enhanced in the accessibility of IGF-I-presenting agarose particles and reflecting the impact of designed multivalence on outcome (Figures 6A, 7, and 8). This insight is opening exciting applications toward tissue regeneration in the future, demonstrating the impact of locally presented IGF-I on cellular performance. Future animal studies are required to detail in vivo consequences of site-specifically modified surfaces of relevant biomaterials and complex materials (e.g., azide functionalized titanium oxide, collagen, and silk fibroin) with plk-IGF-I Ea and investigate the effects of multivalence on regenerative outcome. Other applications may benefit from the site-specific introduction of distinct labels or polymers to probe IGF-I-Ea pharmacokinetics and function for future therapeutic use.

■ ASSOCIATED CONTENT

Supporting Information

The Supporting Information is available free of charge on the ACS Publications website at DOI: 10.1021/acsbiomaterials.7b01016.

Detailed experimental procedures and supplemental figures S1−S3 (PDF)

■ AUTHOR INFORMATION

Corresponding Author

*E-mail: lorenz.meinel@uni-wuerzburg.de.

ORCID

Tessa Lühmann: 0000-0001-7552-6435

Lorenz Meinel: 0000-0002-7549-7627

Author Contributions

All authors designed the experiments. F.W. and A.B. performed the experiments and analyzed the data together with L.M. and T.L. The manuscript was written by F.W, T.L., and L.M.

Notes

The authors declare no competing financial interest.

■ ACKNOWLEDGMENTS

F.W. was supported by China Scholarship Council Grant 201406240097. Financial support from Bundesministerium für Bildung und Forschung (German Federal Ministry of Education and Research; Grant 13N13454) is gratefully acknowledged.

■ REFERENCES

(1) Alland, C.; Moreews, F.; Boens, D.; Carpentier, M.; Chiusa, S.; Lonquety, M.; Renault, N.; Wong, Y.; Cantalloube, H.; Chomilier, J.; Hochez, J.; Pothier, J.; Villoutreix, B. O.; Zagury, J. F.; Tufféry, P. RPBS: a web resource for structural bioinformatics. *Nucleic Acids Res.* **2005**, *33*, W44−W49.

(2) Braun, A. C.; Gutmann, M.; Ebert, R.; Jakob, F.; Gieseler, H.; Lühmann, T.; Meinel, L. Matrix Metalloproteinase Responsive Delivery of Myostatin Inhibitors. *Pharm. Res.* **2017**, *34* (1), 58−72.

(3) Florini, J. R. Hormonal control of muscle growth. *Muscle Nerve* **1987**, *10* (7), 577−598.

(4) Florini, J. R.; Ewton, D. Z.; Coolican, S. A. Growth Hormone and the Insulin-Like Growth Factor System in Myogenesis*. *Endocr. Rev.* **1996**, *17* (5), 481−517.

(5) Florini, J. R.; Ewton, D. Z.; Evinger-Hodges, M. J.; Falen, S. L.; Lau, R. L.; Regan, J. F.; Vertel, B. M. Stimulation and inhibition of myoblast differentiation by hormones. *In Vitro* **1984**, *20* (12), 942−958.

(6) Florini, J. R.; Magri, K. A. Effects of growth factors on myogenic differentiation. *American journal of physiology* **1989**, *256* (4 Pt 1), C701−C711.

(7) Florini, J. R.; Ewton, D. Z.; Magri, K. A. Hormones, Growth Factors, and Myogenic Differentiation. *Annu. Rev. Physiol.* **1991**, *53* (1), 201−216.

(8) Canalis, E. Effect of insulinlike growth factor I on DNA and protein synthesis in cultured rat calvaria. *J. Clin. Invest.* **1980**, *66* (4), 709−719.

(9) SEMSARIAN, C.; SUTRAVE, P.; RICHMOND, D. R.; GRAHAM, R. M. Insulin-like growth factor (IGF-I) induces myotube hypertrophy associated with an increase in anaerobic glycolysis in a clonal skeletal-muscle cell model. *Biochem. J.* **1999**, *339* (2), 443−451.

(10) Stitt, T. N.; Drujan, D.; Clarke, B. A.; Panaro, F.; Timofeyva, Y.; Kline, W. O.; Gonzalez, M.; Yancopoulos, G. D.; Glass, D. J. The IGF-1/PI3K/Akt Pathway Prevents Expression of Muscle Atrophy-Induced Ubiquitin Ligases by Inhibiting FOXO Transcription Factors. *Mol. Cell* **2004**, *14* (3), 395−403.

(11) Musarò, A.; McCullagh, K.; Paul, A.; Houghton, L.; Dobrowolny, G.; Molinaro, M.; Barton, E. R.; L Sweeney, H.; Rosenthal, N. Localized Igf-1 transgene expression sustains hypertrophy and regeneration in senescent skeletal muscle. *Nat. Genet.* **2001**, *27*, 195.

(12) Philippou, A.; Maridaki, M.; Pneumaticos, S.; Koutsilieris, M. The Complexity of the IGF1 Gene Splicing, Posttranslational Modification and Bioactivity. *Mol. Med.* **2014**, *20* (1), 202−214.

(13) Capito, R. M.; Spector, M. Collagen scaffolds for nonviral IGF-1 gene delivery in articular cartilage tissue engineering. *Gene Ther.* **2007**, *14* (9), 721−732.

(14) Lorentz, K. M.; Yang, L.; Frey, P.; Hubbell, J. A. Engineered insulin-like growth factor-1 for improved smooth muscle regeneration. *Biomaterials* **2012**, *33* (2), 494−503.

(15) Mourkioti, F.; Rosenthal, N. IGF-1, inflammation and stem cells: interactions during muscle regeneration. *Trends Immunol.* **2005**, *26* (10), 535−542.

(16) Jabri, N.; Schalch, D. S.; Schwartz, S. L.; Fischer, J. S.; Kipnes, M. S.; Radnik, B. J.; Turman, N. J.; Marcsisin, V. S.; Guler, H.-P. Adverse Effects of Recombinant Human Insulin-like Growth Factor I in Obese Insulin-Resistant Type II Diabetic Patients. *Diabetes* **1994**, *43* (3), 369−374.

(17) Clark, R. G. Recombinant Human Insulin-Like Growth Factor I (IGF-I): Risks and Benefits of Normalizing Blood IGF-I Concentrations. *Horm. Res. Paediatr.* **2005**, *62* (1), 93−100.

(18) Wilkinson-Berka, J.; Wraight, C.; Werther, G. The Role of Growth Hormone, Insulin-Like Growth Factor and Somatostatin in Diabetic Retinopathy. *Curr. Med. Chem.* **2006**, *13* (27), 3307−3317.

(19) Chan, J. M.; Stampfer, M. J.; Giovannucci, E.; Gann, P. H.; Ma, J.; Wilkinson, P.; Hennekens, C. H.; Pollak, M. Plasma Insulin-Like Growth Factor-I and Prostate Cancer Risk: A Prospective Study. *J. Urol.* **1998**, *279* (5350), 563−566.

(20) Hankinson, S. E.; Willett, W. C.; Colditz, G. A.; Hunter, D. J.; Michaud, D. S.; Deroo, B.; Rosner, B.; Speizer, F. E.; Pollak, M. Circulating concentrations of insulin-like growth factor I and risk of breast cancer. *Lancet* **1998**, *351* (9113), 1393−1396.

(21) Meinel, L.; Illi, O. E.; Zapf, J.; Malfanti, M.; Peter Merkle, H.; Gander, B. Stabilizing insulin-like growth factor-I in poly(d,l-lactide-co-glycolide) microspheres. *J. Controlled Release* **2001**, *70* (1), 193−202.

(22) Wenk, E.; Meinel, A. J.; Wildy, S.; Merkle, H. P.; Meinel, L. Microporous silk fibroin scaffolds embedding PLGA microparticles for controlled growth factor delivery in tissue engineering. *Biomaterials* **2009**, *30* (13), 2571−2581.

(23) Uebersax, L.; Merkle, H. P.; Meinel, L. Insulin-like growth factor I releasing silk fibroin scaffolds induce chondrogenic differentiation of

DOI: 10.1021/acsbiomaterials.7b01016
ACS Biomater. Sci. Eng. 2018, 4, 819−825

human mesenchymal stem cells. *J. Controlled Release* **2008**, *127* (1), 12−21.
(24) Meinel, L.; Zoidis, E.; Zapf, J.; Hassa, P.; Hottiger, M. O.; Auer, J. A.; Schneider, R.; Gander, B.; Luginbuehl, V.; Bettschart-Wolfisberger, R.; Illi, O. E.; Merkle, H. P.; Rechenberg, B. v. Localized insulin-like growth factor I delivery to enhance new bone formation. *Bone* **2003**, *33* (4), 660−672.
(25) Franco, E. J.; Hofstetter, H.; Hofstetter, O. A comparative evaluation of random and site-specific immobilization techniques for the preparation of antibody-based chiral stationary phases. *J. Sep. Sci.* **2006**, *29* (10), 1458−1469.
(26) Gaston, M. A.; Jiang, R.; Krzycki, J. A. Functional context, biosynthesis, and genetic encoding of pyrrolysine. *Curr. Opin. Microbiol.* **2011**, *14* (3), 342−9.
(27) James, C. M.; Ferguson, T. K.; Leykam, J. F.; Krzycki, J. A. The amber codon in the gene encoding the monomethylamine methyltransferase isolated from Methanosarcina barkeri is translated as a sense codon. *J. Biol. Chem.* **2001**, *276* (36), 34252−8.
(28) Srinivasan, G.; James, C. M.; Krzycki, J. A. Pyrrolysine Encoded by UAG in Archaea: Charging of a UAG-Decoding Specialized tRNA. *Science* **2002**, *296* (5572), 1459−1462.
(29) Blight, S. K.; Larue, R. C.; Mahapatra, A.; Longstaff, D. G.; Chang, E.; Zhao, G.; Kang, P. T.; Green-Church, K. B.; Chan, M. K.; Krzycki, J. A. Direct charging of tRNA(CUA) with pyrrolysine in vitro and in vivo. *Nature* **2004**, *431* (7006), 333−5.
(30) Lühmann, T.; Schmidt, M.; Leiske, M. N.; Spieler, V.; Majdanski, T. M.; Grube, M.; Hartlieb, M.; Nischang, I.; Schubert, S.; Schubert, U. S.; Meinel, L. Site-specific POxylation of interleukin-4. *ACS Biomater. Sci. Eng.* **2017**, *3* (3), 304−312.
(31) Lühmann, T.; Jones, G.; Gutmann, M.; Rybak, J.-C.; Nickel, J.; Rubini, M.; Meinel, L. Bio-orthogonal Immobilization of Fibroblast Growth Factor 2 for Spatial Controlled Cell Proliferation. *ACS Biomater. Sci. Eng.* **2015**, *1* (9), 740−746.
(32) Tabisz, B.; Schmitz, W.; Schmitz, M.; Luehmann, T.; Heusler, E.; Rybak, J.-C.; Meinel, L.; Fiebig, J. E.; Mueller, T. D.; Nickel, J. Site-Directed Immobilization of BMP-2: Two Approaches for the Production of Innovative Osteoinductive Scaffolds. *Biomacromolecules* **2017**, *18* (3), 695−708.
(33) Philippou, A.; Maridaki, M.; Pneumaticos, S.; Koutsilieris, M. The complexity of the IGF1 gene splicing, posttranslational modification and bioactivity. *Mol. Med.* **2014**, *20*, 202−14.
(34) Glass, D. J.; Fornaro, M. Stabilized insulin-like growth factor polypeptides. Patent Application Publication US 2010/0234290 A1, NOVARTIS AG, United States, 2010−2013.
(35) John Ballard, F.; Wallace, J. C.; Francis, G. L.; Read, L. C.; Tomas, F. M. Des(1−3)IGF-I: a truncated form of insulin-like growth factor-I. *Int. J. Biochem. Cell Biol.* **1996**, *28* (10), 1085−1087.
(36) Schultz, L.; Vollmers, F.; Lühmann, T.; Rybak, J.-C.; Wittmann, R.; Stank, K.; Steckel, H.; Kardziev, B.; Schmidt, M.; Högger, P.; Meinel, L. Pulmonary Insulin-like Growth Factor I Delivery from Trehalose and Silk-Fibroin Microparticles. *ACS Biomater. Sci. Eng.* **2015**, *1* (2), 119−129.
(37) Denley, A.; Cosgrove, L. J.; Booker, G. W.; Wallace, J. C.; Forbes, B. E. Molecular interactions of the IGF system. *Cytokine Growth Factor Rev.* **2005**, *16* (4), 421−439.
(38) Braun, A. C.; Gutmann, M.; Luhmann, T.; Meinel, L. Bioorthogonal strategies for site-directed decoration of biomaterials with therapeutic proteins. *J. Controlled Release* **2018**, *273*, 68−85.
(39) Eger, S.; Scheffner, M.; Marx, A.; Rubini, M. Formation of Ubiquitin Dimers via Azide−Alkyne Click Reaction. In *Ubiquitin Family Modifiers and the Proteasome: Reviews and Protocols*; Dohmen, R. J.; Scheffner, M., Eds.; Humana Press: Totowa, NJ, 2012; pp 589−596.
(40) Eger, S.; Scheffner, M.; Marx, A.; Rubini, M. Synthesis of Defined Ubiquitin Dimers. *J. Am. Chem. Soc.* **2010**, *132* (46), 16337−16339.
(41) Zhang, B.; Yang, Q.; Chen, J.; Wu, L.; Yao, T.; Wu, Y.; Xu, H.; Zhang, L.; Xia, Q.; Zhou, D. CRISPRi-Manipulation of Genetic Code Expansion via RF1 for Reassignment of Amber Codon in Bacteria. *Sci. Rep.* **2016**, *6*, 20000.
(42) Wals, K.; Ovaa, H. Unnatural amino acid incorporation in E. coli: current and future applications in the design of therapeutic proteins. *Front. Chem.* **2014**, *2*, 15.
(43) Gutmann, M.; Memmel, E.; Braun, A. C.; Seibel, J.; Meinel, L.; Lühmann, T. Biocompatible Azide−Alkyne "Click" Reactions for Surface Decoration of Glyco-Engineered Cells. *ChemBioChem* **2016**, *17* (9), 866−875.

DOI: 10.1021/acsbiomaterials.7b01016
ACS Biomater. Sci. Eng. 2018, 4, 819−825

Supporting Information

Article type: Letter

Site specifically conjugated Insulin-like growth factor-I (IGF-I) for anabolic therapy

Fang Wu[1], *Alexandra Braun*[1], *Tessa Lühmann*[1], *Lorenz Meinel*[1]*

[1]Institute of Pharmacy and Food Chemistry, University of Wuerzburg, Am Hubland, 97074, Wuerzburg, Germany

Number of Pages: S1–S14

Number of Figures: S1–S3

Number of tables: None

Experimental Section

Materials

Propargyl-chloroformate, Eagle's minimum essential medium, bovine serum albumin, phenylmethanesulfonyl fluoride (PMSF), copper (II) sulfate, 1,4 dithiothreitol (DTT), sodium L-ascorbate, tris(3-hydroxypropyltriazolylmethyl)amine (THPTA). Acetonitrile (HPLC grade) and trifluoroacetic acid (HPLC grade) were purchased from VWR (Ismaning, Germany). Restriction endonucleases were from New England Biolabs (Ipswitch, USA). Penicillin G and Streptomycin solution, non-essential amino acids (NEA) were purchased from Biochrom AG (Berlin, Germany). Fetal bovine serum (FBS) was from Gibco (Darmstadt, Germany). Boc-protected L-lysine was from P3 BioSystems LLC (Shelbyville, KY, US). Coomassie Brilliant Blue G250, SuperSignal West Dura Substrate, Bradford Protein Assay Kit were from Pierce (Rockford, USA). Water soluble tetrazolium (WST-1) was from Roche (Basel, Switzerland). Anti-phospho-AKT (Ser473) and anti-AKT were from Cell Signaling (Hitchin, UK). Azide Fluor 488 (5/6-Carboxyrhodamine 110-PEG3-Azide; MW = 574.59 g/mol) was from Jena Bioscience (Jena, Germany). Human recombinant IGF-I was from Genentech Inc. (San Francisco, CA). Anti-Insulin-like growth factor-I antibody (produced in goat), monoclonal anti-insulin-like growth factor-1 (produced in mouse), rabbit anti-goat IgG and protease inhibitor cocktail were from Sigma-Aldrich (Schnelldorf, Germany). Horse serum and secondary antibody goat anti-mouse IgG horseradish peroxidase (HRP) conjugate was from Sigma Aldrich. α-tubulin rabbit monoclonal antibody (#2125) and goat anti-rabbit IgG horseradish peroxidase (HRP) conjugate was from Cell signaling (Danvers, MA). Alexa Fluor 488 labelled goat anti-Mouse IgG secondary antibody was from Invitrogen (Darmstadt, Germany). Western Blot against myosin heavy chain (MyHC; MAB4470) were from R&D Systems (Minneapolis, MN), Pierce BCA Protein Assay Kit and M-PER mammalian protein extraction reagent were from Thermo Fisher Scientific (Schwerte, Germany). NHS activated sepharose TM4 Fast flow (crosslinked 4% agarose beads; Mean

particle size 90 µm, particle range 45 µm – 186 µm) was from GE Healthcare (Freiburg, Germany). Centrifugal ultrafiltration devices Vivaspin 500 were from Satorius (Goettingen, Germany). All other chemicals used were at least of pharmaceutical grade and were purchased from Sigma-Aldrich (unless noted otherwise).

Chemical synthesis of propargyl-L-lysine

Propargyl-L-lysine (Plk) as HCl-salt was synthesized as previously described by Milles et al.[1] and Li et al.[2]. A Bruker Advance 400 MHz NMR spectrometer was used for confirmation of the product as reported in [3].

Expression and purification of plk-IGF Ea

Vector construction

A sequence for the modified pro-IGF-I, termed plk-IGF-I Ea, consisting of the 70 amino acid IGF-I and a particular Ea peptide at the C-terminus was engineered [4]. R71, S72 were deleted to inhibit cleavage between mature IGF-I and the E-peptide. Glu-3 of IGF-I was changed to an amber codon (TAG) for the incorporation of the unnatural amino acid plk. The (TAG) IGF-I Ea mutant was amplified by polymerase chain reaction (PCR) using the forward primer including an NdeI restriction site, one additional glycine codon inserted after the methionine start codon and a TAG mutation (5'-CCCCATATGGGCGGCCCGTAG-3'), while deploying a reverse primer including a BamHI restriction site (5'-CCCGGATCCTTATTACATGCGATAGTTCTTGTTGCCCGC-3'). The PCR product was then subcloned into the backbone of a pET11a vector for the generation of pET11a/plk-IGF-I Ea, already containing the gene for the pyrrolysine tRNA, the lipoprotein promotor lpp and the terminator RRN b/c as described by Eger et al.[5] The correct insert was confirmed by DNA sequencing.

Site-specific incorporation of plk into IGF-I Ea

The pET11a/plk-IGF-I Ea construct was co-transformed with the pRSFDuet-1 vector encoding for the gene of the pyrrolysine tRNA synthetase (pylS) into *E. coli* BL21 DE3 or *E.*

coli C321 delA. exp strains for expression as previously reported.[5] General IPTG-induction protein expression was performed to optimize conditions for plk-IGF-I Ea production.[3, 6] Briefly, the saturated culture of the transformed strains was inoculated into standard Terrific Broth (TB) medium containing 100 μg/mL carbenicillin and 34 μg/mL kanamycin. Different plk concentrations were added at OD_{600} = 0.3. Protein expression was induced using 1 mM IPTG at OD_{600} =0.7 according to the optimization procedure. After incubation at 37 °C for 4 h, 1 mL bacterial suspension of each expression was centrifuged and the obtained pellets were resuspended in 1 x SDS-loading buffer, kept at 95 °C for 5 min and centrifuged again. The lysate supernatants were then analyzed by SDS-PAGE followed by Western Blot analysis. The bacteria were harvested by centrifugation at 5,000 g for 30 min at 4 °C, and stored at −80 °C. The modified Studier auto-induction method [7] was applied as an alternative growing method to increase protein yields[8], as confirmed by Western Blot (Figure S1), and was thus used for batch cultivation. Bacteria were cultured in 2 L of auto induced medium (2 L TB medium, 1 mM $MgSO_4$, 50 mM Na_2HPO_4, 50 mM KH_2PO_4, 25 mM $(NH_4)_2SO_4$, 0.5% glycerol, 0.05 % glucose, 0.2 % a-lactose, 6 mM plk, 100 μg/mL carbenicillin and 34 μg/mL kanamycin) inoculated with 5 % overnight culture at 200 rpm under 37 °C for 28 h. Cells were collected and stored as above.

Refolding and purification of plk-IGF-I Ea

After expression, cell pellets were resuspended in the lysis buffer (50 mM Tris, 50 mM NaCl, 1 mM EDTA, 0.1 mM PMSF, pH=8.0)[6a] and lysed via ultrasonication on ice. After centrifuged at 100,000 g for 1 h at 4 °C, the pellets were cleaned once with 50 mL of washing buffer I (20 mM Tris, 2% Triton X-100, 0.5 M NaCl, 2 M urea, pH=8.0), the mixed suspension was placed on ice for 10 minutes, and centrifuged (10,000 g, 4°C, 20 minutes). To remove Triton X-100 and urea, the inclusion bodies were further washed two more times with 50 mL of washing buffer II (20 mM Tris buffer, pH=7.5). The resultant precipitate were dissolved in solubilization buffer (50 mM Tris, 50 mM NaCl, 1 mM EDTA, 0.1 mM PMSF, 6

M guanidine hydrochloride, 2 mM reduced glutathione, 0.2 mM oxidized glutathione, pH = 8.0) and incubated at room temperature with gentle mixing until the inclusion bodies paste dissolved completely. The unfolded proteins were refolded by dialysis against refolding buffer (50 mM Tris, 50 mM NaCl, 1 mM EDTA, 0.4 M L-arginine, 2 mM reduced glutathione, 0.2 mM oxidized glutathione, 30% ethanol, pH = 8.0) at 4 °C for 72 h. The refolded mixture was subsequently centrifuged at 4,000 g for 15 min at 4 °C and the supernatant was buffer-exchanged into 1 x PBS buffer (pH=7.2). The protein was subjected to cation exchange chromatography using an FPLC system (GE Healthcare Äkta Purifier, Life sciences, Freiburg, Germany). The protein was eluted with a linear gradient from 0.4 M to 0.8 M NaCl over 20 column volumes. Fractions containing plk-IGF-I Ea was then pooled and loaded onto an RPC column (SOURCE™ 15RPC ST 4.6/100; GE Healthcare Life Sciences) as a final purification step. The column was equilibrated with 0.1 % (v/v) trifluoroacetic acid (TFA) in acetonitrile/H2O (5:95, v/v), and the IGF variant was eluted from the column with 40 % acetonitrile (v/v) in 0.1% (v/v) TFA. After identification of plk-IGF-I Ea, the pooled fractions were lyophilized. Structure prediction was done by PEP-FOLD 3.0[9] and molecular graphics were created by Chimera[10].

HPLC analysis

Protein purity was assessed by RP-HPLC using a VWR Hitachi LaChromUltra HPLC system. Approximately 2 µg of protein sample was applied to a Zorbax 300SB-CN reversed-phase chromatography column (4.6 mm x 150 mm, 5 µm) at 40 °C, equilibrated by water containing 0.1 % TFA. Wild-type IGF-I and plk-IGF-I Ea were separated under gradient conditions at a flow rate of 0.8 mL/min. Two eluents were used, eluent A consisted of 0.1% TFA in water, and eluent B was 0.1% TFA in acetonitrile. Separation started with 100% (v/v) eluent A and was changed over 30 min to 100% eluent B. Afterwards, initial conditions were set to wash the column. UV-absorbance was monitored at 214 nm.

Mass analysis

The protein samples were desalted using ZipTipC18-tips according to the manufacturer's instructions. Electrospray Ionisation (ESI) -MS spectra were acquired using an ESI micrOTOF Focus from Bruker Daltonics. Theoretical masses of IGF-I Ea were calculated (http://web.expasy.org/peptide_mass/) and adjusted for theoretical masses of the non-unnatural amino acid plk. To confirm the site-specific incorporation of plk into IGF-I Ea, a trypsin in-gel digestion was performed and the resulting fragments were analyzed by NanoLC-MS/MS as described before[3].

Click reaction

5 µg of plk-IGF-I Ea and wild-type IGF-I were mixed with a 5 to 10-fold molar excess of the fluorescence dye Azide Fluor 488 in PBS (pH = 7.2). Formation of catalytic Cu (I) species was achieved by the addition of 250 µM THPTA and 2.5 mM sodium ascorbate to 50 µM $CuSO_4$. In order to prevent Cu induced protein oxidation, the catalytic Cu (I) mixture were flushed with nitrogen for 10 min. Dye Azide Fluor 488 and the protein were added afterwards, and incubated for 1 h at room temperature. The reaction was stopped by addition of 5 mM EDTA, prior before analysis by SDS-PAGE and fluorescence imaging.

SDS-PAGE and Western Blot

Expressed proteins and click reactions were analyzed by standard Tris-glycine SDS-PAGE under reducing conditions as outlined before[11]. Gels were stained with Coomassie Brilliant Blue G250 and documented using a FluorChem FC2 imaging system (Protein Simple, Santa Clara, CA). Protein identity was confirmed by Western Blot through resolving proteins on 15 % SDS-PAGE gels, followed by protein transfer onto nitrocellulose membrane (BioTrace®NT, PN 66485, Pall Life Sciences, Ann Arbor, MI, USA). Membranes were blocked in 1x Roti®-Block (Carl Roth GmbH, Karlsruhe, Germany) for 1 h at room temperature. Membranes were incubated with a goat anti-human IGF-1 antibody (1:1000 dilution) in Tris buffered saline (TBS) solution containing 0.1 % (v/v) Tween 20 (TBST) at 4 °C for overnight. The membrane was washed three times with TBST for 10 min and incubated

with a peroxidase conjugated rabbit anti-goat IgG at a dilution of 1:2000 in TBST solution for 1 hour at room temperature. Membranes were washed again, and proteins were detected using a chemiluminescent substrate (SuperSignal® West Pico Chemiluminescent Substrate, Thermo Fisher Scientific, Lausanne, CH) and photographed using a FluorChem FC2 imaging system.

WST-1 assay

IGF-I stimulates the growth of MG63 cells and has been used as a potency assay[11-12]. Briefly, MG-63 cells (ATCC-Number CRL-1427, ATCC, Manassas, VA) were cultured in growth medium (MEM containing 8.8% FBS, 1.77 mM L-glutamine, 88 U/mL penicillin G and 88 μg/μL streptomycin, 0.88% non-essential amino acids (NEAA), trypsined and resuspended in assay medium (MEM containing 0.452% BSA, 1.82 mM L-Glutamine, 91 U/mL penicillin G and 91 μg/μL streptomycin, 0.91% NEAA) to a concentration of 5×10^4 cells/mL. 100 μL of cell suspension were then added into each well of 96-well format. After 1 day of pre-incubation, the cells were then incubated for 2 days with dilutions of plk-IGF-I Ea or wild-type IGF-I (0.008 nM to 100 nM) in assay medium. After stimulation, 20 μL of WST-1 reagent (diluted 1:1 with assay buffer) was added and cells were incubated for another 4 hours. Cell viability was measured at 450 nm using a Spectramax 250 microplate reader (Molecular Devices, Sunnyvale, USA).

Phosphorylation assay

To test the activation of IGF-I signaling pathways, MG-63 cells were seeded in assay medium in a 24 well plate (100,000 cells per well). After 24 h in culture, 100 nM of plk-IGF-I Ea in assay medium, 100 nM of wild-type IGF-I in assay medium or assay medium without IGF-I were added for 30 min at 37 °C, respectively. Afterwards, MG-63 cells were wash once with cold PBS and extracted with M-PER Mammalian Cell Lysis Buffer containing 1 mM Na_3VO_4, 5 mM NaF, 0.2 mM PMSF and a protease inhibitor cocktail. Insoluble materials were removed by centrifugation at 10, 000 g for 20 min at 4 °C. The cell extracts were used for SDS-PAGE separation and Western Blot analysis with anti-phosphor-AKT (Ser473) antibody,

anti-AKT antibody (both 1: 1000 dilution in TBST). A peroxidase conjugated secondary antibody (1: 2000 dilution in TBST) and a chemiluminescent substrate were used for visualization in a FluorChem FC2 imaging system.

Decoration of NHS activated agarose beads

NHS activated agarose bead slurry solution (100 µL solution corresponds to 4 µmoL NHS) was washed 3 times with PBS followed by modification with equimolar amounts of 11-Azido-3,6,9-trioxaundecan-1-amine (referred to as amino-undecane-azide herein) or ethanolamine in PBS buffer (pH=7.4) for 2 hours with gentile shaking. After incubation, the unreacted NHS groups were quenched by incubating the agarose beads with 500 mM ethanolamine in 100 mM Tris-HCl buffer (pH=8.3) containing 0.5 M NaCl for 1 hour. The modified beads were subsequently washed 5 times with PBS and kept in 20 % ethanol at 4 °C prior before use.

Immobilization of plk-IGF-I Ea onto agarose beads via CuAAC

After washing 3 times with PBS, 25 µl of decorated agarose bead solution were mixed with 20 µl of plk-IGF-I Ea (0.4 mg/mL in PBS, pH=7.4). For CuAAC reaction, final concentrations of 250 µM THPTA, 50 µM $CuSO_4$ and 2.5 mM ascorbic acid were added and immobilization was performed at room temperature for 2 h as described above.

Visualization of immobilized plk-IGF-I Ea

Immobilized plk-IGF-I Ea beads were visualized using an anti-IGF-I antibody. The reacted beads were blocked with 1x Roti®-Block in TBST solution (Roti-TBST) for 1 h at room temperature, followed by incubation with a mouse anti-human IGF-1 antibody (1:500 dilution) in Roti-TBST solution at 4 °C for overnight. After rewashing, a secondary antibody labeled with Alexa Fluor 488 dye was added to the beads in order to detect the presence or absence of bound plk-IGF-I Ea on the bead surface. In detail, protein-loaded agarose beads were immunolabeled with secondary anti-mouse Alexa 488 antibody at a dilution of 1:500 in Roti-TBST solution with gentle rotation for 1 hour at room temperature. After incubation, the

beads were washed with TBST 6-times, followed by incubation with 0.5 % SDS for 1 d and were washed again 3-times in PBS. The agarose beads were subsequently imaged using a Zeiss Observer Z1 epifluorescence microscope (Zeiss, Oberkochen, Germany) at 10 fold magnification.

Quantification of immobilized plk-IGF-I Ea onto azide particles

Intensive washing was applied to remove the physical absorption of protein. In detail, plk-IGF-I Ea coupled onto azide particles were washed 5-times with PBS, incubated with 0.5 % SDS for 1d, thoroughly washed with sterile PBS for 2 d, and kept in sterile PBS at 4 °C prior to use. The amount of plk-IGF-I Ea immobilized to azide-activated agarose beads was determined in triplicates using the BCA protein assay kit[13] according to the manufacturer's protocol.

Cell proliferation in the presence of plk-IGF-I Ea modified agarose beads after CuAAC

100 µL of MG-63 cells were plated at a density of 5000 cells /well in a 96 well-format and allowed to attach overnight in assay medium. Approximately 0.2 mg agarose bead solution (with a loading of approximately 28 µg plk-IGF-I Ea / mg beads, Figure S3) was added to each well and growth of MG-63 cells was stimulated for 48 hours at 37 °C and 5 % CO_2. The cells were washed once with PBS and fixed with an aqueous 2 % (V/V) formaldehyde solution at pH 7.5 for 10 minutes. After washing three times in PBS, the cells were permealized with 0.1 % (V/V) Triton X-100 in PBS for 5 min and stained with DAPI solution, diluted 1:1000 (V/V) in PBS for 10 minutes. After rewashing 4 times with PBS, a Zeiss Observer Z1 epifluorescence microscope at 10-fold or 40-fold magnification was used for imaging.

To assess cell proliferation in proximity to individual agarose beads, 3D stacks of agarose beads with z-stack keeping 10 slices were taken in line with a corresponding phase contrast image. For cell nuclei quantification, the diameter of the bead was determined and the number of cell nuclei per agarose bead within an area with the dimensions of the bead radius + 30 µm

was manually counted as reported before[3]. At least 14 individual agarose beads were analyzed per condition.

C2C12 Differentiation and Immunostaining

C2C12 myoblasts (ATCC CRL-1772) were expanded in growth medium (GM) consisting of 10 % FBS in high-glucose Dulbecco's modified Eagle's medium (DMEM) supplemented with 2 mM L-glutamine, 88 U/mL penicillin G and 88 μg/μL streptomycin at 37°C and 5 % CO_2. For C2C12 differentiation, 50,000 cells/well were seeded in 24-well plates and cultured in the GM until reaching 80% confluence. Media were then replaced with differentiation medium [DM; DMEM with 2% (vol/vol) horse serum], DM + IGF-I (1 nM), DM + plk-IGF-I Ea (1 nM), DM + plk-IGF-I Ea-presenting beads (approximately 0.2 mg, with a loading of 28 μg plk-IGF-I Ea / mg beads, Figure S3)), or DM + plk-IGF-I Ea-free beads (approximately 0.2 mg). Cell differentiation into myotubes was followed for 8 days and the medium was replaced every other day.

After differentiation, cells in wells were washed 2 times with PBS, fixed with ice-cold 100% methanol for 10 min on ice, and stained with anti-myosin heavy chain antibody at 4°C overnight and Alexa Fluor 488 secondary antibody (diluted 1:500 in PBS + 5% BSA) for 60 min at room temperature[9b]. Cell nuclei were counterstained with DAPI. The stained cells were examined at 10-fold magnification using a Zeiss Axio Observer Z1 epifluorescence microscope equipped with a A-Plan 10x/0.25 Ph1 objective (Zeiss, Oberkochen, Germany).

Western Blot of Differentiated C2C12 Cells

After 8 days of differentiation, C212 cells were lysed using M-PER mammalian protein extraction reagent containing 1 mM Na_3VO_4, 5 mM NaF, 0.2 mM PMSF and a protease inhibitor cocktail and cell extracts were centrifuged at 10, 000 g for 20 min at 4°C. The cell supernatants were mixed with 6 × SDS reducing sample buffer, boiling for 5 min at 95°C and then subjected to 5 % SDS polyacrylamide gel electrophoresis. Immunoblotting followed standard procedures with anti-myosin heavy chain (for the upper part of the membrane,

1:1500 final dilution) or anti-α-tubulin (as loading control for the lower part of the membrane; 1:5000 final dilution) primary antibodies, followed by a horseradish peroxidase-conjugated IgG antibody (1:5000 final dilution) and visualized by using SuperSignal West Pico Chemiluminescent Substrate according to the manufacturer's instructions.

Statistics

All data were displayed as mean ± standard deviation (SD) unless specified otherwise. All statistical analyses were performed using GraphPad Prism 6 (GraphPad Software Inc., CA). Statistical significance was calculated using Student's t-test or one-way ANOVA followed by pairwise comparison using Tukey's post-test. Results were considered statistically significant at $*p \leq 0.05$.

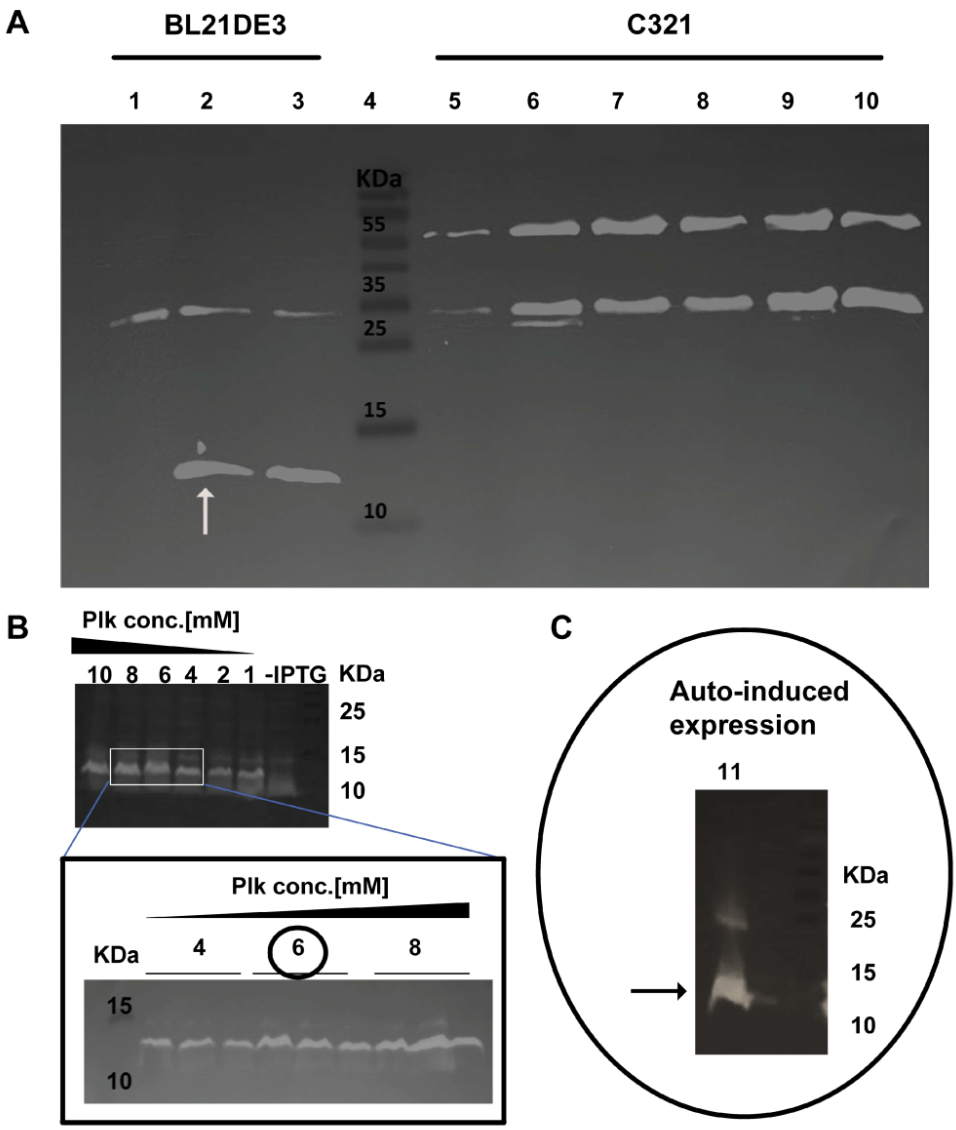

Figure S1. Screening of culture conditions to optimize plk-IGF-I Ea expression (MW: 11579.3 Da). (A) Western Blot analyses of plk-IGF-I Ea expression in different strains using traditional IPTG method. Lanes #4: protein standard, Lanes #1 and #5: protein expression before IPTG induction as control; lanes #2, #3, #6, #7, #8, #9 and #10: protein production after 1.0 mM IPTG induction. *E. coli* BL21 (DE3) was much more efficient for the expression of plk-IGF-1Ea in comparison with *E. coli* C321 delA. exp strains, and thus was employed for the optimization of expression conditions in the following experiments. (B) Western Blot

analyses of plk-IGF-I Ea expression in BL21 (DE3) strain with different plk amount following induction of expression by IPTG. Increasing the plk concentration from 0-6 mM increased plk-IGF-I Ea formation, while further supplementation up to 10 mM did not impact outcome. Thus, the preferable plk amount was set at 6 mM. (C) Western Blot analyses of plk-IGF-I Ea expression levels in BL21 (DE3) following by auto induction (lanes #11).

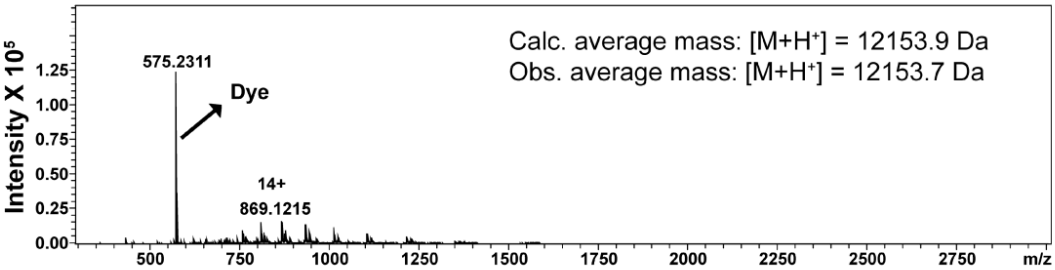

Figure S2. ESI MS analysis of plk-IGF-I Ea after the conjugation with dye Azide Fluor 488 using CuAAC. Obs. Average mass = 12153.7 Da, calc. average mass = 12153.9 Da.

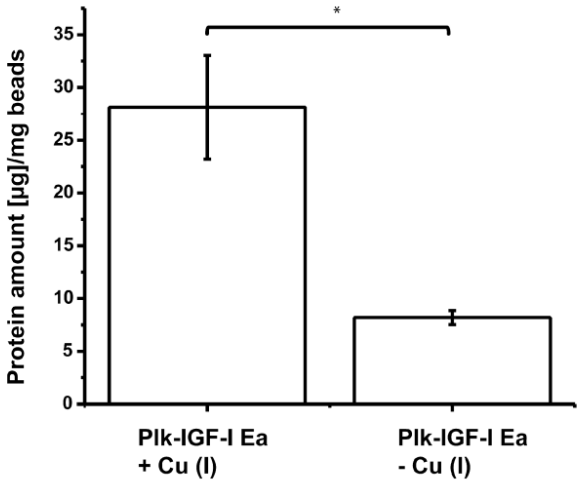

Figure S3. Quantification of immobilized plk-IGF-I Ea onto azide-agarose beads. Data represent mean values ± SD of three individual experiments (n = 3). The asterisk highlights significant differences ($p \leq 0.05$).

.

References:

1. Milles, S.; Tyagi, S.; Banterle, N.; Koehler, C.; VanDelinder, V.; Plass, T.; Neal, A. P.; Lemke, E. A., Click Strategies for Single-Molecule Protein Fluorescence. *Journal of the American Chemical Society* **2012,** *134* (11), 5187-5195.
2. Li, F.; Zhang, H.; Sun, Y.; Pan, Y.; Zhou, J.; Wang, J., Expanding the Genetic Code for Photoclick Chemistry in E. coli, Mammalian Cells, and A. thaliana. *Angewandte Chemie International Edition* **2013,** *52* (37), 9700-9704.
3. Lühmann, T.; Jones, G.; Gutmann, M.; Rybak, J.-C.; Nickel, J.; Rubini, M.; Meinel, L., Bio-orthogonal Immobilization of Fibroblast Growth Factor 2 for Spatial Controlled Cell Proliferation. *ACS Biomaterials Science & Engineering* **2015,** *1* (9), 740-746.
4. (a) Glass, D. J.; Fornaro, M., Stabilized insulin-like growth factor polypeptides. U.S. Patent Nr. 8,343,918, 2013.: 2013; (b) Schultz, I.; Wurzel, J.; Meinel, L., Drug delivery of Insulin-like growth factor I. *European Journal of Pharmaceutics and Biopharmaceutics* **2015,** *97* (Part B), 329-337.
5. Eger, S.; Scheffner, M.; Marx, A.; Rubini, M., Synthesis of Defined Ubiquitin Dimers. *Journal of the American Chemical Society* **2010,** *132* (46), 16337-16339.
6. (a) Lühmann, T.; Spieler, V.; Werner, V.; Ludwig, M.-G.; Fiebig, J.; Mueller, T. D.; Meinel, L., Interleukin-4-Clicked Surfaces Drive M2 Macrophage Polarization. *ChemBioChem* **2016,** *17* (22), 2123-2128; (b) Wandrey, G.; Wurzel, J.; Hoffmann, K.; Ladner, T.; Büchs, J.; Meinel, L.; Lühmann, T., Probing unnatural amino acid integration into enhanced green fluorescent protein by genetic code expansion with a high-throughput screening platform. *Journal of Biological Engineering* **2016,** *10*, 11.
7. Studier, F. W., Protein production by auto-induction in high-density shaking cultures. *Protein Expression and Purification* **2005,** *41* (1), 207-234.
8. Elvin, C. M.; Carr, A. G.; Huson, M. G.; Maxwell, J. M.; Pearson, R. D.; Vuocolo, T.; Liyou, N. E.; Wong, D. C. C.; Merritt, D. J.; Dixon, N. E., Synthesis and properties of crosslinked recombinant pro-resilin. *Nature* **2005,** *437* (7051), 999-1002.
9. (a) Alland, C.; Moreews, F.; Boens, D.; Carpentier, M.; Chiusa, S.; Lonquety, M.; Renault, N.; Wong, Y.; Cantalloube, H.; Chomilier, J.; Hochez, J.; Pothier, J.; Villoutreix, B. O.; Zagury, J. F.; Tufféry, P., RPBS: a web resource for structural bioinformatics. *Nucleic Acids Research* **2005,** *33* (suppl_2), W44-W49; (b) Braun, A. C.; Gutmann, M.; Ebert, R.; Jakob, F.; Gieseler, H.; Lühmann, T.; Meinel, L., Matrix Metalloproteinase Responsive Delivery of Myostatin Inhibitors. *Pharmaceutical Research* **2017,** *34* (1), 58-72.
10. Pettersen, E. F.; Goddard, T. D.; Huang, C. C.; Couch, G. S.; Greenblatt, D. M.; Meng, E. C.; Ferrin, T. E., UCSF Chimera—A visualization system for exploratory research and analysis. *Journal of Computational Chemistry* **2004,** *25* (13), 1605-1612.
11. Germershaus, O.; Schultz, I.; Lühmann, T.; Beck-Broichsitter, M.; Högger, P.; Meinel, L., Insulin-like growth factor-I aerosol formulations for pulmonary delivery. *European Journal of Pharmaceutics and Biopharmaceutics* **2013,** *85* (1), 61-68.
12. (a) Lopaczynski, W.; Harris, S.; Nissley, P., Insulin-like growth factor-I (IGF-I) dependent phosphorylation of the IGF-I receptor in MG-63 cells. *Regulatory Peptides* **1993,** *48* (1), 207-216; (b) Luginbuehl, V.; Wenk, E.; Koch, A.; Gander, B.; Merkle, H. P.; Meinel, L., Insulin-like Growth Factor I—Releasing Alginate-Tricalciumphosphate Composites for Bone Regeneration. *Pharmaceutical Research* **2005,** *22* (6), 940-950.
13. Tabisz, B.; Schmitz, W.; Schmitz, M.; Luehmann, T.; Heusler, E.; Rybak, J.-C.; Meinel, L.; Fiebig, J. E.; Mueller, T. D.; Nickel, J., Site-Directed Immobilization of BMP-2: Two Approaches for the Production of Innovative Osteoinductive Scaffolds. *Biomacromolecules* **2017,** *18* (3), 695-708.

6. Conclusion & Outlook

IGF-I is an inducer of skeletal muscle hypertrophy and blocks atrophy[5-7] by stimulating protein synthesis and suppressing the protein degradation pathway,[177, 178, 385] making it a boon for enhancing muscle function in aging and disease for which localized treatment options are particularly interesting. Furthermore, IGF-I decoration is instrumental for developing IGF-I based therapies with enhanced pharmacological properties. For that, we redesigned the therapeutic via genetic codon expansion leading to an alkyne modified IGF-I, thereby becoming a substrate for biorthogonal click chemistries yielding a decoration in a site-specific fashion. To achieve this, two strategies were adopted to produce uAA incorporated IGF-I: (i) genetically engineered IGF-I fusion variants (Trx-plk-IGF-I); (ii) engineered indigenous IGF-I Ea therapeutic (plk-IGF-I Ea).

Experience has shown that small peptides were especially prone to proteolytic degradation within *E. coli*.[386] For that reason, fusion tag strategies have been applied to enhance expression (reviewed in-depth by [387]). Fusion partners provide several additional advantages, such as alleviating inclusion body formation and generic protein purification schemes.[388, 389] Therefore, we followed a sophisticated protein-fusion system approach for IGF-I production by engineering an IGF-I fusion protein (Trx-IGF-I), containing N-terminal His_6-tagged Trx followed by a thrombin cleavage site and mature human IGF-I. The expression and purification of proteins were facilitated by the use of Trx[257, 276-279] and His_6 tags,[318-322] respectively. After the removal of affinity tags by thrombin, purified IGF-I was demonstrated by SDS-PAGE and Western Blot analysis and further confirmed by mass spectrometry. The preparations were homogeneous as judged by RP-HPLC and SDS-PAGE analysis.

Following the same protein-fusion system strategy, we genetically engineered one IGF-I mutant (Trx-plk-IGF-I) by incorporating the plk at position 3 into the IGF-I amino acid sequence and were able to express sufficient amounts of Trx-plk-IGF-I after systematic optimization of culture conditions (induction time, IPTG concentration, plk amount), and variation of *E. coli* hosts (BL21 (DE3), SHuffle T7, Rosetta (DE3), and C321.ΔA.exp). Soluble and insoluble cell fractions of *E. coli* producing IGF-I variant were analyzed by gel electrophoresis and subsequent Coomassie staining or immunodetection of the recombinant protein. Purified plk-IGF-I was successfully demonstrated by Western Blot. The major drawbacks associated with the fusion tag strategy are the demand of tag removal and multiple chromatography steps. As mentioned in the **Discussion section**, removal of these tags requires endoproteases that lead to unspecific cleavage, the generation of non-native N-terminal amino acids,[390] inefficient processing due to steric hindrance or the presence of unfavorable residues around the cleavage site,[334, 391] low protein yields and failure in recovery active target proteins due to protein precipitation/aggregation,[334, 392] expense of proteases and labor-intensive optimization of cleavage conditions. One approach to mitigate the

risk of unspecific cleavage is to use SUMO protease.[390] Inefficient processing could be alleviated by the inclusion of a spacer or linker (extra amino acid residues) between the cleavage site and target protein.[393, 394]

The other option is to engineer IGF-I (plk-IGF-I Ea) with Ea peptide prolongation at the C-terminus, to bypass the problems associated with the removal of the fusion partner. Another aspect which should be taken into consideration when producing IGF-I in *E. coli*, more than 90% was expressed in insoluble form as inclusion bodies. Hence the subsequent renaturation of this therapeutic into correct conformation is crucial requisite for future application. The proper folding of plk-IGF-I Ea after expression and inclusion body isolation was assessed by WST-1 proliferation assay. The main IGF-I-induced signaling cascade, the AKT pathway, was stimulated to a similar extent by wild-type IGF-I with plk-IGF-I Ea variant, as shown by Western Blot analysis. The promising results suggest that the introduced point mutation did not affect bioactivity as determined by mitogenic effect (long-term exposure) and receptor signaling (short-term exposure). The high purity of plk-IGF-I Ea was as judged by SDS-PAGE and RP-HPLC. The identity was confirmed by Western Blot and mass spectrometry. Moreover, the alkyne group was successfully introduced into IGF-I Ea biosynthetically, as determined by the covalent CuAAC reaction. Additionally, plk-IGF-I Ea was site-specifically immobilized to spatially direct its mitogenic effects and differentiation to the surrounding of a model carrier, providing biological activities in a paracrine manner. Our observations based on locally presented IGF-I on cellular performances, clearly linked the advantageous impact of the designed multi-valence on the outcome. This insight is opening exciting translational applications towards future IGF-I therapeutics. To further investigate the effects of multivalence on the regenerative outcome, *in vivo* consequence of site-specifically decorated surfaces of relevant biomaterials with plk-IGF-I Ea should be detailed in the future.

We further expanded the biomolecule labeling from one single labeling to multiple positions. As demonstrated by Western Blot and mass spectrometry, an IGF-I Ea variant containing plk at two distinct positions was successfully expressed via amber codon suppression. However, attention should be paid to the low natural yield of plk-IGF-I Ea-plk, and associated challenges on the fidelity and suppression efficiency and truncated protein formation with associated downstream purification difficulties. This might be addressed by the use of RF 1 deficient strain (C321.ΔA.exp[309]), evolved ribosomes and developed expression vectors (see **Discussion section**). Afterward, one pot double-labeling would be achieved where terminal alkyne bearing uAAs are incorporated at two distinct positions of IGF-I Ea and then labeled with other molecules (e.g., myostatin antagonist) or surfaces simultaneously via CuAAC chemistry. Further, a bioresponsive linker (e.g., responsive to enzymes, variations in pH, redox potential or hydrogen peroxide levels in disease progression) could be placed in between the biologic and the carrier,[395] supposed to

disintegrate at the site of need readily and the active IGF-I is then released locally from the conjugate in a strictly confined manner. One interesting design to amplify the beneficial anabolic effects of IGF-I is to simultaneously delivery anti-catabolic effect of a myostatin antagonist. Concomitantly, the anabolic effect of IGF-I together with the anti-catabolic effect of a myostatin antagonist might provide synergistic effects in the treatment of sarcopenia or another relevant disease. On the background of the bioresponsive co-delivery system, a myostatin antagonist (MA) with an azide-containing protease cleavable linker (PCL) attached at both its N- and C-terminus is designed and can be manually synthesized. Plk-IGF-I Ea-plk can be linked to the resulted MA in series, as in shape “necklace”. Upon entry into the flamed tissue characterized by upregulated proteases, the inter-positioned PCL is degraded by proteases, releasing IGF-I and MA simultaneously. As a requisite for application, the bioactivity of unconjugated and conjugated plk-IGF-I Ea-plk variant and after protease cleavage has to be demonstrated. Similarly, future work is to be focused on the accomplishment and selectivity of the click reaction and cleavage of the linker by proteases.

As a follow-up, the plk-IGF-I Ea is also a lysine donor substrate for transglutaminase, as determined by SDS-PAGE and fluorescence imaging, providing an option for future dual-functionality labeling. However, the work is still in a preliminary state. Further analysis will be necessary to evaluate the precise cross-linking site(s) within plk-IGF-I Ea. Afterward, plk-IGF-I Ea is sequentially labeled by TGase-catalyzed reaction, followed by separation of FXIIIa using Vivaspin 500 ultrafiltration spin columns and performance of the CuAAC reaction to label the alkyne group of the therapeutic in one pot. Sequential labeling of plk-IGF-I Ea could be exploited for attaching two drugs, or one biologic and one carrier, or one drug and a tracer for imaging in living organisms or a targeted motif for disease-oriented therapy. Apart from the CuAAC strategy, other biorthogonal chemistries can be adopted by exploiting the promiscuity of PylRS to introduce azide functionality into IGF-I Ea, followed by copper-free click chemistry (e.g., SPAAC). For established reactions that have been demonstrated on IGF-I variants, the rate constants for the corresponding model reactions are in the range 10^{-2} M^{-1} s^{-1} to 10^{5} M^{-1} s^{-1} (**Figure 27**). Other emerging approaches, for example, inverse electron-demand Diels–Alder reactions show higher rates in comparison to CuAAC chemistry and approach the rates of enzymatic labeling reactions, can also be utilized by site-specific incorporation of norbornene-, 1,3-disubstituted cyclopropene-, bicyclononyne-, trans-cyclooctene-, or tetrazine-bearing unnatural amino.[396] All in all, the genetically encoded, site-specific incorporation of uAAs that bear bioorthogonal functional groups and natural TGase substrate would allow site-specific dual labeling of IGF-I at defined sites.

Bioresponsive co-delivery of FGF2 and IGF-I based on genetic incorporation of clickable unnatural amino acids were designed to provide an interesting option for tissue engineering. Engineered azide-PCL-FGF2, containing a clickable azide partner, followed by a PCL and FGF2 sequence,[250]

was successfully expressed and purified by heparin-affinity chromatography. The preliminary evidence suggested the successful bioconjugation of plk-IGF-I Ea with engineered azide-PCL-FGF2 by CuAAC reaction.

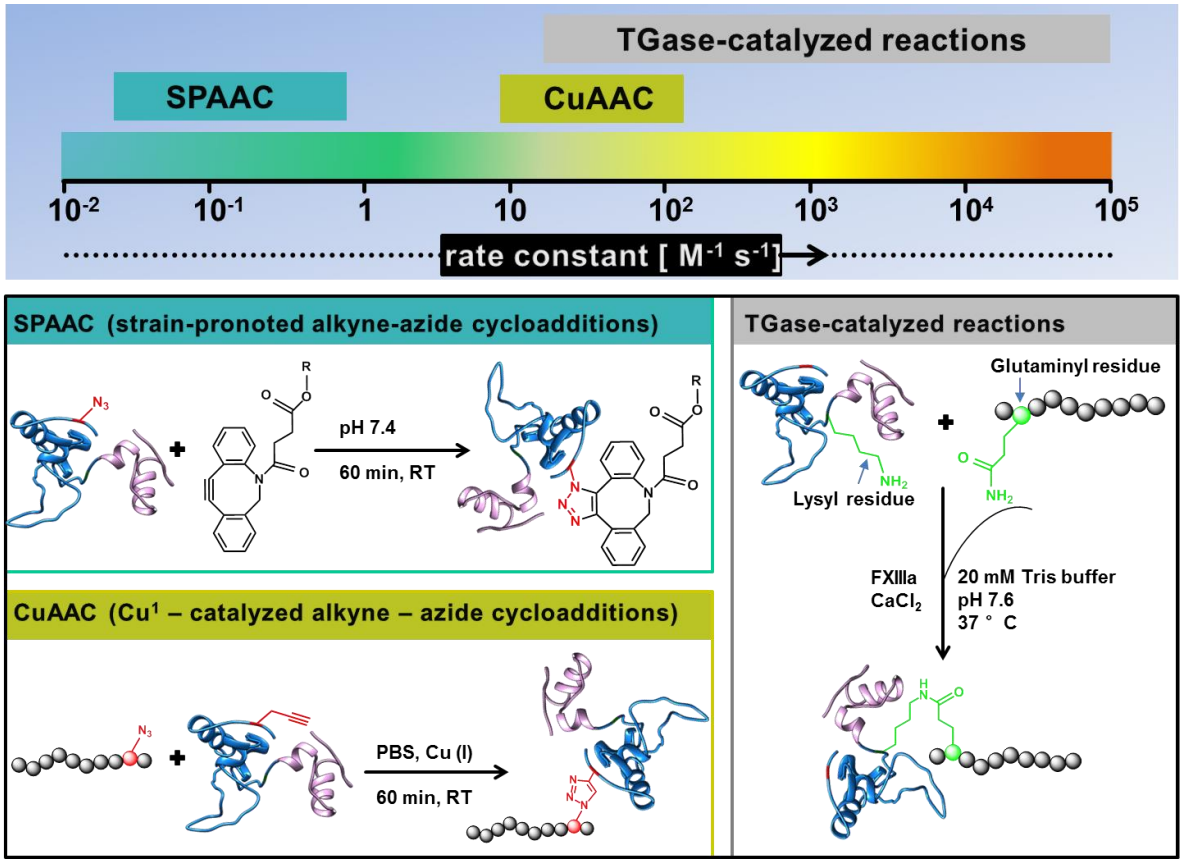

Figure 27. The range of rate constants reported for several bio-orthogonal protein labeling methods[396, 397] and schematic illustration of bio-orthogonal reactions on IGF-I Ea. The rate of CuAAC reaction[398-401] depends on Cu^1. Tailored water-soluble Cu ligands and/or Cu-chelating azides give rate constants of 10–200 $M^{-1}s^{-1}$ in the presence of 10–500 µM Cu^1; TGase-catalyzed labeling depends on different TGase and substrates used, reaction conditions, etc. Kinetic parameters of substrates (kcat/Km) obtained in assays with human FXIII activated by thrombin.[397]

Conjugation efficiency was further optimized after the systematic estimation of reaction temperature, incubation duration, and different molecules ratios. However, insufficient purification was observed for several initial attempts. Further work is to be devoted for the optimization of downstream purification processes with the aim of increasing the yield of IGF-FGF conjugates. Ongoing studies are evaluating the cleavage of the linker by proteases and biological activity of the conjugates before and after cleavage. TGase-reactivity lysine in IGF-I Ea could provide an opportunity to link IGF-FGF conjugates with other molecules possessing a Q-reactive substrate following TGase-catalyzed reaction yielding a site-specific decoration (**Figure 27**). A promising approach is the PEGylation of IGF-FGF conjugates via using a PEG polymer-modified the same

PCL as that of azide-PCL-FGF2. Systemically given “FGF2–PCL–IGF-I–PCL–PEG” conjugates ferry to the site of need, at which providing upregulated enzymes in disease sites can act as triggers for “on-demand” release of FGF2 and IGF-I. Bioresponsive release profiles can be adapted by using two different PCLs for FGF2 and IGF-I in order to match the natural tendon healing process[402] (i.e., a rapid release profile for FGF2 and a gradually slow release profile for IGF-I).

In conclusion, the combination of genetic code expansion and click chemistry allows new functions added to potent therapeutics by site-specific labeling of target proteins with other molecular (e.g., small fluorophores, biologics, polymers). We made considerable progress towards IGF-I based therapies with enhanced pharmacological properties based on genetic incorporation of clickable unnatural amino acids. Still, much work has to be done for the implementation of this strategy and to answer the arising questions.

References

1. Denley, A.; Cosgrove, L. J.; Booker, G. W.; Wallace, J. C.; Forbes, B. E., Molecular interactions of the IGF system. *Cytokine & Growth Factor Reviews* **2005,** 16, (4), 421-439.
2. Firth, S. M.; Baxter, R. C., Cellular actions of the insulin-like growth factor binding proteins. *Endocrine reviews* **2002,** 23, (6), 824-854.
3. Jones, J. I.; Clemmons, D. R., Insulin-like growth factors and their binding proteins: biological actions. *Endocrine Reviews* **1995,** 16, (1), 3-34.
4. Hughes, R.; Sendtner, M.; Thoenen, H., Members of several gene families influence survival of rat motoneurons *in vitro* and *in vivo*. *Journal of neuroscience research* **1993,** 36, (6), 663-671.
5. Semsarian, C.; Sutrave, P.; Richmond, D. R.; Graham, R. M., Insulin-like growth factor (IGF-I) induces myotube hypertrophy associated with an increase in anaerobic glycolysis in a clonal skeletal-muscle cell model. *Biochemical Journal* **1999,** 339, (2), 443-451.
6. Stitt, T. N.; Drujan, D.; Clarke, B. A.; Panaro, F.; Timofeyva, Y.; Kline, W. O.; Gonzalez, M.; Yancopoulos, G. D.; Glass, D. J., The IGF-1/PI3K/Akt pathway prevents expression of muscle atrophy-induced ubiquitin ligases by inhibiting FOXO transcription factors. *Molecular Cell* **2004,** 14, (3), 395-403.
7. Musarò, A.; McCullagh, K.; Paul, A.; Houghton, L.; Dobrowolny, G.; Molinaro, M.; Barton, E. R.; L Sweeney, H.; Rosenthal, N., Localized Igf-1 transgene expression sustains hypertrophy and regeneration in senescent skeletal muscle. *Nature Genetics* **2001,** 27, 195.
8. Puche, J. E.; Castilla-Cortázar, I., Human conditions of insulin-like growth factor-I (IGF-I) deficiency. *Journal of Translational Medicine* **2012,** 10, 224-224.
9. Dodge, J. C.; Haidet, A. M.; Yang, W.; Passini, M. A.; Hester, M.; Clarke, J.; Roskelley, E. M.; Treleaven, C. M.; Rizo, L.; Martin, H., Delivery of AAV-IGF-1 to the CNS extends survival in ALS mice through modification of aberrant glial cell activity. *Molecular Therapy* **2008,** 16, (6), 1056-1064.
10. Franz, C. K.; Federici, T.; Yang, J.; Backus, C.; Oh, S. S.; Teng, Q.; Carlton, E.; Bishop, K. M.; Gasmi, M.; Bartus, R. T., Intraspinal cord delivery of IGF-I mediated by adeno-associated virus 2 is neuroprotective in a rat model of familial ALS. *Neurobiology of disease* **2009,** 33, (3), 473-481.
11. Dodge, J. C.; Treleaven, C. M.; Fidler, J. A.; Hester, M.; Haidet, A.; Handy, C.; Rao, M.; Eagle, A.; Matthews, J. C.; Taksir, T. V., AAV4-mediated expression of IGF-1 and VEGF within cellular components of the ventricular system improves survival outcome in familial ALS mice. *Molecular therapy* **2010,** 18, (12), 2075-2084.
12. Hantai, D.; Akaaboune, M.; Lagord, C.; Murawsky, M.; Houenou, L.; Festoff, B.; Vaught, J.; Rieger, F.; Blondet, B., Beneficial effects of insulin-like growth factor-I on wobbler mouse motoneuron disease. *Journal of the neurological sciences* **1995,** 129, 122-126.
13. Gregorevic, P.; Plant, D. R.; Leeding, K. S.; Bach, L. A.; Lynch, G. S., Improved contractile function of the mdx dystrophic mouse diaphragm muscle after insulin-like growth factor-I administration. *The American journal of pathology* **2002,** 161, (6), 2263-2272.
14. Kaspar, B. K.; Lladó, J.; Sherkat, N.; Rothstein, J. D.; Gage, F. H., Retrograde viral delivery of IGF-1 prolongs survival in a mouse ALS model. *Science* **2003,** 301, (5634), 839-842.
15. Kumar, A.; Yamauchi, J.; Girgenrath, T.; Girgenrath, M., Muscle-specific expression of insulin-like growth factor 1 improves outcome in Lama2 Dy-w mice, a model for congenital muscular dystrophy type 1A. *Human molecular genetics* **2011,** 20, (12), 2333-2343.
16. Adamo, M. L.; Lanau, F.; Neuenschwander, S.; Werner, H.; LeRoith, D.; Roberts, J. C. T., Distinct promoters in the rat insulin-like growth factor-I (IGF-I) gene are active in CHO cells. *Endocrinology* **1993,** 132, (2), 935-937.
17. Yang, H.; Adamo, M. L.; Koval, A. P.; McGuinness, M. C.; Ben-Hur, H.; Yang, Y.; LeRoith, D.; Roberts, J. C. T., Alternative leader sequences in insulin-like growth factor I mRNAs modulate translational efficiency and encode multiple signal peptides. *Molecular Endocrinology* **1995,** 9, (10), 1380-1395.

18. Boor, C.; Kght, R.; R; Kedia, R.; Spiteri, M.; Allen, J., Differential mRNA expression of insulin-like growth factor-1 splice variants in patients with idiopathic pulmonary fibrosis and pulmonary sarcoidosis. *American Journal of Respiratory and Critical Care Medicine* **2001,** 164, (2), 265-272.
19. Adamo, M. L.; Ben-Hur, H.; Leroith, D.; Roberts, C. T., Transcription initiation in the two leader exons of the rat IGF-I gene occurs from disperse versus localized sites. *Biochemical and Biophysical Research Communications* **1991,** 176, (2), 887-893.
20. Wallis, M., New insulin-like growth factor (IGF)-precursor sequences from mammalian genomes: the molecular evolution of IGFs and associated peptides in primates. *Growth Hormone & IGF Research* **2009,** 19, (1), 12-23.
21. D'Ercole, A. J.; Stiles, A. D.; Underwood, L. E., Tissue concentrations of somatomedin C: further evidence for multiple sites of synthesis and paracrine or autocrine mechanisms of action. *Proceedings of the National Academy of Sciences* **1984,** 81, (3), 935-939.
22. Rotwein, P.; Pollock, K. M.; Watson, M.; Milbrandt, J. D., Insulin-like growth factor gene expression during rat embryonic development. *Endocrinology* **1987,** 121, (6), 2141-2144.
23. Adamo, M.; Lowe, J. W. L.; Leroith, D.; Roberts, J. C. T., Insulin-like growth factor I messenger ribonucleic acids with alternative 5'-untranslated regions are differentially expressed during development of the rat. *Endocrinology* **1989,** 124, (6), 2737-2744.
24. Wang, X.; Yang, Y.; Adamo, M. L., Characterization of the rat insulin-like growth factor i gene promoters and identification of a minimal exon 2 promoter. *Endocrinology* **1997,** 138, (4), 1528-1536.
25. O'Sullivan, D. C.; Szestak, T. A. M.; Pell, J. M., Regulation of IGF-I mRNA by GH: putative functions for class 1 and 2 message. *American Journal of Physiology-Endocrinology and Metabolism* **2002,** 283, (2), E251-E258.
26. Woelfle, J.; Chia, D. J.; Rotwein, P., Mechanisms of growth hormone (GH) action identification of conserved STAT5 binding sites that mediate GH-induced insulin-like growth factor-I gene activation. *Journal of Biological Chemistry* **2003,** 278, (51), 51261-51266.
27. Chia, D. J.; Young, J. J.; Mertens, A. R.; Rotwein, P., Distinct alterations in chromatin organization of the two IGF-I promoters precede growth hormone-induced activation of IGF-I gene transcription. *Molecular Endocrinology* **2010,** 24, (4), 779-789.
28. Duguay, S.; Swanson, P.; Dickhoff, W. W., Differential expression and hormonal regulation of alternatively spliced IGF-I mRNA transcripts in salmon. *Journal of molecular endocrinology* **1994,** 12, (1), 25-37.
29. Lund, P. K. In *Insulinlike growth factor I: Molecular biology and relevance to tissue-specific expression and action*, Proceedings of the 1992 Laurentian Hormone Conference, 1994; Elsevier: 1994; pp 125-148.
30. Hameed, M.; Lange, K.; Andersen, J.; Schjerling, P.; Kjaer, M.; Harridge, S.; Goldspink, G., The effect of recombinant human growth hormone and resistance training on IGF-I mRNA expression in the muscles of elderly men. *The Journal of physiology* **2004,** 555, (1), 231-240.
31. Imanaka, M.; Iida, K.; Murawaki, A.; Nishizawa, H.; Fukuoka, H.; Takeno, R.; Takahashi, Y.; Okimura, Y.; Kaji, H.; Chihara, K., Growth hormone stimulates mechano growth factor expression and activates myoblast transformation in C2C12 cells. *Kobe J Med Sci* **2008,** 54, (1), E46-54.
32. Aperghis, M.; Velloso, C. P.; Hameed, M.; Brothwood, T.; Bradley, L.; Bouloux, P. M.; Harridge, S. D.; Goldspink, G., Serum IGF-I levels and IGF-I gene splicing in muscle of healthy young males receiving rhGH. *Growth Hormone & IGF Research* **2009,** 19, (1), 61-67.
33. Moschos, M. M.; Armakolas, A.; Philippou, A.; Pissimissis, N.; Panteleakou, Z.; Nezos, A.; Kaparelou, M.; Koutsilieris, M., Expression of the insulin-like growth factor 1 (IGF-1) and type I IGF receptor mRNAs in human HLE-B3 lens epithelial cells. *In Vivo* **2011,** 25, (2), 179-184.
34. Barton, E. R., The ABCs of IGF-I isoforms: impact on muscle hypertrophy and implications for repair. *Applied Physiology, Nutrition, and Metabolism* **2006,** 31, (6), 791-797.
35. Okazaki, R.; Durham, S. K.; Riggs, B. L.; Conover, C. A., Transforming growth factor-β and forskolin increase all classes of insulin-like growth factor-I transcripts in normal human osteoblast-like cells. *Biochemical and Biophysical Research Communications* **1995,** 207, (3), 963-970.

36. Chew, S. L.; Lavender, P.; Clark, A. J.; Ross, R. J., An alternatively spliced human insulin-like growth factor-I transcript with hepatic tissue expression that diverts away from the mitogenic IBE1 peptide. *Endocrinology* **1995,** 136, (5), 1939-1944.
37. Jansen, E.; Steenbergh, P. H.; van Schaik, F. M. A.; Sussenbach, J. S., The human IGF-I gene contains two cell type-specifically regulated promoters. *Biochemical and Biophysical Research Communications* **1992,** 187, (3), 1219-1226.
38. Hepler, J. E.; Van Wyk, J. J.; Kay Lund, P., Different half-lives of insulin-like growth factor I mRNAs that differ in length of 3' untranslated sequence. *Endocrinology* **1990,** 127, (3), 1550-1552.
39. Lee, E. K.; Gorospe, M., Minireview: posttranscriptional regulation of the insulin and insulin-like growth factor systems. *Endocrinology* **2010,** 151, (4), 1403-1408.
40. Elia, L.; Contu, R.; Quintavalle, M.; Varrone, F.; Chimenti, C.; Russo, M. A.; Cimino, V.; De Marinis, L.; Frustaci, A.; Catalucci, D.; Condorelli, G., Reciprocal regulation of microRNA-1 and insulin-like growth factor-1 signal transduction cascade in cardiac and skeletal muscle in physiological and pathological conditions. *Circulation* **2009,** 120, (23), 2377-2385.
41. Hu, Y.-K.; Wang, X.; Li, L.; Du, Y.-H.; Ye, H.-T.; Li, C.-Y., MicroRNA-98 induces an Alzheimer's disease-like disturbance by targeting insulin-like growth factor 1. *Neuroscience Bulletin* **2013,** 29, (6), 745-751.
42. Rotwein, P., Two insulin-like growth factor I messenger RNAs are expressed in human liver. *Proceedings of the National Academy of Sciences* **1986,** 83, (1), 77-81.
43. Hill, M.; Goldspink, G., Expression and splicing of the insulin-like growth factor gene in rodent muscle is associated with muscle satellite (stem) cell activation following local tissue damage. *The Journal of physiology* **2003,** 549, (2), 409-418.
44. Winn, N.; Paul, A.; Musaro, A.; Rosenthal, N. In *Insulin-like growth factor isoforms in skeletal muscle aging, regeneration, and disease*, Cold Spring Harbor symposia on quantitative biology, 2002; Cold Spring Harbor Laboratory Press: 2002; pp 507-518.
45. Sairam, M. R., Role of carbohydrates in glycoprotein hormone signal transduction. *The FASEB Journal* **1989,** 3, (8), 1915-1926.
46. Taylor, A. K.; Wall, R., Selective removal of alpha heavy-chain glycosylation sites causes immunoglobulin A degradation and reduced secretion. *Molecular and cellular biology* **1988,** 8, (10), 4197-4203.
47. Guan, J.-L.; Machamer, C. E.; Rose, J. K., Glycosylation allows cell-surface transport of an anchored secretory protein. *Cell* **1985,** 42, (2), 489-496.
48. Simmons, J. G.; van Wyk, J. J.; Hoyt, E. C.; Lund, P. K., Multiple transcription start sites in the rat insulin-like growth factor-I gene give rise to IGF-I mRNAs that encode different IGF-I precursors and are processed differently in vitvo. *Growth Factors* **1993,** 9, (3), 205-221.
49. LeRoith, D.; Roberts, C. T., Insulin-like growth factor I (IGF-I): A molecular basis for endocrine versus local action? *Molecular and Cellular Endocrinology* **1991,** 77, (1), C57-C61.
50. Sara, V. R.; Carlsson-Skwirut, C.; Drakenberg, K.; Giacobini, M. B.; Håkansson, L.; Mirmiran, M.; Nordberg, A.; Olson, L.; Reinecke, M.; Ståhlbom, P. A.; Nordqvist, A. C. S., The biological role of truncated insulin-like growth factor-1 and the tripeptide gpe in the central nervous systema. *Annals of the New York Academy of Sciences* **1993,** 692, (1), 183-191.
51. Carlsson-Skwirut, C.; Jörnvall, H.; Holmgren, A.; Andersson, C.; Bergman, T.; Lundquist, G.; Sjögren, B.; Sara, V. R., Isolation and characterization of variant IGF-1 as well as IGF-2 from adult human brain. *FEBS Letters* **1986,** 201, (1), 46-50.
52. Duguay, S. J.; Milewski, W. M.; Young, B. D.; Nakayama, K.; Steiner, D. F., Processing of wild-type and mutant proinsulin-like growth factor-IA by subtilisin-related proprotein convertases. *Journal of Biological Chemistry* **1997,** 272, (10), 6663-6670.
53. Wilson, H. E.; Westwood, M.; White, A.; Clayton, P. E., Monoclonal antibodies to the carboxy-terminal Ea sequence of pro-insulin-like growth factor-IA (proIGF-IA) recognize proIGF-IA secreted by IM9 B-lymphocytes. *Growth Hormone & IGF Research* **2001,** 11, (1), 10-17.
54. Conover, C. A.; Baker, B. K.; Bale, L. K.; Clarkson, J. T.; Liu, F.; Hintz, R. L., Human hepatoma cells synthesize and secrete insulin-like growth factor Ia prohormone under growth hormone control. *Regulatory Peptides* **1993,** 48, (1), 1-8.

55. Conover, C. A.; Baker, B. K.; Hintz, R. L., Cultured human fibroblasts secrete insulin-like growth factor IA prohormone. *The Journal of Clinical Endocrinology & Metabolism* **1989,** 69, (1), 25-30.
56. Bach, M. A.; Roberts, J. C. T.; Smith, E. P.; LeRoith, D., Alternative splicing produces messenger rnas encoding insulin-like growth factor-I prohormones that are differentially glycosylated *in vitro*. *Molecular Endocrinology* **1990,** 4, (6), 899-904.
57. Philippou, A.; Barton, E. R., Optimizing IGF-I for skeletal muscle therapeutics. *Growth hormone & IGF research : official journal of the Growth Hormone Research Society and the International IGF Research Society* **2014,** 24, (5), 157-163.
58. Philippou, A.; Maridaki, M.; Pneumaticos, S.; Koutsilieris, M., The complexity of the IGF1 gene splicing, posttranslational modification and bioactivity. *Molecular Medicine* **2014,** 20, (1), 202-214.
59. Philippou, A.; Papageorgiou, E.; Bogdanis, G.; Halapas, A.; Sourla, A.; Maridaki, M.; Pissimissis, N.; Koutsilieris, M., Expression of IGF-1 isoforms after exercise-induced muscle damage in humans: characterization of the MGF E peptide actions *in vitro*. *In Vivo* **2009,** 23, (4), 567-575.
60. McKay, B. R.; O'Reilly, C. E.; Phillips, S. M.; Tarnopolsky, M. A.; Parise, G., Co-expression of IGF-1 family members with myogenic regulatory factors following acute damaging muscle-lengthening contractions in humans. *The Journal of Physiology* **2008,** 586, (22), 5549-5560.
61. Milingos, D. S.; Philippou, A.; Armakolas, A.; Papageorgiou, E.; Sourla, A.; Protopapas, A.; Liapi, A.; Antsaklis, A.; Mastrominas, M.; Koutsilieris, M., Insulin like growth factor-1Ec (MGF) expression in eutopic and ectopic endometrium: characterization of the MGF E-peptide actions *in vitro*. *Molecular Medicine* **2011,** 17, (1-2), 21-28.
62. Armakolas, A.; Philippou, A.; Panteleakou, Z.; Nezos, A.; Sourla, A.; Petraki, C.; Koutsilieris, M., Preferential expression of IGF-1Ec (MGF) transcript in cancerous tissues of human prostate: Evidence for a novel and autonomous growth factor activity of MGF E peptide in human prostate cancer cells. *The Prostate* **2010,** 70, (11), 1233-1242.
63. Koczorowska, M. M.; Kwasniewska, A.; Gozdzicka-Jozefiak, A., IGF1 mRNA isoform expression in the cervix of HPV-positive women with pre-cancerous and cancer lesions. *Experimental and Therapeutic Medicine* **2011,** 2, (1), 149-156.
64. Kasprzak, A.; Szaflarski, W.; Szmeja, J.; Andrzejewska, M.; Przybyszewska, W.; Kaczmarek, E.; Koczorowska, M.; Kościński, T.; Zabel, M.; Drews, M., Differential expression of IGF-1 mRNA isoforms in colorectal carcinoma and normal colon tissue. *International journal of oncology* **2013,** 42, (1), 305-316.
65. Mourkioti, F.; Rosenthal, N., IGF-1, inflammation and stem cells: interactions during muscle regeneration. *Trends in Immunology* **2005,** 26, (10), 535-542.
66. Temmerman, L.; Slonimsky, E.; Rosenthal, N., Class 2 IGF-1 isoforms are dispensable for viability, growth and maintenance of IGF-1 serum levels. *Growth Hormone & IGF Research* **2010,** 20, (3), 255-263.
67. Philippou, A.; Maridaki, M.; Halapas, A.; Koutsilieris, M., The role of the insulin-like growth factor 1 (IGF-1) in skeletal muscle physiology. *In Vivo* **2007,** 21, (1), 45-54.
68. Lowe, J. W. L.; Lasky, S. R.; LeRoith, D.; Roberts, J. C. T., Distribution and regulation of rat insulin-like growth factor I messenger ribonucleic acids encoding alternative carboxyterminal E-peptides: evidence for differential processing and regulation in liver. *Molecular Endocrinology* **1988,** 2, (6), 528-535.
69. Marshall, R. D., Glycoproteins. *Annual Review of Biochemistry* **1972,** 41, (1), 673-702.
70. Imperiali, B.; O'Connor, S. E.; Hendrickson, T.; Kellenberger, C., Chemistry and biology of asparagine-linked glycosylation. In *Pure and Applied Chemistry*, 1999; Vol. 71, p 777.
71. Durzyńska, J.; Philippou, A.; Brisson, B. K.; Nguyen-McCarty, M.; Barton, E. R., The pro-forms of insulin-like growth factor I (IGF-I) are predominant in skeletal muscle and alter IGF-I receptor activation. *Endocrinology* **2013,** 154, (3), 1215-1224.
72. Ronnett, G. V.; Knutson, V. P.; Kohanski, R. A.; Simpson, T. L.; Lane, M. D., Role of glycosylation in the processing of newly translated insulin proreceptor in 3T3-L1 adipocytes. *Journal of Biological Chemistry* **1984,** 259, (7), 4566-4575.

73. Flintegaard, T. V.; Thygesen, P.; Rahbek-Nielsen, H.; Levery, S. B.; Kristensen, C.; Clausen, H.; Bolt, G., N-glycosylation increases the circulatory half-life of human growth hormone. *Endocrinology* **2010,** 151, (11), 5326-5336.
74. Yu, S. R.; Burkhardt, M.; Nowak, M.; Ries, J.; Petrášek, Z.; Scholpp, S.; Schwille, P.; Brand, M., Fgf8 morphogen gradient forms by a source-sink mechanism with freely diffusing molecules. *Nature* **2009,** 461, 533.
75. Hede, M. S.; Salimova, E.; Piszczek, A.; Perlas, E.; Winn, N.; Nastasi, T.; Rosenthal, N., E-peptides control bioavailability of IGF-1. *PLoS One* **2012,** 7, (12), e51152.
76. Coleman, M. E.; DeMayo, F.; Yin, K. C.; Lee, H. M.; Geske, R.; Montgomery, C.; Schwartz, R. J., Myogenic vector expression of insulin-like growth factor I stimulates muscle cell differentiation and myofiber hypertrophy in transgenic mice. *Journal of Biological Chemistry* **1995,** 270, (20), 12109-12116.
77. Rabinovsky, E. D.; Gelir, E.; Gelir, S.; Lui, H.; Kattash, M.; DeMayo, F. J.; Shenaq, S. M.; Schwartz, R. J., Targeted expression of IGF-1 transgene to skeletal muscle accelerates muscle and motor neuron regeneration. *The FASEB Journal* **2003,** 17, (1), 53-55.
78. Pelosi, L.; Giacinti, C.; Nardis, C.; Borsellino, G.; Rizzuto, E.; Nicoletti, C.; Wannenes, F.; Battistini, L.; Rosenthal, N.; Molinaro, M.; Musarò, A., Local expression of IGF-1 accelerates muscle regeneration by rapidly modulating inflammatory cytokines and chemokines. *The FASEB Journal* **2007,** 21, (7), 1393-1402.
79. Park, S.; Brisson, B. K.; Liu, M.; Spinazzola, J. M.; Barton, E. R., Mature IGF-I excels in promoting functional muscle recovery from disuse atrophy compared with pro-IGF-IA. *Journal of Applied Physiology* **2014,** 116, (7), 797-806.
80. Vinciguerra, M.; Santini, M. P.; Claycomb, W. C.; Ladurner, A. G.; Rosenthal, N., Local IGF-1 isoform protects cardiomyocytes from hypertrophic and oxidative stresses via SirT1 activity. In *Aging (Albany NY)*, 2010; Vol. 2, pp 43-62.
81. Vinciguerra, M.; Santini, M. P.; Martinez, C.; Pazienza, V.; Claycomb, W. C.; Giuliani, A.; Rosenthal, N., mIGF-1/JNK1/SirT1 signaling confers protection against oxidative stress in the heart. *Aging Cell* **2012,** 11, (1), 139-149.
82. Vinciguerra, M.; Musaro, A.; Rosenthal, N., Regulation of muscle atrophy in aging and disease. In *Protein metabolism and homeostasis in aging*, Springer: 2010; pp 211-233.
83. Santini, M. P.; Tsao, L.; Monassier, L.; Theodoropoulos, C.; Carter, J.; Lara-Pezzi, E.; Slonimsky, E.; Salimova, E.; Delafontaine, P.; Song, Y.-H.; Bergmann, M.; Freund, C.; Suzuki, K.; Rosenthal, N., Enhancing Repair of the Mammalian Heart. *Circulation research* **2007,** 100, (12), 1732-1740.
84. Santini, M. P.; Winn, N.; Rosenthal, N. In *Signalling pathways in cardiac regeneration*, Novartis Foundation symposium, 2006; Chichester; New York; John Wiley; 1999: 2006; p 228.
85. Semenova, E.; Koegel, H.; Hasse, S.; Klatte, J. E.; Slonimsky, E.; Bilbao, D.; Paus, R.; Werner, S.; Rosenthal, N., Overexpression of mIGF-1 in keratinocytes improves wound healing and accelerates hair follicle formation and cycling in mice. *The American journal of pathology* **2008,** 173, (5), 1295-1310.
86. Shavlakadze, T.; Winn, N.; Rosenthal, N.; Grounds, M. D., Reconciling data from transgenic mice that overexpress IGF-I specifically in skeletal muscle. *Growth hormone & IGF research* **2005,** 15, (1), 4-18.
87. Shavlakadze, T.; Boswell, J.; Burt, D.; Asante, E.; Tomas, F.; Davies, M.; White, J.; Grounds, M.; Goddard, C., Rskα-actin/hIGF-1 transgenic mice with increased IGF-I in skeletal muscle and blood: Impact on regeneration, denervation and muscular dystrophy. *Growth hormone & IGF research* **2006,** 16, (3), 157-173.
88. LeRoith, D.; Roberts, C. T., Jr., The insulin-like growth factor system and cancer. *Cancer Letters* 195, (2), 127-137.
89. Vajdos, F. F.; Ultsch, M.; Schaffer, M. L.; Deshayes, K. D.; Liu, J.; Skelton, N. J.; de Vos, A. M., Crystal structure of human insulin-like growth factor-1: detergent binding inhibits binding protein interactions. *Biochemistry* **2001,** 40, (37), 11022-11029.
90. Metzger, F.; Sajid, W.; Saenger, S.; Staudenmaier, C.; van der Poel, C.; Sobottka, B.; Schuler, A.; Sawitzky, M.; Poirier, R.; Tuerck, D., Separation of fast from slow anabolism by site-

specific PEGylation of insulin-like growth factor I (IGF-I). *Journal of Biological Chemistry* **2011,** 286, (22), 19501-19510.
91. Owino, V.; Yang, S. Y.; Goldspink, G., Age-related loss of skeletal muscle function and the inability to express the autocrine form of insulin-like growth factor-1 (MGF) in response to mechanical overload. *FEBS Letters* **2001,** 505, (2), 259-263.
92. Philippou, A.; Armakolas, A.; Panteleakou, Z.; Pissimissis, N.; Nezos, A.; Theos, A.; Kaparelou, M.; Armakolas, N.; Pneumaticos, S. G.; Koutsilieris, M., IGF1Ec expression in MG-63 human osteoblast-like osteosarcoma cells. *Anticancer Research* **2011,** 31, (12), 4259-4265.
93. Hill, M.; Wernig, A.; Goldspink, G., Muscle satellite (stem) cell activation during local tissue injury and repair. *Journal of Anatomy* **2003,** 203, (1), 89-99.
94. Dłużniewska, J.; Sarnowska, A.; Beręsewicz, M.; Johnson, I.; Srai, S. K. S.; Ramesh, B.; Goldspink, G.; Górecki, D. C.; Zabłocka, B., A strong neuroprotective effect of the autonomous C-terminal peptide of IGF-1 Ec (MGF) in brain ischemia. *The FASEB Journal* **2005,** 19, (13), 1896-1898.
95. Dai, Z.; Wu, F.; Yeung, E. W.; Li, Y., IGF-IEc expression, regulation and biological function in different tissues. *Growth Hormone & IGF Research* **2010,** 20, (4), 275-281.
96. Hameed, M.; Orrell, R. W.; Cobbold, M.; Goldspink, G.; Harridge, S. D. R., Expression of IGF-I splice variants in young and old human skeletal muscle after high resistance exercise. *The Journal of Physiology* **2003,** 547, (Pt 1), 247-254.
97. Haddad, F.; Adams, G. R., Selected contribution: acute cellular and molecular responses to resistance exercise. *Journal of applied physiology* **2002,** 93, (1), 394-403.
98. Yang, S. Y.; Goldspink, G., Different roles of the IGF-I Ec peptide (MGF) and mature IGF-I in myoblast proliferation and differentiation. *FEBS Letters* **2002,** 522, (1-3), 156-160.
99. Barton, E. R., Viral expression of insulin-like growth factor-I isoforms promotes different responses in skeletal muscle. *Journal of Applied Physiology* **2006,** 100, (6), 1778-1784.
100. Siegfried, J. M.; Kasprzyk, P. G.; Treston, A. M.; Mulshine, J. L.; Quinn, K. A.; Cuttitta, F., A mitogenic peptide amide encoded within the E peptide domain of the insulin-like growth factor IB prohormone. *Proceedings of the National Academy of Sciences* **1992,** 89, (17), 8107-8111.
101. Kuo, Y.-H.; Chen, T. T., Novel activities of pro-IGF-I E Peptides: regulation of morphological differentiation and anchorage-independent growth in human neuroblastoma cells. *Experimental Cell Research* **2002,** 280, (1), 75-89.
102. Durzyńska, J.; Wardziński, A.; Koczorowska, M.; Goździcka-Józefiak, A.; Barton, E. R., Human Eb peptide: not just a by-product of pre-pro-IGF1b processing? *Hormone and metabolic research = Hormon- und Stoffwechselforschung = Hormones et metabolisme* **2013,** 45, (6), 415-422.
103. Deng, M.; Wang, Y.; Zhang, B.; Liu, P.; Xiao, H.; Zhao, J., New proangiogenic activity on vascular endothelial cells for C-terminal mechano growth factor. *Acta Biochim Biophys Sin* **2012,** 44, (4), 316-322.
104. Mills, P.; Dominique, J. C.; Lafrenière, J. F.; Bouchentouf, M.; Tremblay, J. P., A synthetic mechano growth factor E peptide enhances myogenic precursor cell transplantation success. *American Journal of Transplantation* **2007,** 7, (10), 2247-2259.
105. Collins, J. M.; Goldspink, P. H.; Russell, B., Migration and proliferation of human mesenchymal stem cells is stimulated by different regions of the mechano-growth factor prohormone. *Journal of Molecular and Cellular Cardiology* **2010,** 49, (6), 1042-1045.
106. Chen, M. J.; Chiou, P. P.; Lin, P.; Lin, C. M.; Siri, S.; Peck, K.; Chen, T. T., Suppression of growth and cancer-induced angiogenesis of aggressive human breast cancer cells (MDA-MB-231) on the chorioallantoic membrane of developing chicken embryos by E-peptide of pro-IGF-I. *Journal of Cellular Biochemistry* **2007,** 101, (5), 1316-1327.
107. Brisson, B. K.; Barton, E. R., Insulin-like growth factor-I E-peptide activity is dependent on the IGF-I receptor. *PLoS One* **2012,** 7, (9), e45588.
108. Pfeffer, L. A.; Brisson, B. K.; Lei, H.; Barton, E. R., The insulin-like growth factor (IGF)-I E-peptides modulate cell entry of the mature IGF-I protein. *Molecular biology of the cell* **2009,** 20, (17), 3810-3817.

109. Ates, K.; Yang, S. Y.; Orrell, R. W.; Sinanan, A. C. M.; Simons, P.; Solomon, A.; Beech, S.; Goldspink, G.; Lewis, M. P., The IGF-I splice variant MGF increases progenitor cells in ALS, dystrophic, and normal muscle. *FEBS Letters* **2007,** 581, (14), 2727-2732.
110. Kuo, Y.-H.; Chen, T. T., Specific cell surface binding sites shared by human Pro-IGF-I Eb-peptides and rainbow trout Pro-IGF-I Ea-4-peptide. *General and comparative endocrinology* **2003,** 132, (2), 231-240.
111. Musarò, A.; McCullagh, K.; Paul, A.; Houghton, L.; Dobrowolny, G.; Molinaro, M.; Barton, E. R.; Sweeney, H. L.; Rosenthal, N., Localized Igf-1 transgene expression sustains hypertrophy and regeneration in senescent skeletal muscle. *Nature genetics* **2001,** 27, (2), 195.
112. Tan, D. S. W.; Cook, A.; Chew, S. L., Nucleolar localization of an isoform of the IGF-I precursor. *BMC Cell Biology* **2002,** 3, 17-17.
113. McKoy, G.; Ashley, W.; Mander, J.; Yang, S. Y.; Williams, N.; Russell, B.; Goldspink, G., Expression of insulin growth factor-1 splice variants and structural genes in rabbit skeletal muscle induced by stretch and stimulation. *The Journal of Physiology* **1999,** 516, (Pt 2), 583-592.
114. Carpenter, V.; Matthews, K.; Devlin, G.; Stuart, S.; Jensen, J.; Conaglen, J.; Jeanplong, F.; Goldspink, P.; Yang, S.-Y.; Goldspink, G.; Bass, J.; McMahon, C., Mechano-growth factor reduces loss of cardiac function in acute myocardial infarction. *Heart, Lung and Circulation* **2008,** 17, (1), 33-39.
115. Quesada, A.; Micevych, P.; Handforth, A., C-terminal mechano growth factor protects dopamine neurons: A novel peptide that induces heme oxygenase-1. *Experimental Neurology* **2009,** 220, (2), 255-266.
116. Aperghis, M.; Johnson, I. P.; Cannon, J.; Yang, S.-Y.; Goldspink, G., Different levels of neuroprotection by two insulin-like growth factor-I splice variants. *Brain Research* **2004,** 1009, (1), 213-218.
117. Riddoch-Contreras, J.; Yang, S.-Y.; Dick, J. R. T.; Goldspink, G.; Orrell, R. W.; Greensmith, L., Mechano-growth factor, an IGF-I splice variant, rescues motoneurons and improves muscle function in SOD1G93A mice. *Experimental Neurology* **2009,** 215, (2), 281-289.
118. Tang, J. J.; Podratz, J. L.; Lange, M.; Scrable, H. J.; Jang, M.-H.; Windebank, A. J., Mechano growth factor, a splice variant of IGF-1, promotes neurogenesis in the aging mouse brain. *Molecular Brain* **2017,** 10, 23.
119. DurzyŃSka, J.; Barton, E., IGF expression in HPV-related and HPV-unrelated human cancer cells. *Oncology Reports* **2014,** 32, (3), 893-900.
120. Yeh, Y.-H.; Lin, C.-M.; Chen, T. T., Human IGF-I Eb-peptide induces cell attachment and lamellipodia outspread of metastatic breast carcinoma cells (MDA-MB-231). *Experimental Cell Research* **2017,** 358, (2), 199-208.
121. Matheny, R. W.; Nindl, B. C.; Adamo, M. L., Minireview: mechano-growth factor: a putative product of IGF-I gene expression involved in tissue repair and regeneration. *Endocrinology* **2010,** 151, (3), 865-875.
122. Barton, E. R.; Park, S.; James, J. K.; Makarewich, C. A.; Philippou, A.; Eletto, D.; Lei, H.; Brisson, B.; Ostrovsky, O.; Li, Z.; Argon, Y., Deletion of muscle GRP94 impairs both muscle and body growth by inhibiting local IGF production. *The FASEB Journal* **2012,** 26, (9), 3691-3702.
123. Florini, J. R., Hormonal control of muscle growth. *Muscle & Nerve* **1987,** 10, (7), 577-598.
124. Florini, J. R.; Ewton, D. Z.; Coolican, S. A., Growth hormone and the insulin-like growth factor system in myogenesis. *Endocrine reviews* **1996,** 17, (5), 481-517.
125. Florini, J. R.; Ewton, D. Z.; Evinger-Hodges, M. J.; Falen, S. L.; Lau, R. L.; Regan, J. F.; Vertel, B. M., Stimulation and inhibition of myoblast differentiation by hormones. *In Vitro* **1984,** 20, (12), 942-958.
126. Florini, J. R.; Magri, K. A., Effects of growth factors on myogenic differentiation. *The American journal of physiology* **1989,** 256, (4 Pt 1), C701-11.
127. J R Florini; D Z Ewton, a.; Magri, K. A., Hormones, growth factors, and myogenic differentiation. *Annual Review of Physiology* **1991,** 53, (1), 201-216.
128. Koutsilieris, M.; Mitsiades, C.; Sourla, A., Insulin-like growth factor I and urokinase-type plasminogen activator bioregulation system as a survival mechanism of prostate cancer cells in osteoblastic metastases: development of anti-survival factor therapy for hormone-refractory prostate cancer. *Molecular Medicine* **2000,** 6, (4), 251-267.

129. Siddle, K.; Ursø, B.; Niesler, C. A.; Cope, D. L.; Molina, L.; Surinya, K. H.; Soos, M. A., Specificity in ligand binding and intracellular signalling by insulin and insulin-like growth factor receptors. *Biochemical Society Transactions* **2001,** 29, (4), 513-525.
130. Kooijman, R., Regulation of apoptosis by insulin-like growth factor (IGF)-I. *Cytokine & Growth Factor Reviews* **2006,** 17, (4), 305-323.
131. Federici, M.; Porzio, O.; Zucaro, L.; Giovannone, B.; Borboni, P.; Marini, M. A.; Lauro, D.; Sesti, G., Increased abundance of insulin/IGF-I hybrid receptors in adipose tissue from NIDDM patients. *Molecular and Cellular Endocrinology* **1997,** 135, (1), 41-47.
132. Nakae, J.; Kido, Y.; Accili, D., Distinct and overlapping functions of insulin and IGF-I receptors. *Endocrine Reviews* **2001,** 22, (6), 818-835.
133. Taguchi, A.; White, M. F., Insulin-like signaling, nutrient homeostasis, and life span. *Annual Review of Physiology* **2008,** 70, (1), 191-212.
134. Francis, G. L.; Read, L. C.; Ballard, F. J.; Bagley, C. J.; Upton, F. M.; Gravestock, P. M.; Wallace, J. C., Purification and partial sequence analysis of insulin-like growth factor-1 from bovine colostrum. *Biochemical Journal* **1986,** 233, (1), 207-213.
135. Francis, G. L.; Upton, F. M.; Ballard, F. J.; McNeil, K. A.; Wallace, J. C., Insulin-like growth factors 1 and 2 in bovine colostrum. Sequences and biological activities compared with those of a potent truncated form. *Biochemical Journal* **1988,** 251, (1), 95-103.
136. Russo, V. C.; Werther, G. A., Des (1-3) IGF-I potently enhances differentiated cell growth in olfactory bulb organ culture. *Growth Factors* **1994,** 11, (4), 301-311.
137. Carlsson-Skwirut, C.; Lake, M.; Hartmanis, M.; Hall, K.; Sara, V. R., A comparison of the biological activity of the recombinant intact and truncated insulin-like growth factor 1 (IGF-1). *Biochimica et Biophysica Acta (BBA)-Molecular Cell Research* **1989,** 1011, (2-3), 192-197.
138. Francis, G.; Ross, M.; Ballard, F.; Milner, S.; Senn, C.; McNeil, K.; Wallace, J.; King, R.; Wells, J., Novel recombinant fusion protein analogues of insulin-like growth factor (IGF)-I indicate the relative importance of IGF-binding protein and receptor binding for enhanced biological potency. *Journal of molecular endocrinology* **1992,** 8, (3), 213-223.
139. Tomas, F.; Walton, P.; Dunshea, F.; Ballard, F., IGF-I variants which bind poorly to IGF-binding proteins show more potent and prolonged hypoglycaemic action than native IGF-I in pigs and marmoset monkeys. *Journal of endocrinology* **1997,** 155, (2), 377-386.
140. Voorhamme, D.; Yandell, C. A., LONG TM R 3 IGF-I as a more potent alternative to insulin in serum-free culture of HEK293 cells. *Molecular biotechnology* **2006,** 34, (2), 201-204.
141. Stavropoulou, A.; Halapas, A.; Sourla, A.; Philippou, A.; Papageorgiou, E.; Papalois, A.; Koutsilieris, M., IGF-1 expression in infarcted myocardium and MGF E peptide actions in rat cardiomyocytes *in vitro*. *Molecular Medicine* **2009,** 15, (5-6), 127-135.
142. Matheny, J. R. W.; Nindl, B. C., Loss of IGF-IEa or IGF-IEb impairs myogenic differentiation. *Endocrinology* **2011,** 152, (5), 1923-1934.
143. Poudel, B.; Bilbao, D.; Sarathchandra, P.; Germack, R.; Rosenthal, N.; Santini, M. P., Increased cardiogenesis in P19-GFP teratocarcinoma cells expressing the propeptide IGF-1Ea. *Biochemical and Biophysical Research Communications* **2011,** 416, (3-4), 162-166.
144. Adams, G. R., Invited Review: Autocrine/paracrine IGF-I and skeletal muscle adaptation. *Journal of Applied Physiology* **2002,** 93, (3), 1159-1167.
145. Rosenthal, S. M.; Cheng, Z. Q., Opposing early and late effects of insulin-like growth factor I on differentiation and the cell cycle regulatory retinoblastoma protein in skeletal myoblasts. *Proceedings of the National Academy of Sciences* **1995,** 92, (22), 10307-10311.
146. Valentinis, B.; Baserga, R., IGF-I receptor signalling in transformation and differentiation. *Molecular Pathology* **2001,** 54, (3), 133-137.
147. Capito, R. M.; Spector, M., Collagen scaffolds for nonviral IGF-1 gene delivery in articular cartilage tissue engineering. *Gene Ther* **2007,** 14, (9), 721-732.
148. Lorentz, K. M.; Yang, L.; Frey, P.; Hubbell, J. A., Engineered insulin-like growth factor-1 for improved smooth muscle regeneration. *Biomaterials* **2012,** 33, (2), 494-503.
149. Clark, R. G., Recombinant human insulin-like growth factor I (IGF-I): risks and benefits of normalizing blood IGF-I concentrations. *Hormone Research in Paediatrics* **2004,** 62(suppl 1), (Suppl. 1), 93-100.

150. Jennifer, L. W.-B.; Christopher, W.; George, W., The role of growth hormone, insulin-like growth factor and somatostatin in diabetic retinopathy. *Current Medicinal Chemistry* **2006,** 13, (27), 3307-3317.
151. Chan, J. M.; Stampfer, M. J.; Giovannucci, E.; Gann, P. H.; Ma, J.; Wilkinson, P.; Hennekens, C. H.; Pollak, M., Plasma insulin-like growth factor-I and prostate cancer risk: a prospective study. *Science* **1998,** 279, (5350), 563-566.
152. Hankinson, S. E.; Willett, W. C.; Colditz, G. A.; Hunter, D. J.; Michaud, D. S.; Deroo, B.; Rosner, B.; Speizer, F. E.; Pollak, M., Circulating concentrations of insulin-like growth factor I and risk of breast cancer. *The Lancet* **1998,** 351, (9113), 1393-1396.
153. Meinel, L.; Illi, O. E.; Zapf, J.; Malfanti, M.; Peter Merkle, H.; Gander, B., Stabilizing insulin-like growth factor-I in poly(d,l-lactide-co-glycolide) microspheres. *Journal of Controlled Release* **2001,** 70, (1), 193-202.
154. Wenk, E.; Meinel, A. J.; Wildy, S.; Merkle, H. P.; Meinel, L., Microporous silk fibroin scaffolds embedding PLGA microparticles for controlled growth factor delivery in tissue engineering. *Biomaterials* **2009,** 30, (13), 2571-2581.
155. Uebersax, L.; Merkle, H. P.; Meinel, L., Insulin-like growth factor I releasing silk fibroin scaffolds induce chondrogenic differentiation of human mesenchymal stem cells. *Journal of Controlled Release* **2008,** 127, (1), 12-21.
156. Meinel, L.; Zoidis, E.; Zapf, J.; Hassa, P.; Hottiger, M. O.; Auer, J. A.; Schneider, R.; Gander, B.; Luginbuehl, V.; Bettschart-Wolfisberger, R.; Illi, O. E.; Merkle, H. P.; Rechenberg, B. v., Localized insulin-like growth factor I delivery to enhance new bone formation. *Bone* **2003,** 33, (4), 660-672.
157. Germershaus, O.; Schultz, I.; Lühmann, T.; Beck-Broichsitter, M.; Högger, P.; Meinel, L., Insulin-like growth factor-I aerosol formulations for pulmonary delivery. *European Journal of Pharmaceutics and Biopharmaceutics* **2013,** 85, (1), 61-68.
158. Luginbuehl, V.; Zoidis, E.; Meinel, L.; von Rechenberg, B.; Gander, B.; Merkle, H. P., Impact of IGF-I release kinetics on bone healing: a preliminary study in sheep. *European Journal of Pharmaceutics and Biopharmaceutics* **2013,** 85, (1), 99-106.
159. Kletzl, H.; Guenther, A.; Höflich, A.; Höflich, C.; Frystyk, J.; Staack, R. F.; Schick, E.; Wandel, C.; Bleich, N.; Metzger, F., First-in-man study with a novel PEGylated recombinant human insulin-like growth factor-I. *Growth Hormone & IGF Research* **2017,** 33, 9-16.
160. Parker, K.; Berretta, A.; Saenger, S.; Sivaramakrishnan, M.; Shirley, S. A.; Metzger, F.; Clarkson, A. N., PEGylated insulin-like growth factor-I affords protection and facilitates recovery of lost functions post-focal ischemia. *Scientific Reports* **2017,** 7, (1), 241.
161. Sivaramakrishnan, M.; Kashyap, A. S.; Amrein, B.; Saenger, S.; Meier, S.; Staudenmaier, C.; Upton, Z.; Metzger, F., PEGylation of lysine residues reduces the pro-migratory activity of IGF-I. *Biochimica et Biophysica Acta (BBA) - General Subjects* **2013,** 1830, (10), 4734-4742.
162. John Ballard, F.; Wallace, J. C.; Francis, G. L.; Read, L. C.; Tomas, F. M., Des(1–3)IGF-I: a truncated form of insulin-like growth factor-I. *The International Journal of Biochemistry & Cell Biology* **1996,** 28, (10), 1085-1087.
163. Sara, V. R.; Carlsson-Skwirut, C.; Bergman, T.; Jörnvall, H.; Roberts, P. J.; Crawford, M.; Håkansson, L. N.; Civalero, I.; Nordberg, A., Identification of Gly-Pro-Glu (GPE), the aminoterminal tripeptide of insulin-like growth factor 1 which is truncated in brain, as a novel neuroactive peptide. *Biochemical and biophysical research communications* **1989,** 165, (2), 766-771.
164. Robertson, J. G.; Belford, D. A.; Ballard, F. J., Clearance of IGFs and insulin from wounds: effect of IGF-binding protein interactions. *American Journal of Physiology-Endocrinology and Metabolism* **1999,** 276, (4), E663-E671.
165. Bastian, S.; Walton, P.; Wallace, J.; Ballard, F., Plasma clearance and tissue distribution of labelled insulin-like growth factor-I (IGF-I) and an analogue LR3IGF-I in pregnant rats. *Journal of Endocrinology* **1993,** 138, (2), 327-336.
166. Tomas, F. M.; Lemmey, A. B.; Read, L. C.; Ballard, F. J., Superior potency of infused IGF-I analogues which bind poorly to IGF-binding proteins is maintained when administered by injection. *Journal of Endocrinology* **1996,** 150, (1), 77-84.

167. Baserga, R.; Peruzzi, F.; Reiss, K., The IGF-1 receptor in cancer biology. *International journal of cancer* **2003,** 107, (6), 873-877.
168. Musarò, A.; Rosenthal, N., The role of local insulin-like growth factor-1 isoforms in the pathophysiology of skeletal muscle. *Current Genomics* **2002,** 3, (3), 149-162.
169. Bodine, S. C.; Stitt, T. N.; Gonzalez, M.; Kline, W. O.; Stover, G. L.; Bauerlein, R.; Zlotchenko, E.; Scrimgeour, A.; Lawrence, J. C.; Glass, D. J., Akt/mTOR pathway is a crucial regulator of skeletal muscle hypertrophy and can prevent muscle atrophy *in vivo*. *Nature cell biology* **2001,** 3, (11), 1014.
170. Rommel, C.; Bodine, S. C.; Clarke, B. A.; Rossman, R.; Nunez, L.; Stitt, T. N.; Yancopoulos, G. D.; Glass, D. J., Mediation of IGF-1-induced skeletal myotube hypertrophy by PI (3) K/Akt/mTOR and PI (3) K/Akt/GSK3 pathways. *Nature cell biology* **2001,** 3, (11), 1009.
171. Myers, M. G.; Backer, J. M.; Sun, X. J.; Shoelson, S.; Hu, P.; Schlessinger, J.; Yoakim, M.; Schaffhausen, B.; White, M. F., IRS-1 activates phosphatidylinositol 3'-kinase by associating with src homology 2 domains of p85. *Proceedings of the National Academy of Sciences* **1992,** 89, (21), 10350-10354.
172. Myers, J. M. G.; Sun, X. J.; Cheatham, B.; Jachna, B. R.; Glasheen, E. M.; Backer, J. M.; White, M. F., IRS-1 is a common element in insulin and insulin-like growth factor-I signaling to the phosphatidylinositol 3'-kinase. *Endocrinology* **1993,** 132, (4), 1421-1430.
173. Le Roith, D.; Bondy, C.; Yakar, S.; Liu, J.-L.; Butler, A., The somatomedin hypothesis: 2001. *Endocrine Reviews* **2001,** 22, (1), 53-74.
174. Scott, P. H.; Lawrence, J. C., Attenuation of mammalian target of rapamycin activity by increased cAMP in 3T3-L1 adipocytes. *Journal of Biological Chemistry* **1998,** 273, (51), 34496-34501.
175. Nave, B. T.; Ouwens, M.; Withers, D. J.; Alessi, D. R.; Shepherd, P. R., Mammalian target of rapamycin is a direct target for protein kinase B: identification of a convergence point for opposing effects of insulin and amino-acid deficiency on protein translation. *Biochemical Journal* **1999,** 344, (Pt 2), 427.
176. Cross, D. A.; Alessi, D. R.; Cohen, P.; Andjelkovich, M.; Hemmings, B. A., Inhibition of glycogen synthase kinase-3 by insulin mediated by protein kinase B. *Nature* **1995,** 378, (6559), 785.
177. Lu, J.; McKinsey, T. A.; Zhang, C.-L.; Olson, E. N., Regulation of skeletal myogenesis by association of the MEF2 transcription factor with class II histone deacetylases. *Molecular cell* **2000,** 6, (2), 233-244.
178. McKinsey, T. A.; Zhang, C.-L.; Lu, J.; Olson, E. N., Signal-dependent nuclear export of a histone deacetylase regulates muscle differentiation. *Nature* **2000,** 408, 106.
179. Tu, M. K.; Levin, J. B.; Hamilton, A. M.; Borodinsky, L. N., Calcium signaling in skeletal muscle development, maintenance and regeneration. *Cell calcium* **2016,** 59, (2), 91-97.
180. Musarò, A.; McCullagh, K. J. A.; Naya, F. J.; Olson, E. N.; Rosenthal, N., IGF-1 induces skeletal myocyte hypertrophy through calcineurin in association with GATA-2 and NF-ATc1. *Nature* **1999,** 400, 581.
181. Chin, E. R.; Olson, E. N.; Richardson, J. A.; Yang, Q.; Humphries, C.; Shelton, J. M.; Wu, H.; Zhu, W.; Bassel-Duby, R.; Williams, R. S., A calcineurin-dependent transcriptional pathway controls skeletal muscle fiber type. *Genes & development* **1998,** 12, (16), 2499-2509.
182. Naya, F. J.; Mercer, B.; Shelton, J.; Richardson, J. A.; Williams, R. S.; Olson, E. N., Stimulation of slow skeletal muscle fiber gene expression by calcineurin *in vivo*. *Journal of Biological Chemistry* **2000,** 275, (7), 4545-4548.
183. Dunn, S. E.; Chin, E. R.; Michel, R. N., Matching of calcineurin activity to upstream effectors is critical for skeletal muscle fiber growth. *The Journal of Cell Biology* **2000,** 151, (3), 663-672.
184. Parsons, S. A.; Millay, D. P.; Wilkins, B. J.; Bueno, O. F.; Tsika, G. L.; Neilson, J. R.; Liberatore, C. M.; Yutzey, K. E.; Crabtree, G. R.; Tsika, R. W.; Molkentin, J. D., Genetic loss of calcineurin blocks mechanical overload-induced skeletal muscle fiber type switching but not hypertrophy. *Journal of Biological Chemistry* **2004,** 279, (25), 26192-26200.

185. Sandri, M.; Sandri, C.; Gilbert, A.; Skurk, C.; Calabria, E.; Picard, A.; Walsh, K.; Schiaffino, S.; Lecker, S. H.; Goldberg, A. L., Foxo transcription factors induce the atrophy-related ubiquitin ligase atrogin-1 and cause skeletal muscle atrophy. *Cell* **2004,** 117, (3), 399-412.
186. Clemmons, D. R., Role of insulin-like growth factor binding proteins in controlling IGF actions. *Molecular and Cellular Endocrinology* **1998,** 140, (1), 19-24.
187. Clemmons, D. R.; Dehoff, M. L.; Busby, W. H.; Bayne, M. L.; Cascieri, M. A., Competition for binding to insulin-like growth factor (IGF) binding protein-2, 3, 4, and 5 by the IGFs and IGF analogs. *Endocrinology* **1992,** 131, (2), 890-895.
188. Dubaquié, Y.; Lowman, H. B., Total alanine-scanning mutagenesis of insulin-like growth factor I (IGF-I) identifies differential binding epitopes for IGFBP-1 and IGFBP-3. *Biochemistry* **1999,** 38, (20), 6386-6396.
189. Jansson, M.; Andersson, G.; Uhlén, M.; Nilsson, B.; Kördel, J., The insulin-like growth factor (IGF) binding protein 1 binding epitope on IGF-I probed by heteronuclear NMR spectroscopy and mutational analysis. *Journal of Biological Chemistry* **1998,** 273, (38), 24701-24707.
190. Oh, Y.; Müller, H.; Lee, D.; Fielder, P. J.; Rosenfeld, R., Characterization of the affinities of insulin-like growth factor (IGF)-binding proteins 1-4 for IGF-I, IGF-II, IGF-I/insulin hybrid, and IGF-I analogs. *Endocrinology* **1993,** 132, (3), 1337-1344.
191. Baxter, R. C.; Martin, J. L., Structure of the Mr 140,000 growth hormone-dependent insulin-like growth factor binding protein complex: determination by reconstitution and affinity-labeling. *Proceedings of the National Academy of Sciences* **1989,** 86, (18), 6898-6902.
192. Baxter, R. C., Circulating levels and molecular distribution of the acid-labile (α) subunit of the high molecular weight insulin-like growth factor-binding protein complex. *The Journal of Clinical Endocrinology & Metabolism* **1990,** 70, (5), 1347-1353.
193. Twigg, S. M.; Baxter, R. C., Insulin-like growth factor (IGF)-binding protein 5 forms an alternative ternary complex with IGFs and the acid-labile subunit. *Journal of Biological Chemistry* **1998,** 273, (11), 6074-6079.
194. Baxter, R. C.; Meka, S.; Firth, S. M., Molecular distribution of IGF binding protein-5 in human serum. *The Journal of Clinical Endocrinology & Metabolism* **2002,** 87, (1), 271-276.
195. Forbes Briony, E.; Hartfield Perry, J.; McNeil Kerrie, A.; Surinya Kathy, H.; Milner Steven, J.; Cosgrove Leah, J.; Wallace John, C., Characteristics of binding of insulin-like growth factor (IGF)-I and IGF-II analogues to the type 1 IGF receptor determined by BIAcore analysis. *European Journal of Biochemistry* **2002,** 269, (3), 961-968.
196. Uebersax, L.; Merkle, H. P.; Meinel, L., Biopolymer-based growth factor delivery for tissue repair: from natural concepts to engineered systems. *Tissue Engineering Part B: Reviews* **2009,** 15, (3), 263-289.
197. Martin, J. A.; Miller, B. A.; Scherb, M. B.; Lembke, L. A.; Buckwalter, J. A., Co-localization of insulin-like growth factor binding protein 3 and fibronectin in human articular cartilage. *Osteoarthritis and Cartilage* **2002,** 10, (7), 556-563.
198. Gui, Y.; Murphy, L. J., Insulin-like growth factor (IGF)-binding protein-3 (IGFBP-3) binds to fibronectin (FN): demonstration of IGF-I/IGFBP-3/fn ternary complexes in human plasma. *The Journal of Clinical Endocrinology & Metabolism* **2001,** 86, (5), 2104-2110.
199. Jones, J. I.; Gockerman, A.; Busby, W. H., Jr.; Camacho-Hubner, C.; Clemmons, D. R., Extracellular matrix contains insulin-like growth factor binding protein-5: potentiation of the effects of IGF-I. *J Cell Biol* **1993,** 121, (3), 679-87.
200. Conover, C. A.; Khosla, S., Role of extracellular matrix in insulin-like growth factor (IGF) binding protein-2 regulation of IGF-II action in normal human osteoblasts. *Growth Hormone & IGF Research* **2003,** 13, (6), 328-335.
201. Rajaram, S.; Baylink, D. J.; Mohan, S., Insulin-like growth factor-binding proteins in serum and other biological fluids: regulation and functions. *Endocrine reviews* **1997,** 18, (6), 801-831.
202. Werner, H.; Bruchim, I., The insulin-like growth factor-I receptor as an oncogene. *Archives of Physiology and Biochemistry* **2009,** 115, (2), 58-71.

203. Werner, H.; LeRoith, D., The role of the insulin-like growth factor system in human cancer. In *Advances in Cancer Research*, Vande Woude, G. F.; Klein, G., Eds. Academic Press: 1996; Vol. 68, pp 183-223.
204. Headey, S. J.; Keizer, D. W.; Yao, S.; Wallace, J. C.; Bach, L. A.; Norton, R. S., Binding site for the C-domain of insulin-like growth factor (IGF) binding protein-6 on IGF-II; implications for inhibition of IGF actions. *FEBS letters* **2004,** 568, (1-3), 19-22.
205. Carrick, F. E.; Wallace, J. C.; Forbes, B. E., The interaction of Insulin-like Growth Factors (IGFs) with Insulin-like Growth Factor Binding Proteins (IGFBPs): a review. *Letters in Peptide Science* **2001,** 8, (3), 147-153.
206. Ohlsson, C.; Mohan, S.; Sjögren, K.; Tivesten, A. s.; Isgaard, J. r.; Isaksson, O.; Jansson, J.-O.; Svensson, J., The role of liver-derived insulin-like growth factor-I. *Endocrine Reviews* **2009,** 30, (5), 494-535.
207. Naranjo, W. M.; Yakar, S.; Sanchez-Gomez, M.; Perez, A. U.; Setser, J.; LeRoith, D., Protein calorie restriction affects nonhepatic IGF-I production and the lymphoid system: studies using the liver-specific IGF-I gene-deleted mouse model. *Endocrinology* **2002,** 143, (6), 2233-2241.
208. Sjögren, K.; Liu, J.-L.; Blad, K.; Skrtic, S.; Vidal, O.; Wallenius, V.; LeRoith, D.; Törnell, J.; Isaksson, O. G. P.; Jansson, J.-O.; Ohlsson, C., Liver-derived insulin-like growth factor I (IGF-I) is the principal source of IGF-I in blood but is not required for postnatal body growth in mice. *Proceedings of the National Academy of Sciences* **1999,** 96, (12), 7088-7092.
209. Cohick, W.; Clemmons, D., The insulin-like growth factors. *Annual review of physiology* **1993,** 55, (1), 131-153.
210. Mohan, S.; Baylink, D. J., IGF system components and their role in bone metabolism. In *The IGF System*, Springer: 1999; pp 457-496.
211. Stewart, C.; Rotwein, P., Growth, differentiation, and survival: multiple physiological functions for insulin-like growth factors. *Physiological reviews* **1996,** 76, (4), 1005-1026.
212. Butler, A. A.; LeRoith, D., Minireview: tissue-specific versus generalized gene targeting of the IGF1 and IGF1R genes and their roles in insulin-like growth factor physiology. *Endocrinology* **2001,** 142, (5), 1685-1688.
213. Vashisth, H.; Abrams, C. F., All-atom structural models for complexes of insulin-like growth factors IGF1 and IGF2 with their cognate receptor. *Journal of Molecular Biology* **2010,** 400, (3), 645-658.
214. Xu, Y.; Kong, G. K. W.; Menting, J. G.; Margetts, M. B.; Delaine, C. A.; Jenkin, L. M.; Kiselyov, V. V.; De Meyts, P.; Forbes, B. E.; Lawrence, M. C., How ligand binds to the type 1 insulin-like growth factor receptor. *Nature Communications* **2018,** 9, (1), 821.
215. Saenger, S.; Goeldner, C.; Frey, J. R.; Ozmen, L.; Ostrowitzki, S.; Spooren, W.; Ballard, T. M.; Prinssen, E.; Borroni, E.; Metzger, F., PEGylation enhances the therapeutic potential for insulin-like growth factor I in central nervous system disorders. *Growth Hormone & IGF Research* **2011,** 21, (5), 292-303.
216. Saenger, S.; Holtmann, B.; Nilges, M. R.; Schroeder, S.; Hoeflich, A.; Kletzl, H.; Spooren, W.; Ostrowitzki, S.; Hanania, T.; Sendtner, M.; Metzger, F., Functional improvement in mouse models of familial amyotrophic lateral sclerosis by PEGylated insulin-like growth factor I treatment depends on disease severity. *Amyotrophic Lateral Sclerosis* **2012,** 13, (5), 418-429.
217. Braun, A. C.; Gutmann, M.; Mueller, T. D.; Lühmann, T.; Meinel, L., Bioresponsive release of insulin-like growth factor-I from its PEGylated conjugate. *Journal of Controlled Release* **2018**.
218. De Vroede, M. A.; Rechler, M. M.; Nissley, S. P.; Joshi, S.; Burke, G. T.; Katsoyannis, P. G., Hybrid molecules containing the B-domain of insulin-like growth factor I are recognized by carrier proteins of the growth factor. *Proceedings of the National Academy of Sciences* **1985,** 82, (9), 3010-3014.
219. Bayne, M. L.; Applebaum, J.; Chicchi, G. G.; Hayes, N. S.; Green, B. G.; Cascieri, M. A., Structural analogs of human insulin-like growth factor I with reduced affinity for serum binding proteins and the type 2 insulin-like growth factor receptor. *Journal of Biological Chemistry* **1988,** 263, (13), 6233-6239.

220. Kristensen, C.; Andersen, A. S.; Hach, M.; Wiberg, F. C.; Schäffer, L.; Kjeldsen, T., A single-chain insulin-like growth factor I/insulin hybrid binds with high affinity to the insulin receptor. *Biochemical Journal* **1995,** 305, (Pt 3), 981-986.
221. Bagley, C. J.; May, B. L.; Szabo, L.; McNamara, P. J.; Ross, M.; Francis, G. L.; Ballard, F. J.; Wallace, J. C., A key functional role for the insulin-like growth factor 1 N-terminal pentapeptide. *Biochemical Journal* **1989,** 259, (3), 665-671.
222. Schultz, I.; Wurzel, J.; Meinel, L., Drug delivery of insulin-like growth factor I. *European Journal of Pharmaceutics and Biopharmaceutics* **2015,** 97, 329-337.
223. Wang, Z.; Wang, Z.; Lu, W. W.; Zhen, W.; Yang, D.; Peng, S., Novel biomaterial strategies for controlled growth factor delivery for biomedical applications. *Npg Asia Materials* **2017,** 9, e435.
224. Tokunou, T.; Miller, R.; Patwari, P.; Davis, M. E.; Segers, V. F. M.; Grodzinsky, A. J.; Lee, R. T., Engineering insulin-like growth factor-1 for local delivery. *The FASEB Journal* **2008,** 22, (6), 1886-1893.
225. Masters, K. S., Covalent growth factor immobilization strategies for tissue repair and regeneration. *Macromolecular Bioscience* **2011,** 11, (9), 1149-1163.
226. Fischer, S.; Hesse, F.; Knoetgen, H.; Lang, K.; Metzger, F.; Regula, J. T.; Schantz, C.; Schaubmar, A.; Schoenfeld, H.-J., Method for the production of conjugates of insulin-like growth factor-1 and poly (ethylene glycol). In US Patent 7625996B2: 2009.
227. Benjamin, W. U.; Sun, Y.-N., Pharmacokinetics of peptide–Fc fusion proteins. *Journal of Pharmaceutical Sciences* **2014,** 103, (1), 53-64.
228. Glass, D. J.; Yancopoulos, G. D.; Daly, T. J.; Papadopoulos, N. J., IGF-I fusion polypeptides and therapeutic uses thereof. In US Patent 7396918B2: 2008.
229. Wan, A.; Xu, D.; Liu, K.; Peng, L.; Cai, Y.; Chen, Y.; He, Y.; Yang, J.; Jin, J.; Li, H., Efficient expression of stable recombinant human insulin-like growth factor-1 fusion with human serum albumin in Chinese hamster ovary cells. *Preparative Biochemistry and Biotechnology* **2017,** 47, (7), 678-686.
230. Glass, D. J.; Fornaro, M., Stabilized insulin-like growth factor polypeptides. In US Patent 8343918B2: 2013.
231. Vardar, E.; Larsson, H. M.; Engelhardt, E. M.; Pinnagoda, K.; Briquez, P. S.; Hubbell, J. A.; Frey, P., IGF-1-containing multi-layered collagen-fibrin hybrid scaffolds for bladder tissue engineering. *Acta Biomaterialia* **2016,** 41, 75-85.
232. Braun, A. C.; Gutmann, M.; Lühmann, T.; Meinel, L., Bioorthogonal strategies for site-directed decoration of biomaterials with therapeutic proteins. *Journal of Controlled Release* **2018,** 273, 68-85.
233. Sivaramakrishnan, M.; Croll, T. I.; Gupta, R.; Stupar, D.; Van Lonkhuyzen, D. R.; Upton, Z.; Shooter, G. K., Lysine residues of IGF-I are substrates for transglutaminases and modulate downstream IGF-I signalling. *Biochimica et Biophysica Acta (BBA) - Molecular Cell Research* **2013,** 1833, (12), 3176-3185.
234. Griffin, M.; Casadio, R.; Bergamini, C. M., Transglutaminases: nature's biological glues. *Biochemical Journal* **2002,** 368, (Pt 2), 377.
235. Bendele, A.; Seely, J.; Richey, C.; Sennello, G.; Shopp, G., Renal tubular vacuolation in animals treated with polyethylene-glycol-conjugated proteins. *Toxicological sciences* **1998,** 42, (2), 152-157.
236. Chanan-Khan, A.; Szebeni, J.; Savay, S.; Liebes, L.; Rafique, N.; Alving, C.; Muggia, F., Complement activation following first exposure to pegylated liposomal doxorubicin (Doxil®): possible role in hypersensitivity reactions. *Annals of Oncology* **2003,** 14, (9), 1430-1437.
237. Środa, K.; Rydlewski, J.; Langner, M.; Kozubek, A.; Grzybek, M.; Sikorski, A. F., Repeated injections of PEG-PE liposomes generate anti-PEG antibodies. *Cell. Mol. Biol. Lett* **2005,** 10, 37-47.
238. Dams, E. T. M.; Laverman, P.; Oyen, W. J. G.; Storm, G.; Scherphof, G. L.; van der Meer, J. W. M.; Corstens, F. H. M.; Boerman, O. C., Accelerated blood clearance and altered biodistribution of repeated injections of sterically stabilized liposomes. *Journal of Pharmacology and Experimental Therapeutics* **2000,** 292, (3), 1071-1079.

239. Lühmann, T.; Schmidt, M.; Leiske, M. N.; Spieler, V.; Majdanski, T. C.; Grube, M.; Hartlieb, M.; Nischang, I.; Schubert, S.; Schubert, U. S.; Meinel, L., Site-specific poxylation of interleukin-4. *ACS Biomaterials Science & Engineering* **2017,** 3, (3), 304-312.
240. Früh, S. M.; Spycher, P. R.; Mitsi, M.; Burkhardt, M. A.; Vogel, V.; Schoen, I., Functional modification of fibronectin by N-terminal FXIIIa-mediated transamidation. *Chembiochem* **2014,** 15, (10), 1481-1486.
241. De Graaf, A. J.; Kooijman, M.; Hennink, W. E.; Mastrobattista, E., Nonnatural amino acids for site-specific protein conjugation. *Bioconjugate chemistry* **2009,** 20, (7), 1281-1295.
242. Gaston, M. A.; Jiang, R.; Krzycki, J. A., Functional context, biosynthesis, and genetic encoding of pyrrolysine. *Curr Opin Microbiol* **2011,** 14, (3), 342-9.
243. James, C. M.; Ferguson, T. K.; Leykam, J. F.; Krzycki, J. A., The amber codon in the gene encoding the monomethylamine methyltransferase isolated from Methanosarcina barkeri is translated as a sense codon. *J Biol Chem* **2001,** 276, (36), 34252-8.
244. Srinivasan, G.; James, C. M.; Krzycki, J. A., Pyrrolysine encoded by UAG in Archaea: charging of a UAG-decoding specialized tRNA. *Science* **2002,** 296, (5572), 1459-1462.
245. Blight, S. K.; Larue, R. C.; Mahapatra, A.; Longstaff, D. G.; Chang, E.; Zhao, G.; Kang, P. T.; Green-Church, K. B.; Chan, M. K.; Krzycki, J. A., Direct charging of tRNACUA with pyrrolysine *in vitro* and *in vivo*. *Nature* **2004,** 431, 333.
246. Sharon, J.; Puleo, D., Immobilization of glycoproteins, such as VEGF, on biodegradable substrates. *Acta biomaterialia* **2008,** 4, (4), 1016-1023.
247. Hermeling, S.; Crommelin, D. J.; Schellekens, H.; Jiskoot, W., Structure-immunogenicity relationships of therapeutic proteins. *Pharmaceutical research* **2004,** 21, (6), 897-903.
248. Nikić, I.; Lemke, E. A., Genetic code expansion enabled site-specific dual-color protein labeling: superresolution microscopy and beyond. *Current Opinion in Chemical Biology* **2015,** 28, 164-173.
249. Lang, K.; Chin, J. W., Cellular incorporation of unnatural amino acids and bioorthogonal labeling of proteins. *Chemical Reviews* **2014,** 114, (9), 4764-4806.
250. Lühmann, T.; Jones, G.; Gutmann, M.; Rybak, J.-C.; Nickel, J.; Rubini, M.; Meinel, L., Bio-orthogonal immobilization of fibroblast growth factor 2 for spatial controlled cell proliferation. *ACS Biomaterials Science & Engineering* **2015,** 1, (9), 740-746.
251. Lühmann, T.; Spieler, V.; Werner, V.; Ludwig, M. G.; Fiebig, J.; Mueller, T. D.; Meinel, L., Interleukin-4-clicked surfaces drive M2 macrophage polarization. *Chembiochem* **2016,** 17, (22), 2123-2128.
252. Wandrey, G.; Wurzel, J.; Hoffmann, K.; Ladner, T.; Büchs, J.; Meinel, L.; Lühmann, T., Probing unnatural amino acid integration into enhanced green fluorescent protein by genetic code expansion with a high-throughput screening platform. *Journal of Biological Engineering* **2016,** 10, 11.
253. Tabisz, B.; Schmitz, W.; Schmitz, M.; Luehmann, T.; Heusler, E.; Rybak, J.-C.; Meinel, L.; Fiebig, J. E.; Mueller, T. D.; Nickel, J., Site-directed immobilization of BMP-2: two approaches for the production of innovative osteoinductive scaffolds. *Biomacromolecules* **2017,** 18, (3), 695-708.
254. Lang, K.; Davis, L.; Torres-Kolbus, J.; Chou, C.; Deiters, A.; Chin, J. W., Genetically encoded norbornene directs site-specific cellular protein labelling via a rapid bioorthogonal reaction. *Nature Chemistry* **2012,** 4, 298.
255. Fontana, A.; Spolaore, B.; Mero, A.; Veronese, F. M., Site-specific modification and PEGylation of pharmaceutical proteins mediated by transglutaminase. *Advanced Drug Delivery Reviews* **2008,** 60, (1), 13-28.
256. Mero, A.; Schiavon, M.; Veronese, F. M.; Pasut, G., A new method to increase selectivity of transglutaminase mediated PEGylation of salmon calcitonin and human growth hormone. *Journal of Controlled Release* **2011,** 154, (1), 27-34.
257. Sato, H., Enzymatic procedure for site-specific pegylation of proteins. *Advanced Drug Delivery Reviews* **2002,** 54, (4), 487-504.
258. Spolaore, B.; Raboni, S.; Satwekar, A. A.; Grigoletto, A.; Mero, A.; Montagner, I. M.; Rosato, A.; Pasut, G.; Fontana, A., Site-specific transglutaminase-mediated conjugation of interferon α-2b at glutamine or lysine residues. *Bioconjugate chemistry* **2016,** 27, (11), 2695-2706.

259. F., U. H.; Eugene, C.; K., P. M.; D., M. M., Localization of cellular transglutaminase on the extracellular matrix after wounding: Characteristics of the matrix bound enzyme. *Journal of Cellular Physiology* **1991,** 149, (3), 375-382.
260. Schense, J. C.; Hubbell, J. A., Cross-linking exogenous bifunctional peptides into fibrin gels with factor XIIIa. *Bioconjugate chemistry* **1999,** 10, (1), 75-81.
261. Sala, A.; Ehrbar, M.; Trentin, D.; Schoenmakers, R. G.; Vörös, J.; Weber, F. E., Enzyme mediated site-specific surface modification. *Langmuir* **2010,** 26, (13), 11127-11134.
262. Sala, A.; Ehrbar, M.; Trentin, D.; Schoenmakers, R. G.; Vörös, J.; Weber, F. E., Enzyme mediated site-specific surface modification. *Langmuir* **2010,** 26, (13), 11127-11134.
263. Bayne, M. L.; Applebaum, J.; Underwood, D.; Chicchi, G. G.; Green, B. G.; Hayes, N. S.; Cascieri, M. A., The C region of human insulin-like growth factor (IGF) I is required for high affinity binding to the type 1 IGF receptor. *Journal of Biological Chemistry* **1989,** 264, (19), 11004-11008.
264. Gill, R.; Wallach, B.; Verma, C.; Ursø, B.; De Wolf, E.; Grötzinger, J.; Murray-Rust, J.; Pitts, J.; Wollmer, A.; De Meyts, P., Engineering the C-region of human insulin-like growth factor-1: implications for receptor binding. *Protein Engineering, Design and Selection* **1996,** 9, (11), 1011-1019.
265. Zhang, W.; Gustafson, T. A.; Rutter, W. J.; Johnson, J. D., Positively charged side chains in the insulin-like growth factor-1 C-and D-regions determine receptor binding specificity. *Journal of Biological Chemistry* **1994,** 269, (14), 10609-10613.
266. Saegusa, J.; Yamaji, S.; Ieguchi, K.; Wu, C.-Y.; Lam, K. S.; Liu, F.-T.; Takada, Y. K.; Takada, Y., The direct binding of insulin-like growth factor-1 (IGF-1) to integrin αvβ3 is involved in IGF-1 signaling. *The Journal of Biological Chemistry* **2009,** 284, (36), 24106-24114.
267. Fujita, M.; Ieguchi, K.; Prieto, D. C.; Fong, A.; Wilkerson, C.; Chen, J. Q.; Wu, M.; Lo, S.-H.; Cheung, A. T.; Willson, M. D., An integrin-binding-defective mutant of insulin-like growth factor-1 (R36E/R37E IGF1) acts as a dominant-negative antagonist of IGF1R and suppresses tumorigenesis, while the mutant still binds to IGF1R. *Journal of Biological Chemistry* **2013**, jbc. M113. 470872.
268. Denley, A.; Wang, C. C.; McNeil, K. A.; Walenkamp, M. J. E.; van Duyvenvoorde, H.; Wit, J. M.; Wallace, J. C.; Norton, R. S.; Karperien, M.; Forbes, B. E., Structural and functional characteristics of the Val44Met insulin-like growth factor I missense mutation: correlation with effects on growth and development. *Molecular Endocrinology* **2005,** 19, (3), 711-721.
269. Nanjo, K.; Sanke, T.; Miyano, M.; Okai, K.; Sowa, R.; Kondo, M.; Nishimura, S.; Iwo, K.; Miyamura, K.; Given, B. D., Diabetes due to secretion of a structurally abnormal insulin (insulin Wakayama). Clinical and functional characteristics of [LeuA3] insulin. *Journal of Clinical Investigation* **1986,** 77, (2), 514-519.
270. Gauguin, L.; Delaine, C.; Alvino, C. L.; McNeil, K. A.; Wallace, J. C.; Forbes, B. E.; De Meyts, P., Alanine scanning of a putative receptor binding surface of insulin-like growth factor-I. *Journal of Biological Chemistry* **2008,** 283, (30), 20821-20829.
271. Sajid, W.; Holst, P. A.; Kiselyov, V. V.; Andersen, A. S.; Conlon, J. M.; Kristensen, C.; Kjeldsen, T.; Whittaker, J.; Chan, S. J.; De Meyts, P., Structural basis of the aberrant receptor binding properties of hagfish and lamprey insulins. *Biochemistry* **2009,** 48, (47), 11283-11295.
272. De Meyts, P., The structural basis of insulin and insulin-like growth factor-I receptor binding and negative co-operativity, and its relevance to mitogenic versus metabolic signalling. *Diabetologia* **1994,** 37, (2), S135-S148.
273. Schäffer, L., A model for insulin binding to the insulin receptor. *European Journal of Biochemistry* **1994,** 221, (3), 1127-1132.
274. Kiselyov, V. V.; Versteyhe, S.; Gauguin, L.; De Meyts, P., Harmonic oscillator model of the insulin and IGF1 receptors' allosteric binding and activation. *Molecular systems biology* **2009,** 5, (1), 243.
275. Brisson, B. K.; Barton, E. R., New modulators for IGF-I activity within IGF-I processing products. *Frontiers in endocrinology* **2013,** 4, 42.
276. Reva, B.; Antipin, Y.; Sander, C., Predicting the functional impact of protein mutations: application to cancer genomics. *Nucleic Acids Research* **2011,** 39, (17), e118-e118.

277. Zhang, B.; Yang, Q.; Chen, J.; Wu, L.; Yao, T.; Wu, Y.; Xu, H.; Zhang, L.; Xia, Q.; Zhou, D., CRISPRi-manipulation of genetic code expansion via RF1 for reassignment of amber codon in bacteria. *Scientific Reports* **2016,** 6, 20000.
278. Mukai, T.; Hayashi, A.; Iraha, F.; Sato, A.; Ohtake, K.; Yokoyama, S.; Sakamoto, K., Codon reassignment in the *Escherichia coli* genetic code. *Nucleic acids research* **2010,** 38, (22), 8188-8195.
279. Brown, J.; Delaine, C.; Zaccheo, O. J.; Siebold, C.; Gilbert, R. J.; van Boxel, G.; Denley, A.; Wallace, J. C.; Hassan, A. B.; Forbes, B. E.; Jones, E. Y., Structure and functional analysis of the IGF-II/IGF2R interaction. *The EMBO Journal* **2008,** 27, (1), 265-276.
280. Hochuli, E.; Bannwarth, W.; Dobeli, H.; Gentz, R.; Stuber, D., Genetic approach to facilitate purification of recombinant proteins with a novel metal chelate adsorbent. *Nat Biotech* **1988,** 6, (11), 1321-1325.
281. Zhang, D.; Wei, P.; Fan, L.; Lian, J.; Huang, L.; Cai, J.; Xu, Z., High-level soluble expression of hIGF-1 fusion protein in recombinant *Escherichia coli*. *Process Biochemistry* **2010,** 45, (8), 1401-1405.
282. Coligan, J. E., *Short protocols in protein science: a compendium of methods from Current protocols in protein science*. John Wiley & Sons Inc: 2003.
283. Kammerer, R. A.; Schulthess, T.; Landwehr, R.; Lustig, A.; Fischer, D.; Engel, J., Tenascin-C hexabrachion assembly is a sequential two-step process initiated by coiled-coil α-helices. *Journal of Biological Chemistry* **1998,** 273, (17), 10602-10608.
284. Milles, S.; Tyagi, S.; Banterle, N.; Koehler, C.; VanDelinder, V.; Plass, T.; Neal, A. P.; Lemke, E. A., Click strategies for single-molecule protein fluorescence. *Journal of the American Chemical Society* **2012,** 134, (11), 5187-5195.
285. Li, F.; Zhang, H.; Sun, Y.; Pan, Y.; Zhou, J.; Wang, J., Expanding the genetic code for photoclick chemistry in *E. coli*, mammalian cells, and *A. thaliana*. *Angewandte Chemie International Edition* **2013,** 52, (37), 9700-9704.
286. Bradford, M. M., A rapid and sensitive method for the quantitation of microgram quantities of protein utilizing the principle of protein-dye binding. *Analytical Biochemistry* **1976,** 72, (1), 248-254.
287. Lühmann, T.; Spieler, V.; Werner, V.; Ludwig, M.-G.; Fiebig, J.; Mueller, T. D.; Meinel, L., Interleukin-4-clicked surfaces drive M2 macrophage polarization. *ChemBioChem* **2016,** 17, (22), 2123-2128.
288. Lajoie, M. J.; Rovner, A. J.; Goodman, D. B.; Aerni, H.-R.; Haimovich, A. D.; Kuznetsov, G.; Mercer, J. A.; Wang, H. H.; Carr, P. A.; Mosberg, J. A., Genomically recoded organisms expand biological functions. *Science* **2013,** 342, (6156), 357-360.
289. Anita, K.; W., B. M.; H., S. J.; Carole, L.; A., K. R., Expression, renaturation and purification of recombinant human interleukin 4 from *Escherichia coli*. *European Journal of Biochemistry* **1988,** 173, (1), 109-114.
290. Rösner, D.; Schneider, T.; Schneider, D.; Scheffner, M.; Marx, A., Click chemistry for targeted protein ubiquitylation and ubiquitin chain formation. *Nature Protocols* **2015,** 10, 1594.
291. Alland, C.; Moreews, F.; Boens, D.; Carpentier, M.; Chiusa, S.; Lonquety, M.; Renault, N.; Wong, Y.; Cantalloube, H.; Chomilier, J.; Hochez, J.; Pothier, J.; Villoutreix, B. O.; Zagury, J. F.; Tufféry, P., RPBS: a web resource for structural bioinformatics. *Nucleic Acids Research* **2005,** 33, (suppl_2), W44-W49.
292. Braun, A. C.; Gutmann, M.; Ebert, R.; Jakob, F.; Gieseler, H.; Lühmann, T.; Meinel, L., Matrix Metalloproteinase Responsive Delivery of Myostatin Inhibitors. *Pharmaceutical Research* **2017,** 34, (1), 58-72.
293. Wu, F.; Braun, A.; Lühmann, T.; Meinel, L., Site-specific conjugated insulin-like growth factor-I for anabolic therapy. *ACS Biomaterials Science & Engineering* **2018,** 4, (3), 819-825.
294. Burgess, R. R., Chapter 17 Refolding solubilized inclusion body proteins. In *Methods in Enzymology*, Burgess, R. R.; Deutscher, M. P., Eds. Academic Press: 2009; Vol. 463, pp 259-282.
295. Volker, N.; Norbert, A.; Dieter, T.; Wolfgang, E., Improved staining of proteins in polyacrylamide gels including isoelectric focusing gels with clear background at nanogram sensitivity using Coomassie Brilliant Blue G-250 and R-250. *ELECTROPHORESIS* **1988,** 9, (6), 255-262.

296. Jeno, P.; Mini, T.; Moes, S.; Hintermann, E.; Horst, M., Internal sequences from proteins digested in polyacrylamide gels. *Analytical Biochemistry* **1995,** 224, (1), 75-82.
297. Rosenfeld, J.; Capdevielle, J.; Guillemot, J. C.; Ferrara, P., In-gel digestion of proteins for internal sequence analysis after one- or two-dimensional gel electrophoresis. *Analytical Biochemistry* **1992,** 203, (1), 173-179.
298. Coin, I.; Beyermann, M.; Bienert, M., Solid-phase peptide synthesis: from standard procedures to the synthesis of difficult sequences. *Nature protocols* **2007,** 2, (12), 3247.
299. Per, J.; Sissela, L.; Per-A˚ke, N.; Stefan, S., Genetic design for facilitated production and recovery of recombinant proteins in *Escherichia coli*. *Biotechnology and Applied Biochemistry* **2002,** 35, (2), 91-105.
300. Sørensen, H. P.; Mortensen, K. K., Soluble expression of recombinant proteins in the cytoplasm of *Escherichia coli*. *Microbial cell factories* **2005,** 4, (1), 1.
301. Donovan, R. S.; Robinson, C. W.; Glick, B. R., Review: optimizing inducer and culture conditions for expression of foreign proteins under the control of thelac promoter. *Journal of Industrial Microbiology* **1996,** 16, (3), 145-154.
302. Xu, Z.; Zhong, Z.; Huang, L.; Peng, L.; Wang, F.; Cen, P., High-level production of bioactive human beta-defensin-4 in *Escherichia coli* by soluble fusion expression. *Applied Microbiology and Biotechnology* **2006,** 72, (3), 471-479.
303. Peng, L.; Xu, Z.; Fang, X.; Wang, F.; Cen, P., High-level expression of soluble human β-defensin-2 in *Escherichia coli*. *Process Biochemistry* **2004,** 39, (12), 2199-2205.
304. Wang, J.; Chen, J.; Xu, R.; Xu, Z., Batch and fed-batch cultivation for excretive production of human epidermal growth factor (hEGF) with recombinant *E. coli* K12 system. *Preparative biochemistry & biotechnology* **2008,** 38, (3), 271-281.
305. LaVallie, E. R.; Lu, Z.; Diblasio-Smith, E. A.; Collins-Racie, L. A.; McCoy, J. M., Thioredoxin as a fusion partner for production of soluble recombinant proteins in *Escherichia coli*. In *Methods in enzymology*, Elsevier: 2000; Vol. 326, pp 322-340.
306. Wals, K.; Ovaa, H., Unnatural amino acid incorporation in *E. coli*: current and future applications in the design of therapeutic proteins. *Frontiers in Chemistry* **2014,** 2, 15.
307. Johnson, D. B. F.; Xu, J.; Shen, Z.; Takimoto, J. K.; Schultz, M. D.; Schmitz, R. J.; Xiang, Z.; Ecker, J. R.; Briggs, S. P.; Wang, L., RF1 knockout allows ribosomal incorporation of unnatural amino acids at multiple sites. *Nat Chem Biol* **2011,** 7, (11), 779-786.
308. Lajoie, M. J.; Rovner, A. J.; Goodman, D. B.; Aerni, H.-R.; Haimovich, A. D.; Kuznetsov, G.; Mercer, J. A.; Wang, H. H.; Carr, P. A.; Mosberg, J. A.; Rohland, N.; Schultz, P. G.; Jacobson, J. M.; Rinehart, J.; Church, G. M.; Isaacs, F. J., Genomically recoded organisms expand biological functions. *Science* **2013,** 342, (6156), 357-360.
309. Zheng, Y.; Lajoie, M. J.; Italia, J. S.; Chin, M. A.; Church, G. M.; Chatterjee, A., Performance of optimized noncanonical amino acid mutagenesis systems in the absence of release factor 1. *Molecular BioSystems* **2016,** 12, (6), 1746-1749.
310. Hart, R. A.; Lester, P. M.; Reifsnyder, D. H.; Ogez, J. R.; Builder, S. E., Large scale, in situ isolation of periplasmic IGF-I from *E. coli*. *Bio/Technology* **1994,** 12, 1113.
311. Swiderska, K. W.; Szlachcic, A.; Czyrek, A.; Zakrzewska, M.; Otlewski, J., Site-specific conjugation of fibroblast growth factor 2 (FGF2) based on incorporation of alkyne-reactive unnatural amino acid. *Bioorganic & Medicinal Chemistry* **2017,** 25, (14), 3685-3693.
312. Samuelsson, E.; Moks, T.; Uhlen, M.; Nilsson, B., Enhanced *in vitro* refolding of insulin-like growth factor I using a solubilizing fusion partner. *Biochemistry* **1994,** 33, (14), 4207-4211.
313. Khow, O.; Suntrarachun, S., Strategies for production of active eukaryotic proteins in bacterial expression system. *Asian Pacific Journal of Tropical Biomedicine* **2012,** 2, (2), 159-162.
314. Rosano, G. L.; Ceccarelli, E. A., Recombinant protein expression in *Escherichia coli*: advances and challenges. *Frontiers in Microbiology* **2014,** 5, (172).
315. Huang, C., Jr.; Lin, H.; Yang, X., Industrial production of recombinant therapeutics in *Escherichia coli* and its recent advancements. *Journal of Industrial Microbiology & Biotechnology* **2012,** 39, (3), 383-399.
316. Mostafa, K.; Reza, S. M.; Maryam, B.; Cordian, B., High-level expression and purification of soluble bioactive recombinant human heparin-binding epidermal growth factor in *Escherichia coli*. *Cell Biology International* **2015,** 39, (7), 858-864.

317. Zhao, H.; Heusler, E.; Jones, G.; Li, L.; Werner, V.; Germershaus, O.; Ritzer, J.; Luehmann, T.; Meinel, L., Decoration of silk fibroin by click chemistry for biomedical application. *Journal of Structural Biology* **2014,** 186, (3), 420-430.
318. Janknecht, R.; De Martynoff, G.; Lou, J.; Hipskind, R. A.; Nordheim, A.; Stunnenberg, H. G., Rapid and efficient purification of native histidine-tagged protein expressed by recombinant vaccinia virus. *Proceedings of the National Academy of Sciences* **1991,** 88, (20), 8972-8976.
319. Lichty, J. J.; Malecki, J. L.; Agnew, H. D.; Michelson-Horowitz, D. J.; Tan, S., Comparison of affinity tags for protein purification. *Protein expression and purification* **2005,** 41, (1), 98-105.
320. Arnau, J.; Lauritzen, C.; Petersen, G. E.; Pedersen, J., Current strategies for the use of affinity tags and tag removal for the purification of recombinant proteins. *Protein expression and purification* **2006,** 48, (1), 1-13.
321. Schmitt, J.; Hess, H.; Stunnenberg, H. G., Affinity purification of histidine-tagged proteins. *Molecular biology reports* **1993,** 18, (3), 223-230.
322. Bornhorst, J. A.; Falke, J. J., Purification of proteins using polyhistidine affinity tags. In *Methods in enzymology*, Elsevier: 2000; Vol. 326, pp 245-254.
323. Lobstein, J.; Emrich, C. A.; Jeans, C.; Faulkner, M.; Riggs, P.; Berkmen, M., SHuffle, a novel *Escherichia coli* protein expression strain capable of correctly folding disulfide bonded proteins in its cytoplasm. *Microbial Cell Factories* **2012,** 11, 56-56.
324. Patrick, O. D.; Laure, P.; U., H. I.; Jiqiang, L.; Keturah, O.; R., L. W.; Dieter, S., Near-cognate suppression of amber, opal and quadruplet codons competes with aminoacyl-tRNAPyl for genetic code expansion. *FEBS Letters* **2012,** 586, (21), 3931-3937.
325. Heinemann, I. U.; Rovner, A. J.; Aerni, H. R.; Rogulina, S.; Cheng, L.; Olds, W.; Fischer, J. T.; Söll, D.; Isaacs, F. J.; Rinehart, J., Enhanced phosphoserine insertion during *Escherichia coli* protein synthesis via partial UAG codon reassignment and release factor 1 deletion. *FEBS letters* **2012,** 586, (20), 3716-3722.
326. Wang, L.; Johnson, D.; Wang, C.; Xu, J.; Schultz, M.; Schmitz, R.; Ecker, J., Release factor one is nonessential in *Escherichia coli*. **2012**.
327. Mukai, T.; Hoshi, H.; Ohtake, K.; Takahashi, M.; Yamaguchi, A.; Hayashi, A.; Yokoyama, S.; Sakamoto, K., Highly reproductive *Escherichia coli* cells with no specific assignment to the UAG codon. *Scientific reports* **2015,** 5, 9699.
328. Johnson, D. B. F.; Xu, J.; Shen, Z.; Takimoto, J. K.; Schultz, M. D.; Schmitz, R. J.; Xiang, Z.; Ecker, J. R.; Briggs, S. P.; Wang, L., RF1 knockout allows ribosomal incorporation of unnatural amino acids at multiple sites. *Nature Chemical Biology* **2011,** 7, 779.
329. Gallwitz, M.; Enoksson, M.; Thorpe, M.; Hellman, L., The extended cleavage specificity of human thrombin. *PLoS One* **2012,** 7, (2), e31756.
330. Jui-Yoa, C., Thrombin specificity. *European Journal of Biochemistry* **1985,** 151, (2), 217-224.
331. Cera, E.; Cantwell, A. M., Determinants of thrombin specificity. *Annals of the New York Academy of Sciences* **2001,** 936, (1), 133-146.
332. Jansson, M.; Dixelius, J.; Uhlen, M.; Nilsson, B. O., Binding affinities of insulin-like growth factor-I (IGF-I) fusion proteins to IGF binding protein 1 and IGF-I receptor are not correlated with mitogenic activity. *FEBS Letters* **1997,** 416, (3), 259-264.
333. Rajalingam, D.; Kathir, K. M.; Ananthamurthy, K.; Adams, P. D.; Kumar, T. K. S., A method for the prevention of thrombin-induced degradation of recombinant proteins. *Analytical biochemistry* **2008,** 375, (2), 361-363.
334. Waugh, D. S., An overview of enzymatic reagents for the removal of affinity tags. *Protein expression and purification* **2011,** 80, (2), 283-293.
335. Woeldicke, H. F.; Zhang, X.; Liu, Y.; Tong, W., Modified enterokinase light chain. In US Patent 9611466B2: 2017.
336. Terpe, K., Overview of tag protein fusions: from molecular and biochemical fundamentals to commercial systems. *Applied Microbiology and Biotechnology* **2003,** 60, (5), 523-533.
337. Nominé, Y.; Ristriani, T.; Laurent, C.; Lefèvre, J.-F.; Weiss, É.; Travé, G., Formation of soluble inclusion bodies by HPV E6 oncoprotein fused to maltose-binding protein. *Protein expression and purification* **2001,** 23, (1), 22-32.

338. Studier, F. W., Protein production by auto-induction in high-density shaking cultures. *Protein expression and purification* **2005,** 41, (1), 207-234.
339. Holmes, W.; Smith, R.; Bill, R., Evaluation of antifoams in the expression of a recombinant FC fusion protein in shake flask cultures of Saccharomyces cerevisiae &Pichia pastoris. *Microbial Cell Factories* **2006,** 5, (1), P30.
340. Routledge, S. J.; Bill, R. M., The effect of antifoam addition on protein production yields. In *Recombinant Protein Production in Yeast: Methods and Protocols*, Bill, R. M., Ed. Humana Press: Totowa, NJ, 2012; pp 87-97.
341. Routledge, S. J.; Hewitt, C. J.; Bora, N.; Bill, R. M., Antifoam addition to shake flask cultures of recombinant Pichia pastoris increases yield. *Microbial Cell Factories* **2011,** 10, (1), 17.
342. Rackham, O.; Chin, J. W., A network of orthogonal ribosome·mRNA pairs. *Nature Chemical Biology* **2005,** 1, 159.
343. Wang, K.; Neumann, H.; Peak-Chew, S. Y.; Chin, J. W., Evolved orthogonal ribosomes enhance the efficiency of synthetic genetic code expansion. *Nature Biotechnology* **2007,** 25, 770.
344. Guo, J.; Melançon Charles , E.; Lee Hyun, S.; Groff, D.; Schultz Peter , G., Evolution of amber suppressor tRNAs for efficient bacterial production of proteins containing nonnatural amino acids. *Angewandte Chemie International Edition* **2009,** 48, (48), 9148-9151.
345. Park, H.-S.; Hohn, M. J.; Umehara, T.; Guo, L.-T.; Osborne, E. M.; Benner, J.; Noren, C. J.; Rinehart, J.; Söll, D., Expanding the genetic code of *Escherichia coli* with phosphoserine. *Science* **2011,** 333, (6046), 1151-1154.
346. Neumann, H.; Wang, K.; Davis, L.; Garcia-Alai, M.; Chin, J. W., Encoding multiple unnatural amino acids via evolution of a quadruplet-decoding ribosome. *Nature* **2010,** 464, 441.
347. A., C. I.; Michael, S., Quadruplet codons: One small step for a ribosome, one giant leap for proteins. *BioEssays* **2010,** 32, (8), 650-654.
348. Pott, M.; Schmidt, M. J.; Summerer, D., Evolved sequence contexts for highly efficient amber suppression with noncanonical amino acids. *ACS Chemical Biology* **2014,** 9, (12), 2815-2822.
349. Young, T. S.; Ahmad, I.; Yin, J. A.; Schultz, P. G., An enhanced system for unnatural amino acid mutagenesis in *E. coli*. *Journal of Molecular Biology* **2010,** 395, (2), 361-374.
350. Chatterjee, A.; Sun, S. B.; Furman, J. L.; Xiao, H.; Schultz, P. G., A versatile platform for single- and multiple-unnatural amino acid mutagenesis in *Escherichia coli*. *Biochemistry* **2013,** 52, (10), 10.1021/bi4000244.
351. Chatterjee, A.; Xiao, H.; Bollong, M.; Ai, H.-W.; Schultz, P. G., Efficient viral delivery system for unnatural amino acid mutagenesis in mammalian cells. *Proceedings of the National Academy of Sciences* **2013,** 110, (29), 11803-11808.
352. Ganim, Z.; Rief, M., Mechanically switching single-molecule fluorescence of GFP by unfolding and refolding. *Proceedings of the National Academy of Sciences* **2017**.
353. Abrams, J. L.; Morano, K. A., Coupled assays for monitoring protein refolding in Saccharomyces cerevisiae. *Journal of visualized experiments : JoVE* **2013**, (77), 10.3791/50432.
354. Trésaugues, L.; Collinet, B.; Minard, P.; Henckes, G.; Aufrère, R.; Blondeau, K.; Liger, D.; Zhou, C.-Z.; Janin, J.; Van Tilbeurgh, H., Refolding strategies from inclusion bodies in a structural genomics project. *Journal of structural and functional genomics* **2004,** 5, (3), 195-204.
355. Vincentelli, R.; Canaan, S.; Campanacci, V.; Valencia, C.; Maurin, D.; Frassinetti, F.; Scappucini-Calvo, L.; Bourne, Y.; Cambillau, C.; Bignon, C., High-throughput automated refolding screening of inclusion bodies. *Protein Science* **2004,** 13, (10), 2782-2792.
356. Townsend, M. W.; Deluca, P. P., Stability of ribonuclease A in solution and the freeze-dried state. *Journal of pharmaceutical sciences* **1990,** 79, (12), 1083-1086.
357. Dong, A.; Prestrelski, S. J.; Allison, S. D.; Carpenter, J. F., Infrared spectroscopic studies of lyophilization-and temperature-induced protein aggregation. *Journal of pharmaceutical sciences* **1995,** 84, (4), 415-424.
358. Costantino, H. R.; Schwendeman, S. P.; Griebenow, K.; Klibanov, A. M.; Langer, R., The secondary structure and aggregation of lyophilized tetanus toxoid. *Journal of pharmaceutical sciences* **1996,** 85, (12), 1290-1293.

359. Chan, H.-K.; Ongpipattanakul, B.; Au-Yeung, J., Aggregation of rhDNase occurred during the compression of KBr pellets used for FTIR spectroscopy. *Pharmaceutical research* **1996,** 13, (2), 238-242.
360. Jordan, G. M.; Yoshioka, S.; Terao, T., The aggregation of bovine serum albumin in solution and in the solid state. *Journal of pharmacy and pharmacology* **1994,** 46, (3), 182-185.
361. Prestrelski, S. J.; Pikal, K. A.; Arakawa, T., Optimization of lyophilization conditions for recombinant human interleukin-2 by dried-state conformational analysis using fourier-transform infrared spectroscopy. *Pharmaceutical research* **1995,** 12, (9), 1250-1259.
362. Costantino, H. R.; Griebenow, K.; Mishra, P.; Langer, R.; Klibanov, A. M., Fourier-transform infrared spectroscopic investigation of protein stability in the lyophilized form. *Biochimica et Biophysica Acta (BBA) - Protein Structure and Molecular Enzymology* **1995,** 1253, (1), 69-74.
363. Prestrelski, S. J.; Tedeschi, N.; Arakawa, T.; Carpenter, J. F., Dehydration-induced conformational transitions in proteins and their inhibition by stabilizers. *Biophysical Journal* **1993,** 65, (2), 661-671.
364. Shahrokh, Z.; Eberlein, G.; Buckley, D.; Paranandi, M. V.; Aswad, D. W.; Stratton, P.; Mischak, R.; Wang, Y., Major degradation products of basic fibroblast growth factor: detection of succinimide and iso-aspartate in place of aspartate ^{15}. *Pharmaceutical research* **1994,** 11, (7), 936-944.
365. Wang, Y. J.; Shahrokh, Z.; Vemuri, S.; Eberlein, G.; Beylin, I.; Busch, M., Characterization, stability, and formulations of basic fibroblast growth factor. In *Formulation, Characterization, and Stability of Protein Drugs: Case Histories*, Springer: 2002; pp 141-180.
366. Costantino, H. R.; Langer, R.; Klibanov, A. M., Moisture-induced aggregation of lyophilized insulin. *Pharmaceutical research* **1994,** 11, (1), 21-29.
367. Chang, B. S.; Beauvais, R. M.; Dong, A.; Carpenter, J. F., Physical factors affecting the storage stability of freeze-dried interleukin-1 receptor antagonist: glass transition and protein conformation. *Archives of biochemistry and biophysics* **1996,** 331, (2), 249-258.
368. Fink, A. L., Protein aggregation: folding aggregates, inclusion bodies and amyloid. *Folding and Design* **1998,** 3, (1), R9-R23.
369. Chang, J. Y.; McFarland, N. C.; Swartz, J. R., Method for refolding insoluble, misfolded insulin-like growth factor-I into an active conformation. In US Patent 5288931: 1994.
370. Miller, J. A.; Narhi, L. O.; Hua, Q. X.; Rosenfeld, R.; Arakawa, T.; Rohde, M.; Prestrelski, S.; Lauren, S.; Stoney, K. S., Oxidative refolding of IGF-1 yields two products of similar thermodynamic stability: A bifurcating protein-folding pathway. *Biochemistry* **1993,** 32, (19), 5203-5213.
371. Miller, J. A.; Hsieh, P. K.; Tsai, L. B., Production of biologically active insulin-like growth factor i from high expression host cell systems. In US Patent 5158875A: 1992.
372. Takahashi, T.; Ogasawara, T.; Kishimoto, J.; Liu, G.; Asato, H.; Nakatsuka, T.; Uchinuma, E.; Nakamura, K.; Kawaguchi, H.; Chung, U.-i., Synergistic effects of FGF-2 with insulin or IGF-I on the proliferation of human auricular chondrocytes. *Cell transplantation* **2005,** 14, (9), 683-693.
373. Frederick, T. J.; Wood, T. L., IGF-I and FGF-2 coordinately enhance cyclin D1 and cyclin E–cdk2 association and activity to promote G1 progression in oligodendrocyte progenitor cells. *Molecular and Cellular Neuroscience* **2004,** 25, (3), 480-492.
374. Jiang, F.; Frederick, T. J.; Wood, T. L., IGF-I synergizes with FGF-2 to stimulate oligodendrocyte progenitor entry into the cell cycle. *Developmental Biology* **2001,** 232, (2), 414-423.
375. Kessler, M. W.; Barr, J.; Greenwald, R.; Lane, L. B.; Dines, J. S.; Dines, D. M.; Drakos, M. C.; Grande, D. A.; Chahine, N. O., Enhancement of Achilles tendon repair mediated by matrix metalloproteinase inhibition via systemic administration of doxycycline. *Journal of Orthopaedic Research* **2014,** 32, (4), 500-506.
376. Gutmann, M.; Memmel, E.; Braun, A. C.; Seibel, J.; Meinel, L.; Lühmann, T., Biocompatible azide–alkyne “click” reactions for surface decoration of glyco-engineered cells. *ChemBioChem* **2016,** 17, (9), 866-875.
377. Reihl, O.; Lederer, M. O.; Schwack, W., Characterization and detection of lysine–arginine cross-links derived from dehydroascorbic acid. *Carbohydrate research* **2004,** 339, (3), 483-491.

378. Kay, P.; Wagner, J. R.; Gagnon, H.; Day, R.; Klarskov, K., Modification of peptide and protein cysteine thiol groups by conjugation with a degradation product of ascorbate. *Chemical research in toxicology* **2013,** 26, (9), 1333-1339.
379. Hong, V.; Presolski, S. I.; Ma, C.; Finn, M., Analysis and optimization of copper-catalyzed azide–alkyne cycloaddition for bioconjugation. *Angewandte Chemie International Edition* **2009,** 48, (52), 9879-9883.
380. Liu, Y.; Sun, G.; David, A.; Sayre, L. M., Model studies on the metal-catalyzed protein oxidation: structure of a possible His-Lys cross-link. *Chemical research in toxicology* **2004,** 17, (1), 110-118.
381. Mori, S.; Barth, H. G., *Size exclusion chromatography*. Springer Science & Business Media: 2013.
382. Janson, J.-C., *Protein purification: principles, high resolution methods, and applications*. John Wiley & Sons: 2012; Vol. 151.
383. Plass, T.; Milles, S.; Koehler, C.; Schultz, C.; Lemke, E. A., Genetically encoded copper-free click chemistry. *Angewandte Chemie (International Ed. in English)* **2011,** 50, (17), 3878-3881.
384. Plass, T.; Milles, S.; Koehler, C.; Szymański, J.; Mueller, R.; Wießler, M.; Schultz, C.; Lemke, E. A., Amino acids for Diels–Alder reactions in living cells. *Angewandte Chemie International Edition* **2012,** 51, (17), 4166-4170.
385. Handayaningsih, A.-E.; Iguchi, G.; Fukuoka, H.; Nishizawa, H.; Takahashi, M.; Yamamoto, M.; Herningtyas, E.-H.; Okimura, Y.; Kaji, H.; Chihara, K.; Seino, S.; Takahashi, Y., Reactive oxygen species play an essential role in IGF-I signaling and IGF-I-induced myocyte hypertrophy in C2C12 myocytes. *Endocrinology* **2011,** 152, (3), 912-921.
386. Narang, S., *Synthesis and applications of DNA and RNA*. Elsevier: 2012.
387. Hannig, G.; Makrides, S. C., Strategies for optimizing heterologous protein expression in *Escherichia coli*. *Trends in Biotechnology* **1998,** 16, (2), 54-60.
388. Makrides, S. C., Strategies for achieving high-level expression of genes in *Escherichia coli*. *Microbiological reviews* **1996,** 60, (3), 512-538.
389. LaVallie, E. R.; McCoy, J. M., Gene fusion expression systems in *Escherichia coli*. *Current Opinion in Biotechnology* **1995,** 6, (5), 501-506.
390. Butt, T. R.; Edavettal, S. C.; Hall, J. P.; Mattern, M. R., SUMO fusion technology for difficult-to-express proteins. *Protein Expression and Purification* **2005,** 43, (1), 1-9.
391. Li, Y., Self-cleaving fusion tags for recombinant protein production. *Biotechnology Letters* **2011,** 33, (5), 869-881.
392. Costa, S.; Almeida, A.; Castro, A.; Domingues, L., Fusion tags for protein solubility, purification and immunogenicity in *Escherichia coli*: the novel Fh8 system. *Frontiers in Microbiology* **2014,** 5, (63).
393. Esposito, D.; Chatterjee, D. K., Enhancement of soluble protein expression through the use of fusion tags. *Current Opinion in Biotechnology* **2006,** 17, (4), 353-358.
394. Malhotra, A., Chapter 16 tagging for protein expression. In *Methods in Enzymology*, Burgess, R. R.; Deutscher, M. P., Eds. Academic Press: 2009; Vol. 463, pp 239-258.
395. Lühmann, T.; Meinel, L., Nanotransporters for drug delivery. *Current Opinion in Biotechnology* **2016,** 39, 35-40.
396. Lang, K.; Chin, J. W., Bioorthogonal reactions for labeling proteins. *ACS Chemical Biology* **2014,** 9, (1), 16-20.
397. Pietsch, M.; Wodtke, R.; Pietzsch, J.; Löser, R., Tissue transglutaminase: An emerging target for therapy and imaging. *Bioorganic & Medicinal Chemistry Letters* **2013,** 23, (24), 6528-6543.
398. Nguyen, D. P.; Lusic, H.; Neumann, H.; Kapadnis, P. B.; Deiters, A.; Chin, J. W., Genetic encoding and labeling of aliphatic azides and alkynes in recombinant proteins via a pyrrolysyl-tRNA synthetase/tRNACUA pair and click chemistry. *Journal of the American Chemical Society* **2009,** 131, (25), 8720-8721.
399. Wang, Q.; Chan, T. R.; Hilgraf, R.; Fokin, V. V.; Sharpless, K. B.; Finn, M. G., Bioconjugation by copper(I)-catalyzed azide-alkyne [3 + 2] cycloaddition. *Journal of the American Chemical Society* **2003,** 125, (11), 3192-3193.

400. Presolski, S. I.; Hong, V.; Cho, S.-H.; Finn, M. G., Tailored ligand acceleration of the Cu-catalyzed azide−alkyne cycloaddition reaction: practical and mechanistic implications. *Journal of the American Chemical Society* **2010,** 132, (41), 14570-14576.
401. Chayasith, U.; Anupong, T.; Scott, G.; Scott, C.; Upinder, S.; Peter, S.; R., G. K.; Y., T. A., Fast, cell-compatible click chemistry with copper-chelating azides for biomolecular labeling. *Angewandte Chemie International Edition* **2012,** 51, (24), 5852-5856.
402. Docheva, D.; Müller, S. A.; Majewski, M.; Evans, C. H., Biologics for tendon repair. *Advanced Drug Delivery Reviews* **2015,** 84, 222-239.
403. Alibolandi, M.; Mirzahoseini, H., Chemical assistance in refolding of bacterial inclusion bodies. *Biochemistry Research International* **2011,** 2011, 631607.
404. Snyder, G. H., Free energy relationships for thiol-disulfide interchange reactions between charged molecules in 50% methanol. *Journal of Biological Chemistry* **1984,** 259, (12), 7468-7472.
405. Hejnaes, K. R.; Bayne, S.; Nørskov, L.; Holmegaard, H.; Sørensen, H. H.; Thomsen, J.; Schäffer, L.; Wollmer, A.; Skriver, L., Development of an optimized refolding process for recombinant Ala–Glu–IGF-1. *Protein Engineering, Design and Selection* **1992,** 5, (8), 797-806.

Appendix

Appendix A.

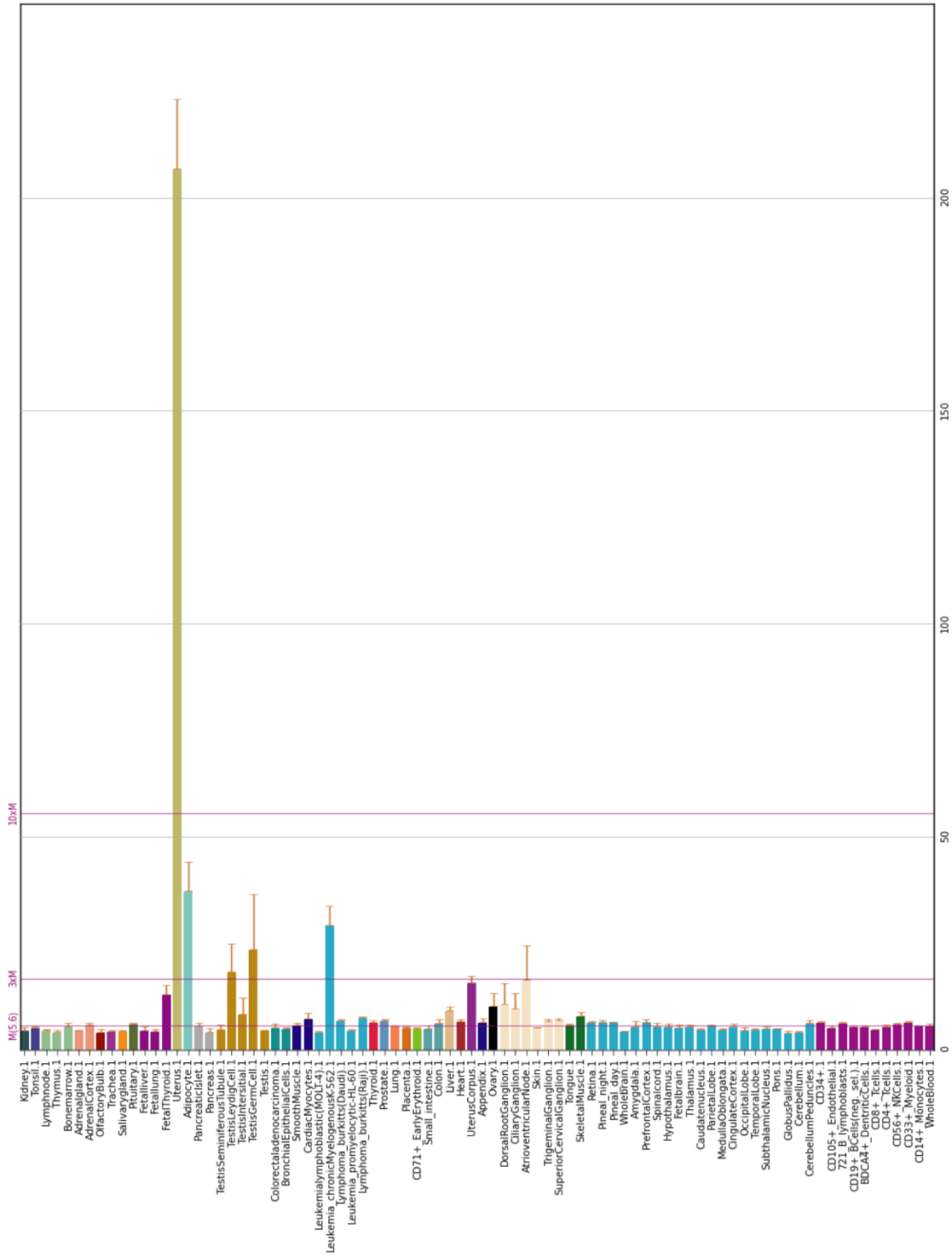

Figure 28. IGF-I gene expression profiles built by BioGPS platform

Appendix B.

```
                 1         10        20        30        40        50        60        70
Human            G P E T L C G A E L V D A L Q F V C G D R G F Y F N K P T G Y G S S S R R A P Q T G I V D E C C F R S C D L R R L E M Y C A P L K P A K S A
Rat              - - - - - - - - - - - - - - - - - - - - P - - - - - - - - - - - - - - - I - - - - - - - - - - - - - - - - - - - - - - - - - - - - T - - -
Kangaroo         - - - - - - - - - - - - - - - - - - - - E - - - - - S - - - - - - - - - - - - - - L H H - - - - - - - - - - - - - - - - - - - - - - I - - - - - -
Chicken          - - - - - - - - - - - - - - - - - - - - - - - - - - S - - - - - - - - - - - - - L H H K - - - - - - - - Q - - - - - - - - - - - - - - - I - - P - - -
Frog             - - - - - - - - - - - - - T - - - - - - - - - - - - S - - - - - - - N N - - S H H R - - - - - - - - Q - - - F - - - - - - - - - - A - - - - - -
Salmon           - - - - - - - - - - - - - T - - - - - - E - - - - - S - - - - - - - P - - - - S H N R - - - - - - - - Q - - E - - - - - - - - - - - V - SG - A -
Barramundi       - - - - - - - - - - - - - T - - - - - - E - - - - - S - - # - - - - N A - - S # # R - - - - - - - - Q - - E - - - - - - - - - - - P - T # - A -
Pig              - - - - - - - - - - - - - - - - - - - - - - - - - - - - - - - - - - - - - - - - - - - - - - - - - - - - - - - - - - - - - - - - - - - - - - - -
Cow              - - - - - - - - - - - - - - - - - - - - - - - - - - - - - - - - - - - - - - - - - - - - - - - - - - - - - - - - - - - - - - - - - - - - - - - -
Goat             - - - - - - - - - - - - - - - - - - - - - - - - - - - - - - - - - - - - - - - - - - - - - - - - - - - - - - - - - - - - - - - - - - - - T - - -
Dog              - - - - - - - - - - - - - - - - - - - - - - - - - - - - - - - - - - - - - - - - - - - - - - - - - - - - - - - - - - - - - - - - - - - - - - - -
Equine           - - - - - - - - - - - - - - - - - - - - - - - - - - - - - - - - - - - - - - - - - - - - - - - - - - - - - - - - - - - - - - - - - - - - - - - -
Rhesus macaque   - - - - - - - - - - - - - - - - - - - - - - - - - - - - - - - - - - - - - - - - - - - - - - - - - - - - - - - - - - - - - - - - - - - - - - - -
Chimpanzee       - - - - - - - - - - - - - - - - - - - - - - - - - - - - - - - - - - - - - - - - - - - - - - - - - - - - - - - - - - - - - - - - - - - - - - - -
Rabbit           - - - - - - - - - - - - - - - - - - - - - - - - - - - - - - - - - - - - - - - - - - - - - - - - - - - - - - - - - - - - - - - - - - - - - - A -
```

Figure 29. Sequence alignment of human, rat, kangaroo, chicken, frog, salmon, barramundi, pig, cow, goat, dog, equine, rhesus macaque, chimpanzee and rabbit IGF-I. Dash lines represent amino acids that are identical to those found in human IGF-I. Hash (#) symbols were used to frame shift the proteins for maximal alignment between sequences.

Appendix C.

Table 9. Examples of buffer additives which may be used to facilitate protein refolding[403] (unless noted specifically)

Additive	Concentration	Effect
CHAPS	30 mM	Detergent
Glycerol	10–50%	Stabilizer
Guanidine HCl	0.1–1 M	Chaotroph
L-arginine	0.4–0.5 M	Stabilizer
Laroylsarcosin	Up to 4 M	Detergent
$MgCl_2$/$CaCl_2$	2–10 mM	Cation
NaCl/Ammonium sulfate	0.2–0.5 M	Salt
Non-detergent sulfo betain	Up to 1 M	Solubilizer
PEG 3350	Up to 0.5% W/V	Osmolyte
SDS	0.1%	Detergent
Sodium citrate/sulfate	0.2–0.5 M	Salt
Sucrose/glucose	Up to 0.75 M	Stabilizer
TMAO	1–3 M	Osmolyte
Triton X-100	0.1–1%	Detergent
Tween-80	0.01%	Detergent
Glycine	Up to 1 M	Osmolyte
Proline	Up to 1 M	Osmolyte
Urea	0.1–2 M	Chaotroph
Methanol[404]	5-20%	Enhancement of selected disulfide pairings
Ethanol[405]	5-20%	Hydrophobic
Cysteine[405]	Up to 2 mM	Reducing agents

Appendix D.

Table 10. Protease inhibitors.

Inhibitor	**Working concentration**	**Stock concentration**	**Solvent**	**Application**
Aprotinin	1–2 µg/ml	10 mg/ml	water	serine proteases
Benzamidine	15 µg/ml	10 mg/ml	water	serine proteases
EDTA, EGTA	1–10 mM	0.5 M (pH 8)	water	metallo proteases
Leupeptin	1–2 µg/ml	10 mg/ml	water	cysteine and serine proteases
PMSF	0.1–1.0 mM	100 mM	isopropanol	serine proteases
Pepstatin A	1µg/ml	1 mg/ml	methanol	aspartic proteases
Sodium orthovanadate (Na_3VO_4)	1–10 mM	200 mM	water	ATPases alkaline and acid phosphatases protein-phosphotyrosine phosphatases
Sodium fluoride (NaF)	5–50 mM	500 mM	water	Ser/Thr and acidic phosphatases

Abbreviations

ALS	Acid-labile subunit
BSA	Bovine serum albumin
CAM	Carbamidomethylation
CamK	Calcium-calmodulin dependent protein kinase
cIGF-I	Commercial IGF-I
CTC	Chlorotrityl chloride resin
CuAAC	Copper-catalyzed azide-alkyne 1,3-dipolar cycloaddition
CV	Column volumes
DCM	Dichloromethane
DIC	N, N′-Diisopropylcarbodiimide
DIPEA	N, N-Diisopropylethylamine
DMF	N, N-Dimethylformamide
DTT	1,4-Dithiothreitol
ECM	Extracellular matrix
EF-Tu	Elongation factor Tu
FGF2	Fibroblast growth factor 2
FXIIIa	Factor XIIIa
GRAS	generally recognized as safe
Grb2	Growth receptor binding protein -2
HDACs	Histone Deacetylases
His6	Hexahistidine
HSA	Human serum albumin
IGFBPs	IGF-binding proteins
IGF-I	Insulin-like growth factor I
IGF-IR	Type I IGF receptor
IGF-IIR	Type II IGF receptor

IR	Insulin receptor
IRS	Insulin receptor substrate
IMAC	Immobilized metal affinity chromatography
IB	Inclusion body
IAM	Iodoacetamide
IPTG	Isopropyl-β-d-thiogalactopyranosid
LB	Lysogeny broth
MAFbx	Muscle Atrophy F-box
MALDI-TOF-MS	Matrix-assisted laser desorption/ionization time-of-flight mass spectrometry
MAP	Mitogen-activated protein
MEF2	Myocyte enhancer factor 2
MGF	Mechano growth factor
MiRNA	MicroRNA
mTOR	Mammalian target of Rapamycin
MuRF1	Muscle Ring Finger1
MyHC	Myosin heavy chain
NEB	New England Biolabs
NHS	N-hydroxysuccinimide
NMDA	N-methyl-D-aspartate
JNK	Jun kinase
PCL	Protease cleavable linker
PCR	Polymerase chain reaction
PI3K	Phosphatidylinositol 3 kinase
Plk	Propargyl-l-lysine
PMSF	Phenylmethylsulfonyl fluoride
PSL	Protease-sensitive peptide linker
Pyl	Pyrrolysyl

PylRS	Pyrrolysyl tRNA synthetase
RF1	Release factor 1
ROS	Reactive oxygen species
SDS-PAGE	Sodium dodecyl sulfate polyacrylamide gel electrophoresis
SPAAC	Strain-promoted alkyne-azide cycloaddition
TB	Terrific Broth
TBS	Tris-buffered saline
TBST	Tris buffered saline solution containing 0.1 % (v/v) tween 20
TFA	Trifluoroacetic acid
TGases	Transglutaminases
Trx	Thioredoxin
uAA	Unnatural amino acid
α2PI1–8	α-2 plasmin inhibitor

Curriculum vitae

Personal Details

Name	Fang Wu
Date of birth	1989-05-09
Place of birth	Hunan, China

Education

Nov. 2014 - present	Ph.D., Institute of Pharmacy and Food Chemistry, University of Würzburg, Germany
	Supervisor: Prof. Dr. Dr. Lorenz Meinel
Sep. 2011 – Jul. 2014	M.E., National Engineering Research Center for Biomaterials, Sichuan University, China.
Sep. 2007 – Jul. 2011	B.S., School of Chemical Technology, Huaqiao University, China

Publication:

F. Wu, A. Braun, T. Lühmann, L. Meinel, "'Site-Specific Conjugated Insulin-like Growth Factor-I for Anabolic Therapy," *ACS Biomater. Sci. Eng.*, 2018, 4 (3), pp 819-825.

Posters:

F. Wu, M. Gutmann, T. Lühmann, L. Meinel. (2018) Bioresponsive co-delivery of FGF2 and IGF-I based on genetic incorporation of clickable unnatural amino acids, EMBO Workshop: Chemical Biology (29.08.2018–01.09.2018), Poster No. 221.

F. Wu, J. Ritzer, T. Lühmann, L. Meinel. (2017) Genetically engineered insulin-like growth factor-I (IGF-I) for site-specific bioconjugation, 21st Annual Meeting of the Controlled Release Society - German Local Chapter (02.03.2017–03.03.2017), Poster No. 48.

F. Wu, J. Ritzer, T. Lühmann, L. Meinel. (2016) Site-directed incorporation of propargyl-L-lysine into insulin-like growth factor-I (IGF-I) for site-specific decoration, Chem-SyStM 2016 (08.12.2016), Poster No. 60.

Acknowledgments

I would like to express my sincere gratitude to my supervisor Prof. Dr. Dr. Lorenz Meinel, who offered me the opportunity to come to Germany to work in his group. Particularly, I want to thank him for giving me the possibility to access many scientific methods, and for his continuous guidance, great support and kind advice throughout my Ph.D. study.

Furthermore, I would like to thank PD Dr. Tessa Lühmann, for the much productive discussions and help with both practical problems and writing, in particular with abstracts, posters, and manuscript.

I would like to thank Dr. Jennifer Ritzer for all her help and kindness, for her expertise and for training me in protein expression, peptide synthesis, for improving my biannual CSC study reports and for the nice time we spent together.

I would like to thank Alexandra Braun for the great cooperation, for the open exchange of ideas and inspiring conversations, for her crucial contribution to the manuscript.

I would also like to thank Marcus Gutmann for the support with 3D stacks of agarose beads, FGF2 knowledge, and skills, for his great support with the EMBO poster.

I would further like to thank all my colleagues of the group for interesting conversations at lunch, during cake breaks or at different activities outside of working hours. I am very grateful to Dr. Johannes Wiest, Valerie Spieler, Tobias Miesler, Katharina Güntzel, Doris Moret, Cornelius Hermann, Martina Raschig, Niklas Hauptstein, Dr. Sascha Zügner, Christine Schneider, and Joel Wurzel, who all helped me in numerous ways during various stages of my Ph.D. Furthermore, a big “Thank you!” to Jonas Schlauersbach and Valerie Spieler for their help in translating the summary of my thesis to German.

To all my close friends in Europe and China, I thank them for their always unconditional friendship and support throughout these years.

My special thanks go to Dongliang for supporting me in everything I did, keeping me in touch with the “real” world outside of the research, and for being always there for me when I needed him.

I would like to thank my family for all their love and encouragement. I thank my niece XuanXuan and nephew DuoDuo who are my stress relievers during thesis writing.

And finally, I acknowledge the financial support from “China Scholarship Council 201406240097”.

Documentation of authorship

This section contains a list of the individual contribution for each author to the **publication** reprinted in this thesis.

P1	**Wu F, Braun A, Lühmann T, Meinel L** (2018) Site-Specific Conjugated Insulin-like Growth Factor-I for Anabolic Therapy. ACS Biomaterials Science & Engineering **4**: 819-825.			
Author	**1**	**2**	**3**	**4**
Subcloning	x			
Protein expression	x			
Inclusion body purification	x			
SDS-PAGE	x			
Western Blot	x			
Protein purification	x			
HPLC analysis	x			
Click reaction	x			
WST-1 assay	x	x		
Phosphorylation assay	x			
Decoration of NHS activated agarose beads	x			
Immobilization of plk-IGF-I Ea onto agarose beads via CuAAC	x			
Visualization of immobilized plk-IGF-I Ea	x	x		
Quantification of immobilized plk-IGF-I Ea onto azide particles	x			
Cell proliferation in the presence of plk-IGF-I Ea modified agarose beads after CuAAC	x			
C2C12 Differentiation and Immunostaining	x			
Western Blot of Differentiated C2C12 Cells	x			
Data analysis and interpretation	x	x	x	x
Manuscript planning	x		x	x
Manuscript writing	x		x	x
Correction of manuscript	x		x	x
Supervision of Fang Wu				x

Documentation of unpublished experimental work not done by me

All unpublished experimental work described in this **monograph (from Introduction to Discussion section)** was done by me, except the following:

Operator	Institute	Chapter
Dr. Isabel Schultz	Department of Pharmaceutical Technology and Biopharmacy, University of Würzburg, Germany	2.3.1.1 Prepared glycerol stock of BL (21) DE3/plk-IGF-I Ea-plk
Dr. Werner Schmitz	Department of Biochemistry and Molecular Biology, University of Würzburg, Germany	2.3.1.4 Performed trypsin digest of the excised bands and performed LC/ESI-MS analysis
Katharina Güntzel	Department of Pharmaceutical Technology and Biopharmacy, University of Würzburg, Germany	2.3.2.1.1 Acquired LC-MS spectra
Marcus Gutmann	Department of Pharmaceutical Technology and Biopharmacy, University of Würzburg, Germany	2.3.3.1 Prepared glycerol stock of BL (21) DE3/azide-PCL-FGF2, and provided part of the purified azide-PCL-FGF2 protein
Martina Raschig	Department of Pharmaceutical Technology and Biopharmacy, University of Würzburg, Germany	2.3.3.1 Synthesis of azide-L-lysine

Erklärung zu den Eigenanteilen des Doktoranden sowie der weiteren Doktoranden als Koautoren an Publikationen und Zweitpublikationsrechten bei einer kumulativen Dissertation.

Für alle in dieser kumulativen Dissertation verwendeten Manuskripte liegen die notwendigen Genehmigungen der Verlage (‚reprint permission') für die Zweitpublikation vor, außer das betreffende Kapitel ist noch gar nicht publiziert. Dieser Umstand wird einerseits durch die genaue Angabe der Literaturstelle der Erstpublikation auf der ersten Seite des betreffenden Kapitels deutlich gemacht oder die bisherige Nichtveröffentlichung durch den Vermerk „unpublished" oder „nicht veröffentlicht" gekennzeichnet.

Die Mitautoren der in dieser kumulativen Dissertation verwendeten Manuskripte sind sowohl über die Nutzung als auch über die oben angegebenen Eigenanteile informiert und stimmen dem zu.

Die Anteile der Mitautoren an den Publikationen sind in den vorausgehenden Tabellen aufgeführt.

Prof. Dr. Dr. Lorenz Meinel Unterschrift

Fang Wu Unterschrift